THE UNIVERSITY OF CHICAGO

EVOLUTION AND DEVELOPMENT OF THE VERTEBRAL COLUMN IN JAWED VERTEBRATES

A DISSERTATION SUBMITTED TO
THE FACULTY OF THE DIVISION OF THE BIOLOGICAL SCIENCES
AND THE PRITZKER SCHOOL OF MEDICINE
IN CANDIDACY FOR THE DEGREE OF
DOCTOR OF PHILOSOPHY

DEPARTMENT OF ORGANISMAL BIOLOGY AND ANATOMY

BY

KATHARINE ELIZABETH CRISWELL

CHICAGO, ILLINOIS

DECEMBER 2016

Table of Contents

List of Tables

List of Figures

Acknowledgements

I consider myself extremely fortunate to have had the opportunity to complete my Ph.D. in the Organismal Biology and Anatomy Department at the University of Chicago. I truly love this place, and feel that interactions with my committee specifically, and the entire department more generally, have shaped who I am as a scientist. I thank my dissertation committee first and foremost: Mike Coates, Andrew Gillis, Robert Ho, and Melina Hale. These scientists took the time to advise me on paleontology, development, and biomechanics, and these insights helped to guide my dissertation research. Mike has taught me many things, from the importance of precise language to broad-scale phylogenetic thinking to the intricacies of "British" English. Mike has been the exact type (ha!) of advisor that I needed – pushing me to think critically about all aspects of paleontology and evolution, while giving me enough space to pursue the research questions I became most interested in. I will be forever grateful for that freedom, as it has shaped my future research path. Andrew has been an amazing mentor and friend over the past several years, and large portions of this dissertation would not have been possible without his guidance. He took the time to work with me in the summers at MBL and in the winter in Cambridge to ensure I learned the skills I needed. He is one of the nicest people I have ever met, and I look forward to working (and sharing more Dogfish Head happy hours!) with him in the future. Robert has given me his time, lab space, and reagents over the years, ensuring that I had a place to do developmental biology while I was in Chicago. I am grateful that he opened his lab doors to me, and I am sorry for all those times I made the lab smell (dead fish, glacial acetic acid, histosol, burnt wax/wood, etc.). Melina is a phenomenal role model for a young woman scientist

like me, and I appreciate her advice and useful suggestions for my project throughout my time in Chicago.

The OBA department boasts so many truly excellent faculty members that I have benefitted from knowing throughout this process. Vicky Prince has taught me not just about developmental biology, but about how a biology program runs. I have shared many useful conversations with Zhe-Xi Luo on paleontology, CT scanning, and the scientific process. Mike LaBarbera taught me the importance of thinking biomechanically through our project on the spine brush, which we will one day finish! I am grateful to Neil Shubin for sharing skate tank space, embryos, and his microtome with me.

I wouldn't have made it through grad school with my sanity intact without the other students also undergoing this journey with me. My Darwinian cohort is simply amazing and I am in awe of all of them. Haley Stinnett was my rock, my other half, the Hate to my Kaley, my accountability. Because of her I know that everything gets done before it is due, black is always an acceptable color, and sometimes you just need to let it out. Thank you for always being there for me. Molly Gallagher, Christina Masco, Amy Henry, and Misha Blizard shared all of their good news and heartbreak over wine and cheese nights. You all are some of the most thoughtful people I know and I am so lucky to have found friends that can make me both laugh and think at the same time. I have so many other friends in the huge family that is the Darwinian cluster that made my time at UofC not just bearable, but enjoyable. Max Winston, Daniel Hooper, Lu Yao, and Nicole Bitler rounded out the 2011 cohort and provided a lot of laughs and solidarity. My former lab mates Lauren Sallan and Tom Stewart provided feedback and advice, as well as inspiration to live up to their high standard. I thank Tom for hours of heart to heart talks on the

nature of Academia, publishing, and combining comparative anatomy with developmental biology. Many others offered scientific advice, technical help, and good company, including Jon Mitchell, Brett Aiello, Tim Sosa, Justin Lemberg, Andrew Gehrke, Tetsuya Nakamura, Joyce Pieretti, Carrie Albertin, Dallas Krentzel, Courtney Orsbon, Peter Smits, Dave Grossnickle, Darcy Ross, Adam Hardy, Jackie Lungmus, Kyler Brown, Doreen Rhee, Eric Blair, Julie Szymaszek, Alana Beadell, Qiyan Mao, Chris Quintanilla, and Erin Boyle. Adam Kuuspalu and Kristen Tietjen provided assistance with reagents and CT scans. I was also part of two wonderful athletic teams while at UofC – the Anatomy Cremasters softball team and the Darwin's Revenge Broomball team. Cremasters: thank you for giving me an outlet for my frustrations and a supply of Old Style. Darwin's Revenge: 2nd place champions all the way!

Part of the way through my Ph.D. I decided to explore developmental biology, despite having very little experience in the field. That changed in the summer of 2014 when I took the Embryology course at MBL. This experience transformed my life and I am so thankful for all of my fellow students and the instructors and TAs that taught me how to work with their respective animals. Through Embryology I discovered a whole world of questions that I want to explore, and I learned the confidence to begin doing so. I am grateful to Alejandro Sanchez-Alvarado and Richard Behringer for taking a chance on a paleontologist, and then for allowing me to come back for two more years to pursue my own research. I am also thankful to have met and worked with Jon Henry and Dede Lyons in Loeb 257A. Never a dull moment! Nipam Patel helped me to understand and work with all of the confocal microscopes at MBL, and has since been a wonderful friend and colleague. I also thank Clare Baker, who I first met at MBL, and who then shared her lab space and advice with me in Cambridge. Many people at the Marine Resources

Center at MBL helped to provide me with embryos for my experiments, including Dave Remsen, Scott Bennett, and Dan Calzarette.

The paleontology portion of this project required a lot of travel and time spent browsing through fossil fish collections. Many curators and collections managers opened their doors to me, including Bill Simpson at the Field Museum, Amy Henrici at the Carnegie Museum, Alana Gishlick at the American Museum, Ted Daescher and Fred Mullison at the Academy of Natural Sciences, Gael Clement at the Museum National d'Histoire Naturelle, David Pickering and Erich Fitzgerald at the Museum Victoria, Stig Walsh at the National Museum of Scotland, and Olivier Matton and Johanne Kerr at the Parc National d'Miguasha.

I thank the many funding agencies that found my project interesting enough to support. I was fortunate enough to be awarded a National Science Foundation Doctoral Dissertation Improvement Grant (DEB-1501749), a Society of Vertebrate Paleontology Albert E. Wood Award, a Paleontological Society Kenneth E. and Annie Caster Student Research Grant, a Company of Biologists Travelling Fellowship, A University of Chicago Hinds Fund Award, an MBL/UChicago Graduate Research Award, an MBL Post-Course Research Award, a Society of Vertebrate Paleontology Patterson Fieldwork Grant, a Society of Vertebrate Paleontology Jackson School of Geosciences Travel Award, a University of Chicago BSD Student Travel Award, a Jones-Fenleigh Memorial Fund Award through the SVPCA, and a University of Chicago Graduate Council Travel Award.

I wouldn't have been able to register, apply to graduate, get paid, or use my grant money without the many administrators who drop everything to help their students. Thank you to Alison

Anastasio, Audrey Aronowski, Libby Eakin, Carolyn Johnson, Deb Hawkins, Cindy King, Stephanie Manick, Norma Del Real, Annetha Bartley, and Josh Berg.

I had the great fortune of spending three years in Austin, Texas studying for my Master's degree, where I met three of the most amazing scientists and people I will ever meet. Michelle Stocker, Jen Olori, and Kerin Claeson, I am so happy to know that five years later we are still close, still communicate with each other every month, and still share our science. You three were my inspiration when I was a brand-new graduate student, and look at me now! I feel like I am finally approaching your level.

I would also like to thank my amazing and supportive family. We biologists know that offspring receive 50% of their genes from each parent, and I think that is quite evident in my case. I have obviously inherited my love of science and fish from my Dad, who introduced me to nature at an early age and fostered my curiosity. When I started graduate school I knew that I loved science, but I didn't realize that I also loved teaching. I believe I got that from my mom. Both of my parents have instilled in me a drive to work hard and push myself to reach the pinnacle of my field. They have listened to my joy and disappointment and have never stopped encouraging me. My brother Jason has kept me going with jokes, weird voices, and the reminder that there's more to life than a lab and a computer.

Finally, to my husband, Justin Garber. You have done everything in your power to make my dreams come true. Thank you so much for cooking dinner, for picking me up when I worked late, and for always believing in me. I am so lucky to have had you by my side throughout all of this and I can't wait to share the next adventure with you.

Abstract

This dissertation focuses on a fundamental feature of the jawed vertebrate (gnathostome) body plan, the vertebral column. The vertebral column has long been used to diagnose the vertebrate clade, but its development and evolutionary history are not well understood. Vertebrae can consist of neural arches and spines, hemal arches and spines, and either a persistent notochord or a series of centra. Vertebral columns preserved in early jawed vertebrate fossils show diversity in morphology and construction, leading to the hypothesis that many components of vertebrae have evolved independently throughout the evolutionary history of jawed vertebrates. Accompanying the hypotheses of independent evolution is evidence that centra in teleost fishes are, at least in part, derived from the notochord, while centra in tetrapods are formed from somitic cells. This dissertation seeks to explore the evolution of vertebral morphology and development across non-tetrapod gnathostomes, to test the hypotheses that vertebral modifications have evolved numerous times and determine how differences in vertebral development have shaped the vertebrae of major gnathostome subgroups. Chapter one provides an introduction to vertebral morphology, gnathostome phylogeny, and the history of the study of vertebral column evolution and development. In chapter two I compile a supertree representing hypotheses of gnathostome relationships and infer ancestral vertebral conditions using parsimony, maximum likelihood, and Bayesian inference. I recover up to ten independent originations of centra, five originations of anterior fusions, and eight originations of polyspondyly throughout gnathostomes. In chapter three I describe vertebral development in the little skate (*Leucoraja erinacea*), a taxon representative of a neglected group of gnathostomes, the elasmobranchs. I use traditional techniques including histology and whole mount skeletal

preparations, as well as modern microCT methods to study embryonic vertebral morphology in a series of little skate embryos. My findings include that the neural arches develop from an unsegmented layer of condensed mesenchyme that extends the length of the body, that centra in the little skate comprise three layers of tissue, and that the mineralized areolar calcification arises from a layer of spindle-shaped cells that seem to be mesenchyme-derived. I test the embryonic origin of the centra and arches in the little skate in chapter four by injecting a fluorescent dye into 1) the ventral portions of the somites and 2) notochord progenitor cells and allowing embryos to develop to near-hatching. I recover dye-labeled cells from the somites in all components of the vertebral skeleton including the neural arches, hemal arches, and all layers of the centra, while notochord-labeled cells remain in the notochord and notochord epithelium. These fate mapping experiments indicate that the vertebral skeleton is primitively somite-derived. Taken together, the data presented in this dissertation demonstrate that actinopterygians, elasmobranchs, and tetrapods all evolved centra independently and have invented distinct patterns and processes in which to build them.

Chapter 1: Introduction: The evolution and homoplasy of the axial skeleton of jawed vertebrates

"I define a vertebra, as *one of those segments of the endo-skeleton which constitute the axis of the body, and the protecting canals of the nervous and vascular trunks*: such a segment may also support *diverging appendages*."

- Richard Owen, On the Archetype and Homologies of the Vertebrate Skeleton, 1848, page 81

The vertebral column is traditionally presented as the defining feature of vertebrates. It consists of a series of repeated cartilaginous mineralizations that extend the length of the body axis and correspond in some sense to each segment of the axial musculature. Vertebrae provide a scaffold for the muscles and connective tissue that facilitates locomotion, and protect the nervous tissue of the spinal cord. Despite this general role, a striking diversity of morphology, composition, and developmental mechanisms is present in the vertebral column across vertebrates. The relationship between the morphology and the evolutionary history of this ancient feature creates intriguing questions about how this morphological diversity came to be.

Vertebral columns comprise some combination of a notochord or series of centra, neural and hemal arches, and may include transverse processes, intercalary components, ribs, and fusions (the synarcual in chondrichthyans and 'placoderms', and the Weberian apparatus in otophysan actinopterygians) (Figure 1.1). Neural arches (neurapophyses) are variable in their morphology, but always form skeletal arcs enclosing and protecting the dorsal portion of the spinal cord. Hemal arches (hemapophyses) are most often found posterior to the pelvic fin and protect the caudal artery and vein, in addition to providing ventral extensions that dorsoventrally support the tail. Intercalary components, interdorsals and interventrals, consist of separate

mineralizations that exist between the neural and hemal arches in some taxa. Transverse processes, as well as parapophyses and diapophyses, provide lateral facets for rib or muscle attachment. A notochord persists, in varying degrees, into the adult vertebral column in many extant vertebrates, from an unconstricted state in lampreys and coelacanths, to intervertebral discs in mammals. In most living vertebrates, however, the embryonic notochord is gradually replaced by repeating ossified or chondrified structures called centra. When centra are present, they may constrict the notochord completely, forming spool- or hourglass-shaped structures, or they may simply form rings around the notochord. Most jawed vertebrates tend to have a one-to-one correspondence of vertebrae with myotomal segments, but several groups evolved multiple centra or vertebrae for each segment of the axial musculature, termed polyspondyly.

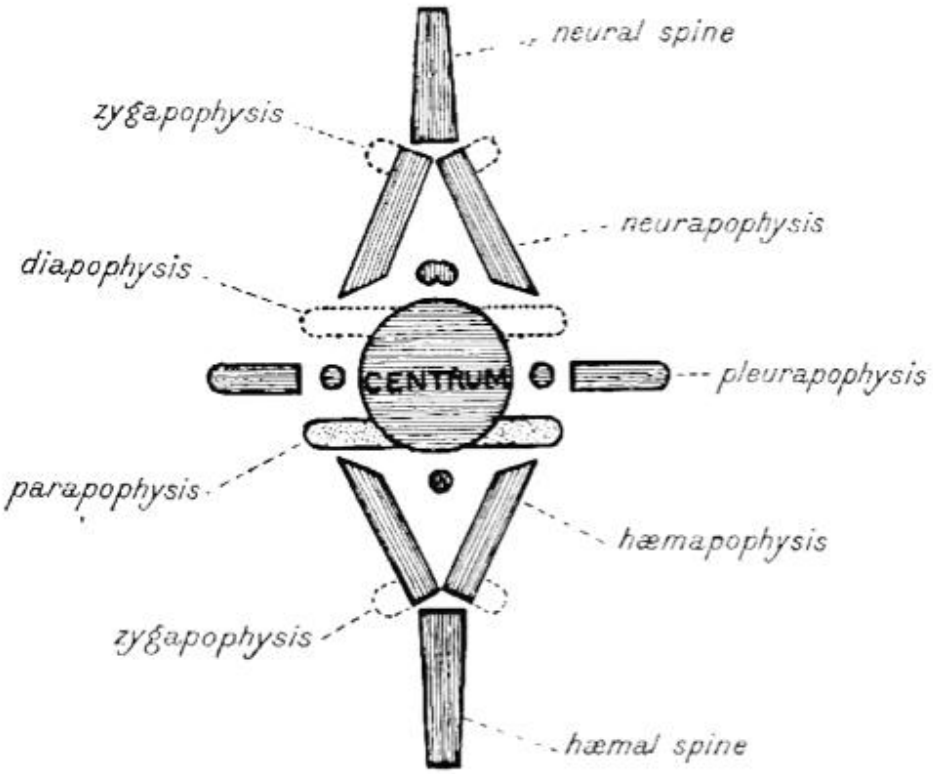

Figure 1.1. Owen's (1848) ideal, typical vertebra. Not all of the figured and labeled components

Figure 1.1 continued. are always present in actual vertebrae, but this figure represents those that possibly could exist in one vertebra.

In addition to morphology, vertebral tissue composition varies drastically. Teleost vertebrae generally consist of acellular bone, in which the bone-forming osteoblasts are not incorporated into the skeletal tissue after formation, but retreat laterally as they deposit bone matrix (Ekanayake and Hall, 1987; Hall, 2005). The vertebrae of chondrichthyans are primarily cartilaginous, with fibrous cartilage at the edges of the centra and densely calcified areolar cartilage in the center (Kemp and Westrin, 1979; Bordat, 1987; Dean and Summers, 2006). In addition to several kinds of cartilage, a perichondral bone-like tissue has been documented in the neural arches of the dogfish and the swell shark (Peignoux-Deville et al., 1982; Eames et al., 2007).

Vertebrate phylogeny and the origin of vertebrae

Crown vertebrates include all living jawed and jawless vertebrates, as well as several extinct clades. Within the jawed vertebrates, crown gnathostomes comprise chondrichthyans (cartilaginous fishes including chimaeras, sharks, skates, and rays) and osteichthyans (bony fishes including the sarcopterygians and the actinopterygians). The extinct 'acanthodians' fall within the gnathostome crown, on the chondrichthyan stem, and several grades of extinct 'placoderms', as well as the several groups of jawless fish, such as the cyclostomes (lampreys and hagfish) and the extinct clades Galeaspida and Osteostraci, group on the gnathostome stem (Figure 1.2).

Hypotheses of jawed vertebrate phylogenetic relationships have been changing drastically in recent years (Brazeau, 2009; Davis et al., 2012; Zhu et al., 2013; Dupret et al.,

2014; Giles et al., 2015). Among these changes, the once-monophyletic ‘placoderms’ are now recognized as a paraphyletic grade leading to crown gnathostomes, and the ‘acanthodians’ are consistently being recovered as paraphyletic stem chondrichthyans (Zhu et al., 2013; Dupret et al., 2014; Giles et al., 2015) (Figure 1.2). This phylogenetic rearrangement results in changes in our understanding of which stem gnathostomes are most closely related to the crown group and which characters and morphologies might be ancestral for gnathostomes. For example, the antiarchs, including *Bothriolepis* and *Yunnanolepis*, seem to be one of the earliest branches of jawed vertebrates, while arthrodires, including *Coccosteus* and *Incisoscutum*, and the Silurian *Entelognathus*, are more closely related to crown gnathostomes (Zhu et al., 2013) (Figure 1.2). Additionally, as new fossils have been discovered, the timing of the origin of modern gnathostome clades has shifted, with divergence estimates now placed firmly within the Silurian (Zhu et al., 2009; Brazeau and Friedman, 2015).

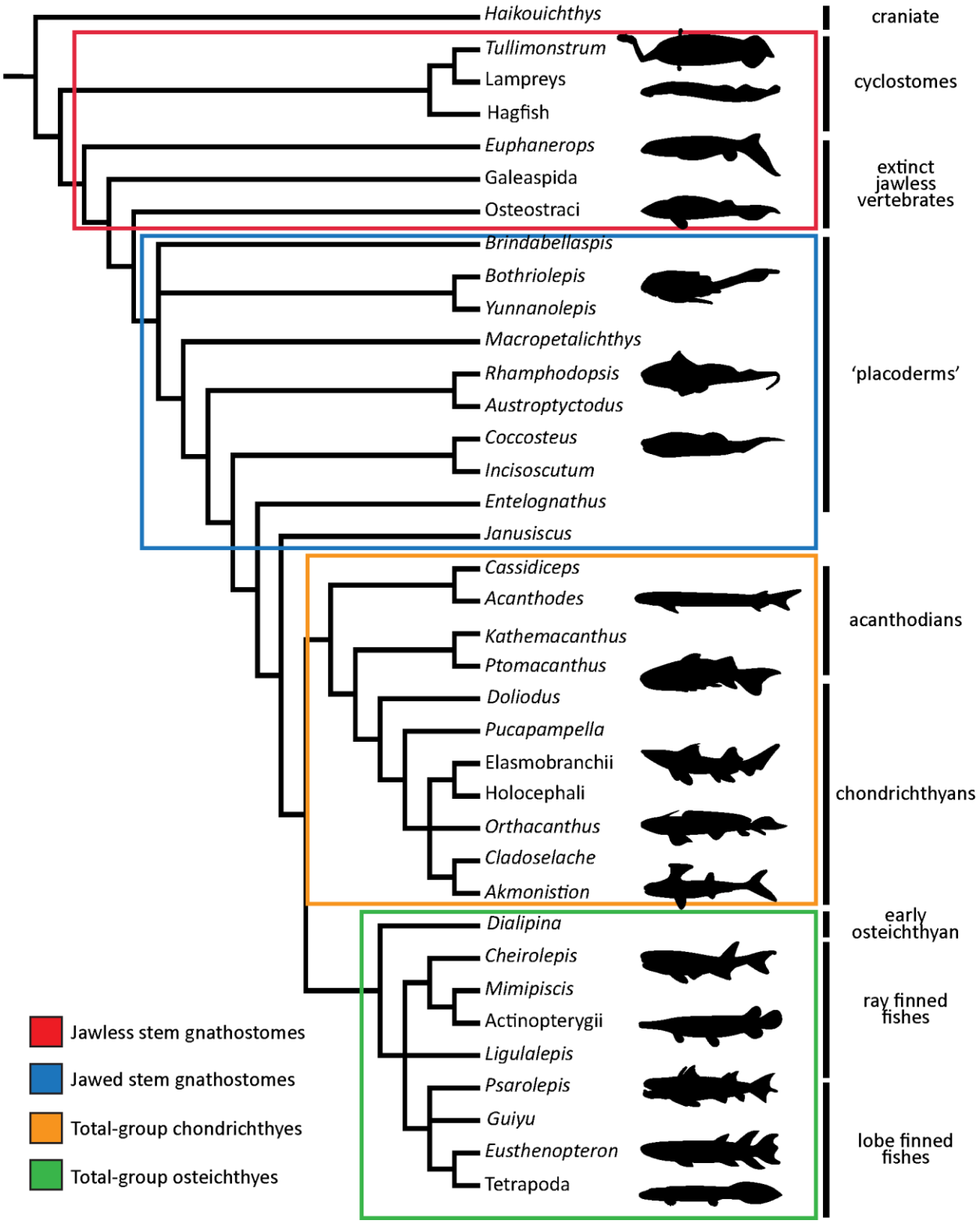

Figure 1.2. Simplified current hypothesis of early vertebrate relationships based on Sansom et al. (2013), Giles et al. (2015), and McCoy et al. (2016). Previously thought to be a monophyletic

Figure 1.2, continued. group, 'placoderms' are now considered to be paraphyletic grades leading to crown gnathostomes. All fish genera represented in this tree are extinct.

Conducting a new phylogenetic analysis of early gnathostomes is beyond the scope of this thesis. However, many different phylogenetic analyses have recovered similar successive groupings of placoderm grades leading to crown gnathostomes, but some of the resolution at the base of the split between osteichthyans and chondrichthyans seems premature. For instance, the character-taxon matrices used in many of these analyses under sample the chondrichthyan branches of the tree (Zhu et al., 2013; Giles et al., 2015), leading to greater resolution on the osteichthyan side, but an overall unbalanced analysis. Additionally, when new taxa are added to a character-taxon matrix, large sections of characters may remain uncoded for those taxa, even when the morphological data are available to fill in those gaps (e.g. Zhu et al. (2013)). When compared to one another, discrepancies in the results of many of the recent phylogenetic analyses, as well as large sections of the tree that lack resolution, highlight the instability of the base of the gnathostome tree. These include large polytomies within the 'acanthodians' as well as a lack of agreement as to both the most proximate outgroups to crown gnathostomes and the most basally branching members of the crown (Zhu et al., 2013; Dupret et al., 2014; Giles et al., 2015). These incongruences suggest that the relationships recovered are not well supported, and that one or two new taxa with an unconventional character set could collapse many of those nodes.

Vertebral mineralizations in some form are present in all known jawed vertebrate groups and some jawless vertebrates. Of the extant jawless vertebrates, lampreys and hagfish, only lampreys have obvious vertebral elements, possessing a series of irregularly patterned and often

asymmetrical neural arches that lack any ventral arches or centra (Figure 1.3 a,d,e) (Marinelli and Strenger, 1954; Janvier, 1996). For many years hagfish were thought to lack evidence of

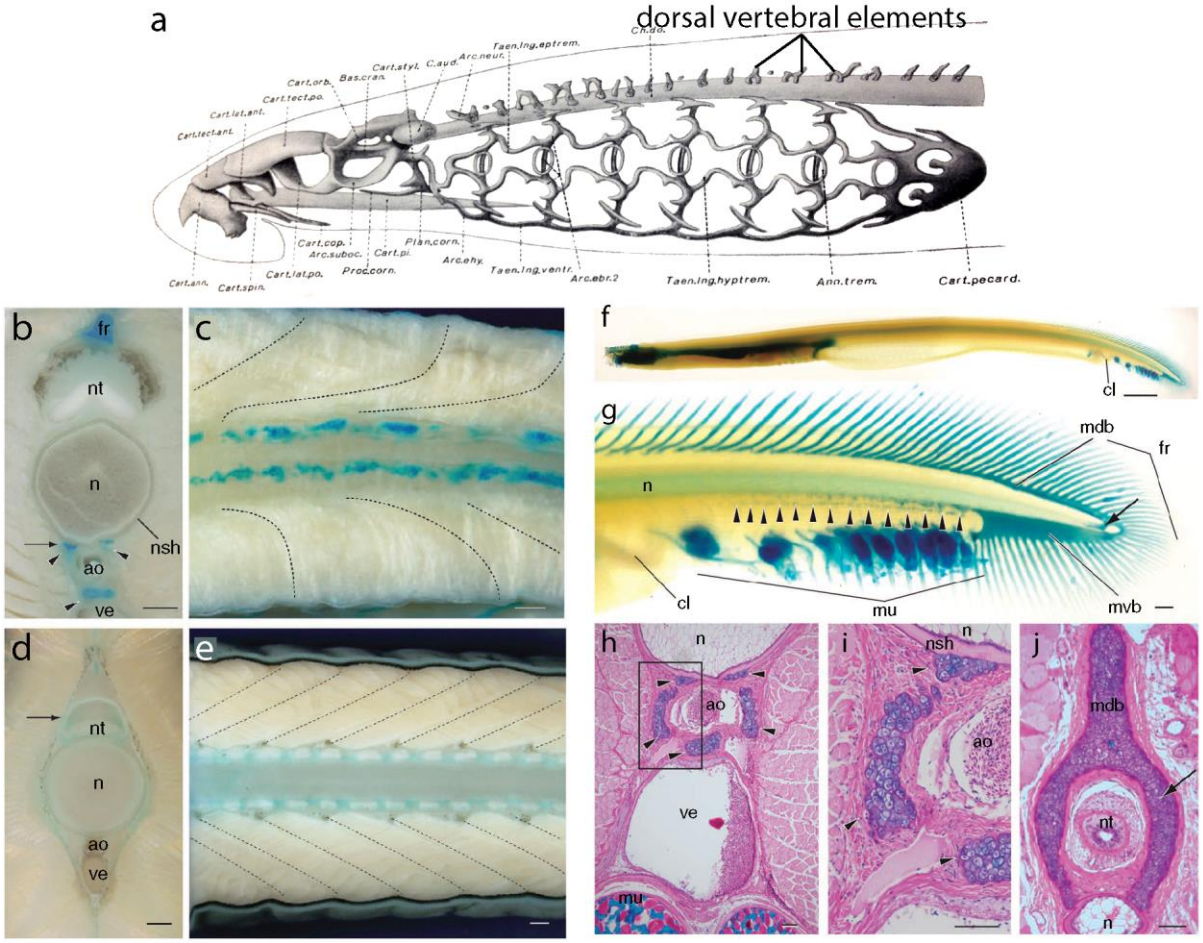

Figure 1.3. Vertebrae in jawless fishes. a, line drawing of the dorsal vertebral elements present in lampreys, from Marinelli and Strenger (1954), b-e) transverse and horizontal sections through the axial column in a hagfish; b,c, and a lamprey; d,e, from Ota et al. 2011, arrows indicate level of horizontal section; f, g, whole mount Alcian blue staining highlights the cartilaginous nodules present ventrally in the tail of the hagfish, *Eptatretus burgeri*; h-j, transverse sections through the tail of the hagfish stained with hematoxylin, eosin, and Alcian blue to show the morphology the ventral cartilaginous nodules, from Ota et al. 2011. Arrowheads indicate ventral cartilaginous nodules. ao, dorsal aorta; cl, cloaca; fr, fin ray; mdb, median dorsal bar; mu, mucus gland; mvb, median ventral bar; n, notochord; nsh, notochordal sheath; nt, neural tube; ve, vein.

vertebrae, with their axial support consisting of solely the notochord. However, Ota et al. (2011) discovered a series of small ventral cartilaginous nodules in the very posterior portion of the tail

of the hagfish *Eptatretus burgeri* (Figure 1.3 b,c,f-j) that express several genes in common with the jawed vertebrate sclerotome. Despite this suggestive genetic evidence, those nodules have little in common morphologically with the vertebrae of any other vertebrate. Additionally, they are positioned only ventral to the notochord, an arrangement that has not been seen in any other vertebrate, and the functional aspects of these data are unknown.

Evidence of vertebrae in jawless fishes is not limited to extant species. Up to ten variably-shaped structures are preserved around the notochord in fossils of the Early Cambrian chordate *Haikouichthys ercaicunensis* (Figure 1.4 a-d) (Shu et al., 2003). Also, an early jawless vertebrate from the Upper Devonian of Canada, *Euphanerops longus*, preserves both dorsal and ventral vertebral elements in its axial skeleton (Figure 1.4 e-g) (Janvier and Arsenault, 2007). The Mazon Creek (late Carboniferous) Tully monster, *Tullimonstrum gregarium,* which was recently designated a vertebrate based on the presence of a notochord, vertebral arches, and gill pouches, among others, seems to have repeated cartilaginous structures that correspond to each myomere, although these do not extend into the tail (Figure 1.4 h,i) (McCoy et al., 2016). The morphology of *Euphanerops* has been interpreted by some (e.g. Ota et al. 2011) as evidence that the ancestral vertebrate axial skeleton consisted of dorsal and ventral cartilages, and that the extant jawless fish lineages of lampreys and hagfish have lost their ventral and dorsal axial skeletons, respectively. Despite the hypothesized phylogenetic positions of *Euphanerops* as either sister to cyclostomes or sister to the rest of jawless plus jawed vertebrates (Sansom et al., 2013; Conway Morris and Caron, 2014), and of the Tully Monster as a lamprey (McCoy et al., 2016), they are known from the Upper Devonian and Carboniferous, respectively, by which time many other vertebrate lineages (with substantial vertebral skeletons) have not only evolved, but greatly diversified. It is possible that the morphologies of *Euphanerops*, *Eptatretus,* and

Tullimonstrum are apomorphic, and do not represent general or primitive conditions for the entire vertebrate clade, but rather have been independently derived. At this point, with so few data points for jawless vertebrates, drawing conclusions about the ancestral vertebrae for all of vertebrates should be done cautiously.

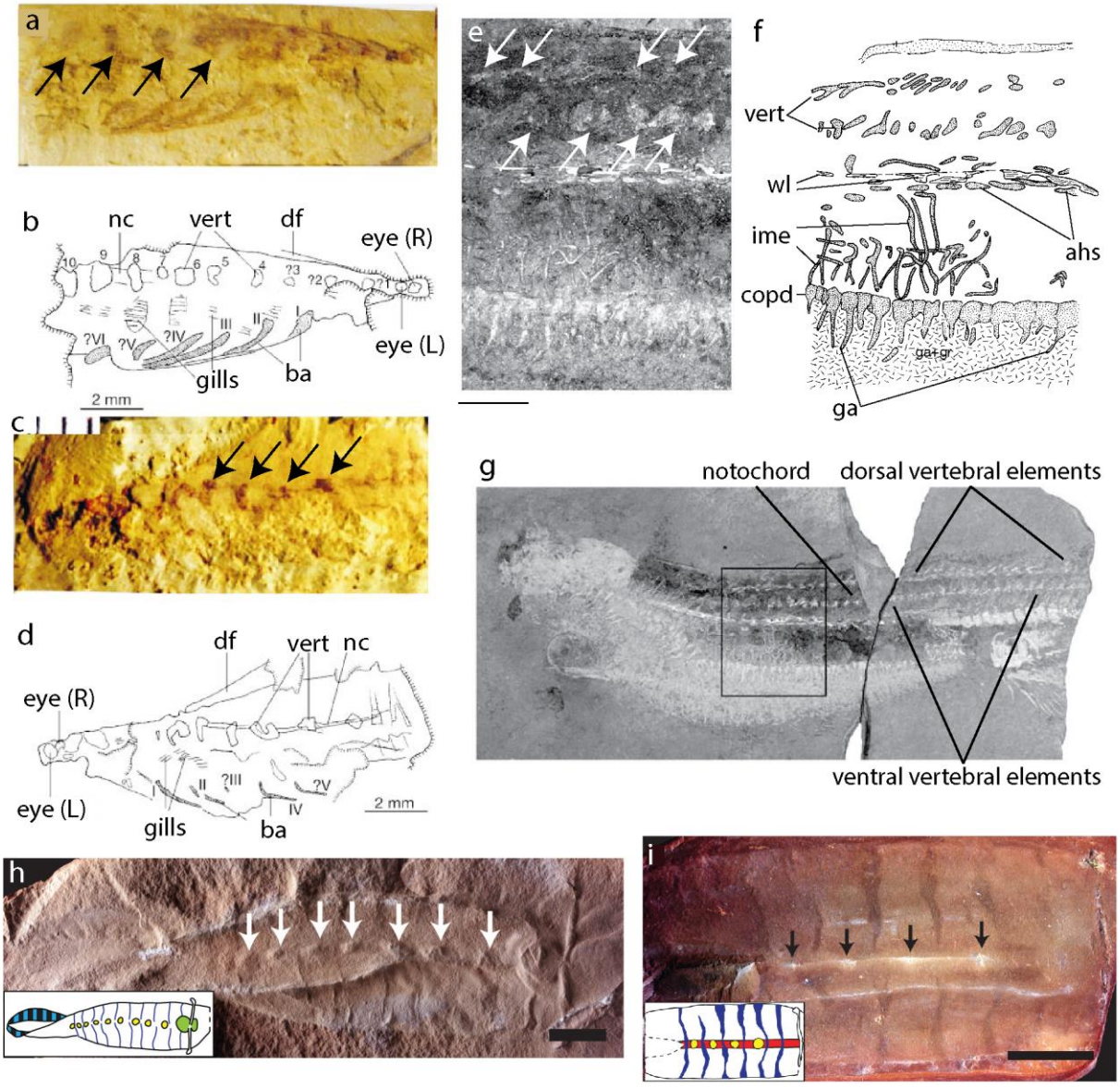

Figure 1.4. Cartilaginous nodules present in the axial columns of three jawless vertebrates. a-d, nodules that seem to surround the notochord in the Cambrian chordate *Haikouichthys*, indicated by black arrows (Shu et al., 2003); e-g, dorsal and ventral vertebral elements in the Devonian *Euphanerops*, indicated by white arrows (Janvier and Arsenault, 2007); and h-i cartilaginous

Figure 1.4 continued. nodules present in each precaudal body segment in the Carboniferous *Tullimonstrum* (McCoy et al., 2016).

Vertebral conditions in the earliest jawed vertebrates are slightly clearer than in their jawless cousins. Early members of all major vertebrate groups, including the grades of 'placoderms' leading to crown gnathostomes and early members of the Chondrichthyes and Osteichthyes themselves, lack centrum mineralization yet possess neural arches. Ventral arcualia, or hemal arches that are not just present in the caudal fin, are less common, but are present in some ptyctodonts (e.g. *Campbellodus* (Johanson et al., 2013) and *Materpiscis* (Long et al., 2008)) and arthrodires (e.g. *Compagopiscis* (Gardiner and Miles, 1994) and *Incisoscutum* (Johanson et al., 2013)). Throughout the Devonian Period, however, multiple gnathostome clades evolved repeated mineralizations that replaced the notochord to provide axial support. An analysis of the patterns of centrum evolution, along with many other aspects of the vertebral column, and the ancestral conditions in each major vertebrate group, make up a significant portion of this dissertation.

History of the study of vertebral column evolution in fishes

Schematic representations and discussions of general vertebral composition date back to the 1800s and focused on several vertebrate groups, including elasmobranchs, teleosts, and amniotes (Geoffroy-Saint-Hilaire, 1822; Owen, 1848; Balfour, 1878; Hasse, 1879; Klaatsch, 1893a; Gadow and Abbott, 1895). Although many early authors debated the correct terminology of the many vertebral components, only those of Owen (1848) and Gadow and Abbott (1895) have persisted into the present nomenclature.

Geoffroy-Saint-Hilaire (1822) described vertebral organization in the flatfish

Pleuronectes, and was one of the first to assign names to each of the vertebral components he discussed. Geoffroy-Saint-Hilaire's (1822) terminology consisted of a cycléal, the equivalent of the centrum, périals and épials as the neural arch and dorsal intercalary components, respectively, and paraals and cataals as the hemal arches and spines, and ventral intercalary elements. The cyclopérial corresponds to the neural arch and the metapérial to the neural spine, while the cycloparaal and metaparaal correspond to the hemal arch and spine. For those components that were endoskeletal, the prefix en- was added to each term, while pro- was added to dermal axial elements, like median fin rays.

Owen (1848) rejected Geoffory-Saint-Hilaire's vertebral terminology and instead presented a new terminology, noting that Geoffroy-Saint-Hilaire "had sometimes applied the same term to two distinct elements, and sometimes two distinct names to one and the same element" (Owen, 1848, p. 83). Owen's terminology, seen in Figure 1.1, included new terms that are now established in the literature: neurapophysis and hemapophysis for the neural and hemal arches, and additional specific names for each of the processes projecting laterally: the diapophysis, pleurapophysis, and parapophysis. Owen (1848) described the archetypal vertebra as one that possesses four canals around the centrum: the neural canal dorsally, the hemal canal ventrally, and laterally, canals are formed by the fusion of the pleurapophysis with either the diapophysis or parapophysis. The ideal, or perfect, vertebra is stated to often be found in the human thorax or in the necks of birds. This typical vertebra was crucial to Owen's vertebrate archetype because he reduced the entire vertebrate skeleton to a series of homologous vertebrae that were modified based on their location in the body (Owen, 1848).

Gadow and Abbott (1895) described yet another model and set of terms for the basic composition of fish vertebrae that became one of the most widely known and cited works on the

subject. This model, founded on histological observations of vertebral development in a number of chondrichthyan and osteichthyan embryos, proposes that each vertebral unit consists of four pairs of growth centers, called arcualia. These arcualia condense around, and proliferate dorsally and ventrally from, the notochord, forming the basidorsalia, basiventralia, interdorsalia, and interventralia (Figure 1.5). According to Gadow and Abbott (1895), the basidorsalia are produced by the dorsal halves of the sclerotomes, correspond to the neural arches, and were states to be present in all vertebrates.

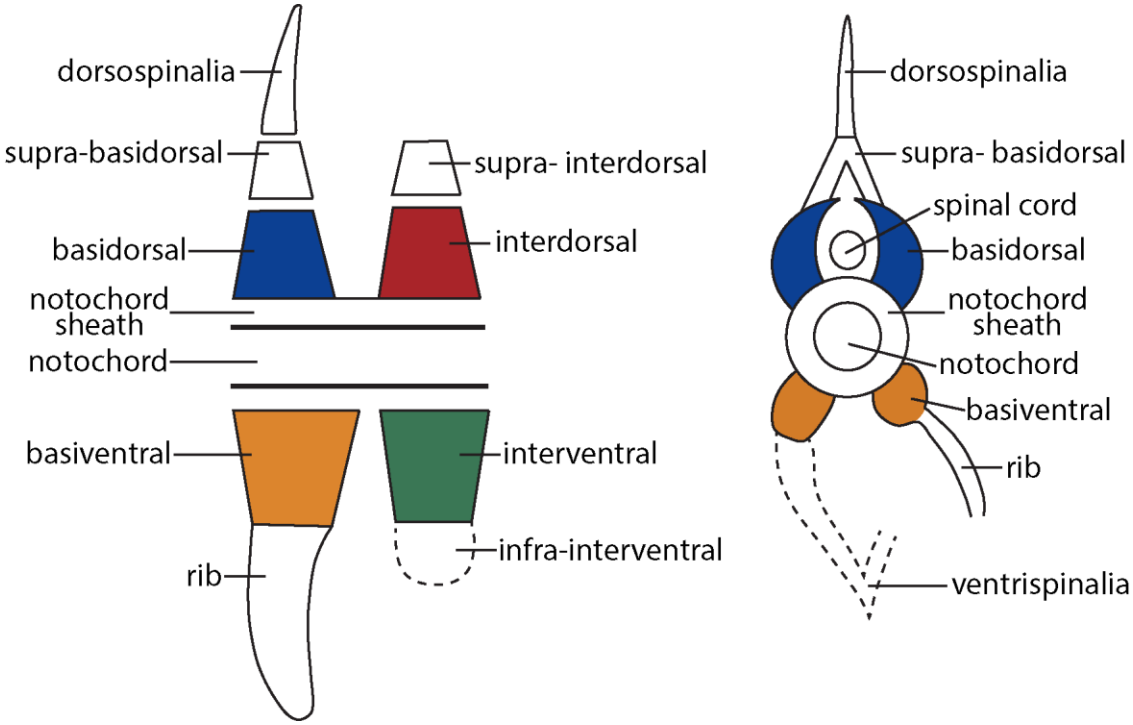

Figure 1.5. Reproductions of Gadow's (1933) ideal gnathostome vertebrae in sagittal and transverse views. The four pairs of embryonic growth centers are colored in blue, yellow, red, and green.

The interdorsalia, by contrast, form from the cell masses of the ventral halves of the sclerotome that have grown dorsally, and they are located between successive basidorsals. Gadow and Abbott (1895) named three additional dorsal components, the supra-basi-dorsals and

supra-inter-basals, grouped collectively as the supradorsalia, and the dorsospinalia. The supra-basi-dorsals are paired cartilages that extend from the top of the basidorsals, and can be seen in fish such as the gar, *Lepisosteus*, and the African lungfish, *Protopterus*. The supra-inter-basals are paired cartilages that are situated just posterior to the supra-basi-dorsals, as their interdorsal complement, and are present in young *Amia* (the bowfin), *Lepisosteus*, and *Protopterus*. Lastly, the dorsospinalia are midline extensions of the dorsalia, also known as neural spines or spinous processes.

The basiventralia develop from the ventral-ward extension of the ventral halves of the sclerotomes, and correspond to the hemal arches. The interventralia are situated between the basiventralia, form the ventral intercalary components, and are produced by the ventral extensions of the dorsal halves of the sclerotomes. In addition to the basiventrals and interventrals, Gadow and Abbott (1895) suggested that infraventralia were present in some elasmobranchs and chondrosteans as paired ventral structures, and ventrispinalia existed in many groups as unpaired extensions of the basiventrals.

Lastly, Gadow and Abbott (1895) identified two kinds of centra: chorda-centra, those formed by the notochord sheath, and arch-centra, those formed from skeletogenous extensions of the arches that surround the notochord. Chorda-centra were stated to form through an invasion of cartilaginous cells into the notochord sheath (supported by Klaatsch, 1893), and are present in elasmobranch fishes. The cartilaginous rings formed around the notochord in holocephalans are considered to be partial chorda-centra. Formation of arch-centra occurs when the skeletogenous cells condense on the outside of the notochord sheath, and have no interaction with the sheath at all. Gadow and Abbott (1895) state that arch-centra are present in gars, teleosts, amphibians, and amniotes.

In addition to the organization and terminology of the vertebral column in fishes, Gadow and Abbott (1895) and Gadow (1933) discussed the process of vertebral segmentation and the relationship of the somites to each basidorsal and basiventral vertebral component. Gadow and Abbott (1895) incorrectly suggest that somites are 'resegmented' into skleromeres, or vertebral segments composed of dorsal and ventral alternating halves. This notion of 'resegmentation' was proposed and discussed by several authors previously (Gegenbaur, 1862; Corning, 1891), but there was no consensus as to the details of the process. 'Resegmentation' in some form is now known to occur in representatives from several vertebrate clades, including amniotes (Bagnall et al., 1988), amphibians (Piekarski and Olsson, 2014), and bony fishes (Morin-Kensicki et al., 2002). Instead of dorsal and ventral segments, each vertebra is actually composed of the caudal half of the anterior sclerotome (the incipient basidorsal), along with the cranial half of the posterior sclerotome (the corresponding basiventral) (Bagnall et al., 1988; Aoyama and Asamoto, 2000).

Currently, the most commonly accepted vertebral terminology includes a combination of those proposed by both Owen (1848) and Gadow and Abbott (1895), with both neural arch/hemal arch and basidorsal/basiventral employed to describe the dorsal and ventral arch elements, despite the original developmental implications of basidorsal and basiventral. Intercalary elements describe interdorsals and interventrals, those repeating elements dorsal and ventral to the notochord, that alternate with the main arch elements. For the rest of this dissertation I will refer to dorsal arch elements as neural and interdorsal arches, and ventral elements as hemal and interventral arches, and will avoid using arcualia terminology.

Homology of vertebral elements

When reviewing the differences in both vertebral morphology and developmental mechanisms across vertebrate diversity, it becomes clear that no one pattern or process is general for all of jawed vertebrates. Instead, similar structures seem to have evolved multiple times within different gnathostome groups. The homology of many of these vertebral components has been hypothesized for several groups, including lungfishes and some actinopterygians, but no comprehensive or quantitative analysis has been undertaken to examine the evolutionary patterns of vertebrae across all gnathostome groups. Schaeffer (1967) discussed osteichthyan vertebrae, giving a brief overview of the variation in morphology present among non-teleost actinopterygians, teleosts, lungfish, and coelacanths, and remarking that "the arch components and the centra are clearly homologous throughout the Osteichthyes…" (p. 194). Miles (1970) reviewed all of the acanthodian vertebrae known at the time, describing in detail the vertebral morphology of *Acanthodes*, the most completely known acanthodian. Laerm focused on isolated osteichthyan groups, such as tetrapod-line sarcopterygians (1979a), chondrosteans (1979b), and neopterygians (1982), but never combined his analyses to consider actinopterygian axial evolution as a whole. Arratia et al. (2001) focused on dipnoan vertebrae, and discussed vertebral morphology in many other groups, including several other actinopterygian and sarcopterygian clades, but largely omitted both chondrichthyans and 'placoderms'. Arratia et al. (2001) also explored the homology of neural spines, supraneurals, and radials, suggesting sarcopterygians and actinopterygians evolved supraneurals independently. Centra are also concluded to be independently evolved in several major gnathostome groups, including chondrichthyans, dipnoans, tetrapod-line sarcopterygians, and actinopterygians, but this conclusion is arrived at qualitatively and based on morphological differences between the centra in these groups.

Vertebral development across gnathostomes

Like morphology, vertebral development is also diverse among extant gnathostome groups, but much of the current knowledge comes from historical, histological studies of vertebral development or from detailed developmental analyses in a small number of model organisms, namely chick and mouse (Christ and Wilting, 1992; Peters et al., 1999; Christ et al., 2000). Among teleost fishes, developmental studies have focused on the zebrafish, *Danio rerio*, the Japanese medaka, *Oryzias latipes*, and the Atlantic salmon, *Salmo salar* (Ekanayake and Hall, 1987; Morin-Kensicki et al., 2002; Grotmol et al., 2003; Fleming et al., 2004; Nordvik et al., 2005). This taxonomic sampling is reasonable, as all three species are spread out among the teleost tree. Zebrafish are cypriniforms, a group of ostariophysans (mostly freshwater fishes), salmon are part of a separate major radiation, the Euteleostei, and medaka are nested much further within the euteleosts, as part of the percomorph clade (Near et al., 2012).

Several key works from the 19th century contributed greatly to our current understanding of vertebral development. Hasse (1879) observed and figured vertebral development, with most of his embryonic material derived from sharks of the genus *Scyllium*. Additionally, Hasse (1879) described the morphological diversity of adult chondrichthyan vertebrae in great detail, sampling two holocephalan genera, close to 40 shark genera, and 10 genera of batoids, some of which included fossil material. Balfour's (1885) treatise on comparative embryology compared vertebral development across different groups, including chondrichthyans, osteichthyan fishes, and tetrapods. Gadow and Abbott (1895) provide one of the most complete descriptions of the notochord, its sheath, and the developmental processes that combine to create a vertebra. Included in these descriptions were histological studies of vertebral development and

organization in numerous species of fish, including elasmobranchs, holocephalans, lungfishes, and non-teleost actinopterygians, with a brief mention of cyclostomes. Some aspects of vertebral development seem to be conserved. In vertebrates, the core of the axial column is the notochord. The notochord begins as a flexible rod of vacuolated cells that develops a thickened sheath that differentiates into two layers, the elastica interna and elastica externa (Gadow and Abbott, 1895). The elastica interna thickens considerably during development and forms concentric rings of fibrous tissue, while the elastica externa remains thin and refracting.

Once the notochord sheath has thickened and divided into several layers, vertebral development commences with cells migrating from the ventral portion of the somite, the sclerotome, to encircle the notochord, where they condense to form proliferating centers that develop into the neural and hemal arches (Figure 1.6) (Gadow and Abbott, 1895). The somites form from presomitic mesoderm that has segmented in the craniocaudal direction into cellular blocks that extend the length of the body axis on either side of the notochord and neural tube (Christ et al., 2004). It is this segmentation that seems to guide the development of other metamerically-arranged structures such as the vertebrae, ribs, and muscle blocks. Subsequent to segmentation, the somites undergo an epithelial to mesenchymal transition (EMT), forming the sclerotomal and dermomyotomal subdivisions. After the cells in the ventral somite undergo this EMT they express the sclerotome markers *Pax1* and *Pax9* (Christ et al., 2004).These somitic subdivisions, the sclerotome and dermomyotome, go on to give rise to the vertebrae and ribs, and the muscles and dermis, respectively.

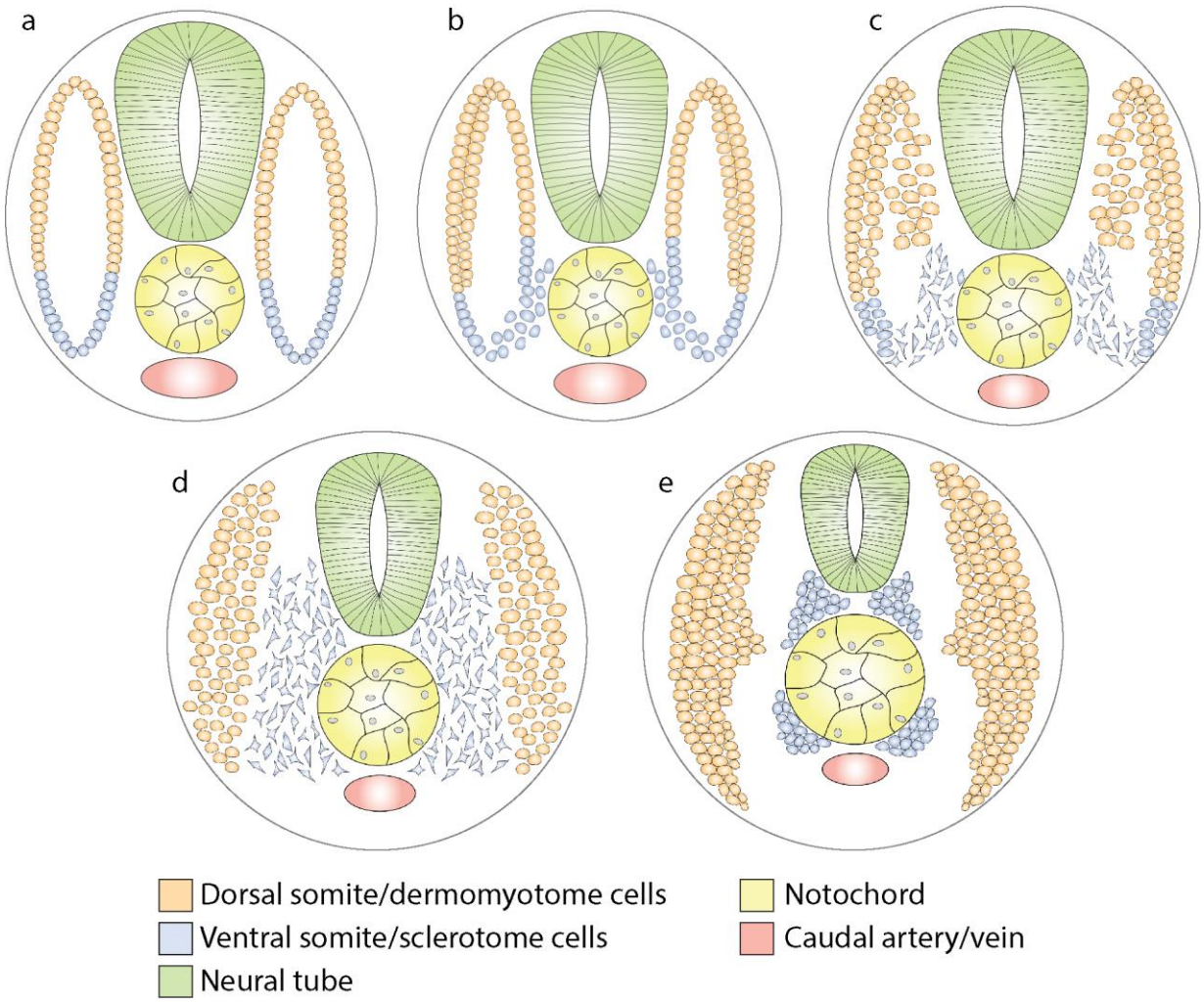

Figure 1.6. Schematic transverse sections through the caudal region of a hypothetical vertebrate, showing the early process of sclerotome migration and condensation of mesenchyme around the notochord. a, Somites are present as epithelial blocks of paraxial mesoderm. Dorsal somites, which go on to form the dermomyotomes, are colored orange and ventral somites, which go on to form the sclerotome, are colored blue; b, the ventral somites undergo an epithelial to mesenchymal transition and begin to migrate toward the notochord and neural tube; c, d, The sclerotomal cells continue to proliferate and migrated; e, The sclerotomal cells condense around the notochord and begin the process of vertebral development.

The involvement of numerous genes has been documented in sclerotome differentiation and vertebral development. *Pax1* and *Pax9* are expressed in the ventral portion of the somite in many different vertebrates, marking the sclerotomal cells as they go through an EMT and begin to migrate towards the notochord (Peters et al., 1999; Christ et al., 2004; Fleming et al., 2004). Additionally, *Bapx1* is activated by *Pax1* and *Pax9* and helps to initiate sclerotome differentiation in mouse (Peters et al., 1999; Rodrigo et al., 2003). *Twist* is expressed in the sclerotome and is considered a sclerotome marker, but also is expressed in other tissues such as the neural crest and trunk mesoderm (Barnes and Firulli, 2009; Yeo et al., 2009). Sclerotome initiation is activated by *Shh* and *Noggin,* genes that are both expressed in the notochord during sclerotome formation (Fan and Tessier-Lavigne, 1994; McMahon et al., 1998). Specifically, in *Noggin* mutants, there is a reduction in the number of sclerotomal cells and *Pax1* expression is delayed and decreased (McMahon et al., 1998).

Once the sclerotome has migrated, and has begun to condense as vertebral anlagen, a different set of genes becomes activated to induce chondrogenesis or osteogenesis. *Pax1* and *Pax9* have been shown to regulate *NK3.2* in mice (Rodrigo et al., 2003), which in turn induces expression of the chondrocyte marker *Sox9* (Zeng et al., 2002) and *Runx2,* a gene essential for osteoblast generation (Lengner et al., 2005). During cartilage development, expression of *Sox9* precedes collagen genes such as *Col2a1* and *Col10a1,* or osteoblast markers such as *Sp7*/*Osterix* (Zhao et al., 1997; Nakashima et al., 2002; Mori-Akiyama et al., 2003; Avaron et al., 2006). In elasmobranchs, *Col2a1* is expressed in the developing centrum and interior tissue of the neural arches, while *Col1a1*and *Col1a2* are expressed in the perichondrium surrounding the neural arches (Enault et al., 2015). In teleost fishes, *Osterix,* which is essential for osteoblast

differentiation and bone formation, is expressed in both the developing centra (at 6 days post fertilization) and neural and hemal arches (at 11 days post fertilization) (Renn and Winkler, 2009).

When present, centra can develop either inside the notochord sheath, as chordacentra, or outside, as arcocentra, as discussed above. However, the actual cellular contribution of the notochord in this process seems to vary among taxa. Centrum development has been documented in only a small number of vertebrates, including chicken, mouse, and several species of teleost. In chick and mouse, both arches and centra are derived entirely from somite cells (Bagnall et al., 1988; Peters et al., 1999; Christ et al., 2000), but teleost fish employ several modes of centrum development. Zebrafish centra form directly from a secretion of bone matrix from within the notochord, with no apparent contribution from the somites and no cartilaginous precursors (Fleming et al., 2004). Conversely, in medaka, centrum bone forms from mesenchymal cells that condense around the notochord (Ekanayake and Hall, 1987). Salmon seem to combine the two processes, with centra developing from a layer of bone deposited within the notochord sheath, as well as sclerotome-derived mesenchyme condensing on the outer surface of the sheath (Grotmol et al., 2003, 2005). Additionally, in salmon, segmented notochordal constrictions formed by a layer of "chordoblast" cells may help to direct centrum formation. Lineage tracing data for vertebral development in the sister group of the osteichthyans, the chondrichthyans, are lacking, with all evidence to date coming from descriptive histology. Both Klaatsch (1893a) and Gadow and Abbott (1895) reported that arches and centra form from sclerotomal cells in the elasmobranchs, and independently concluded based on histological evidence that sclerotomal cells invade the notochord sheath to form centra. However, no tests of this hypothesis have since been carried out using modern developmental techniques such as fate mapping and computed

tomography.

Despite the rich historical literature on vertebral development, little work has been done since the late 1800s and early 1900s to elucidate the timing and patterns of vertebral development in cartilaginous fishes. The most recent works include those of Balfour (1878), Hasse (1879), and Gadow and Abbott (1895). These early descriptions are extremely useful, but the embryonic series presented are often incomplete, including no more than a handful of embryos for each taxon, and skipping large portions of developmental time. Additionally, embryonic descriptions are available for several shark genera (e.g., *Squalus* and *Scyllium*), but coverage of skate and ray development in general lags behind the sharks. This taxonomic coverage is not sufficient to infer generalizable developmental patterns across elasmobranchs. Many of the detailed experimental analyses that have been undertaken have focused on a small number of bony vertebrates, providing a depth of information, but not covering the breadth of vertebrate diversity. This approach is problematic because the potential developmental diversity present across vertebrate groups may be overlooked. Results collected from these few model organisms are often used extrapolated to, and generalized for, all vertebrates, when the processes they document may actually be specific to a single clade. Additionally, variation in vertebral morphology across both extinct and extant vertebrates is poorly documented, and patterns of character change in the axial columns of both living and fossil fishes have not been studied comprehensively across the breadth of jawed vertebrate diversity.

Gadow and Abbott's (1895) work remains the standard, authoritative text on vertebral evolution, and is still used widely in textbooks, and in paleontological and developmental research (Grande and Bemis, 1998; Arratia et al., 2001; Bird and Mabee, 2003; Kardong, 2009). The 'Arcualia Theory' suggests that the four sclerotomally-derived growth centers (basidorsals,

basiventrals, interdorsals, and interventrals) are modified in both position and shape throughout vertebrate diversity to form the vertebral structures seen in all major vertebrate clades. This mode of organization has been proven inapplicable for many tetrapod groups. In fact Gadow's (1933) book detailing the application of the arcualia theory to tetrapods was subsequently scrutinized and rejected by Williams (1959) on the grounds that several of the growth centers are not present in many tetrapod groups, and centra develop as autonomous structures not related to the arches. The arcualia model has not been adequately evaluated in a similar fashion for chondrichthyan and osteichthyan fishes.

Summary of Research

The focus of this dissertation is on analyzing the evolution and development of the gnathostome axial column, using quantitative methods and modern developmental techniques. Cartilaginous fishes are key to this analysis because the lack of experimental data and taxonomic diversity present in the existing literature limit the broad-scale conclusions that can be drawn about independent evolution and ancestral developmental processes. The aims of this dissertation are to reexamine and test accepted hypotheses of vertebral origin, to estimate primitive conditions, including morphologies and developmental processes, for the gnathostome axial skeleton, and to determine whether the axial skeleton is formed in the same way across the gnathostome tree. Chapter two provides both a descriptive and quantitative analysis of vertebral evolution to determine how much independent evolution has occurred in the axial skeleton of jawed vertebrates. This analysis includes more genera of fossil and living fish than any previous study and examines the distribution of many different morphological characters in a time-scaled phylogenetic context. Chapter three contributes a characterization of vertebral development in

the little skate, *Leucoraja erinacea*, using histological and microtomographic methods. These techniques allow for the visualization of embryonic anatomy in cross section, as well as in three dimensions. In chapter four I present experimental data testing the embryological origin of the centra and arches in the little skate. These fate mapping experiments test the hypothesis that vertebrae are built by the same embryonic tissues in all vertebrate groups. Chapter five evaluates the evidence of the homoplasy of gnathostome centra in both a phylogenetic and molecular context, proposes future experiments to complement those discussed here, and reexamines Gadow and Abbott's (1895) hypothesis of vertebral construction for non-tetrapod gnathostomes. All work presented here is my own unless cited otherwise.

Chapter 2: Independent evolution in the axial column of jawed vertebrates

Summary

Vertebrae have traditionally been used as the defining feature of vertebrates: they diagnose the clade and provide structural support central to the vertebrate skeleton. Vertebral morphologies play pivotal roles in systematics and functional anatomy, and vary dramatically across gnathostome taxa and geologic time. The earliest vertebral skeletons found in fossil vertebrates consist solely of a series of neural arches articulating to a persistent notochord. However, by the first appearance of the major gnathostome clades (elasmobranchs, holocephalans, actinopterygians, sarcopterygians) vertebral columns included additional components and disparate morphologies. Here I use new methods and time-scaled phylogenetic hypotheses to analyze the evolutionary diversification of this fundamental structure. To investigate the phylogenetic and ontogenetic histories of individual vertebral components I compiled a character matrix focused on the vertebral anatomy of over 230 genera of fossil and living fish, using both historical literature and personal observation. I combined hypotheses of relationships representing gnathostome crown and stem clades to build a supertree that I then scaled to geologic time using reference dates from the included fossils. I then implemented several methods of ancestral state reconstruction to estimate the number of times vertebral structures and morphologies, including centra, anterior vertebral fusions, and polyspondyly evolved independently within gnathostomes. Methods used include maximum parsimony, the Mk1 model of maximum likelihood, and the threshold model incorporating Bayesian inference. My results indicate that centra have evolved independently at least ten times, while series of

fused vertebrae have each evolved at least five times, and polyspondyly has up to eight independent originations. Likelihood values and posterior probabilities were higher within gnathostome subgroups, while nodes representing the split between osteichthyans and chondrichthyans, and sarcopterygians and actinopterygians, were less certain. The diversity of vertebral components and homoplasy in this system indicates that vertebrae are not composed of single units, but rather consist of separate arch and centrum components with independent evolutionary trajectories. These independent originations raise questions about the evolutionary advantages of evolving centra and the diversity of developmental mechanisms employed.

Introduction

To reconstruct the history of vertebral evolution and test hypotheses of homology in the vertebral columns of gnathostomes, a broad sample of the variation in vertebral morphology present across the gnathostome tree is necessary. Vertebrae in all gnathostomes include a series of neural arches rostrally and hemal arches caudally, but beyond these features, vertebrae are quite variable. The embryonic notochord may persist into adulthood or it may be surrounded or replaced altogether by centra. In addition to one set of neural arches for each myotomal segment, a second set of intercalary arches, or small intercalary plates, is present in many taxa. Neural spines can be fused to the neural arches or separate, segmented into many smaller components. Within the caudal region, several gnathostome groups have developed polyspondyly, in which centra or entire vertebrae are duplicated within each myotomal segment.

In this chapter I will focus on investigating this variation in vertebral morphology in the major groups of non-tetrapod gnathostomes, which include the various grades of ‘placoderms’ (arthrodires, antiarchs, phyllolepids, ptyctodonts, and rhenanids) that branch as successive sister

groups to the rest of gnathostomes and the 'acanthodians', early gnathostomes that form a paraphyletic cloud at the base of the chondrichthyans (see Figure 1.2). Within the chondrichthyans I will discuss vertebral morphology in elasmobranchs and holocephalans. Here I use elasmobranchs to include sharks, skates, and rays (neoselachians), along with extinct clades like the hybodonts, and stem chondrichthyans to refer to the symmoriids and early sharks such as *Pucapampella* and *Doliodus*. The holocephalans include the extant chimaeras and additional early representatives. On the osteichthyan side of the gnathostome crown the sarcopterygians include the lungfish and their stem relatives, the porolepiforms, the coelacanths, and the tetrapodomorphs. Actinopterygians are represented in this chapter by the teleosts, holosteans (bowfins and gars plus their extinct relatives), neopterygians (teleosts plus holosteans), chondrosteans (sturgeon and paddlefish), *Polypterus*, and a number of early fossils.

As discussed in chapter one, hypotheses of early gnathostome relationships are currently undergoing large-scale revision: 'placoderms' are now considered to be successive grades of stem gnathostomes instead of a separate clade of early gnathostomes, and 'acanthodians' have been recovered as paraphyletic stem chondrichthyans in multiple analyses (Brazeau, 2009; Davis et al., 2012; Zhu et al., 2013; Giles et al., 2015; Long et al., 2015). However, the optimization of certain anatomical features, such as the presence and homology of claspers in 'placoderms' and chondrichthyans, may yet influence these accepted relationships (see review by Brazeau and Friedman, 2015). Despite recent advances in elucidating gnathostome relationships, unevenness in gnathostome taxon sampling remains. The sarcopterygian portion of the tree benefits from more phylogenetic analyses and greater resolution, reflecting a concerted research emphasis on identifying and describing close tetrapod relatives. Early chondrichthyans and actinopterygians have suffered from a paucity of phylogenetic data, with few early chondrichthyan-focused

phylogenies published in recent years, apart from the taxon-poor analysis of Pradel et al. (2011), and with few trees sampling the full diversity of the early Devonian and Carboniferous actinopterygians. Despite these uncertainties, the new trees provide an opportunity to test previously-proposed models of vertebral evolution against new interpretations of jawed vertebrate relationships to determine how this foundational structure came to be as morphologically diverse as it is today.

Variability in vertebral columns of fishes

Variation in vertebral morphology and in centrum construction have been documented for many groups of gnathostomes. Centra come in a variety of forms, from mineralized rings of calcified cartilage or bone around a persistent notochord, to heavily calcified discs that constrict the notochord completely. Centra have been divided into four categories based on their developmental construction. Arcocentra develop when cartilage from the arch bases surrounds the notochord and ossifies, holocentra are formed by proliferating chondrocytes that surround the notochord and are later replaced by bone, autocentra ossify directly, with no cartilaginous precursors, and chordacentra form when cartilage from the arches invades the fibrous notochord sheath and mineralizes (Arratia et al., 2001). All categories of centra, and associated kinds of centrum construction, can be found in different actinopterygian groups. As yet, it is unclear whether they represent independent originations or parts of a continuum of centrum variation.

Fusions of the anterior region of the vertebral column can form a synarcual, in which vertebral units are fused into a single continuous structure that can be functionally linked to a skeletal feature such as the pectoral girdle or dorsal fins (Johanson et al., 2013), or a Weberian apparatus, in which the anterior vertebrae function to transmit sound from the swim bladder to

the otic region (Coburn and Grubach, 1998; Ladich, 2001). Several patterns of polyspondyly have been observed: when caudal vertebrae develop two centra or two full vertebrae for each myotomal segment (diplospondyly) or when the number of centra for each body segment is greater than two throughout the vertebral column (polyspondyly).

The axial skeleton in 'placoderms' is insubstantial, consisting in most genera of a series of paired neural, and often hemal, arches and in some instances a synarcual (known in several arthrodires, ptyctodonts, and phyllolepids). As such, there have been very few papers discussing vertebral evolution within this gnathostome clade or grade. Johanson et al. (2010, 2013) described the anterior fusion of the synarcual in numerous 'placoderm' taxa, such as *Cowralepis, Materpiscis,* and *Jagorina*. Placoderm preservation often consists solely of the dermal head and trunk shields, but the post-cranial axial skeleton has been preserved in arthrodires such as *Coccosteus, Plourdosteus, Incisoscutum,* ptyctodonts including *Austroptyctodus* and *Campbellodus,* and the rhenanids *Gemuendina* and *Jagorina*. Usefully, the 'placoderms' included in many of the recent early gnathostome phylogenetic analyses (e.g. Long et al., 2015) actually have substantially preserved axial remains.

Acanthodian fishes are notoriously poorly preserved, with fossil skeletons often consisting of a flattened skull and blanket of body scales. There are, however, several 'acanthodians' known to preserve at least some portions of the axial skeleton, including *Acanthodes, Kathemacanthus, Ischnacanthus, Parexus* and *Diplacanthus* (Miles, 1970; Gagnier and Wilson, 1996). Significantly, in all of these taxa the vertebrae are represented by paired neural and hemal arches that bracket a persistent notochord, just as in the majority of 'placoderms'.

Centra in actinopterygians are likely primitively absent, and the early history of

actinopterygian centra is difficult to establish because the stems of extant subgroups are barely populated before the Mesozoic. The earliest taxa in the group, Middle to Upper Devonian genera such as *Mimipiscis* and *Moythomasia*, generally lack centra, but centra are known from many more recent taxa throughout the clade, including *Tarrasius* (Carboniferous), *Australosomus* (Triassic), *Hulettia* (Permo-Triassic), and *Ionoscopus* (Triassic). Laerm (1979a, 1982) examined vertebrae from a number of extant actinopterygian subgroups, including *Acipenser*, *Polyodon*, *Polypterus*, *Birgeria* (Triassic), *Amia*, *Lepisosteus*, and the Cretaceous fossil amiid *Caturus*, and concluded that when centra are present they are often built in different ways. Within neopterygians, vertebral development has been studied in *Amia*, *Lepisosteus*, and several species of teleost, and centra in each of these groups are constructed differently (Balfour and Parker, 1882; Hay, 1895; Fleming et al., 2004; Nordvik et al., 2005). Centra in *Amia* originate with expanding arch bases that encircle the notochord, while *Lepisosteus* centra begin to mineralize within a perichordal tube of cartilage that surrounds the notochord. In *Polypterus* centra form independently of the cartilaginous anlagen of the arches, through intramembranous ossification around the notochord (Bartsch and Gemballa, 1992). Early fossil neopterygians also show variations in centrum structure including inner and outer layers of bone (*Ophiopsis*), caudal diplospondyly (*Macrepistius*), and the presence of hemicentra (*Caturus*) (Laerm, 1982).

Unlike the actinopterygians, many early sarcopterygian vertebral columns are well known, including examples from Devonian lungfishes *Uranolophus* and *Griphognathus*, Devonian coelacanths *Miguashaia* and *Holopterygius*, and the tetrapodomorphs *Eusthenopteron* and *Osteolepis*. Arratia et al. (2001) conducted a thorough synthesis of vertebral evolution in sarcopterygian fishes. This includes extensive descriptions of extant lungfish vertebrae and selected comparisons to other gnathostomes, most of them osteichthyans. Extant lungfish and

most fossil lungfish clearly lack vertebral centra, but several Paleozoic taxa are known with fully mineralized centra. Additionally, complicated ring centra that consist of a dorsal component, the pleurocentrum and a ventral ring, the intercentrum, are found in the Devonian porolepiform (stem lungfish) *Glyptolepis*. Tetrapod-line sarcopterygians, including *Eusthenopteron* and *Osteolepis*, as well as the earliest tetrapods themselves, also preserve two-part "rhachitomous" ring centra.

Chondrichthyan vertebrae have been studied by Gadow and Abbott (1895), Ridewood (1899, 1921), Daniel (1922), and Goodrich (1930), among others. These works focused on vertebral development, but did not discuss evolutionary patterns or fossil forms throughout the elasmobranchs and holocephalans because few completely preserved fossils were known at this point. Many of the earliest chondrichthyan fossils (*Doliodus* and *Pucapampella*) do not preserve vertebral elements (Maisey, 2001; Miller et al., 2003), but some Devonian and several Carboniferous fossils show complete axial preservation. These earliest chondrichthyans lack centra, suggesting that an absence of centra was ancestral for chondrichthyans. Several early holocephalans (*Chondrenchelys* and *Harpagofututor*), as well as extant chimaeras, have ring centra (Lund, 1982; Didier, 1995; Finarelli and Coates, 2014), while elasmobranchs develop full centra (Cappetta, 1987), indicating that centra may have evolved independently twice in chondrichthyans. Few phylogenetic analyses have focused on early chondrichthyan relationships, and as such there is a paucity of hypotheses of chondrichthyan relationships. Therefore, aside from descriptions of axial morphology in selected chondrichthyan fossils, no analyses of the evolutionary patterns of chondrichthyan vertebrae exist.

How much independent vertebral evolution has occurred across gnathostomes?

This variation in centrum morphology and construction across the gnathostome tree and absences in early members of most major clades raises questions about homoplasy. Independent origins of centra have been proposed for several osteichthyan taxa, including actinopterygians (e.g. *Polypterus*, *Australosomus*, and *Lepisosteus*) and lungfish (*Griphognathus* and *Soederberghia*) (Schaeffer, 1967a; Laerm, 1976, 1979a, 1979b, 1982; Arratia et al., 2001), but no comprehensive or quantitative analysis has examined the evolutionary patterns of vertebrae across all gnathostome groups. Additionally, the last thorough studies of chondrichthyan vertebral evolution date back to Gadow and Abbott (1895) and Goodrich (1930). Gardiner (1983) provides a thorough overview of vertebral development throughout gnathostomes and highlights some of the variation in morphology seen across each major group. Included in these highlights are discussions of evolutionary patterns for non-tetrapod gnathostomes, but none of these are placed in a phylogenetic context. Within these qualitative discussions of vertebral evolution (Laerm, 1979a, 1982; Gardiner, 1983; Arratia et al., 2001), there is little use of statistical methods to study macroevolutionary patterns in a quantitative fashion. Since these influential works, numerous statistical methods and evolutionary software packages have been developed to study the patterns of character evolution, making a quantitative analysis of vertebral evolution possible.

Here I utilize the new phylogenetic trees available for early gnathostomes, as well as statistical methods of inferring ancestral conditions, to test the hypotheses of Laerm (1979a, 1982), Arratia et al. (2001), and Gardiner (1983) that centra are independently derived in many groups. In addition to the centrum, I also assess independent evolution in other portions of the axial column across evolutionary time. I focus on the most functionally advantageous vertebral

characters, including whether anterior vertebral segments have fused to form a synarcual or a Weberian apparatus, the presence and degree of polyspondyly, whether the neural arches are paired or fused, and if intercalary elements are present. I use parsimony-based ancestral state reconstructions to obtain an estimate of the number of independent originations of centra and other vertebral modifications across gnathostomes. I also performed Bayesian inference- and maximum likelihood-based analyses to determine how different models of evolution and prior probabilities impact the inferred ancestral conditions.

Materials and Methods

Taxon Sampling

Ancestral state reconstruction analyses rely on input data from reliable phylogenetic hypotheses of relationships. The taxa I examined were either present in one of the source phylogenies, or represented a group that was not included in a previous analysis, but still provided valuable anatomical information. The clades and taxa that were incorporated into this analysis from source trees include: antiarch 'placoderms', ptyctodont 'placoderms', arthrodire 'placoderms', and rhenanid 'placoderms'; the earliest known chondrichthyans (*Doliodus* and *Pucapampella*); ctenacanths and hybodonts (stem elasmobranchs) and symmoriids (stem chondrichthyans); extant elasmobranchs including batoids and selachians; both early and extant holocephalans; climatiiform and acanthodiform 'acanthodians'; early osteichthyans such as *Janusiscus* and *Ligulalepis*; non-teleost actinopterygians such as *Polypterus*, *Moythomasia*, and *Australosomus*; several representative teleosts; Devonian, ceratodontid, and lepidosirenid lungfishes; both early and late coelacanths; and tetrapod-line sarcopterygians. I collected vertebral data at the genus level. An additional 22 fossil genera with well-preserved axial

columns were examined and included to populate sections of the supertree that were lacking in representation (see section on phylogenetic comparative methods). These taxa did not alter the shape of the tree, but served only to provide necessary vertebral data.

Vertebral Character Data

Data were collected for five characters from specimens described and figured in the literature and from examining specimens in museum collections housed at the Field Museum of Natural History (FMNH), Carnegie Museum of Natural History (CM), Academy of Natural Sciences of Drexel University (ANSP), American Museum of Natural History (AMNH), National Museum of Scotland (NMS), Natural History Museum in London (NHM), Museum National d'Histoire Naturelle (MNHN), Museum Victoria (MV), and the Parc National de Miguasha (MHNM) (see Appendix 1 for a table of specimens examined and literature sources). Characters were only scored when the anatomy in each taxon was unambiguously preserved or discussed in a published study. For example, if the entire body of a fossil was well preserved, with some axial elements visible, it was coded into the character matrix. Fossils consisting of only a head and some isolated postcranial remains were not included unless centra or other parts of the axial skeleton were able to be clearly interpreted. Each specimen was examined and photographed using a Canon EOS 20D on a black velvet background.

Computed Tomography

CT scans of the early actinopterygian *Mesopoma* (NHM P11656) and stem elasmobranch *Tristychius* (NMS 1972.27.481D, E) were obtained from the University of Texas Computed

Tomography Facility (UTCT) on a North Star Imaging, Inc. ACTIS scanner. A second scan of *Mesopoma* and a scan of another early actinopterygian, *Moythomasia* (MV 222915), as well as microCT scans of the little skate *Leucoraja erinacea* were obtained in the Department of Organismal Biology and Anatomy at the University of Chicago, using a GE v|tome|x Phoenix CT scanner. A scan of the madtom catfish *Noturus eleutherus* was obtained on a SkyScan 1176 CT scanner at Pennsylvania State University. See Table 1 for scanning parameters.

Taxon	**kV**	**μA**	**Time (ms)**	**Voxel Size (μm)**
Moythomasia	160	28	1000	39.86
Mesopoma	160	85	333	10.57
Tristychius	450	130	96	25.00
Noturus	40	600	35	12.63
Leucoraja precaudal	80	70	4000	3.76
Leucoraja caudal	100	100	2000	3.08

Table 2.1. CT scanning parameters for four taxa included in this analysis.

Phylogenetic Comparative Methods

Supertree construction

The phylogenetic tree onto which ancestral state reconstructions were run was created by combining tree topologies from eleven recent phylogenetic analyses: Cloutier and Ahlberg (1995) for early sarcopterygians, Maisey et al. (2004) for hybodont sharks, Schultze (2004) for Mesozoic lungfish, Gardiner et al., (2005) for early actinopterygians, Cavin et al., (2007) for Mesozoic and Cenozoic lungfish, Friedman (2007a) for early lungfish, Inoue et al. (2010) for extant chondrichthyans, Pradel et al. (2011) for early chondrichthyans, Gess and Coates (2015) for coelacanths, Giles et al. (2015) for early gnathostomes focusing on Osteichthyans, and Long et al. (2015) for early gnathostomes focusing on placoderms. These trees were chosen because

they represent the most recently published examples of phylogenetic analyses for each respective taxon group. Numerous trees sampling the same portion of gnathostome phylogeny were avoided. All of these analyses sampled different, but slightly overlapping, parts of vertebrate evolutionary history, and when combined, provide a comprehensive picture of recent hypotheses of gnathostome interrelationships. The goal of this supertree is to focus on the early representatives of each gnathostome group, to broadly sample the early diversity of vertebral morphology. In addition to the earliest members, this supertree includes representatives of each clade through the Mesozoic and Cenozoic, as well as extant taxa, to sufficiently sample the range of possible morphologies.

To assure that the matrix associated with each tree produced the published results, I conducted phylogenetic analyses using the dataset and parameters specified in each paper. In several studies the tree reconstruction methods were vague and the results of my replication did not match the published results (e.g. Pradel et al., 2011). In the case of Pradel et al. (2011) the tree I recovered had a total of 68 steps, while the published tree was stated to have only 65 steps and the placements of several taxa were significantly different. Despite these discrepancies, the published tree topologies are used here; the differences in tree topology have little to no effect on the overall ancestral state reconstruction results.

There are several methods available for creating hypotheses of relationships for large numbers of taxa, including concatenating character-taxon matrices and the Matrix Representation with Parsimony (MRP) method of supertree construction used here. Because this dataset includes gnathostomes with an extremely wide range of morphologies, existing character matrices have too little overlap to produce reasonable results. For example, the braincases of extant chondrichthyans are difficult to compare to extant lungfish and extant actinopterygians

because these taxa have been evolving independently of one another for close to one billion years. Even if the goal was to create a character matrix for all gnathostomes, a large proportion of characters could not be coded for many taxa, resulting in large percentages of missing data and a lack of resolution. An alternative method is to combine source tree topologies instead of character matrices to achieve a supertree. MRP works by coding taxa represented in each node (and its descendants) in each source tree with a 0 if absent and a 1 if present (Baum, 1992; Ragan, 1992). This method of supertree construction does not produce a primary hypothesis of relationships, but rather combines existing hypotheses into one large scaffold onto which character transformations can be analyzed. Concerns that supertrees will recover novel tree topologies incongruent with the character-based source trees have been raised a number of times, but spurious groups like these usually have little impact on the overall tree topology and can be easily edited (Bininda-Emonds and Sanderson, 2001; Pisani and Wilkinson, 2002; Ruta et al., 2003)

Tree preparation and supertree matrix construction was performed in Mesquite (Maddison and Maddison 2015). To obtain input tree files from published phylogenetic analyses, each tree topology was drawn manually in Mesquite and concatenated into one tree block. Uncertain taxonomic assignments or genera represented by more than one species in a single tree (e.g. *Ptychoceratodus* in Cavin et al. 2007 and *Griphognathus* and *Chirodipterus* in Friedman 2007) were collapsed into a single genus. Additionally, the extant tetrapods in the Inoue et al. (2010) tree were removed because they were not relevant to this analysis. A MRP matrix was constructed in Mesquite using the MRP matrices from trees function (see Appendix 2 for MRP matrix). The MRP matrix was then exported as a nexus file and run in PAUP* 4.0a147 (Swofford 2015) using a parsimony ratchet to achieve a supertree. The tree was rooted with

Galeaspida and Osteostraci as outgroups and a heuristic search was run using TBR branch swapping and 100,000 random addition sequence replicates. One most parsimonious tree was recovered, with 319 steps.

Once a most parsimonious supertree was computed, the tree topology was adjusted slightly by hand to correct severe and obvious errors in taxon placement, such as spurious clades not represented in any of the source trees. Additionally, several taxa were added to the tree topology by hand in Mesquite, to add fullness to the tree in the Mesozoic Era and a more thorough sample of vertebral morphology. These are taxa with well-preserved axial skeletons that were not incorporated into one of the phylogenetic hypotheses used to compute a supertree, but for which good taxonomic and phylogenetic information is available. Taxa added and references to their phylogenetic or taxonomic position are as follows:

Belonostomus – Bogan et al.(2011) (2011)

Caturus – Grande and Bemis (1998)

Ctenurella – Trinajstic and Long (2009)

Dapedium – Xu et al. (2012)

Discoserra – Hurley et al. (2007)

Falcatus – Lund et al. (2014)

Harpacanthus – Lund et al. (2014)

Harpagofututor – Lund (1982)

Hopleacanthus – Coates and Sequeira (2001a)

Howidipterus – Long and Clement (2009)

Hulettia – Hurley et al. (2007)

Ionoscopus – Grande and Bemis (1998)

Lepisosteus – Xu et al. (2012)

Leptolepis – Xu et al. (2012)

Mesopoma – Coates (1999)

Pachycormus – Arratia and Schultze (2013)

Phanerosteon – Sallan (2012)

Pholidophorus – Xu et al. (2012)

Plourdosteus – Carr (2004)

Semionotus – Grande (2010)

Squaloraja – Stahl (1999)

Tarrasius – Sallan (2012)

Time calibration of supertree

Age range data were collected from the literature for each taxon present in the supertree, at the genus level (see Appendix 3). Where possible, the smallest interval of dates was entered, but whenever only rough dating information was available the age range for the relevant geologic stage or set of stages was used. The supertree was time calibrated using the paleotree package (Bapst, 2012) in the R software environment. Within paleotree, two tables were imported, including a set of geologic stages and a set of age range intervals corresponding to those stages. The cal3 method was utilized, which stochastically samples from a distribution of potential ages within the range specified by the age range table. The results of this stochastic sampling mean that for future analyses for which branch lengths may affect models of evolution a sample of time-scaled trees should be analyzed and compared.

Character descriptions (see Appendix 4 for character matrix)

1. Vertebral centra: present or absent

    0 – absent

    1 – ring centra

    2 – fully developed centra

Mineralizations around or invading the notochord are common among gnathostomes, but can vary greatly in their form. Vertebral columns with no centrum mineralization consist solely of neural and/or hemal arches and a notochord that persists unconstricted into adulthood (state 0). Examples of gnathostomes with no centra include the extant sturgeons and lungfish (Arratia et al., 2001; Hilton et al., 2011). Ring centra consist of cartilage or bone deposited on the outside of the notochord sheath as a complete or partial ring (hemicentrum) or within the sheath itself as a chorda-centrum, but does not replace the notochord (state 1). The notochord persists in conjunction with ring centra and remains large into adulthood, but is surrounded by mineralized rings in a metameric pattern. Here I consider the rhachitomous vertebrae of tetrapodomorphs, in which a small dorsal pleurocentrum and a ventral ring-shaped intercentrum combine, to be ring centra in most cases because the notochord is not substantially constricted in adulthood. Complete ring centra can be seen in the ratfish *Hyrolagus,* while, hemicentra are present in fossil holocephalans such as *Chondrenchelys* (Didier, 1995; Finarelli and Coates, 2014). Fully developed centra occur when those rings of mineralization also constrict the notochord, drastically reducing its width (state 2). Fully mineralized centra can be composed of cartilage or bone, fully replace the notochord, and occasionally have a small foramen that passes through their center, as in the actinopterygian *Amia* (Grande and Bemis, 1998).

2. Anterior vertebral fusions

0 – absent

1 – one fusion

Vertebrae are usually separate units that might articulate to one another, but do not actually fuse together (state 0). In some taxa, however, fusions of the anterior-most vertebrae may be present, in the form of a synarucal or Weberian apparatus (state 1). In otophysan actinopterygians the Weberian apparatus comprises the anterior portion of the vertebral column, including up to the first five vertebrae. These vertebrae are either modified into ossicles, (e.g. cypriniforms such as the zebrafish *Danio*) or fully fused into a single structure (e.g. siluriforms, such as the madtom catfish *Noturus*) to aid in the transmission of sound waves from the swim bladder to the otic region (Coburn and Grubach, 1998; Bird and Mabee, 2003).

3. Polyspondyly – multiple centra per body segment

0 – none at all

1 – diplospondyly or polyspondyly only in caudal region

2 – polyspondyly in entire column

The general state of vertebral organization consists of one set of neural arches and one centrum for each myotomal segment (state 0). However, the condition in which there are multiple centra present for each myotomal segment is termed polyspondyly. Polyspondyly can take the form of a simple duplication of the number of centra, resulting in two centra for each set of neural arches, which is termed diplospondyly (state 1). Diplospondyly is present in some actinopterygians, such as the bowfin *Amia*, and can also be seen in a slightly different arrangement in elasmobranch fishes, where each myotomal segment contains two entire vertebrae (Ridewood, 1899; Grande and Bemis, 1998). A more extreme version of polyspondyly is commonly seen in holocephalans

such as *Hydrolagus*, in which more than two centra form for each body segment (state 2) (Didier, 1995).

4. Neural arches

    0 – paired

    1 – fused anteriorly

    2 – fused throughout

Neural arches are present in all known gnathostomes, but their morphology varies among different groups. Arches can be present as paired structures that are aligned on either side of the neural tube and in each body segment, and whose apices meet in the midline (state 0). Most 'placoderms' have paired neural arches. Neural arches also can fuse at the midline, forming a singular structure either in the anterior region only (state 1) or throughout the entire body (state 2).

5. Intercalary elements

    0 – absent

    1 – interdorsals and interventrals present

    2 – just interdorsals

In many fishes the neural and hemal arches are not the only arch structures present. Intercalary elements are absent in many early gnathostomes, including 'placoderms' and 'acanthodians'(state 0) (Miles, 1970; Johanson et al., 2013). However, the vertebrae of some gnathostomes, including the elasmobranchs, include both dorsal intercalaries (Gadow and Abbott's (1895) interdorsals) and ventral intercalaries (interventrals) that alternate with the

primary arch elements (state 1) (Daniel, 1922). In some groups, such as skates, only dorsal intercalaries are present (state 2) (see chapter three).

Ancestral state reconstructions

Reconstructions of ancestral states were performed on discrete characters using three methods: maximum parsimony, the Mk1 model of maximum likelihood (both in the phylogenetics program Mesquite (Maddison and Maddison, 2015)), and Bayesian inference via the ancthresh function in the phytools package in R (Revell, 2014). I decided to test hypotheses of centrum homoplasy using a variety of methods to 1) determine how congruent the results were when various models of evolution and prior assumptions are employed and 2) to implement measures of uncertainty that accurately reflect missing data into the analysis. Parsimony-based ancestral state reconstructions were performed in Mesquite using an unordered model in which any state change counts as one step. The ancestral state reconstructed as most parsimonious therefore has the fewest state changes across the trajectory of each branch. Parsimony has been frequently used when evaluating character evolution in analyses that incorporate paleontological data, in which large portions of the data matrix might consist of missing data. Parsimony is able to infer ancestral states even when the proportion of missing data is high, but it has been shown to produce incorrect results in cases of unequal probabilities of gains and losses and rapid evolution (Cunningham et al., 1998).

The maximum likelihood model of ancestral state reconstructions computed in Mesquite is the Markov k-state 1 parameter (Mk1) model (Lewis, 2001). The Mk1 model assumes a single parameter, the rate of state change, as equally probable from all directions. Mesquite outputs include color-coded branches and either raw or proportional likelihoods. Proportional likelihoods

are reported here. Unfortunately, the Mk1 model is the only likelihood model available in the current version of Mesquite, so I was not able to test whether different assumptions in the rate of state change would have had an impact on the reconstructed ancestral states. Additionally, the maximum likelihood results plotted on trees in Mesquite are hard to interpret without the interactive interface of the software program, so the trees are not shown in this chapter. Instead, proportional likelihoods at major nodes are reported.

The ancthresh command runs an ancestral state reconstruction using the threshold model, which is based on evolutionary quantitative genetics experiments. The threshold model assumes an underlying continuous value, or "liability" that corresponds to each observed character state for a particular taxon. When the value of the liability crosses a fixed threshold the observed character state changes. The ancthresh command assumes a Brownian motion model of liability evolution and uses Bayesian Markov chain Monte Carlo to sample liability values from their posterior probabilities. The function requires a table of prior probabilities for each character state, for each taxon (see Appendix 5). Prior probabilities were calculated based on character state coding, with a 1.00 probability assigned for a tip with a presence of a known character state and a 0.00 probability assigned for states that are known to not occur. For taxa with uncertainties (i.e., vertebrae are not preserved) the probability was assigned as one divided by the number of character states, which provided uninformative or equiprobable values. For polymorphic characters, the two observed character states were given equal probability. The ancthresh function was run with 1,000,000 generations and the Brownian motion model of evolution. The output from the threshold model analysis comes in the form of a phylogenetic tree with pie charts located at each tip and node, giving the posterior probability for each character state at each

position on the tree. Tables of posterior probabilities for each character at each node are also provided (summarized in Appendix 6).

The input of prior probabilities in Bayesian analyses can be both beneficial and potentially harmful when analyzing character evolution. Because the prior probabilities in this case represent the known character states of taxa in the tree, the Bayesian analysis does not ignore uncertainty, but rather incorporates it as missing data and produces measures of confidence (posterior probabilities) for each node (Ronquist, 2004). However, because uncertain taxa are coded as equiprobable for each character state, states that have not been observed in any taxa in a given group will be up-weighted more than they would be in other methods. This can increase uncertainty at nodes where nearby taxa are missing vertebral data, but particular character states are more likely to be observed.

The threshold model can be greatly influenced by features of the input tree, such as branch lengths and divergence estimates. Because the cal3 model of time scaling described above samples stochastically for each node, I obtained a sample of ten trees with slightly different divergence dates and ran the Bayesian analysis on each of those. Taken together, the resulting posterior probabilities can provide an estimate of whether the result at a given node is well supported. I selected three characters on which to run the threshold model analysis because Bayesian analyses are time consuming and require extensive computing power: presence of centra, anterior fusions, and polyspondyly. These characters were easy to evaluate in fossil and recent specimens and have been hypothesized to be functionally advantageous (Schaeffer, 1967a; Lauder, 1980; Denison, 1983; Koob and Long, 2000; Johanson et al., 2013). I tested the threshold model on ten trees with slightly different time-scaled divergence dates (see Appendix 7) and averaged the resulting posterior probabilities to evaluate confidence at each node.

Results

Primitively, gnathostome vertebrae comprised only paired neural and hemal arches

The primitive vertebral condition for jawed vertebrates consisted of a notochord that persisted into adulthood, one set of paired neural arches per myotomal segment, and one set of hemal arches for each caudal myotomal segment. The absence of centra is not just primitive for gnathostomes, but is also reconstructed as the ancestral condition for all 'placoderm' subgroups, chondrichthyans (including 'acanthodians'), and actinopterygians (Figures 2.1, 2.2). Vertebral modifications like centra, anterior fusions, polyspondyly, neural arch fusions, and intercalary components originated within each respective clade independently of other gnathostomes, and will be discussed in detail throughout this chapter.

Bayesian inference, maximum likelihood, and parsimony ancestral state reconstructions on a supertree of 232 taxa recover at least ten originations of centra, five originations of anterior vertebral fusions, and eight originations of polyspondyly. Neural arches have transitioned from a paired to a fused state at least ten times independently and intercalary components have arisen independently potentially six times. The evolutionary patterns within each gnathostome group for each of these characters will be described in detail.

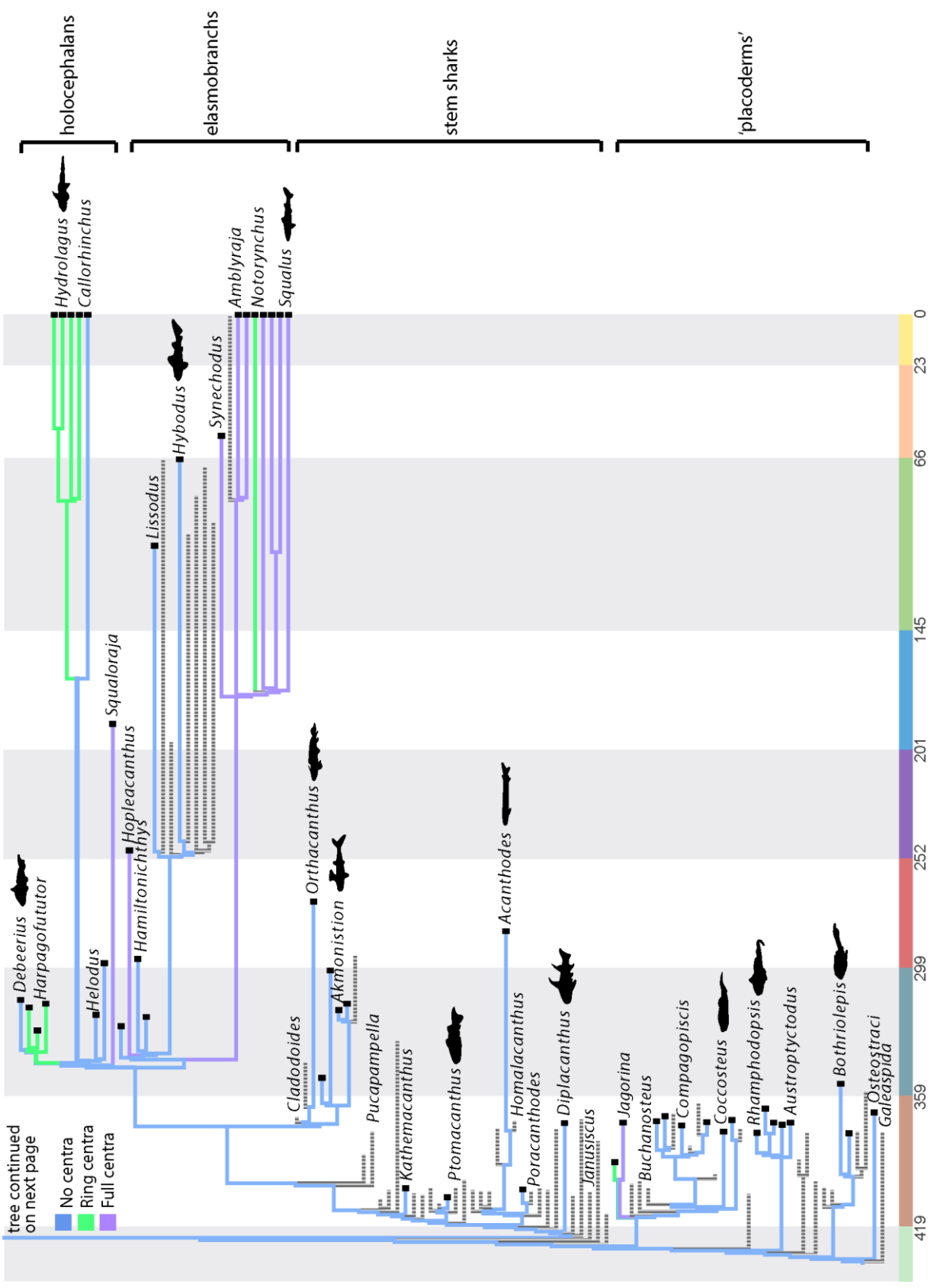

Figure 2.1. Supertree showing parsimony ancestral state reconstructions for vertebral centra.

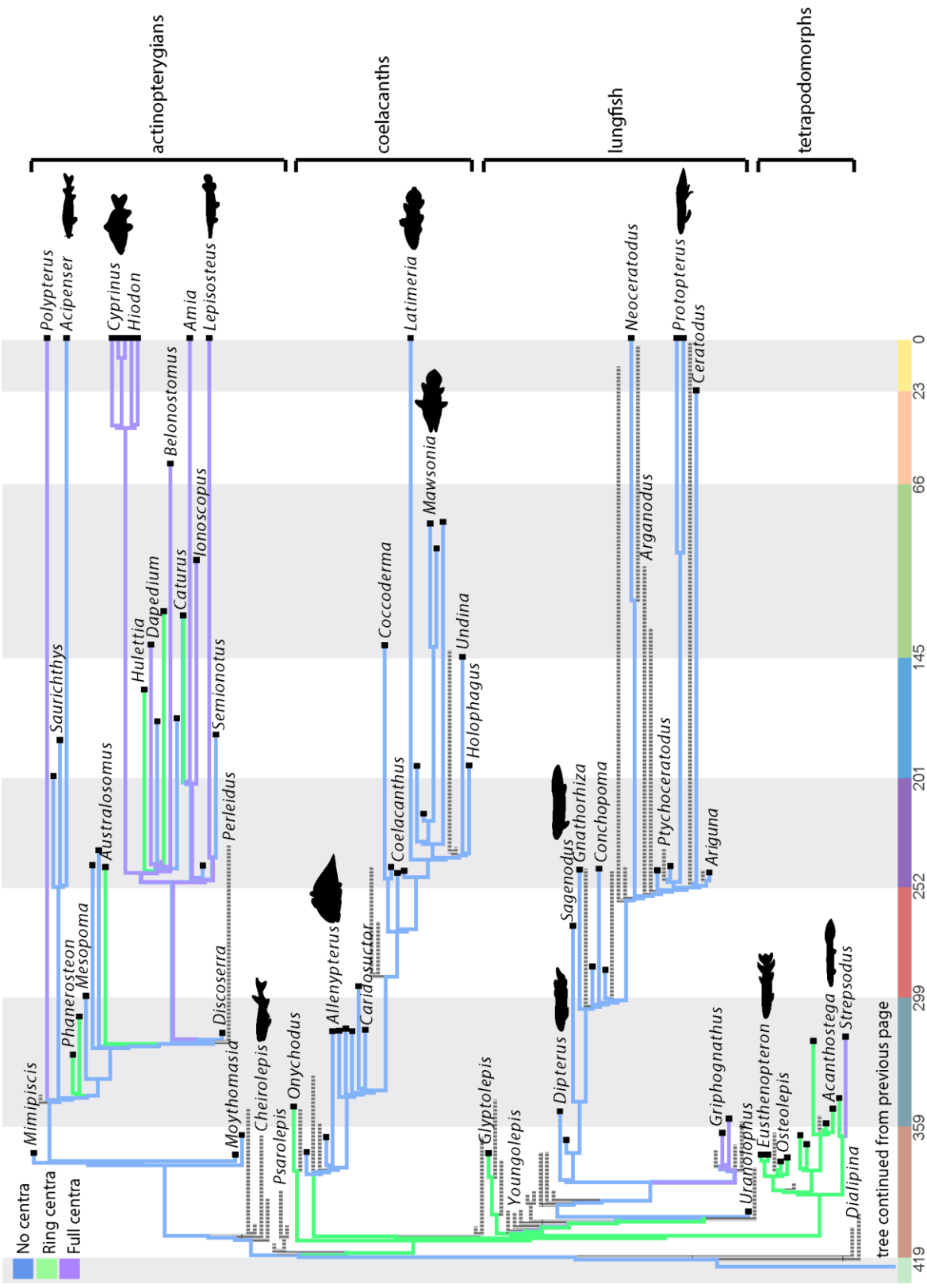

Figure 2.1 continued. Supertree showing parsimony ancestral state reconstructions for centra.

Figure 2.1 continued. Absence of centra is colored blue, ring centra are colored green, and full centra are colored purple. Silhouettes highlight key taxa and clades are denoted by brackets. The tree is time-scaled and plotted over geologic time, with dates and time scale colors added to the bottom.

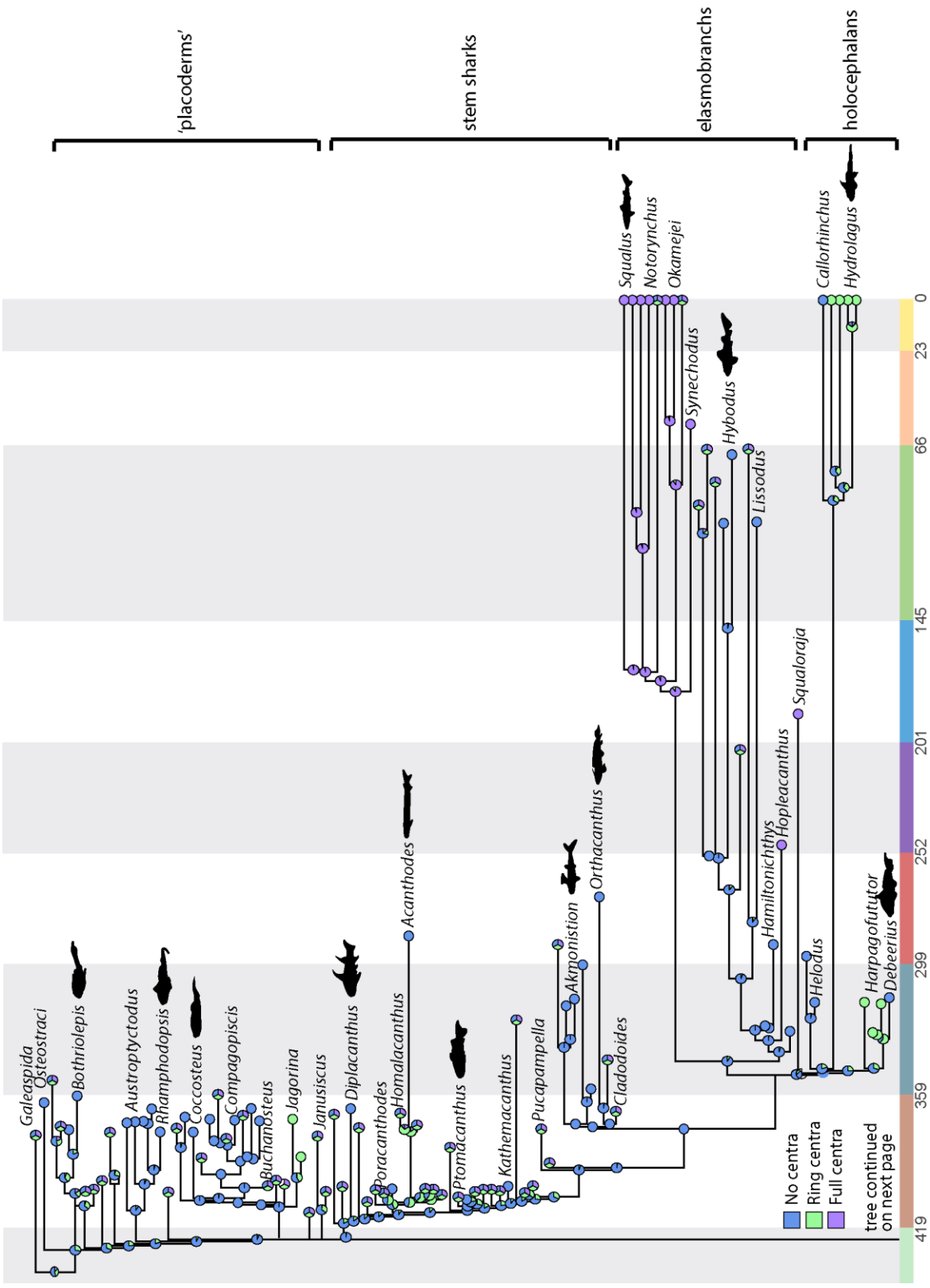

Figure 2.2. Supertree showing threshold model-based ancestral state reconstructions for centra.

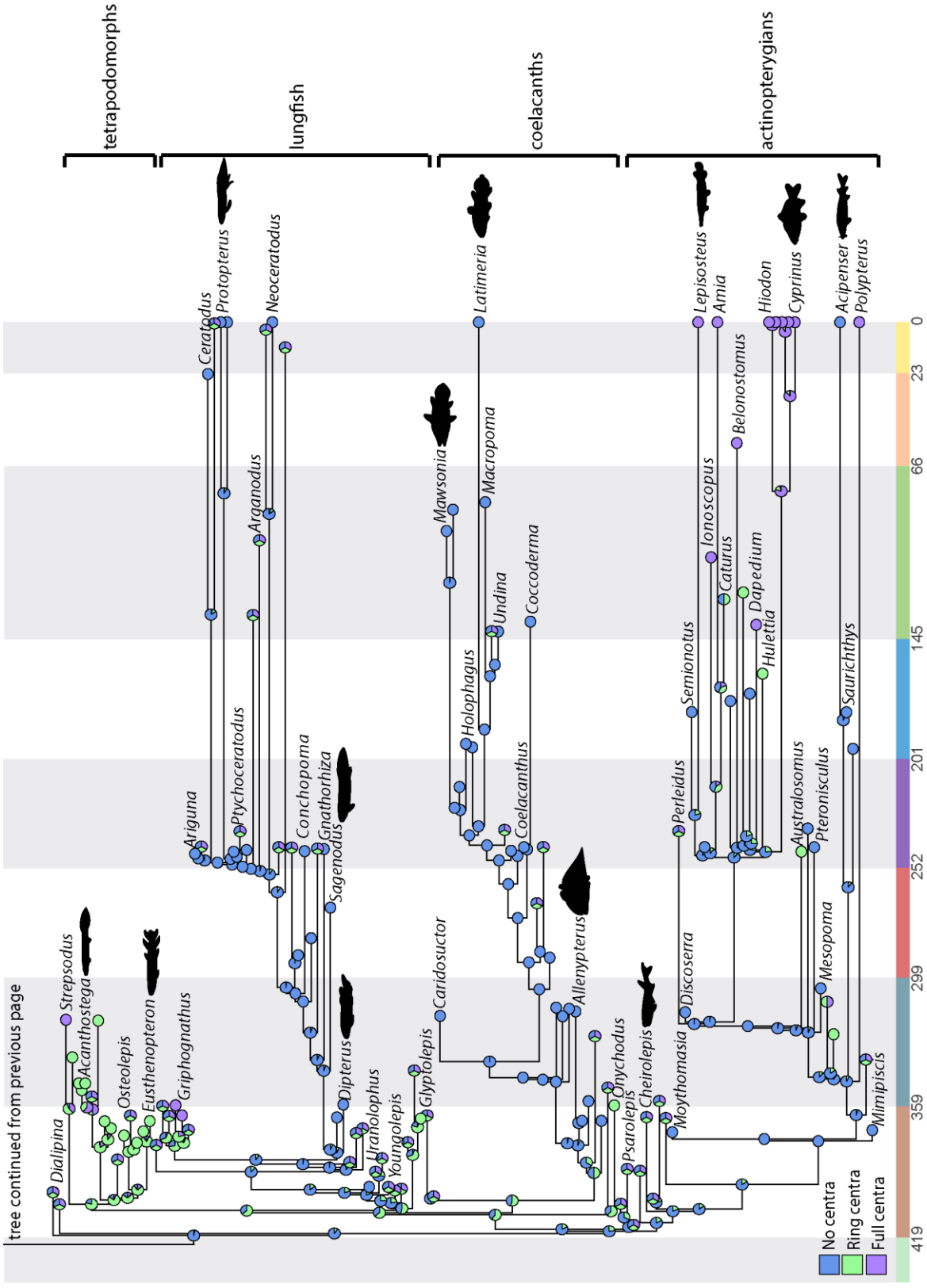

Figure 2.2 continued. Supertree showing threshold model-based ancestral state reconstructions

Figure 2.2 continued. for centra, separated over two pages. Absence of centra is colored blue, ring centra are colored green, and full centra are colored purple. Silhouettes highlight key taxa and clades are denoted by brackets. The tree is time-scaled and plotted over geologic time, with dates and time scale colors added to the bottom.

Centra evolved at least ten times independently

Maximum likelihood and parsimony ancestral state reconstructions both show strong support for a primitive lack of centra in jawed vertebrates, although posterior probabilities from the Bayesian analysis are weaker (Table 2.1). This absence is clearly visible in numerous 'placoderms' (e.g. *Plourdosteus, Phyllolepis, Ctenurella, Coccosteus,* and *Austroptyctodus* (Figure 2.3a-e)), 'acanthodians' (e.g. *Acanthodes, Diplacanthus, Kathemacanthus*), chondrichthyans (e.g., *Debeerius, Orthacanthus, Xenacanthus* (Figure 2.4a-c)), and even some of the earliest known osteichthyans with vertebral preservation (*Mimipiscis, Uranolophus, Onychodus*). Additionally, several groups of extant osteichthyans, including the chondrosteans, lungfish, and coelacanths, all lack mineralized centra (Figures 2.1, 2.2).

Centra remain absent through the origins of all major gnathostome groups except for the sarcopterygians (Figures 2.1, 2.2). Both parsimony and Bayesian inference reconstruct ring centra as ancestral for sarcopterygian clades including coelacanths, lungfish, and tetrapodomorphs, but absence of centra is recovered as most likely for sarcopteryians (proportional likelihood 0.9127) (Figures 2.1, 2.2). However, the most proximate outgroup taxa, early osteichthyans such as *Guiyu, Psarolepis,* and *Achoania,* preserve only skulls or braincases, so the reconstruction of ring centra as ancestral is not based on complete taxon sampling. This missing data localized around the major gnathostome splits adds to uncertainty in inferring ancestral states.

Clade	Reconstruction Method	Model	Missing data	Ancestral state	Likelihood/ Probability
Antiarchs	Parsimony	Unordered		Absent	
	Maximum likelihood	Mk1	67%	Equivocal	
	Bayesian Inference	Threshold		Absent	0.7815
Ptyctodonts	Parsimony	Unordered		Absent	
	Maximum likelihood	Mk1	0%	Absent	0.9999
	Bayesian Inference	Threshold		Absent	0.9470
Arthrodires + others	Parsimony	Unordered		Absent	
	Maximum likelihood	Mk1	50%	Absent	0.9986
	Bayesian Inference	Threshold		Absent	
Chondrichthyans	Parsimony	Unordered		Absent	
	Maximum likelihood	Mk1	30%	Equivocal	
	Bayesian Inference	Threshold		Equivocal	
Elasmobranchs	Parsimony	Unordered		Absent	
	Maximum likelihood	Mk1	33%	Absent	0.9999
	Bayesian Inference	Threshold		Absent	0.8468
Holocephalans	Parsimony	Unordered		Absent	
	Maximum likelihood	Mk1	0%	Absent	0.9945
	Bayesian Inference	Threshold		Absent	0.7178
All Osteichthyans	Parsimony	Unordered		Absent	
	Maximum likelihood	Mk1	37%	Absent	0.9988
	Bayesian Inference	Threshold		Absent	0.6063
Tetrapodomorphs	Parsimony	Unordered		Ring	
	Maximum likelihood	Mk1	21%	Ring	0.9931
	Bayesian Inference	Threshold		Ring	0.7826
Actinistians	Parsimony	Unordered		Absent	
	Maximum likelihood	Mk1	29%	Absent	0.9283
	Bayesian Inference	Threshold		Equivocal	
Porolepiforms	Parsimony	Unordered		Absent	
	Maximum likelihood	Mk1	55%	Absent	0.9016
	Bayesian Inference	Threshold		Equivocal	
Actinopterygians	Parsimony	Unordered		Absent	
	Maximum likelihood	Mk1	6%	Absent	0.9999
	Bayesian Inference	Threshold		Absent	0.7377
Neopterygians	Parsimony	Unordered		Absent	
	Maximum likelihood	Mk1	0%	Absent	0.9991
	Bayesian Inference	Threshold		Absent	0.7650
Teleosts	Parsimony	Unordered		Full	
	Maximum likelihood	Mk1	0%	Full	0.9997
	Bayesian Inference	Threshold		Equivocal	

Table 2.2. Ancestral states inferred for centrum presence and absence, using parsimony, the Mk1

Table 2.2 continued. likelihood model, and Bayesian inference. Included are the model of evolution and the percent missing data for each clade listed. Proportional likelihoods and posterior probabilities are reported for maximum likelihood and Bayesian analyses.

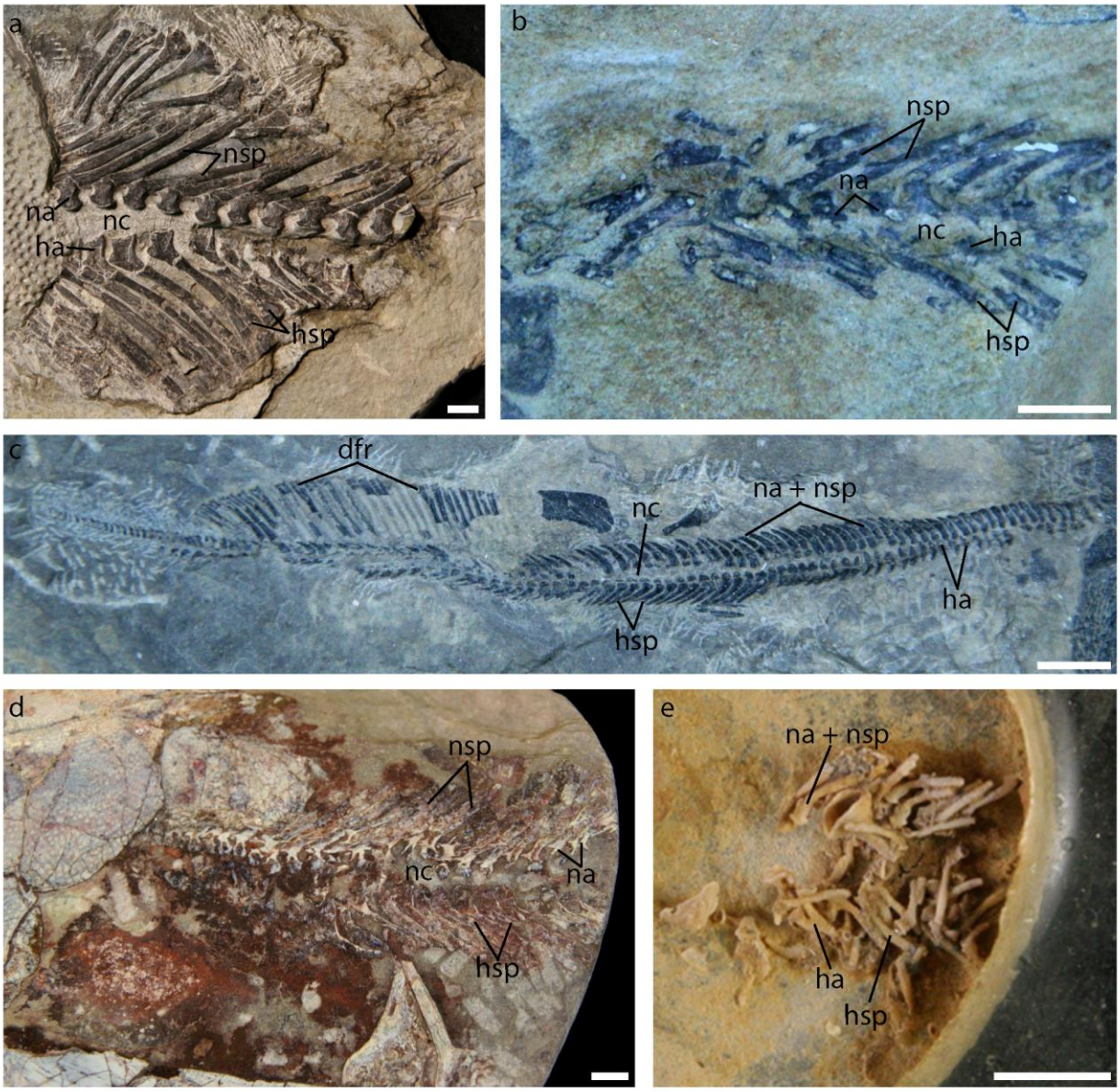

Figure 2.3. Examples of placoderm vertebral columns lacking centra. a, *Plourdosteus canadensis* MHNM02-3375*;* b, *Phyllolepis woodwardi*, NHM P11912; c, *Ctenurella* ARD 231; d, *Coccosteus cuspidatus* NMS1895.190.1; and e, *Austroptyctodus* MV P230240. dfr, dorsal fin rays; ha, hemal arch; hsp, **hFemal** spine; na, neural arch; nc, notochord; nsp, neural spine. Scale bar equals one cm.

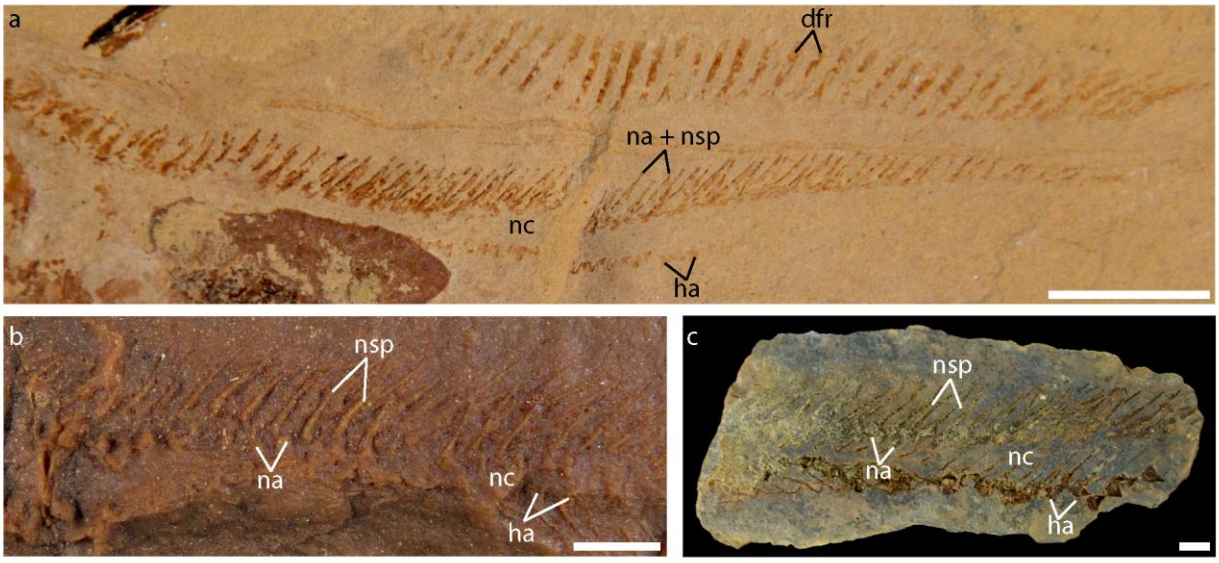

Figure 2.4. Examples of chondrichthyans that show neural and hemal arches and spines, but lack centra. a, *Debeerius ellefseni* CM 46027A; b, *Orthacanthus* sp. NHM P24431; c, *Xenacanthus decheni* NMS 1891.41.6B. dfr, dorsal fin rays; ha, hemal arch; hsp, hemal spine; na, neural arch; nc, notochord; nsp, neural spine. Scale bars equal one cm.

Absence of centra is recovered by parsimony and maximum likelihood as primitive for the clade encompassing rhenanids, arthrodires, and ptyctodonts (proportional likelihoods greater than 0.99). Only the rhenanids, including *Gemuendina* and *Jagorina*, have been documented to have centra (Gross, 1963; Stensiö, 1969; Johanson et al., 2010). These taxa are known from few specimens, but photographs and published line drawings show neural arches fused in the form of synarcuals articulating to mineralized centra.

Parsimony and maximum likelihood results suggest that centra evolved independently at three times in the holocephalans, in the chondrenchelyids, such as *Harpagofututor*, (proportional likelihood 0.80) and crown chimaeras, such as *Hydrolagus*, (proportional likelihood 0.98), as well as *Squaloraja* (proportional likelihood 0.98) (Figure 2.5a-c), and up to twice in the elasmobranchs (proportional likelihoods greater than 0.99 for both). Among these independent originations, centrum morphology is variable: ring centra were present in Carboniferous

holocephalans like *Chondrenchelys* and *Harpagofututor* (Figure 2.5a) as well as in extant holocephalans (Figure 2.5b), while the Jurassic holocephalan *Squaloraja* preserves fully mineralized centra with only a small foramen remaining in the center (Figure 2.5c).

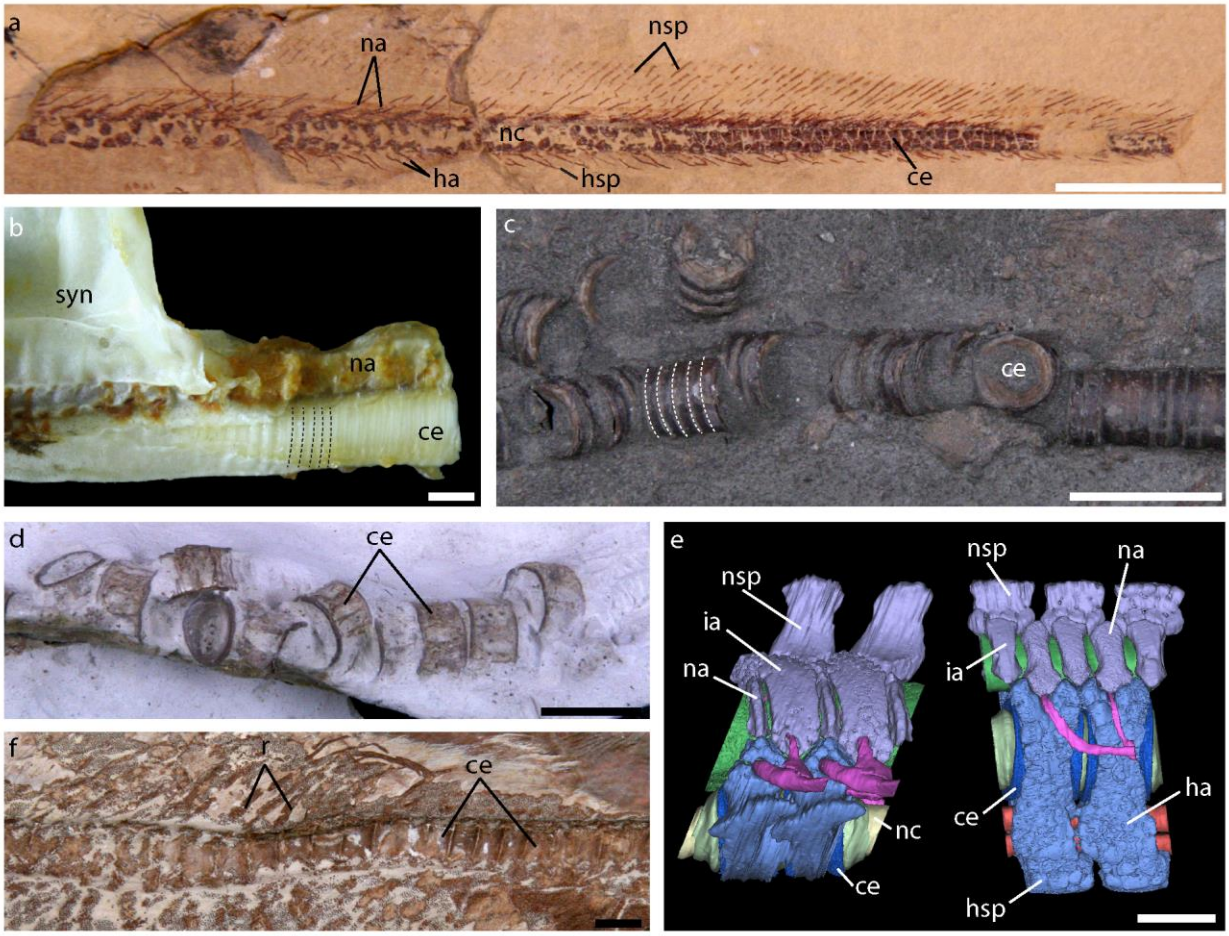

Figure 2.5. Examples of holocephalan and elasmobranch vertebral columns showing ring centra and full centra. a, *Harpagofututor volsellorhinus* CMNH 27326A; b, *Hydrolagus novezealandia* ANSP 177827 c, *Squaloraja dolichognatha* NHM P2276; d, *Synechodus dubrisiensis* NHM 49032 e, *Leucoraja erinacea;* f, *Rhinobatos intermedius* NHM 49516. Scale bar equals one cm for all except e, in which scale bars equal 200 µm.

Many of the earliest stem elasmobranchs lacked centrum mineralization, as is seen in early sharks like the Carboniferous *Tristychius* and the Permian shark *Hamiltonichthys*. The earliest non-holocephalan chondrichthyan known to exhibit centra is the Permian stem elasmobranch *Hopleacanthus* (Schaumberg, 1982). Centra are likely homologous for extant

elasmobranchs, and consist of an hourglass-shaped double-cone of calcified cartilage that incorporates growth rings and is easily preserved in the fossil record, along with an inner layer of hyaline cartilage, and in some taxa, an outer layer of hyaline cartilage extending from the neural arches to the hemal arches (Hasse, 1879; Daniel, 1922). Examples of elasmobranch centra can be seen in *Synechodus*, *Leucoraja*, and *Rhinobatos* (Figure 2.5d-f).

Within the osteichthyans, the most parsimonious and most likely ancestral condition was again the persistence of a notochord into adulthood, with neural and hemal arches functioning as the sole vertebral elements (Table 2.1). The Bayesian analysis, however, recovers equivalent posterior probabilities for both absence of centra and presence of ring centra, suggesting that neither state is well supported (see Appendix 6). The ancestral state of actinopterygian vertebrae appears to persist in extant chondrosteans, paddlefish and sturgeons. Chondrostean vertebrae include a series of neural and intercalary arches, along with hemal arches and a persistent notochord. The Carboniferous actinopterygians *Mesopoma* and *Discoserra* retain the ancestral condition of a persistent notochord (although they are derived with respect to other characters, such as the fusion of neural spines and appearance of transverse processes), and new data from CT scans of *Mesopoma* might provide insights into early neopterygian and chondrostean vertebral morphology. *Mesopoma* vertebrae consist of sets of paired neural arches with non-articulating, midline neural spines (Figure 2.6a). Ventral arches are present anterior in the body in the form of small ossifications ventral to the notochord. In the first two vertebral segments these ventral arches meet and fuse at the midline, forming u-shaped canals. No mineralized centra are present. *Discoserra* also shows the primitive lack of centra and a set of ventral arches in the anterior portion of the vertebral column (Figure 2.6b). Within the neopterygians some taxa retain the primitive condition, such as *Dapedium*, or show polymorphic expression of centra, in

the case of *Caturus* (Figure 2.6c, d). Within *Caturus*, different species have been identified that lack centra as well as possess ring and hemi-chordacentra (Laerm, 1982).

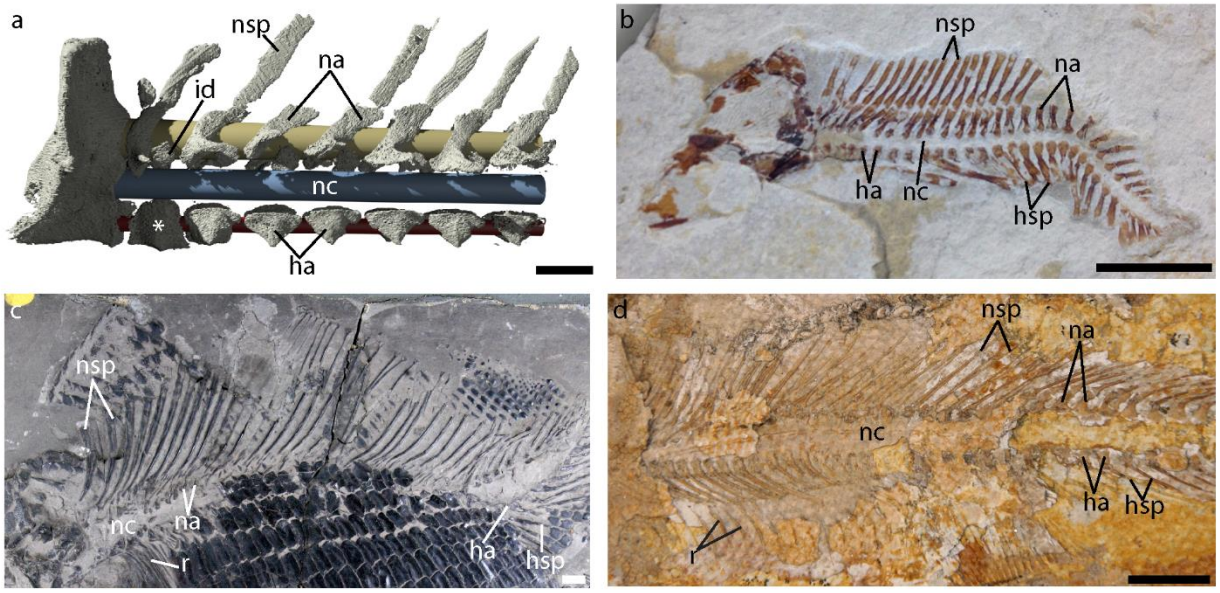

Figure 2.6. Vertebrae in actinopterygian fishes showing taxa that lack centra. a, *Mesopoma planti* NHM P11656, asterisk marks fused ventral arches; b, *Discoserra pectinodon* CM35547A2; c, *Dapedium* sp. NHM P3508*;* d, *Caturus furcatus* CMNH 869. ha, hemal arch; hsp, hemal spine; id, interdorsal; na, neural arch; nc, notochord; nsp, neural spine; r, ribs. Scale bars equal one cm.

Using all methods, independent origins of actinopterygian centra are recovered in early actinopterygians such as *Phanerosteon* and *Australosomus*, the bichir (*Polypterus*), teleosts, and holosteans, including the bowfin (*Amia*) and the gar (*Lepisosteus*) (Figure 2.1) (posterior probabilities greater than 0.73 and proportional likelihoods greater than 0.99). However, within the neopterygians, maximum likelihood reconstructs more independent evolution than the other methods, with centrum originations in the amiids, gars, teleosts, and several other extinct taxa, including *Hulettia, Belonostomus,* and *Pholidophorus* (proportional likelihoods >0.98).

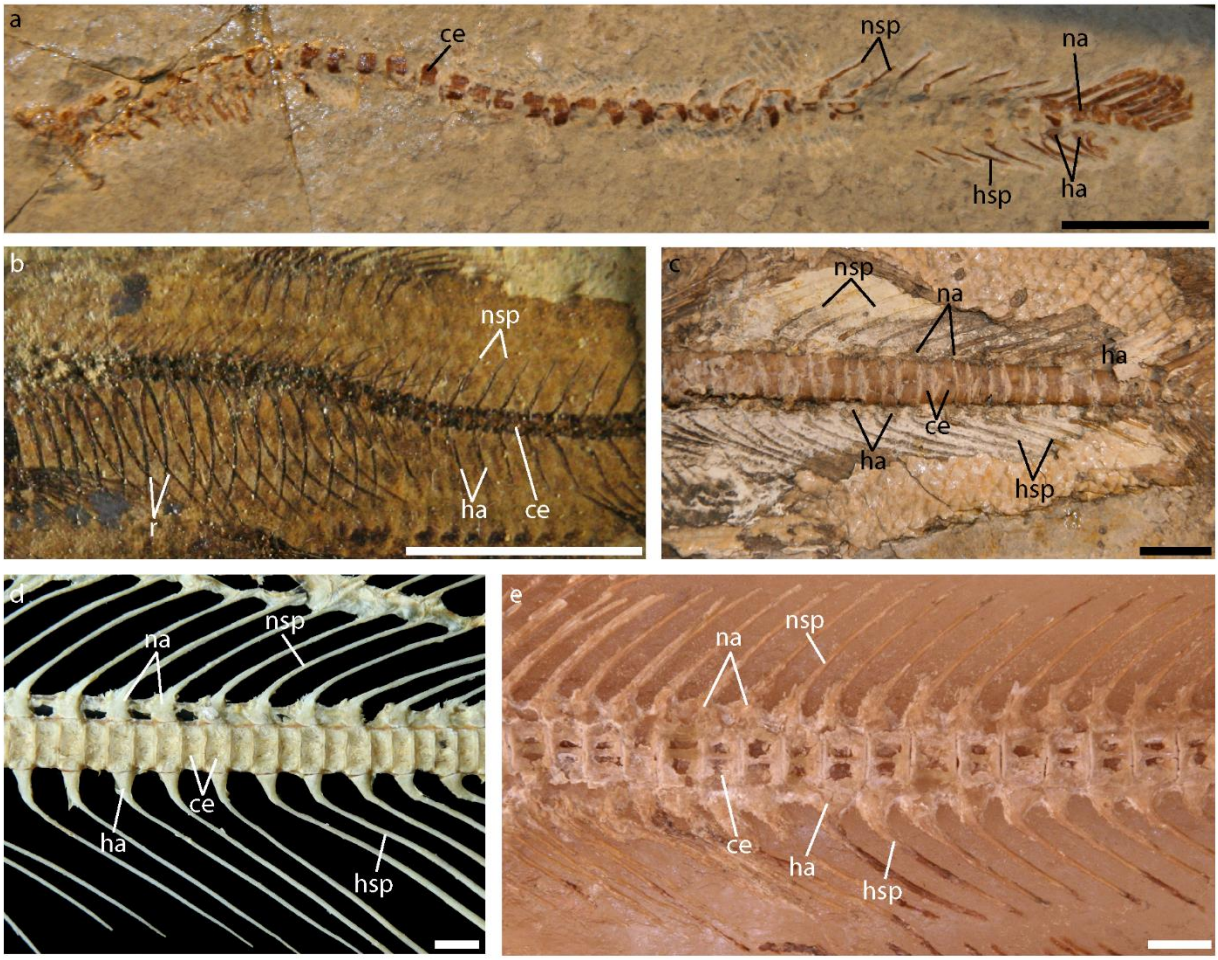

Figure 2.7. Actinopterygian fishes that have evolved vertebral centra. a, *Hulettia americana* AMNH 10917; b, *Leptolepis koonwam* MV P251233; c, an example of a specimen of *Caturus* sp. CM 4697; with ring centra and caudal diplospondyly; d, *Amia calva* ANSP 78258; e, *Ionoscopus cyprinoides* CM 4036. ce, centrum; ha, hemal arch; hsp, hemal spine; na, neural arch; nc, notochord; nsp, neural spine; r, ribs. Scale bar equals one cm.

There is considerable variation in actinopterygian centrum morphology, even between closely related taxa. The centra in the early actinopterygians *Australosomus* and *Phanerosteon* consist of rings of bone that do not replace the notochord (Nielsen, 1949; Sallan, 2012). Ring centra are present in the neopterygian *Hulettia* (Figure 2.7a), while full centra can be found in its cousin, *Leptolepis* (Figure 2.7b). The stem amiid *Caturus*, as discussed earlier, has been found

lacking centra (Figure 2.6d) or with ring centra (Figure 2.7c), while centra in *Amia* and another amiid, *Ionoscopus,* are robust (Figure 2.7d, e). *Lepisosteus* centra also are unique among fishes in their opisthocoelous shape, in which the anterior face is concave and the posterior face is convex (Grande, 2010).

It is difficult to discern with certainty the number of centrum originations within sarcopterygians because so many of the earliest stem sarcopterygians, such as *Guiyu, Psarolepis*, and *Achoania,* do not preserve any postcranial axial skeleton. However, within stem lungfish, coelacanths, and tetrapodomorphs, preserved vertebral columns are more numerous. Results from maximum likelihood and parsimony analyses are consistent, and suggest that centra are ancestrally absent for coelacanths, with the absence of centra persisting throughout the clade, and no instances of coelacanth centra are known (Figures 2.1; 2.8a, b) (proportional likelihood 0.9283). Primitive conditions are similar for lungfish, (proportional likelihood 0.9016), which is evident from the lack of centra in some of the earliest known lungfish, *Uranolophus* and *Dipterus*. Absence of centra is a general condition for most of lungfish, with many additional Paleozoic taxa (e.g. *Conchopoma,* Figure 2.8c) and virtually all known Mesozoic and Cenozoic taxa lacking centra (e.g. *Neoceratodus*, Figure 2.8d).

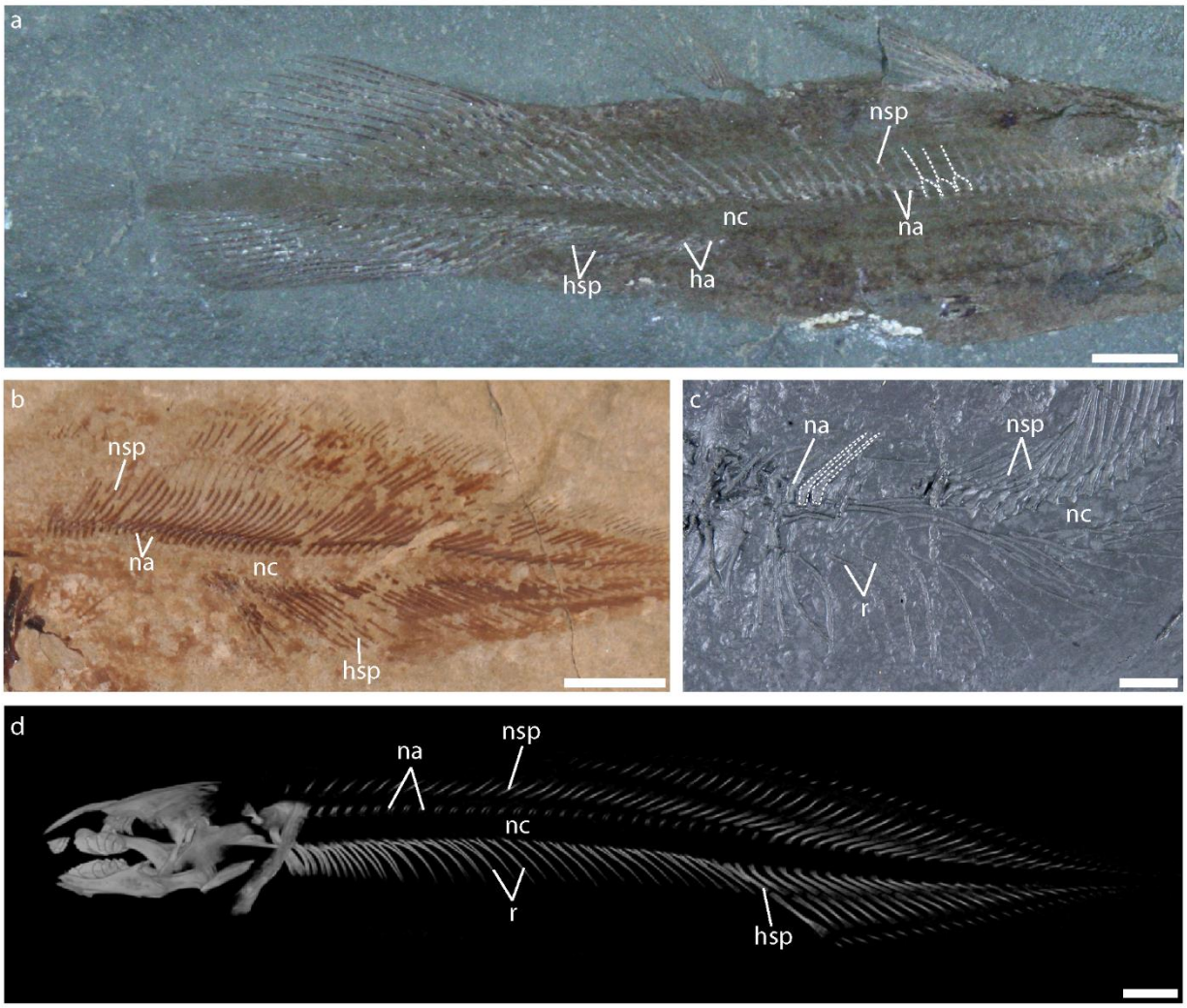

Figure 2.8. Sarcopterygians lacking centra. a, The coelacanth *Caridosuctor populosum* MNHN ANP 116A; b, the coelacanth *Allenypterus montanus* CM 27284A; c, the lungfish *Conchopoma gadiforme* NHM P58467; d, the extant lungfish *Neoceratodus forsteri* AMS I-40438-001. In all specimens except *Caridosuctor* anterior is to the left. ha, hemal arch; hsp, hemal spine; na, neural arch; nc, notochord; nsp, neural spine; r, rib. Scale bars equal one cm.

Several Devonian lungfish, including *Soederberghia* and *Griphognathus*, do develop mineralized centra that completely replace the notochord (Figure 2.9a), and because these taxa are nested within the lungfish clade, it can be concluded that this is an additional independent origin of centra. Ring centra are present in the porolepiform *Glyptolepis* (Figure 2.9b) and tetrapodomorphs, including Devonian stem tetrapods like *Eusthenopteron* (Figure 2.9c) and a

sarcopterygian of indeterminate affinities, *Onychodus*. Parsimony, maximum likelihood, and Bayesian inference all reconstruct these instances as homologous (proportional likelihood 0.9931, posterior probability 0.7826). Centra in *Glyptolepis* consist of a ventral ring of bone forming the intercentrum that transitions into hemal arches in the caudal region and a small dorsal pleurocentrum (Figure 2.9b). Centra in the earliest branching tetrapodomorphs consist of rings of bone surrounding a somewhat substantial notochord (e.g. *Eusthenopteron* and *Megalichthys;* Figure 2.9c, d), while more deeply nested tetrapodomorphs develop more heavily mineralized centra (e.g. *Acanthostega*, *Ichthyostega*). These centra are rhachitomous, forming dorsal pleurocentrum and ventral intercentrum components that together constrict the notochord but do not replace it entirely (Coates, 1996; Pierce et al., 2013).

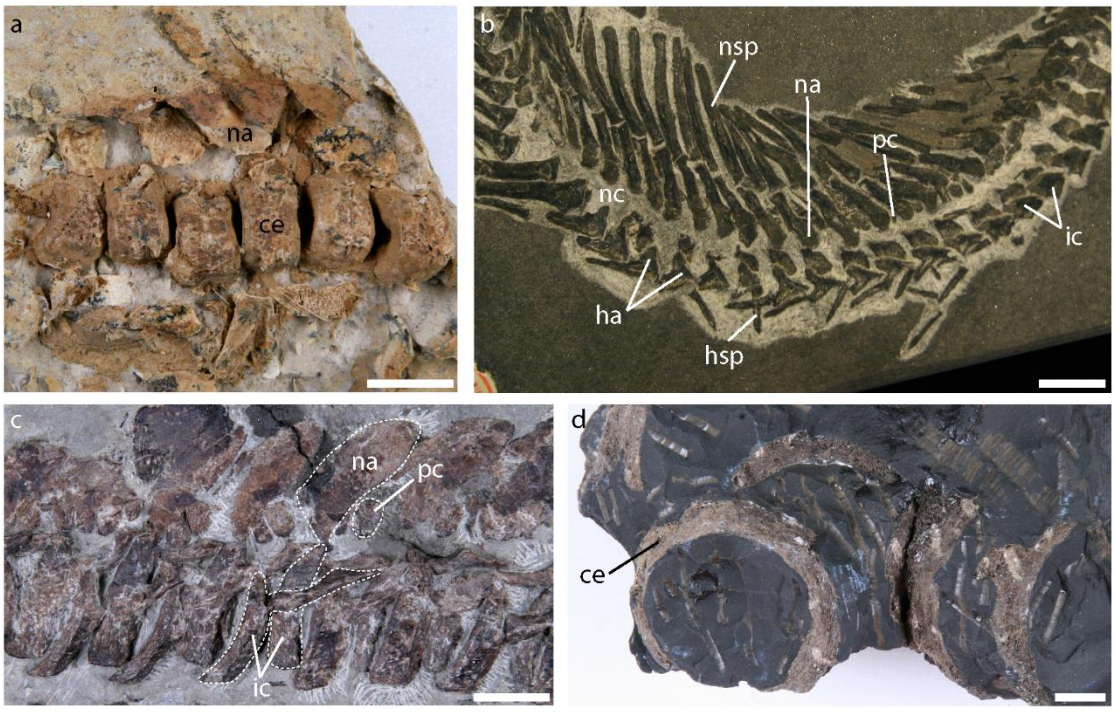

Figure 2.9. Sarcopterygians with ring centra or full centra. a, the Devonian lungfish *Griphognathus whitei* NHM P52571; b, the porolepiform *Glyptolepis paucidens* NMS 1898.120.40; c, *Eusthenopteron foordi* NHM P60387; d, *Megalichthys hibberti* NHM P3326 anterior is to the right in *Griphognathus* and *Glyptolepis* and to the left in *Eusthenopteron*. ce,

Figure 2.9 continued. centrum; ha, hemal arch; hsp, hemal spine; ic, intercentrum; na, neural arch; nc, notochord; nsp, neural spine; pc, pleurocentrum. Scale bars equal one cm.

Synarcuals are common among chondrichthyans and 'placoderms'

Ancestrally, synarcuals and other anterior fusions were lacking for jawed vertebrates, being absent in some of the earliest branching 'placoderms' as well as jawless fishes like the osteostracans (Figures 2.10, 2.11) (Janvier et al., 2004). However, anterior fusions of the vertebral column are common throughout other 'placoderms' and chondrichthyans, and all methods of analysis reconstruct anterior fusions as having evolved at least five times independently in gnathostome fishes. Two of these instances of synarcual origination can be seen in the rhenanids (*Nefudina* (Figure 2.12a), *Jagorina*, and *Gemuendina*), arthrodires (*Compagopiscis* and *Incisoscutum*), and the ptyctodonts (*Austroptyctodus*, *Campbellodus*, and *Cowralepis*) (posterior probabilities greater than 0.8 and proportional likelihoods greater than 0.98 for arthrodires and ptyctodonts, see Table 2.2) (Figures 2.10, 2.11). The number of vertebral elements incorporated into synarcuals, as well as the degree of fusion, in 'placoderms' varies. In the arthrodire *Incisoscutum ritchiei*, the synarcual incorporates only the first two segments, while *Compagopiscis* synarcuals consist of at least six neural arches and *Dunkleosteus* synarcual include at least eight neural arch segments (Johanson et al., 2013).

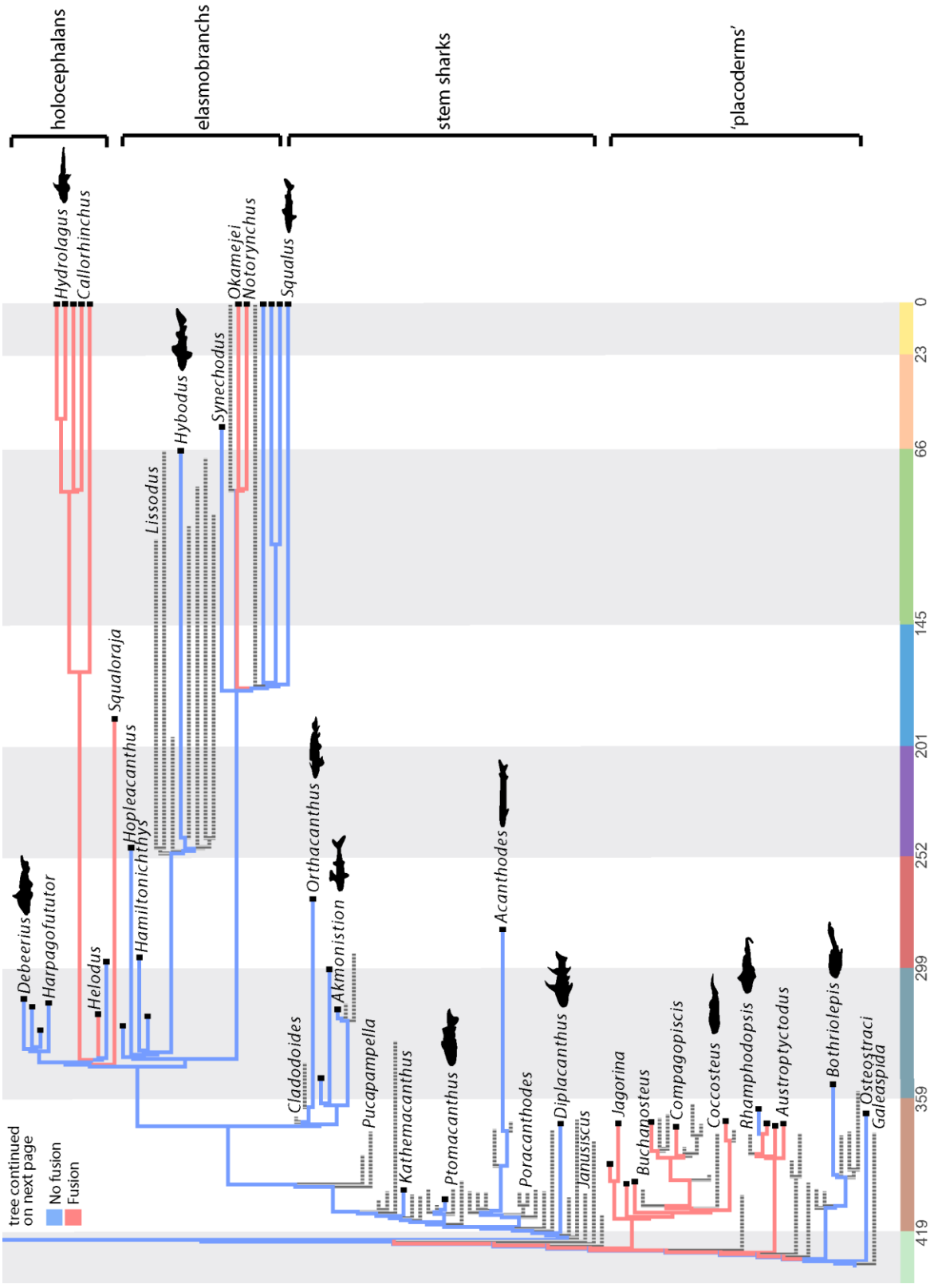

Figure 2.10. Parsimony ancestral state reconstructions for anterior fusions.

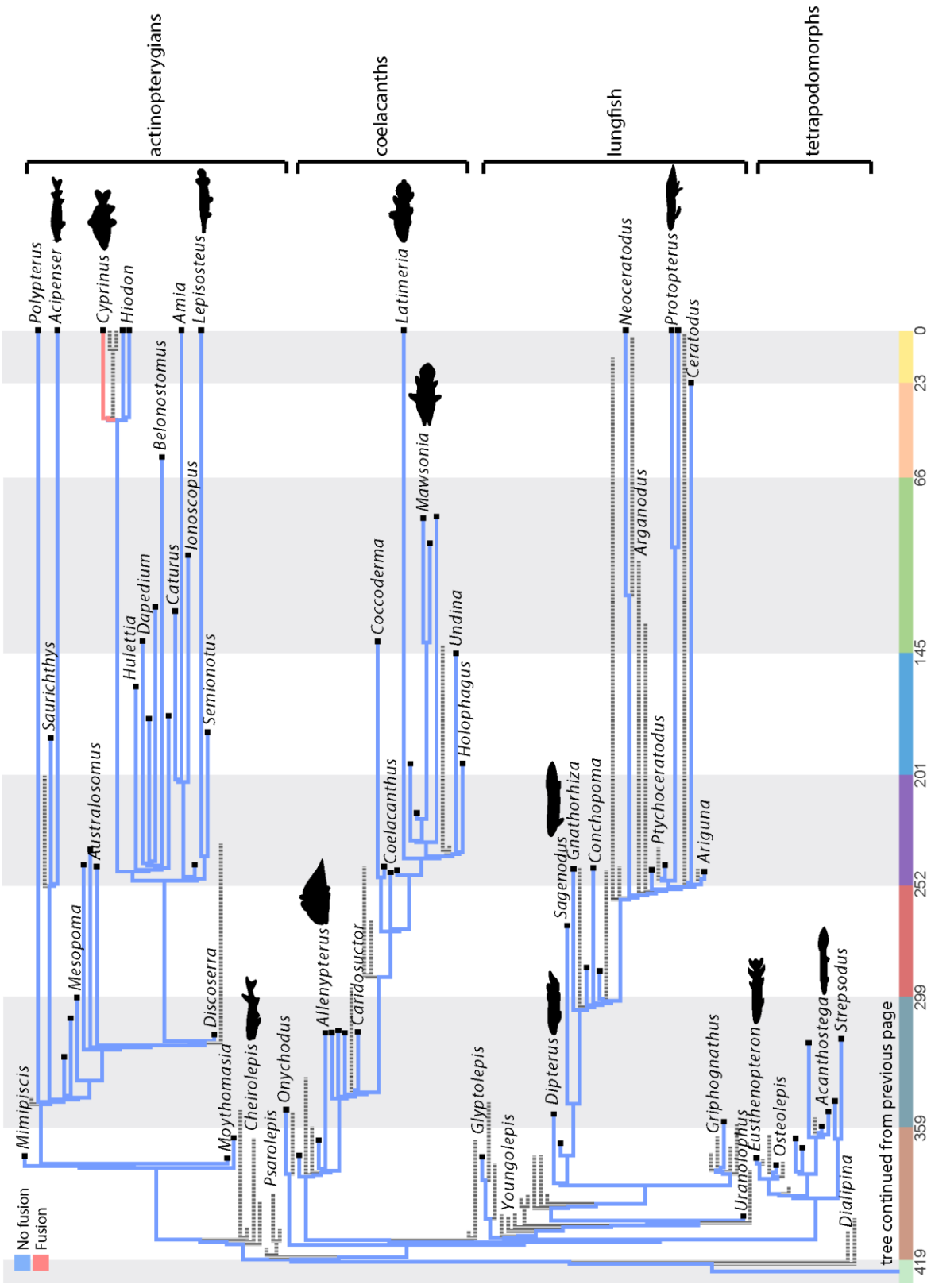

Figure 2.10 continued. Parsimony ancestral state reconstructions for anterior fusions

Figure 2.10 continued. of the vertebral column, separated over two pages. Absence of fusions is colored blue, while fusions are colored red. Silhouettes highlight key taxa and clades are denoted by brackets. The tree is time-scaled and plotted over geologic time, with dates and time scale colors added to the bottom.

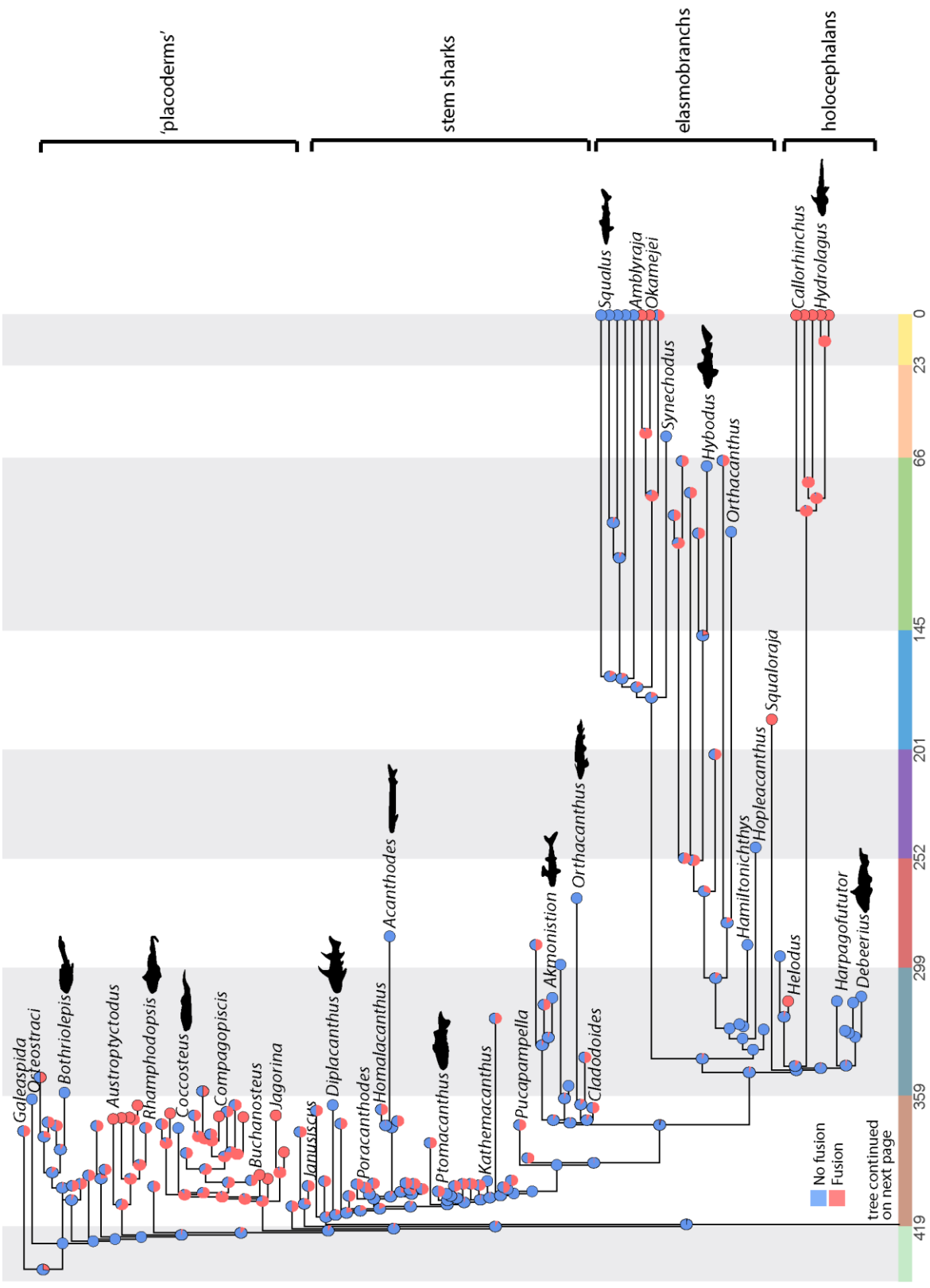

Figure 2.11. Threshold model-based ancestral state reconstructions for anterior fusions

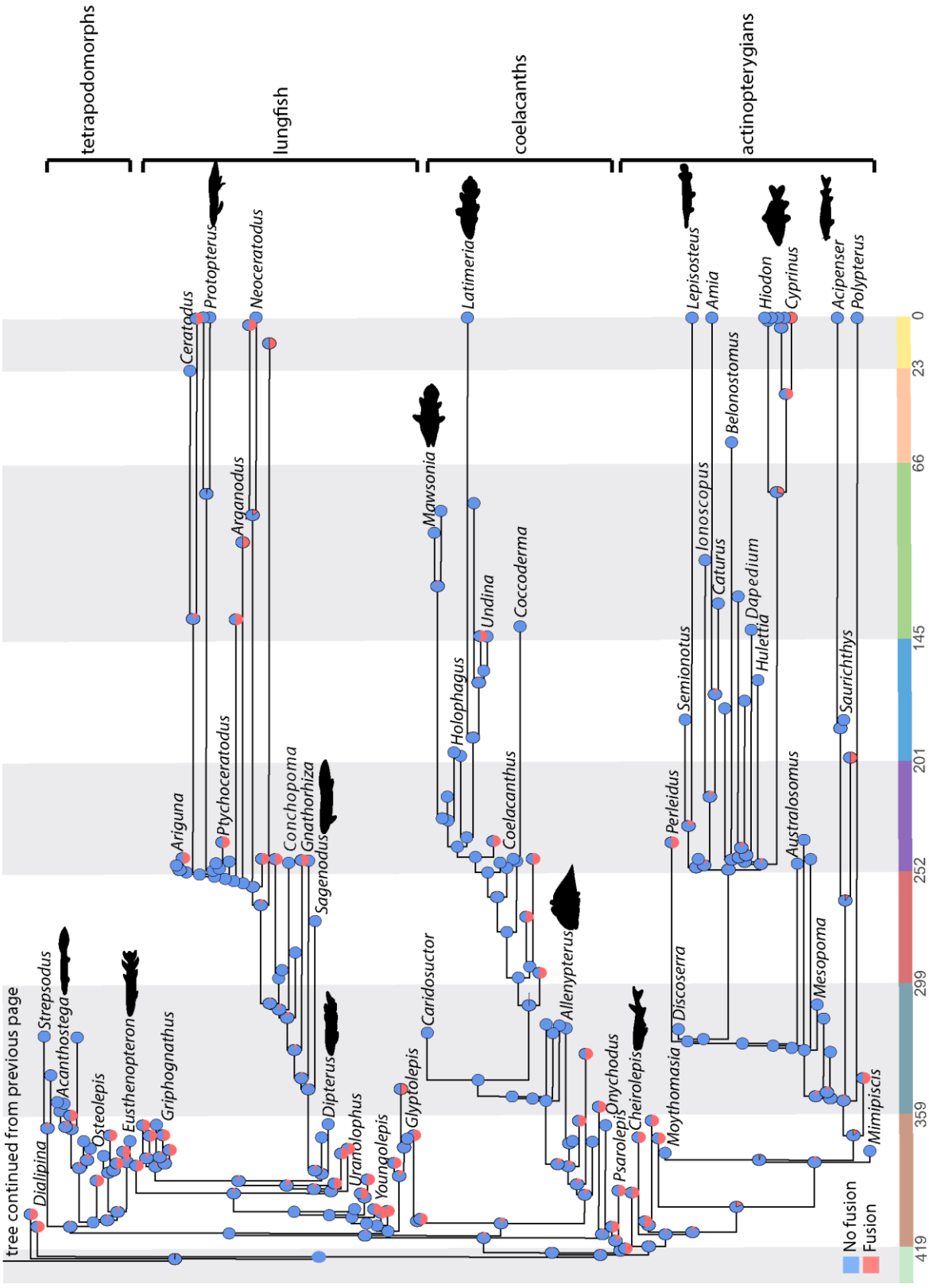

Figure 2.11 continued. Threshold model-based ancestral state reconstructions for anterior

Figure 2.11 continued. fusions of the vertebral column, separated over two pages. Absence fusions is colored blue, while fusions are colored red. Silhouettes highlight key taxa and clades are denoted by brackets. The tree is time-scaled and plotted over geologic time, with dates and time scale colors added to the bottom.

In chondrichthyans, synarcuals have originated independently in both the chimaeroids, as a support for the dorsal fin spine and associated musculature (Figure 2.12b), and in the batoids, to absorb the force of the massive pectoral girdle and fins (Johanson et al., 2013) (Figure 2.10, 2.11). Synarcuals evolved only once in elasmobranchs, in the monophyletic batoids, for which they are a synapomorphy (Claeson, 2011; Aschliman et al., 2012) (Claeson, 2011; Aschliman et al., 2012). Maximum likelihood reconstructs the absence of a synarcual as the primitive state in the holocephalans, while parsimony reconstructs both absence and presence as equally. In all analyses synarcuals are absent at the base of both the Holocephali (0.9999 proportional likelihood and 0.9278 posterior probability) and the Elasmobranchii (0.9945 proportional likelihood and 0.9790 posterior probability), providing strong evidence these instances represent independent originations.

One additional anterior vertebral fusion/modification occurs in the otophysan teleosts, in the form of the Weberian apparatus. This structure usually incorporates the first three to five vertebrae with various degrees of fusion (Bird and Mabee, 2003) and functions in transmitting sound vibrations from the swim bladder anterior to the otoliths (Coburn and Grubach, 1998). In some groups, such as catfishes, these vertebrae are completely fused to form a single structure (Figure 2.12c), but in others, such as the cyprinids, they are modified into ossicles and articulated to form this specialized organ.

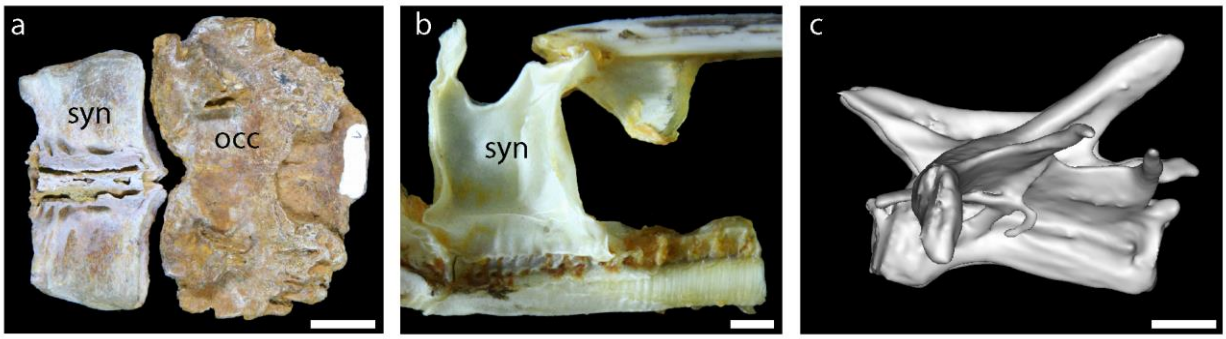

Figure 2.12. Anterior vertebral fusions in ‘placoderms’, chondrichthyans, and otophysan actinopterygians. a, dorsal view of the synarcual and occipital of the ‘placoderm’ *Nefudina qalibahensis* MNHN ARB 237 JW2B7; b, lateral view of the synarcual of the holocephalan *Hydrolagus novezealandia* ANSP 177827; c, lateral view of the Weberian apparatus of the madtom catfish *Noturus eleutherus*. syn, synarcual; occ, occiput. Anterior is to the left and scale bars equal one cm.

Clade	Reconstruction Method	Model	Missing data	Ancestral state	Likelihood/ Probability
Antiarchs	Parsimony	Unordered		Absent	
	Maximum likelihood	Mk1	83%	Equivocal	
	Bayesian Inference	Threshold		Absent	0.7766
Ptyctodonts	Parsimony	Unordered		Present	
	Maximum likelihood	Mk1	20%	Present	0.9811
	Bayesian Inference	Threshold		Present	0.8860
Arthrodires + others	Parsimony	Unordered		Present	
	Maximum likelihood	Mk1	44%	Present	0.9984
	Bayesian Inference	Threshold		Present	0.8222
Chondrichthyans	Parsimony	Unordered		Absent	
	Maximum likelihood	Mk1	26%	Equivocal	
	Bayesian Inference	Threshold		Absent	0.6711
Elasmobranchs	Parsimony	Unordered		Absent	
	Maximum likelihood	Mk1	52%	Absent	0.9945
	Bayesian Inference	Threshold		Absent	0.9790
Holocephalans	Parsimony	Unordered		Absent	
	Maximum likelihood	Mk1	0%	Absent	0.9999
	Bayesian Inference	Threshold		Absent	0.9278
Osteichthyans	Parsimony	Unordered		Absent	
	Maximum likelihood	Mk1	41%	Equivocal	
	Bayesian Inference	Threshold		Absent	0.6891
Tetrapodomorphs	Parsimony	Unordered		Absent	
	Maximum likelihood	Mk1	29%	Absent	0.9999
	Bayesian Inference	Threshold		Absent	0.9259
Actinistians	Parsimony	Unordered		Absent	
	Maximum likelihood	Mk1	32%	Absent	0.9999
	Bayesian Inference	Threshold		Absent	0.7876
Porolepiforms	Parsimony	Unordered		Absent	
	Maximum likelihood	Mk1	60%	Absent	0.9999
	Bayesian Inference	Threshold		Absent	0.8752
Actinopterygians	Parsimony	Unordered		Absent	
	Maximum likelihood	Mk1	17%	Absent	0.9999
	Bayesian Inference	Threshold		Absent	0.8940
Neopterygians	Parsimony	Unordered		Absent	
	Maximum likelihood	Mk1	0%	Absent	0.9999
	Bayesian Inference	Threshold		Absent	0.9522
Teleosts	Parsimony	Unordered		Absent	
	Maximum likelihood	Mk1	0%	Absent	0.9993
	Bayesian Inference	Threshold		Absent	0.9484

Table 2.3. Ancestral states inferred for the evolution of anterior fusions, using parsimony, the

Table 2.3 continued. Mk1 likelihood model, and Bayesian inference. Included are the model of evolution and the percent missing data for each clade listed. Proportional likelihoods and posterior probabilities are reported for maximum likelihood and Bayesian analyses.

Polyspondyly has evolved independently in chondrichthyans and actinopterygians

Ancestrally for jawed vertebrates, the relationship between vertebrae and myotomal segments, as well as centra and arches, was one to one (Figures 2.13, 2.14). Additionally, absence of polyspondyly has been reconstructed as the primitive condition for almost every major group of jawed vertebrates, with all reconstruction methods generally in agreement (Table 2.3). Like many other characters discussed here, polyspondyly seems to have evolved many times, with two independent originations within the chondrichthyans, and up to five separate originations within actinopterygians.

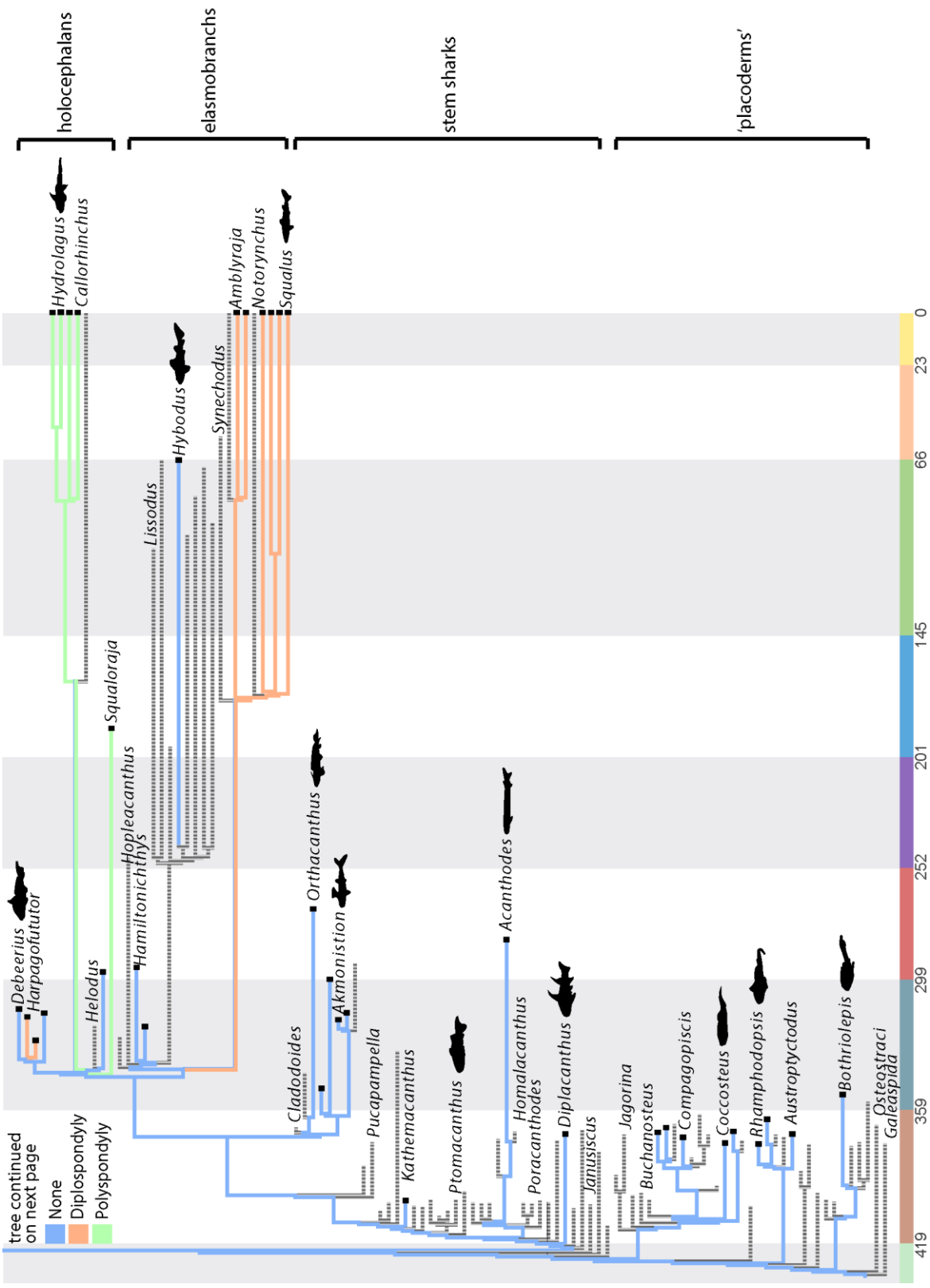

Figure 2.13. Parsimony ancestral state reconstructions for polyspondyly.

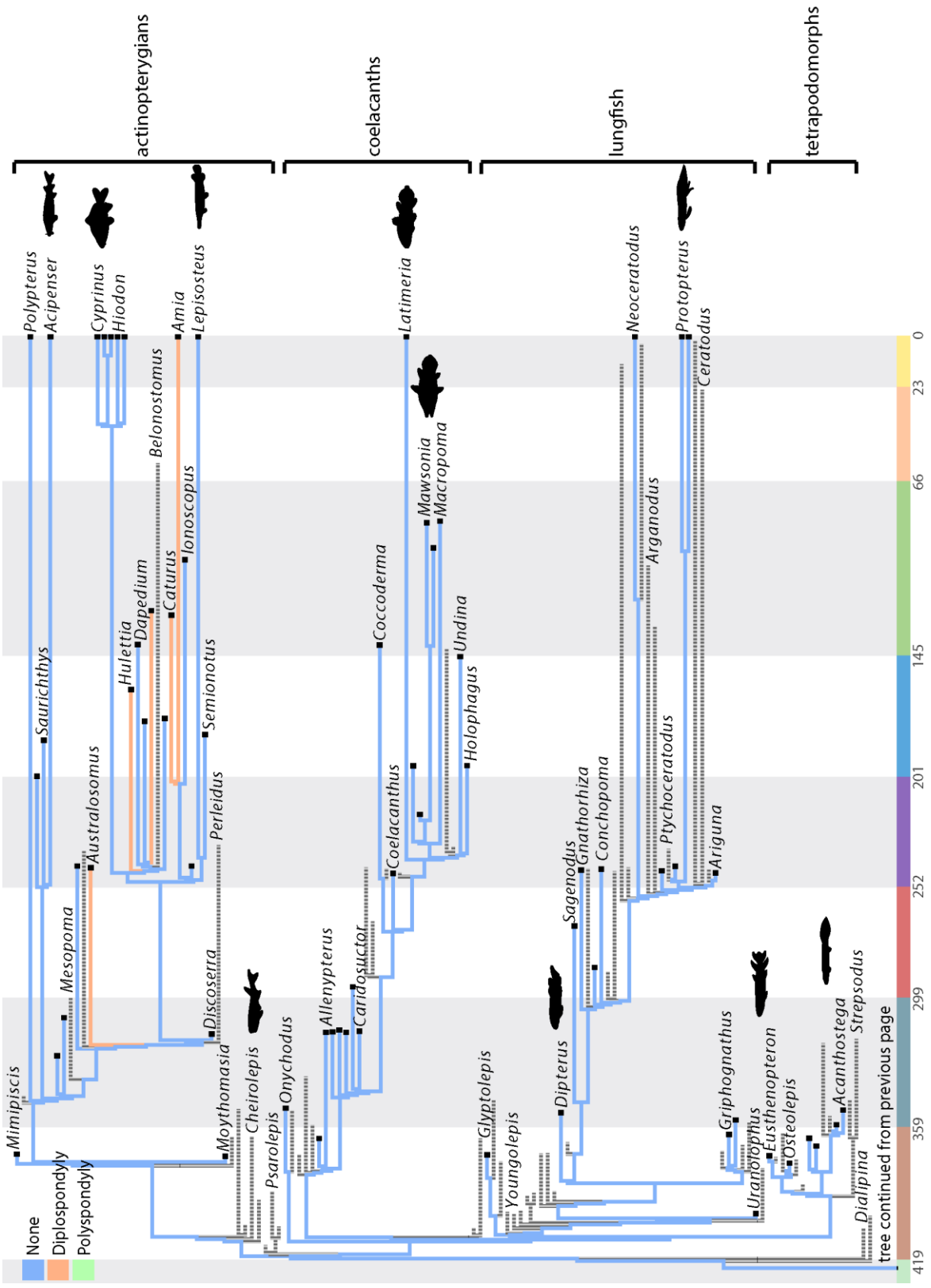

Figure 2.13 continued. Parsimony ancestral state reconstructions for polyspondyly,

Figure 2.13 continued. separated over two pages. Absence of polyspondyly is colored blue, caudal diplospondyly is colored orange, and polyspondyly throughout the vertebral column is colored green. Silhouettes highlight key taxa and clades are denoted by brackets. The tree is time-scaled and plotted over geologic time, with dates and time scale colors added to the bottom.

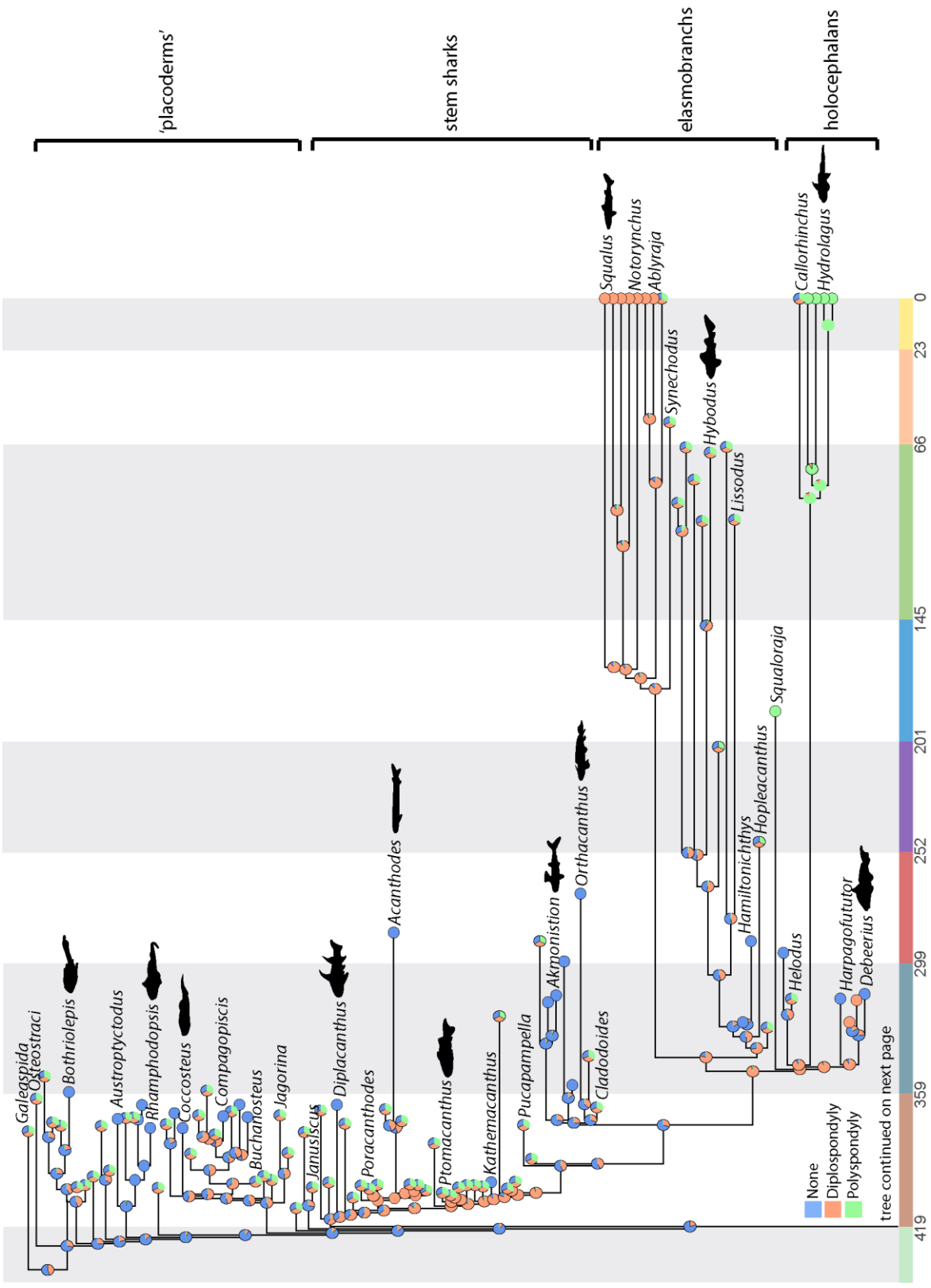

Figure 2.14. Threshold model-based ancestral state reconstructions for polyspondyly.

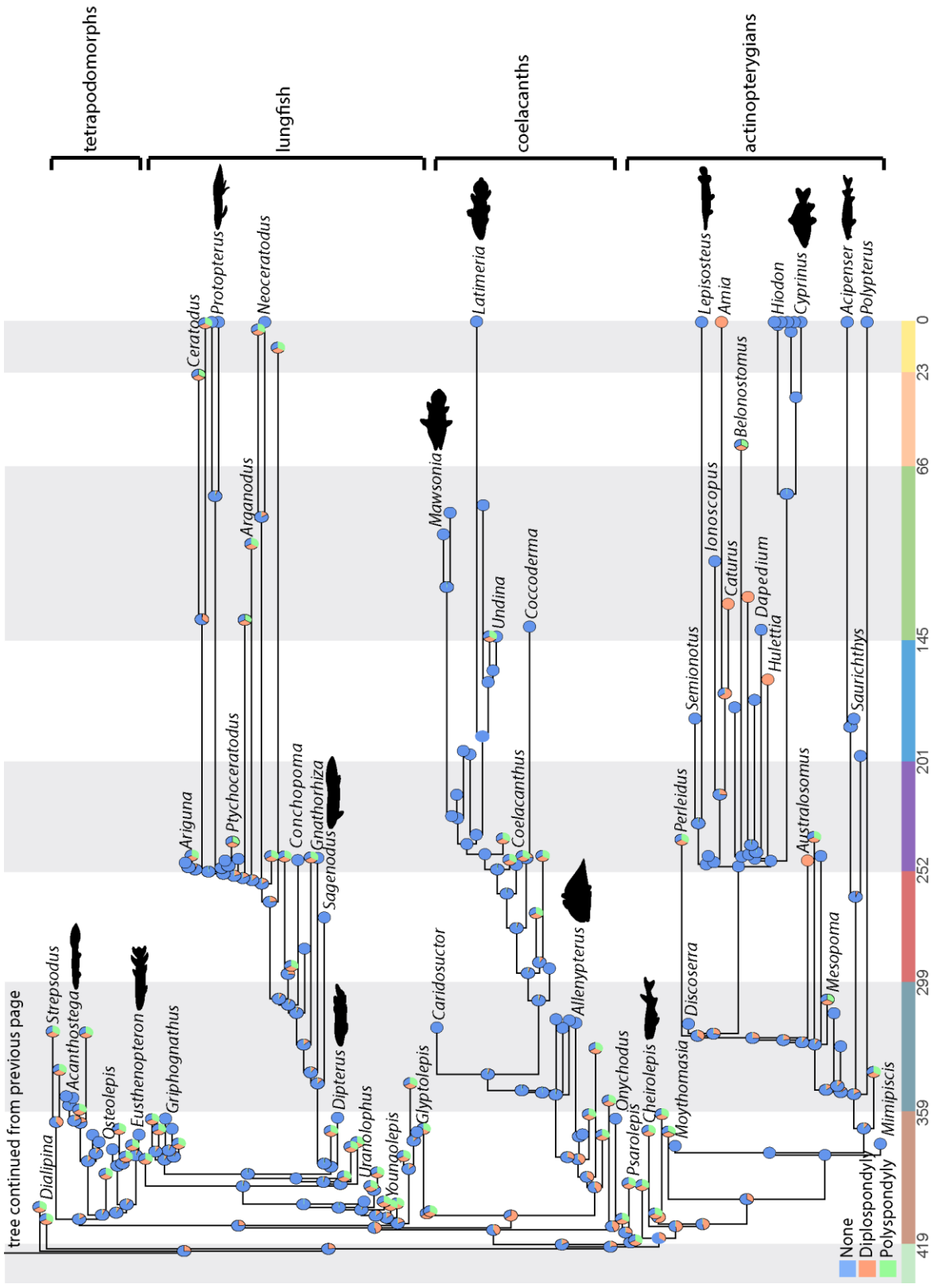

Figure 2.14 continued. Threshold model-based ancestral state reconstructions for polyspondyly,

Figure 2.14 continued. separated over two pages. Absence of polyspondyly is colored blue, caudal diplospondyly is colored orange, and polyspondyly throughout the vertebral column is colored green. Silhouettes highlight key taxa and clades are denoted by brackets. The tree is time-scaled and plotted over geologic time, with dates and time scale colors added to the bottom.

Within chondrichthyans, holocephalans show both caudal diplospondyly or polyspondyly (e.g. *Harpagofututor*, Figure 2.5a; *Chondrenchelys*) and extreme polyspondyly throughout the axial column, in the form of up to five centra, or calcified rings, for each body segment (e.g. *Squaloraja*, *Hydrolagus*) (Figure 2.5b, c). The centra of *Squaloraja* are substantially different than those of extant chimaeras, with thoroughly mineralized centra and a nearly-completely constricted notochord. In extant chimaeras, the polyspondyly comes in the form of rings that calcify around the notochord, but do not constrict it, very late in development (Didier 1995).

Within extant elasmobranchs, the caudal regions of both sharks and batoids show a duplication of entire vertebrae in the caudal region, a form of caudal diplospondyly that is different from other groups of jawed vertebrates (Ridewell 1899). This duplication can be easily seen by comparing the position of the spinal nerve roots in the caudal and precaudal regions (Figure 2.5e, also see chapter three of this dissertation).

Vertebrae change from a monospondylous state to a diplospondylous condition in the caudal regions of several neopterygian species, including *Hulettia, Caturus,* and *Amia* (Figure 2.7a, c, d). In all of these taxa the centra are duplicated in the caudal region, showing two centra for each set of arches, and therefore each myotomal segment. Parsimony reconstructs absence of polyspondyly as the ancestral condition for actinopterygians, as well as for each successive node in the actinopterygian clade, suggesting that all taxa that have evolved diplospondyly have done so independently of one another. The threshold model recovers similar results with slightly less confidence, with the absence of polyspondyly showing posterior probabilities of 0.8446, 0.8879,

and 0.8295 for actinopterygians as a whole, neopterygians, and teleosts, respectively. Maximum likelihood reconstructions were equivocal for most actinopterygian nodes.

Diplospondyly has also been documented in several species of extinct teleost, which were not included in this analysis, such as *Lycoptera*, *Galkinia*, and *Enchelion* (Gardiner, 1983; Filleul and Dutheil, 2004), indicating that diplospondyly may have evolved a fifth time within the osteoglossomorphs, a sister group to most other teleosts. An interesting, and seemingly unique, elaboration of the neural arches has been documented in the extinct and elongate actinopterygian *Saurichthys* (Maxwell et al., 2013). All known species of *Saurichthys* lack centra but have both neural and intercalary arches. In a well-preserved specimen of the Triassic *Saurichthys curionii*, the relationship between myosepta and vertebrae has been documented in detail, showing that the intercalary arches have been elongated to form two sets of neural arches for each centrum and myotomal segment.

Clade	Reconstruction Method	Model	Missing data	Ancestral state	Likelihood/ Probability
Antiarchs	Parsimony	Unordered	83%	None	
	Maximum likelihood	Mk1		Equivocal	
	Bayesian Inference	Threshold		None	0.6066
Ptyctodonts	Parsimony	Unordered	40%	None	
	Maximum likelihood	Mk1		None	0.9999
	Bayesian Inference	Threshold		None	0.9151
Arthrodires + others	Parsimony	Unordered	69%	None	
	Maximum likelihood	Mk1		Equivocal	
	Bayesian Inference	Threshold		None	0.6885
Chondrichthyans	Parsimony	Unordered	44%	None	
	Maximum likelihood	Mk1		Equivocal	
	Bayesian Inference	Threshold		None/diplo	0.5450/0.4544
Elasmobranchs	Parsimony	Unordered	57%	None/diplo	
	Maximum likelihood	Mk1		Equivocal	
	Bayesian Inference	Threshold		None	0.6882
Holocephalans	Parsimony	Unordered	17%	None	
	Maximum likelihood	Mk1		None	0.9999
	Bayesian Inference	Threshold		None	0.6444
Osteichthyans	Parsimony	Unordered	49.6%	None	
	Maximum likelihood	Mk1		Equivocal	
	Bayesian Inference	Threshold		None	0.7098
Tetrapodomorphs	Parsimony	Unordered	57%	None	
	Maximum likelihood	Mk1		Equivocal	
	Bayesian Inference	Threshold		None	0.8729
Actinistians	Parsimony	Unordered	39%	None	
	Maximum likelihood	Mk1		Equivocal	
	Bayesian Inference	Threshold		None	0.7511
Porolepiforms	Parsimony	Unordered	45%	None	
	Maximum likelihood	Mk1		None	0.9999
	Bayesian Inference	Threshold		None	0.8364
Actinopterygians	Parsimony	Unordered	24%	None	
	Maximum likelihood	Mk1		Equivocal	
	Bayesian Inference	Threshold		None	0.8446
Neopterygians	Parsimony	Unordered	6%	None	
	Maximum likelihood	Mk1		Equivocal	
	Bayesian Inference	Threshold		None	0.8879
Teleosts	Parsimony	Unordered		None	
	Maximum likelihood	Mk1	0%	None	0.9999
	Bayesian Inference	Threshold		None	0.8253

Table 2.4. Ancestral states inferred for polyspondyly, using parsimony, the Mk1 likelihood model, and Bayesian inference. Included are the model of evolution and the percent missing data

Table 2.4 continued. for each clade listed. Proportional likelihoods and posterior probabilities are reported for maximum likelihood and Bayesian analyses.

Additional variation in gnathostome vertebrae

In addition to centra, anterior fusions, and polyspondyly, I examined the evolution of characters such as fusions of the neural and hemal arches and presence of intercalary elements using parsimony-based ancestral state reconstructions. These features have less obvious functional advantages, and were often more difficult to code because they require exceptional preservation. Fossil fish also are often mediolaterally compressed, making characters like neural arch fusions difficult to detect.

Ancestrally, the neural arches arose as paired structures that developed on either side of the spinal cord and remained separate at the midline of the body, but throughout gnathostome evolution the arches have repeatedly fused to form singular, midline structures. Fusion of the neural arches in all or part of the axial column has occurred independently in the arthrodires, in the chondrichthyans (both in extant elasmobranchs and in Carboniferous sharks like *Tristychius*), throughout the coelacanths, twice in the porolepiforms, and numerous times throughout the actinopterygians.

Intercalary arches form along with the main neural and hemal arches in a number of different groups, including elasmobranchs, holocephalans, actinopterygians, and lungfish. Many of these, including the 'placoderms', 'acanthodians', symmoriid sharks, coelacanths, most lungfish, and numerous early actinopterygians, including *Mimipiscis* and *Moythomasia,* have no interdorsals or interventrals. Within elasmobranchs, the vertebrae of many taxa comprise both dorsal and ventral intercalary elements (e.g. *Rhinobatis, Heterodontus*) while in others only the dorsal intercalary arches are present (e.g. *Leucoraja*). Dorsal intercalary elements are present in

Carboniferous and Permian as well as extant holocephalans, but it is unclear whether interdorsals are ancestral for Holocephali. Within lungfish, small interdorsal cartilages have been found occasionally in the very posterior portion of the tail, but are not known throughout the rest of the group (Arratia et al., 2001). Intercalary elements seem to have evolved independently within actinopterygians at least three times: once in the chondrosteans, once in the lineage leading to *Amia*, and once along the neopterygian stem.

Discussion

Missing data preclude strong conclusions at the largest evolutionary splits

Within most major clades there are enough well-preserved fossils with axial columns to infer ancestral states, and therefore, independent originations. However, the nodes representing the primary gnathostome divisions: the split between osteichthyans and chondrichthyans, the actinopterygian and sarcopterygian divergence, and the elasmobranch-holocephalan split are populated by taxa lacking vertebral preservation. Some of these key taxa include *Lophosteus*, *Youngolepis*, *Psarolepis*, *Achoania*, and *Ligulalepis* (Figure 2.1), which consist largely of isolated heads without postcranial preservation (Zhu and Fan, 1995; Yu, 1998; Basden and Young, 2001; Zhu et al., 2001; Schultze and Märss, 2004). The ancestral state reconstruction results from the maximum likelihood- and Bayesian inference-based analyses were equivocal or poorly supported for the bases of Chondrichthyes and Osteichthyes, suggesting that at present primitive vertebral conditions cannot be assigned confidently.

Within each major clade, however, sufficient vertebral preservation is present in early members, providing more robust estimates of ancestral states. For example, although the earliest sarcopterygian fossils lack vertebral columns (as well as most of their postcrania), evidence from

early coelacanths (*Holopterygius, Serenichthys*), early porolepiforms and lungfish (*Glyptolepis, Uranolophus*), and early tetrapodomorphs (*Eusthenopteron, Osteolepis*) help to polarize the character transformations within each clade. By shifting the focus of each group slightly crownward, ancestral states can be confidently estimated, with any character state changes occurring in deeply nested taxa likely to be independent of other clades.

In addition to missing data, another problem with the threshold model lies in the assignment of prior probabilities for uncertain taxa. In the threshold model analysis, when the character state for a given taxon is unknown, the prior probability assigned to each state is equal, with no reference to outgroup conditions (Revell, 2014). When character states for multiple taxa in a clade are unknown, the equal prior probabilities can artificially increase the weight of some character states that are unlikely to occur, and decrease the weight of more likely states. For example, no 'acanthodian' fossils have ever been recovered with centra, and the primitive condition for nodes both crownward and stemward is an absence of centra, but still there are many 'acanthodians' for which no vertebrae are known. It seems more likely that the taxa for which we have no data lack centra, like all of the known 'acanthodians', but the threshold model reconstructs higher posterior probabilities for ring centra than seem realistic (see Figure 2.2, at the node between *Homalacanthus* and *Acanthodes*, where the posterior probability for ring centra is >0.5). These equivalent priors for unknown taxa could be lowering the confidence of reconstructed states for many nodes throughout the tree that include taxa without vertebral preservation.

Because ancestral state reconstructions require a source tree onto which to test models of character evolution, the resulting inferences are dependent on the phylogenetic resolution available. Some hypotheses of gnathostome relationships included in the supertree presented in

this chapter, such as the fossil actinopterygians and early chondrichthyans, are (or until very recently were) lacking in reliable phylogenetic analyses. For example, numerous early actinopterygian fossils with axial preservation exist, but they have not been incorporated into phylogenetic analyses, resulting in a supertree that likely undersamples actinopterygian vertebral morphology. Therefore, this tree likely includes several outdated or spurious sets of relationships that will be corrected in the near future with pending new phylogenetic analyses.

When did modern vertebral morphologies arise in each clade?

Modern vertebral morphologies (i.e. centra) originated at different times in the history of each respective gnathostome clade. Some clades evolve centra midway through their history, while others seem to experiment with centra early in their existence and then settle on one condition that persists to the present. For example, chondrichthyans (including 'acanthodians' as stem chondrichthyans) likely diverged from the osteichthyans late in the Silurian Period (~425 MA). Within the chondrichthyans, the first holocephalan centra are known from the Carboniferous chondrenchelyids (~330 MA) while elasmobranch centra are not known until the Permian (~255 MA), in the stem elasmobranch *Hopleacanthus* (Schaumberg, 1982).

Within the osteichthyans, lungfish are an interesting example of early experimentation and then apparent stabilization, as several taxa (*Soederberghia* and *Griphognathus*) evolved full centra in the Devonian Period (~385 MA), but since then no other members of the clade have been found with mineralized centra. Ring centra are present in tetrapodomorphs from the earliest appearance of the clade in the mid Devonian, and remain the general condition until they are modified by tetrapods in the Carboniferous. Coelacanths do not seem to have ever evolved centra

and their vertebrae have changed very little since the first appearance of the clade in the Devonian Period.

The lack of early actinopterygians with reliable phylogenetic location data mentioned previously is problematic when trying to determine the earliest appearances of centra. The range extensions displayed in the time-scaled supertrees suggest that actinopterygian taxa seem to have evolved a variety of vertebral morphologies early in their evolutionary history. When examined in more detail however, the earliest known fossils exhibiting those morphologies are dated to much later than the trees indicate. For example, the ghost lineage inferred on the time-scaled tree for *Polypterus*, a taxon with full centra, extends back to the early Carboniferous, well before any other actinopterygians with centra are known. In reality very few fossil polypterids exist, with the Late Cretaceous *Serenoichthys* being the oldest (Friedman, 2015). Some of the earliest known actinopterygians with centra include the Carboniferous forms with ring centra, *Tarassius* and *Phanerosteon* (Sallan, 2012). The haplolepids from the Carboniferous also exhibit ring centra just posterior to the head, although the phylogenetic position of these actinopterygians is not known (Baum and Lund, 1974). Apart from these taxa, actinopterygians with centra are not known until the Mesozoic *Australosomus* (~250 MA) (Nielsen, 1942). These discrepancies highlight the problems of using supertrees to study macroevolutionary patterns, and will hopefully be resolved with the addition of new fossils and source phylogenies.

Why do vertebral modifications evolve frequently, and why are they rarely lost?

Centra have evolved many times in nearly every gnathostome clade, but loss of centra is rare among gnathostomes, suggesting that it is evolutionarily advantageous to have centra. One of the hypothesized advantages of centra suggests that adding mineralized rings to the axial

column, along with other morphological adaptations such as horizontal septa in the axial muscles and an epicercal tail, stiffened the body and allowed for a faster rate of bending during swimming (Koob and Long, 2000). Faster bending would, in turn, result in faster steady swimming and greater starting accelerations. When plotted on a simplified early gnathostome phylogenetic tree, the appearance of centra correlates with the proposed evolution of pelagic carangiform swimming (Koob and Long, 2000). Indeed, the few extant taxa known to lack or have reduced centra (coelacanths, lungfish, paddlefish, sturgeons, and hexachiform sharks) are generally slow-moving and are filter feeders, omnivores, or scavengers. Adding to this evidence, many of the clades that lack centra are known for persisting for millions of years with largely unchanged ecological lifestyles and morphologies. However, these correlations are merely qualitative and the proposed mechanical changes and evolutionary functions are speculative and have not been tested.

Beyond the speculation about the possible mechanical advantages centra might provide, there have been several quantitative tests of the function of centra within living sharks. Porter and Long (2010) performed compressive load-bearing experiments on the vertebral column including 1) the arches and centra, and 2) on centra dissected from the arches, in the gray smoothhound shark (*Mustelus californicus*) to determine whether centra are the major load-bearing component of the vertebral column. They found that dissected centra were able to support loads similar to those of whole vertebral columns (centra plus arches), which suggests that the arches provide little load-bearing support and that evolving centra is mechanically beneficial. Centrum proportions have also been shown to correlate with potential body curvature in several species of sharks. Porter et al. (2009) compared morphometric data from shark centra to the minimum bending angle in six species and found that second moment of area, centrum

length, and centrum height are all significantly correlated. These results again provide evidence that the presence and proportions of centra can have measureable effects on axial mobility. However, biomechanical testing of the relationship between the presence of centra and axial mobility seems to be a neglected area of research in need of additional study.

In addition to centra, synarcuals have evolved multiple times to result in a stiffening of the anterior trunk. Synarcuals have a clear functional purpose in providing a base for the muscles that raise and lower the dorsal fin and spine in chimaeras, and in absorbing the force of the pectoral fins in batoids, and have not been lost in any known lineages (Figure 2.10; 2.11). In 'placoderms', the functional advantage of the synarcual has been hypothesized that fusing the anterior neural arches facilitated the actions of raising the head to eat or breathe (Denison, 1983). The function of the ossicles and fused vertebraeWeberian apparatus of otophysan actinopterygians as a sound transport mechanism is well understood (Ladich, 2001). In some otophysans, such as the armored catfishes, the fused Weberian apparatus may also have helped to stiffen the neck within the armored scales, as it likely did in 'placoderms' (Denison, 1983). Anterior vertebral fusions (termed syncervicals) are actually known also in numerous tetrapods, including rodents, cetaceans, xenarthrans, squamates, dinosaurs, ichthyosaurs, and plesiosaurs (Van Buren and Evans, 2016). The functional significance of these fusions varies, from adaptations for fossoriality in moles and amphisbaenians, to support for heavy skulls with cranial ornamentation in ornithischian dinosaurs.

It has also been speculated that diplospondyly in the caudal region of sharks and actinopterygians is biomechanically advantageous. It was originally thought that diplospondyly evolved to provide increased flexibility to the tail during swimming (Ridewood, 1899; Schaeffer, 1967a). With additional vertebrae or centra in each myotomal segment, the tail can achieve

greater control over the pattern of locomotion (Lauder, 1980). However, these hypotheses have not been tested with biomechanical models. Additionally, few explanations exist in the literature for the function of the polyspondyly seen in the vertebrae of holocephalans, in which up to five calcified rings surround the notochord. Extant holocephalans swim using pectoral fin-based flapping motion, while keeping their axial column steady (Foster and Higham, 2010), suggesting that a flexible vertebral column is not necessary or advantageous. It is possible that adding calcified rings to the notochord would increase the stiffness of the axial column, although experiments are needed to test this hypothesis. Morphological data from several tetrapod taxa, including whales and tanystropheid archosaurs, support this hypothesis. Tanystropheids have an elongate and flexible vertebral column and the cervical vertebrae are, in turn, elongated (Pritchard et al., 2015). Conversely, whales have shortened necks, and whale cervical vertebrae are either fused or shortened to provide stiffness, in a pattern similar to that of extant holocephalans (Buchholtz, 2001).

How does centrum development differ in instances of independent origination?

These results raise intriguing questions about the developmental mechanisms behind the many different iterations of centra described here. Are the centra that evolved repeatedly within teleosts, elasmobranchs, and tetrapodomorphs, and seem to be constructed in different patterns, built using the same genetic pathways and embryonic tissues? Centrum development has been studied, in some manner, in several species of chondrichthyan (*Scyliorhinus, Cephaloscyllium*), non-teleost actinopterygian (*Amia, Lepisosteus, Polypterus*), teleost (*Danio, Salmo*), and tetrapod (*Ambystoma, Gallus, Mus).* In chondrichthyans, centra seem to develop from cells migrating into a fibrous sheath that surrounds the notochord, although these observations are based on sharks

and little data exist for batoids (Gadow and Abbott, 1895; Eames et al., 2007). As described above, centra in *Amia* form from expanding arch bases, *Lepisosteus* centra form through the condensation of a cartilaginous tube of tissue surrounding the notochord, and *Polypterus* centra are deposited as intramembranous ossifications (Balfour and Parker, 1882; Hay, 1895; Bartsch and Gemballa, 1992). Within teleosts centra also differ in their construction, although these likely represent a single origination. Centra in *Salmo* first appear as a small ring of chordoblast cells surrounding the notochord and grow through deposition of mesenchymal cells (Nordvik et al., 2005) and *Danio* centra form without cartilaginous precursors and do not develop the layers seen in salmon (Bird and Mabee, 2003). Although the mechanisms of centrum growth differ among these many examples, little is known about the genetic pathways and tissues of origin involved in creating this diversity. Thorough studies of vertebral development in taxa such as extant holocephalans, batoids, and early-branching teleosts like osteoglossomorphs or elopomorphs would provide further information on the diversity of centrum construction. More specifically, experiments documenting the embryonic origins of centra and arches and genetic controls of vertebral development in key taxa such as *Lepisosteus, Polypterus*, an early-branching teleost, and a cartilaginous fish are crucial for understanding whether these similar, but independently-derived structures are produced using the same, or widely divergent developmental processes.

Conclusions

In this chapter I have shown that vertebral modifications, including the presence of centra, anterior fusions of the vertebral column, polyspondyly, fusions of the neural arches, and intercalary elements all evolved repeatedly throughout the gnathostome evolutionary tree.

Additionally, those modifications arose early in the history of each clade and remained constant into the present, indicating that many of these features were evolutionarily advantageous.

The vertebral column provides an excellent system in which to study convergent evolution in a wide variety of taxa. The diversity of vertebral construction documented to date suggests that the developmental mechanisms that build centra may vary in each independent origination, but it is still unclear what those mechanisms are. The vertebral skeletons of the taxa discussed in this chapter show some differences, but still are comparable enough that by doing the same experiments, and investigating the same genes, in chondrichthyans, actinopterygians, and tetrapods, we can come to understand the evolutionary pathways that centra have taken within each lineage.

Vertebrae have long been considered a clear synapomorphy of vertebrates, but each vertebral character analyzed in this chapter (presence of centra, anterior fusions, polyspondyly, and fusion of the neural arches) showed multiple independent originations across gnathostomes using all methods of ancestral state reconstruction. A deep-time perspective and the inclusion of data from fossil gnathostomes in addition to extant taxa are key to understanding evolutionary patterns on a broad scale. In addition to the near lack of vertebral skeleton found in jawless fishes like lampreys, hagfish, and osteostracans, my findings indicate that vertebrae as most biologists know them are not homologous. Each vertebra should not be considered to be a single unit, but rather to consist of many individual components with separate evolutionary histories. There is no one ideal, archetypal vertebra, as vertebrae as they are commonly regarded did not exist in the last common ancestor of vertebrates.

Chapter 3: Embryonic development of the axial column in the little skate, *Leucoraja erinacea*[1]

Summary

The morphological patterns and molecular mechanisms of vertebral column development are well understood in bony fishes (osteichthyans). However, vertebral column morphology in elasmobranch chondrichthyans (e.g. sharks and skates) differs from that of osteichthyans, and its development has not been extensively studied. Here, I characterize vertebral development in an elasmobranch fish, the little skate, *Leucoraja erinacea*, using microCT, paraffin histology, and whole-mount skeletal preparations. Vertebral development begins with the condensation of mesenchyme, first around the notochord, and subsequently around the neural tube and caudal artery and vein. Mesenchyme around the notochord differentiates into a continuous sheath of spindle-shaped cells, which is the precursor to the mineralized areolar calcification of the centrum. Mesenchyme around the neural tube and caudal artery/vein becomes united by a population of mesenchymal cells that condenses lateral to the sheath of spindle-shaped cells, with this mesenchymal complex eventually differentiating into the hyaline cartilage of the future neural arches, hemal arches and outer centrum. The initially continuous layers of areolar tissue and outer hyaline cartilage eventually subdivide into discrete centra and arches, with the notochord constricted in the center of each vertebra by a late-forming "inner layer" of hyaline cartilage, and by a ring of areolar calcification located medial to the outer vertebral cartilage. The vertebrae of elasmobranchs are distinct among vertebrates, both in terms of their composition (i.e. with centra consisting of up to three tissues layers – an inner cartilage layer, a calcified

[1] This chapter has been modified from a paper currently in revision at the Journal of Morphology.

areolar ring, and an outer layer of hyaline cartilage), and their mode of development (i.e. the subdivision of arch and outer centrum cartilage from an initially continuous layer of hyaline cartilage). Given the striking variation in patterns of vertebral construction, broad taxon sampling and comparative developmental analyses are required to understand the diversity of mechanisms at work in the developing axial skeleton of vertebrates.

Introduction

The vertebral column is a key component of the vertebrate skeleton, providing structural support for the skull and appendicular skeleton, as well as protection for the spinal cord and axial blood vessels. Vertebrae are a defining feature of the vertebrate clade, but different components of the vertebral skeleton, namely the arches and centra, have evolved independently of one another, are variable in their construction, and may therefore be patterned by separate developmental mechanisms (Arratia et al., 2001). In order to gain insight into developmental and evolutionary basis of axial column morphological variation, broad taxon sampling of developmental and anatomical data within vertebrates – and particularly, within jawed vertebrates (gnathostomes) – is needed. However, at present, most data on vertebral column development have been collected from few osteichthyan taxa (i.e. bony fishes and tetrapods) (Fleming et al., 2015). There is a notable paucity of developmental data for the vertebral columns of chondrichthyans (cartilaginous fishes – sharks, skates, rays, and holocephalans), and this results in a biased and incomplete picture of vertebral column evolution within vertebrates.

The onset of vertebral development begins in a similar fashion in all taxa studied to date, when a subpopulation of mesodermal cells undergoes an epithelial to mesenchymal transformation from the ventral somites, and migrates medially as sclerotome (Gadow and

Abbott, 1895; Christ and Wilting, 1992). These sclerotomal cells are thought to condense at dorsolateral and ventrolateral positions, relative to the notochord, and form the neural arch and hemal arch rudiments. After sclerotome migration and condensation, vertebral development, and centrum formation in particular, is more variable. Depending on the taxon, centra may arise via a combination of four general processes: 1) Through arch primordia encircling the notochord (arcocentra); 2) through sclerotomal cells that invade and chondrify within the notochord sheath (chordacentra); 3) through chondrocytes that differentiate around the notochord sheath (holocentra); or 4) through direct ossification outside the notochord sheath (autocentra) (Arratia et al., 2001).

The developmental mechanisms and tissues underlying vertebral formation differ greatly among different vertebrate clades. In teleost fishes (actinopterygians) the vertebrae are composed of acellular bone, in which bone-forming osteoblasts are not incorporated into the skeletal tissue after bone matrix is secreted (Hall, 2005). Centra in zebrafish (*Danio rerio*) form before the arches, by nine days post fertilization, and vertebrae ossify directly, without cartilaginous precursors (Fleming et al., 2004; Bensimon-Brito et al., 2012). The arches form from sclerotomal cells that condense both dorsal to and ventral to the notochord, but centra form from bone matrix that seems to be deposited by the notochord itself (Fleming et al., 2004). In Atlantic salmon (*Salmo salar*), neural and hemal arch cartilages form first and are then encased in bone, with centra developing later through four layers of mineralization. These four layers include the chordacentrum, which mineralizes within the notochord sheath, a thin, continuous perinotochordal layer that covers the notochord, an outer layer of laminin bone making up each centrum, and lastly, cancellous bone with longitudinal trabeculae (Nordvik et al., 2005; Wang et al., 2013). As a third example, chordacentra in the Japanese medaka (*Oryzias latipes*) develop

within the notochord sheath prior to being surrounded by perichordal bone (Ekanayake and Hall, 1987).

In tetrapods (salamander, chick, and mouse), vertebrae have been documented to form entirely from migrating sclerotomal cells that condense around the notochord to form a perichordal tube of tissue that then differentiates into individual vertebral units (Bagnall et al., 1988; Christ and Wilting, 1992; Piekarski and Olsson, 2014). In chick (*Gallus gallus*), the ventral portion of the somite has been fate mapped to specific vertebral components, with the medial-most cell population contributing to the centra, the dorsal sclerotomal cells giving rise to neural spines, and the lateral portion of the sclerotome making up the remainder of the neural arches and ribs (Bagnall et al., 1988; Christ et al., 2000). In the axolotl (*Ambystoma mexicanum*), an amphibian, fate mapping of somites three to five shows somitic contributions to all parts of the vertebrae, including the centra, arches, and intervertebral discs (Piekarski and Olsson, 2014). This variation in vertebral development across vertebrates highlights the need for more data from the sister group of osteichthyans, the cartilaginous fishes (chondrichthyans).

Extant chondrichthyans belong to one of two lineages: the holocephalans and the elasmobranchs. Extant holocephalans comprise the chimaeroids, a small group of largely deep-sea fishes, while extant elasmobranchs include skates and rays (collectively known as batoids) and sharks. Vertebral column anatomy in adult elasmobranchs differs markedly from that of osteichthyans. The elasmobranch vertebral column consists of a zipper-like set of neural and intercalary arches dorsally, along with centrum cartilages that support transverse processes precaudally and hemal arches caudally (Daniel, 1922). A series of mediolaterally flattened neural spines sits in between vertebral boundaries on the dorsal-most surface of the vertebral column throughout the length of the body. The arches consist of a core of hyaline cartilage covered by a

mosaic of blocks of calcified tissue called tesserae in adults (Dean and Summers, 2006). Most elasmobranchs have mineralized chordacentra (centra formed within the notochord sheath), in which cells differentiate into dense rings within the fibrous notochord sheath and are surrounded by apatite in their intercellular spaces, forming a highly cellular, netlike mineralized tissue called areolar calcification (Gadow and Abbott, 1895; Applegate, 1967; Dean and Summers, 2006). These centra take on an hourglass shape, expanding anteriorly and posteriorly, and constrict the notochord considerably at their center, with remnants of the notochord persisting at the intervertebral boundaries. Caudal diplospondyly – a condition in which two vertebrae correspond to each myomere and set of spinal nerves – is well known in many sharks (Ridewood, 1899), but occurs in batoids as well.

Within elasmobranchs, vertebral morphology is variable. In the broadnose seven-gill shark (*Notorynchus cepedianus*), the notochord is surrounded by an unsegmented cartilaginous tube and supports thin, mineralized ring centra that persist into adulthood (Daniel, 1922). In the porbeagle shark (*Lamna nasus*), the hammerhead (*Sphyrna blochii*), the basking shark (*Cetorhinus maximus*), and the guitarfish (*Rhinobatos productus*), heavily mineralized centra form within the fibrous notochord sheath and expand throughout ontogeny to engulf the neural and hemal arches (Ridewood, 1921; Daniel, 1922; Goodrich, 1930). In many elasmobranchs, such as the horn shark (*Heterodontus francisci*), small-spotted catshark (*Scyliorhinus canicula*), little skate (*Leucoraja erinacea),* and some rays (e.g. *Myliobatis aquila*), the cartilage of the arches expands dorsally and ventrally to envelop the calcified centra (Hasse, 1879; Daniel, 1922).

Current understanding of elasmobranch vertebral development derives largely from historical studies on sharks, with only sparse data from skates and rays (for shark data see

Gegenbaur, 1872; Hasse, 1879; Klaatsch, 1893a, 1893b, 1895; Gadow and Abbott, 1895; Goodrich, 1958; and see Klaatsch, 1893b for a discussion of vertebral development in the electric ray *Torpedo ocellata*). These studies demonstrated that the initiation of shark vertebral development proceeds, as in osteichthyans, with the migration of sclerotomal cells toward the notochord sheath. The notochord sheath thickens into a ring of fibrous, spindle-shaped cells, surrounded by a thin membrane, the elastica externa. Sclerotomal mesenchyme is thought to both condense around the notochord, forming cartilaginous units that give rise to the neural and hemal arches, and migrate through the perforated elastica externa and into the fibrous sheath where it differentiates into the cartilage of the centrum.

Historically, sharks have been used as representatives of generalized, and by implication primitive, gnathostome anatomical conditions (e.g. Goodrich 1930). As a result, the classic, and most used, model of vertebral construction, based on vertebral development in sharks, was widely applied to gnathostomes as a whole (Gadow and Abbott, 1895; Gadow, 1933). It suggests that for all gnathostomes each vertebral unit is composed of four pairs of embryonic cartilages, or 'arcualia': two pairs of dorsal elements (basidorsals and interdorsals) and two pairs of ventral elements (basiventrals and interventrals) (Gadow and Abbott, 1895). The basidorsals form the adult neural arches and, when present, the dorsal intercalary arches, and the basiventrals form the hemal arches and ventral intercalary arches. Several key works have pointed out that the 'Arcualia Theory' is not compatible with published evidence for osteichthyan (Schaeffer, 1967a) and acanthodian fishes (Miles, 1970) and the theory has been rejected outright for tetrapods (Williams, 1959). Despite this apparent incongruity, the simplistic arcualia model, and its associated terminology, remains influential and is often used to describe the vertebrae of non-tetrapod gnathostomes in the paleontological and comparative anatomical literature (Jarvik,

1980a, 1980b; Arratia et al., 2001). Additionally, it is unclear whether all elasmobranchs develop according to Gadow and Abbott's (1895) model or whether some clades, such as batoids, deviate from this pattern.

It is clear from the bias of developmental studies towards osteichthyans (zebrafish, chick, and mouse), the lack of studies on vertebral column development in cartilaginous fishes utilizing modern microtomographic (microCT) techniques, and the confusion over current embryological terminology and models, that tests of historical hypotheses and a renewed focus on vertebral column evolution are needed. In order to reconstruct sequences of character evolution for the gnathostome vertebral column – i.e. to determine which developmental processes are general for gnathostomes, and to distinguish between homologous and homoplastic vertebral structures – it is necessary to collect morphological and developmental data from numerous osteichthyan and chondrichthyan taxa. Additionally, an assessment of whether the processes of vertebral development that have been described in sharks are representative for all elasmobranchs requires data on axial column development in batoids. Here, I use computed tomography, histology, and whole mount skeletal preparation to visualize the embryonic development of the axial column in a batoid elasmobranch, the little skate *Leucoraja erinacea*. Crucially, the use of high-resolution microCT scans allowed for the interpretation of detailed anatomy in three dimensions that has not previously been possible. The little skate is an emerging model for studies of gnathostome development and evolution, and as such, the methods employed here will be broadly useful to researchers studying other anatomical systems.

Materials and Methods

Animal collection, husbandry, and fixation

Developmental series of the little skate, *Leucoraja erinacea,* from stages 27 to 34, were obtained from the Marine Resources Center (MRC) at the Marine Biological Laboratory in Woods Hole, MA, USA. Embryonic stages correspond to those described in the staging table of the winter skate, *Leucoraja ocellata* (Maxwell et al., 2008). Little skate embryos reach stage 27 after approximately four weeks of development at 18ºC and have developed small pectoral and pelvic fins. By stage 34, after approximately five months of development, embryos are close to hatching, with dark pigmentation and little external yolk remaining. Embryos were maintained at approximately 18ºC in seawater while at the MRC, until stage 27, and were then maintained at 15ºC in reconstituted Instant Ocean (Aquarium Systems) on at 12-hour light-dark cycle. Upon reaching the appropriate developmental stage, embryos were removed from their keratinous egg cases using a razor blade and euthanized with an overdose of MS-2222 (Ethyl 3-aminobenzoate methanesulfonate – Sigma-Aldrich) (1g/L bath). Embryos were then fixed for 24-48 hours in 4% paraformaldehyde, rinsed three times in 1X phosphate buffered saline (3x5 minutes), and graded into either 100% methanol (MeOH) or ethanol (EtOH) through an ascending series (25%, 50%, 75%, and 100% in 1X PBS, 5min/rinse) and stored at -20º C.

microCT scanning

Embryos of all stages were stained with Iodine Potassium Iodide (IKI) (2% w/v iodine and 1% w/v potassium iodide in water), diluted to 10% in water, for three to five days to provide contrast to soft tissues. Two stage 31 embryos were stained with 5% w/v phosphomolybdic acid (PMA) in MeOH for five days. Both IKI and PMA provide contrast to soft tissues, but PMA is

actually taken up by cartilage, and presents as an even, mid-range gray tone in the CT slices.

Embryos at stages 28-30 and 32-33 were microCT scanned at the University of Texas at Austin CT Laboratory (UTCT) using an XRadia microXCT 400 scanner. Embryos at stages 30, 31, 32, and 34 were microCT scanned in the Department of Organismal Biology at the University of Chicago, using a General Electric Phoenix v|tome|x 240 MicroCT scanner with two X-ray tubes and 16'x16' detector panel of 2048 x 2048 pixel resolution (see Table 1 for scanning parameters). The 180kV 15W high-power NanoFocus tube achieves a maximum voxel resolution of 0.5 μm and can scan organisms in a size range of 15 cm in length by 12 cm in diameter. Resulting scans were segmented using Mimics versions 17.0 and 18.0 (Materialise, Leuven, Belgium).

Stage	**# Scanned**	**Stain**	**kV**	**uA**	**Timing**	**Voxel size**
28	2	IKI	60 70	167 143	3 sec 2 sec	2.90 3.08
29	1	IKI	60	167	3 sec	2.47
30	4	IKI	100 70 70 60	100 143 143 167	2 sec 3 sec 3 sec 2.5	2.63 2.93 2.93 3.08
31	3	PMA PMA IKI	100 40 110	100 250 70	2 sec 4 sec 2 sec	2.95 2.79 3.12
32	1PC 2 C	IKI	100 60 60	100 167 167	2 sec 2 sec 2 sec	2.58 4.16 4.16
33	2 C	IKI	60	167	1.5 sec	4.99
34	1 PC 1 C	IKI	80 100	70 100	4 sec 2 sec	3.76 3.08

Table 3.1. microCT scanning parameters for skate embryos scanned and used in this study. C = caudal region, IKI = iodine potassium iodide, kV = kilovolts, PC = precaudal region, PMA = phosphomolybdic acid, uA = microamps, voxel size in micrometers.

Skeletal preparations

A second series of embryos, corresponding to the stages discussed above, were cleared and stained in whole mount with Alcian blue to visualize the proteoglycan-rich matrix present in vertebral cartilage. This protocol was based on a standard clearing and staining protocol for fishes (Klymkowsky and Hanken, 1991) that was optimized for use on elasmobranch fishes (Gillis et al., 2009). From 100% EtOH, embryos were transferred to 70% EtOH, soaked in acetic EtOH for two hours (3:7 glacial acetic acid:EtOH), and then stained with Alcian blue (0.2mg/ml acetic EtOH) for 24 hours or more. After staining, embryos were destained in acetic EtOH for 24 hours, graded from 70% EtOH into diH_2O, and neutralized in a solution of 30% saturated sodium borate in diH_2O over 24 hours. Embryos were digested in 0.5% trypsin in sodium borate, then rinsed in 30% sodium borate and graded into diH_2O. Embryos were then transferred into 0.5% KOH for at least 24 hours, graded into glycerol over several days to clear, and stored in glycerol. Alcian blue-stained embryos were imaged using a Leica MZFLIII microscope with a Nikon D5000 camera, and the Camera Control Pro software. White balance was adjusted in Adobe Photoshop CS6 using the levels tool; no other editing was performed.

Paraffin histology and staining

A third series of embryos (two specimens per stage) was paraffin embedded and sectioned for histochemical staining with Hematoxylin, Eosin, and Alcian blue (HEA). Hematoxylin is a positively charged, basic dye that stains acidic structures, such as cell nuclei containing DNA and RNA, with a dark violet to bluish color (Fischer et al., 2008). Eosin is a negatively charged, acidic dye that stains basic tissues that include proteins, such as cytoplasm

and sometimes extracellular matrix, pink. As mentioned previously, Alcian blue was used to identify proteoglycan-rich extracellular matrix in section. Older embryos with heavily calcified vertebrae and dermal denticles (stage 32 and above) were demineralized in 10% ethylenediaminetetraacetic acid (EDTA) for 14 days prior to embedding. The embedding process consisted of three 20-minute rinses in histosol (National Diagnostics), followed by two 30-minute rinses in a 50:50 paraffin:histosol solution at 67º C. The tissue was then placed in 100% paraffin overnight at 67º C, and during the following day the paraffin was changed five times before the tissue was placed in embedding blocks and positioned. The tissue was sectioned in transverse or sagittal orientation at a thickness of 8 μm using a Microm HM 330 microtome with Thermo Fisher HP 35 coated blades.

HEA staining was performed on sections according to established protocols (Gillis et al., 2009). Slides were de-waxed with histosol (National Diagnostics) (2 x 5 minutes), and then rehydrated through a descending EtOH series (2 x 5 minutes in 100% EtOH, then 2 minutes each in 90%, 70%, 50%, 30% EtOH), and rinsed in distilled water (2 x 2 minutes). Slides were stained with Mayers Hematoxylin (15 minutes), rinsed in running tap water for 20 minutes, stained with 2mg/mL Alcian blue in acetic EtOH (1 minute), rinsed in 95% EtOH (2 x 2 minutes), and stained with 0.1% Eosin Y (30 seconds to 1 minute). Slides were then rinsed in 95% EtOH (2 minutes), 100% EtOH (2 x 2 minutes), and histosol (2 x 5 minutes) prior to coverslipping with permount. Sections were imaged with a Zeiss Axioplan microscope, Nikon D5000 camera, and Camera Control Pro software. White balance was adjusted in Adobe Photoshop CS6 using the levels tool; no other editing was performed.

Results

Embryonic morphology of the little skate through a series of stages from the beginning of vertebral development to hatching will be presented here. A summary of the major events and tissues present throughout this process will follow this description.

Stage 27

Initially during stage 27, loose mesenchyme appears to surround the notochord as a single layer of cells just peripheral to the notochord epithelium (Figure 3.1a, a'). As development progresses additional mesenchymal cells condense around the notochord, up to five cells thick, to form a continuous layer that extends the length of the body (Figure 3.1b, b').

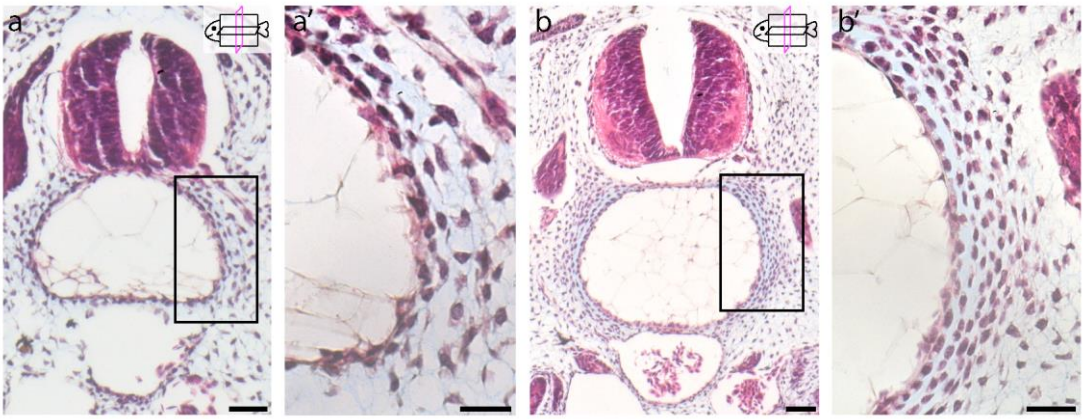

Figure 3.1. Embryonic vertebral morphology in stage 27 skate embryos. a, cross section through an early HEA-stained stage 27 embryo; a', 20x magnification of cells surrounding the notochord in a; b, cross section through a late HEA-stained stage 27 embryo; b', 20x magnification of mesenchymal cells condensing around the notochord in b. Icons in upper right corner indicate plane of section. Scale bars represent 50 µm for a and b, and 25 µm for a' and b'.

Stage 28-29

Incipient vertebral structures (neural and hemal arch mesenchyme) appear at stage 28 and remain largely unchanged through stage 29. The notochord sheath consists of an inner layer that

is approximately two cells thick, surrounded by an outer layer of elongate, spindle-shaped cells arranged concentrically around the notochord and forming a thickened fibrous tube (Figure 3.2a-c'). The spindle-shaped cells surrounding the notochord are embedded in Alcian blue-stained (and therefore presumably proteoglycan-rich) extracellular matrix, and microCT scans show that both neural and hemal arch mesenchyme and this layer of spindle-shaped cells are deposited as unsegmented tubes along the entire anterior-posterior axis (Figure 3.2d-f). Mesenchymal cells condense dorsal and ventral to the notochord, to form the nascent neural and hemal arches, but at this point the mesenchyme has not yet reached the dorsal-most portion of the neural tube (Figure 3.2g-k). Sagittal and horizontal sections reveal that the notochord is unconstricted (Figure 3.2f, l).

Precaudally, small lateral condensations of mesenchyme, also continuous along the anterior-posterior axis of the notochord, begin to form transverse processes (Figure 3.2c, c'). The dorsal aorta is present as a wide canal just ventral to the notochord. Dorsal root ganglia are large and teardrop-shaped, are spaced close to one another, and have corresponding nerves extending posteroventrally down the length of the incipient vertebrae (Figure 3.2d, e). Nervous tissue stains brightly with IKI in young embryos (Figure 3.2b, h, l), providing clear markers of each axial segment, even when the vertebral tissue is continuous.

Caudally, development is largely contemporaneous with the precaudal region. Mesenchymal cells extend ventrally and condense around caudal artery and vein, but these cells are not spindle-shaped in appearance and the matrix surrounding these cells does not stain with Alcian blue. The dorsal-most and ventral-most extensions of condensed mesenchyme are thicker than the rest of the tissue, giving it a bulging square shape in cross section (Figure 3.2g, h, i). The incipient neural arch tissue extends dorsally from the base, near the notochord, but does not yet

fully enclose the neural tube, as in the precaudal region. The dorsal root ganglia and spinal nerves are spaced farther apart caudally than in the precaudal region (Figure 3.2k), foreshadowing that each set of nerves will correspond with two vertebrae in the caudal region, as opposed to a single vertebral unit in the precaudal region. The caudal artery and vein are large, with small foramina forming in the hemal arch cartilage to admit blood vessels (Figure 3.2j, k). In stage 28 and 29 whole mount cleared and stained specimens, Alcian blue-stained cartilage is not yet visible (not shown).

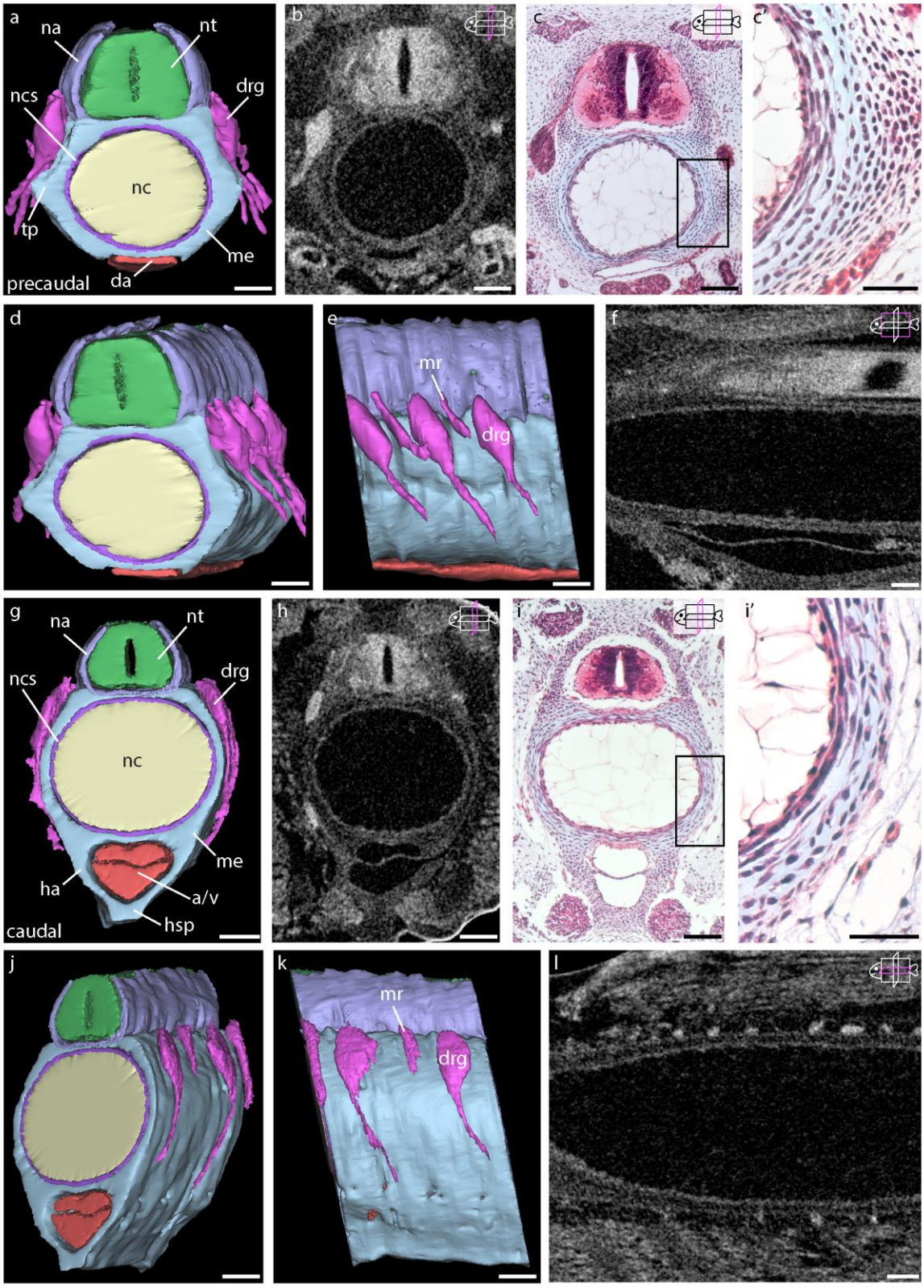

Figure 3.2. Embryonic vertebral morphology in stage 28-29 skate embryos. a, anterior view of a

Figure 3.2 continued. CT reconstruction of the precaudal vertebrae; b, transverse section through the IKI-stained CT scan; c, transverse section stained with HEA, showing the thickened layer of spindle-shaped cells; c', 20x magnification of the layer of spindle-shaped cells; d, anterolateral view of the precaudal CT reconstruction; e, lateral view of the precaudal CT reconstruction; f, sagittal section through the precaudal CT scan; g, anterior view of the caudal CT reconstruction; h, transverse section of the caudal CT scan; i, transverse section through the caudal vertebrae stained with HEA; i', 20x magnification of the layer of spindle-shaped cells; j, anterolateral view of the caudal CT reconstruction; k, lateral view of the caudal CT reconstruction; l, sagittal section of the caudal CT scan. a/v, caudal artery and vein, da, dorsal aorta, drg, dorsal root ganglion, ha, hemal arch, hsp, hemal spine, me, mesenchymal sheath, mr, motor nerve root, na, neural arch, nc, notochord, ncs, notochord sheath, nt, neural tube, tp, transverse process. Icons in upper right corner indicate plane of section. Scale bars represent 100 μm for most images; scale bars represent 50 μm for c' and i'.

Stage 30

In the precaudal region in stage 30 skate embryos, the neural tube, dorsal root ganglia, and spinal nerves remain unchanged from previous stages (Figure 3.3a-e). Vertebral tissues at stage 30 are very similar to those at stage 29, though several subtle differences are observed. The sheath of spindle-shape cells remains continuous, but has increased in thickness (Figure 3.3f). Hints of future notochord constriction (and, eventually, vertebral boundaries) can be seen in sagittal and horizontal sections in both the precaudal and caudal regions as the notochord begins to segmentally decrease in size (Figure 3.3f-g). The morphology of the caudal vertebrae is similar to that of the precaudal region, with a thickened layer of spindle-shaped cells (Figure 3.3h-k), but with spinal nerves that are more spread out, indicating future diplospondyly, in which each myotomal segment will eventually include two vertebrae instead of one (Figure 3.3k-l).

Mesenchymal condensations surrounding the neural tube dorsally and caudal artery and vein ventrally now meet at the dorsal and ventral midline, respectively, to fully enclose the axial column (Figure 3.3c, m-n). At this stage, the tissue of the transverse processes has condensed,

but remains undifferentiated (Figure 3.3b, c, c'). Compared to stage 29, the tissue connecting the nascent hemal arches to the hemal spines has thinned slightly (Figure 3.3h, k-l).

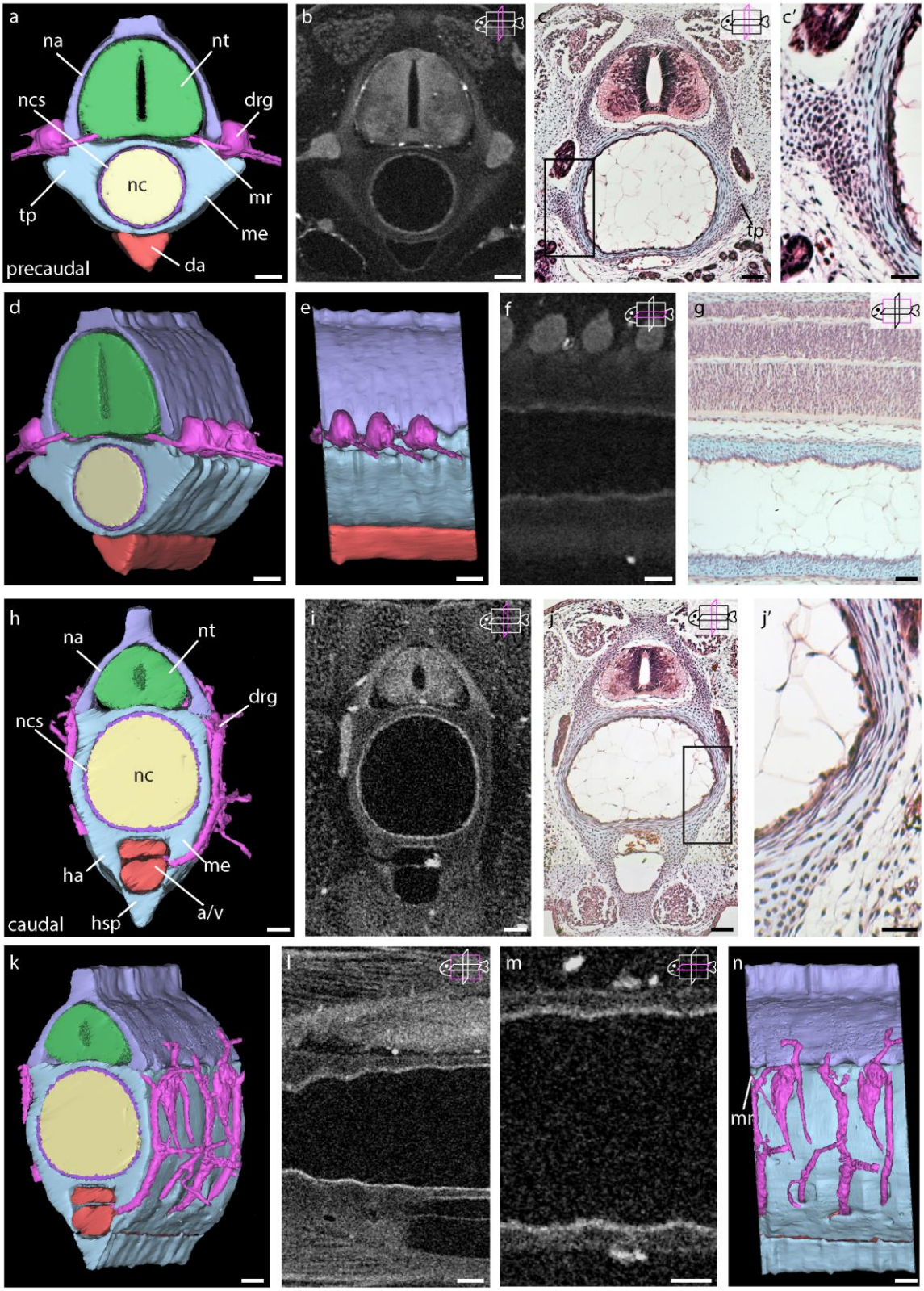

Figure 3.3. Embryonic vertebral morphology in stage 30 skate embryos. a, anterior view of a CT

Figure 3.3 continued. reconstruction of the precaudal vertebrae; b, transverse section through the IKI-stained CT scan; c, transverse section stained with HEA showing the layer of spindle-shaped cells and condensed mesenchyme of the transverse processes; c', 20x zoom of the layer of spindle-shaped cells; d, anterolateral view of a CT reconstruction of the precaudal vertebrae; e, lateral view of a CT reconstruction of the precaudal vertebrae; f, horizontal section through a CT scan of the precaudal vertebrae; g, sagittal section stained with HEA; h, anterior view of a CT reconstruction of the caudal vertebrae; i, transverse section through a CT scan of the caudal vertebrae; j, transverse section through the caudal vertebrae, stained with HEA; j', 20x zoom of the layer of spindle-shaped cells shown in j; k, anterolateral view of a CT reconstruction of caudal vertebrae; l, sagittal section through a CT scan of the caudal vertebrae; m, horizontal section of a CT scan through the caudal vertebrae; n, lateral view of a CT reconstruction of caudal vertebrae. a/v, caudal artery and vein, da, dorsal aorta, drg, dorsal root ganglion, ha, hemal arch, hsp, hemal spine, me, mesenchymal sheath, mr, motor nerve root, na, neural arch, nc, notochord, ncs, notochord sheath, nt, neural tube, tp, transverse process. Icons in upper right corner indicate plane of section. Scale bars are 100 μm for most images, and 50 μm for c' and j'.

Stage 31

During stage 31 the condensed mesenchyme of the neural and hemal arches differentiates into cartilage and is continuous with cartilage enveloping the notochord and its surrounding layer of spindle-shaped cells. The notochord continues to decrease in diameter relative to the vertebrae, and boundaries between vertebral elements (centrum cartilages, neural and intercalary arches) become apparent. Late in stage 31, the cartilage surrounding the notochord becomes restricted to each vertebral segment, and thins at presumptive vertebral boundaries. This cartilaginous tube remains continuous, but variations in thickness can be seen on the outer surface of the centrum cartilage in CT reconstructions (Figure 3.4g, i; Figure 3.5d, e).

Precaudally, the mesenchyme of the neural arches and spines has differentiated into cartilage and stains strongly with Alcian blue (Figure 3.4a-d). Boundaries are now present separating the arches and cartilage of the centra, and clear spinal nerve foramina have developed (Figure 3.4c, e-f). The neural arch tissue still appears continuous throughout the anterior-posterior axis in microCT scans, but arches have begun to form shallow grooves, corresponding

with myotomal segments (Figure 3.4g-i). In sagittal section, boundaries separating the neural and intercalary arches are visible (Figure 3.4j). The transverse processes are well formed by late stage 31, extending posterolaterally, and have begun to segment by subdividing medially, although the lateral-most extensions remain continuous (Figure 3.4b, c, f, i).

In the thicker cartilaginous regions (centra), a middle layer of eosin-stained tissue can be seen in section, which represents the first appearance of the mineralized areolar tissue (Figure 3.4c, c'). In the thinner, intervertebral regions, the layer of spindle-shaped cells has increased in thickness, forming dense, concentric rings around the notochord (Figure 3.4f, f'). In one CT scan of a PMA-stained embryo, small bands of tissue seem to intrude into the notochord, forming on the inside of the notochord sheath, and at the widest part of the notochord in each myotomal segment (Figure 3.4b, d, h). These rings are only present precaudally and are positioned just medial to and in line with the grooves visible on the surface of the outer cartilage, suggesting that they may have a role in directing the subdivision of the continuous cartilage. However, these structures have not yet been observed in any other specimens, indicating either that this specimen might be anomalous, or that this tissue is ephemeral, being present only for a short time in development.

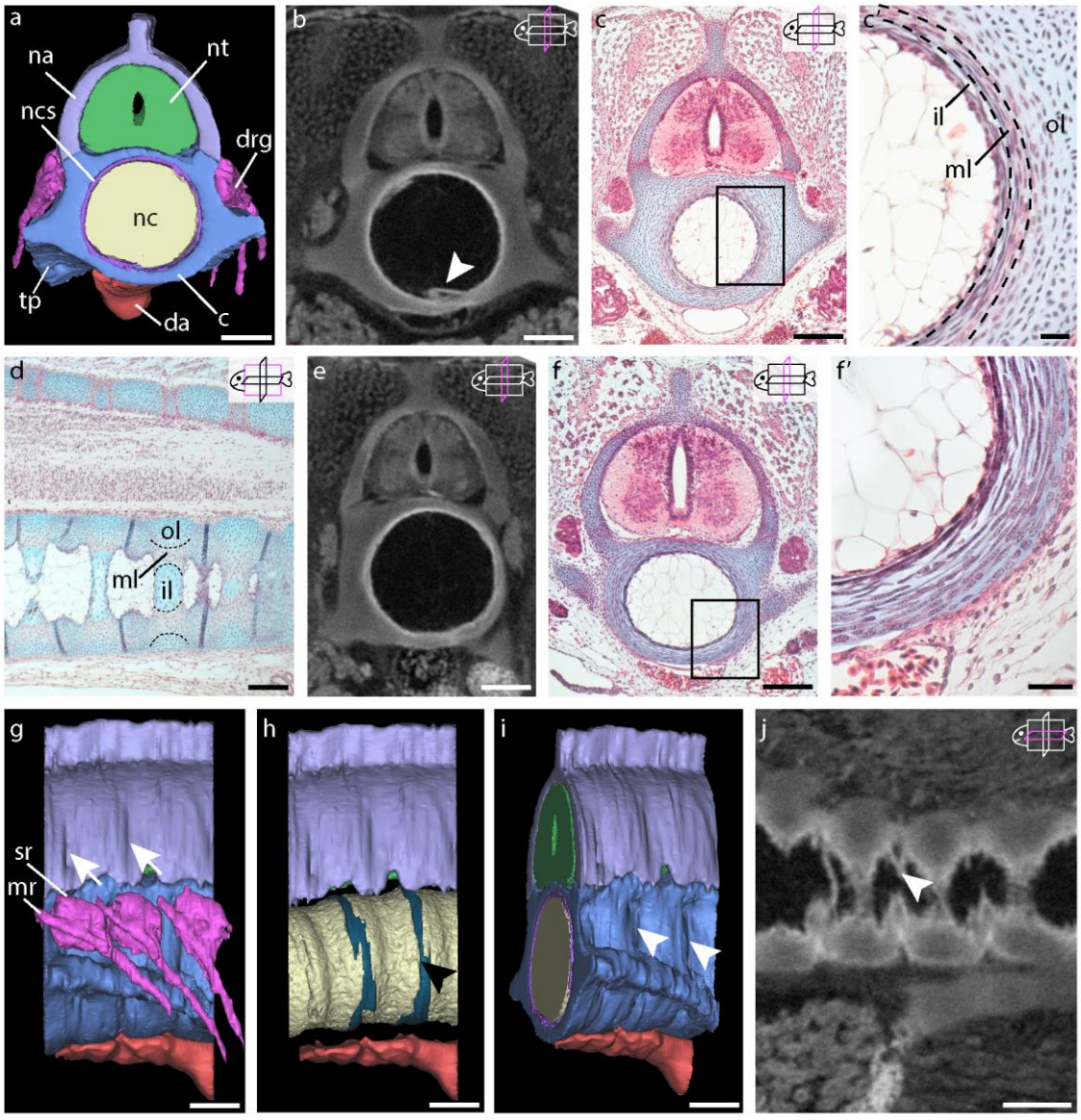

Figure 3.4. Precaudal embryonic vertebral morphology in stage 31 skate embryos. a, anterior view of a CT reconstruction of the precaudal vertebrae; b, transverse section through the PMA-stained CT scan showing the widest part of the vertebra, arrowhead refers to notochord band; c, transverse section stained with HEA, showing the thickened continuous cartilage; c', 20x zoom of the centrum cartilage, dashed lines indicate first appearance of areolar tissue; d, sagittal section through a late stage 31 skate embryo stained with HEA, dashed lines indicate areolar tissue; e, transverse section through the CT scan showing the morphology of the intervertebral region; f, transverse section stained with HEA, showing the narrow, fibrous nature of the intervertebral region; f', 20x zoom of the fibrous rings; g, lateral view of the CT reconstruction showing dorsal root ganglia and spinal nerves, arrows indicate grooves of incipient arch boundaries; h, lateral view of the CT reconstruction with centrum cartilage removed, arrowhead indicates notochord band; i, anterolateral view of the CT reconstruction showing the grooves of

Figure 3.4 continued. incipient vertebral boundaries, arrowheads depict location of grooves indicating incipient subdivision; j, horizontal section through the CT scan, arrowhead indicates notochord band. da, dorsal aorta, drg, dorsal root ganglion, c, cartilage, il, inner layer of cartilage, ml, middle layer of centrum/areolar calcification, mr, motor nerve root, na, neural arch, ncs, notochord sheath, nt, neural tube, ol, outer layer of hyaline cartilage, sr, sensory nerve root, tp, transverse process. Icons in upper right corner indicate plane of section. Scale bars are 200 μm for most images, scale bars are 100 μm for c' and f'.

Embryonic morphology of the caudal vertebrae differs slightly from the precaudal vertebrae by the end of stage 31. The neural and intercalary arches have begun to separate, with small slits forming in the cartilage, although they remain continuous at the level of the neural spines and at their bases (Figure 3.5a-e). The centrum cartilages have also begun to thicken at intervals corresponding to each myotomal boundary, but the grooves representing incipient vertebral boundaries are not as deep as in the precaudal region (Figure 3.5e). Both the fibrous intervertebral regions and the widest parts of the centrum are similar to the precaudal vertebrae, with a ring representing the early areolar tissue medially and Alcian blue-stained cartilage in the outer layer (Figure 3.5f, g, g', h, h'). Segmental constriction of the notochord has increased from stage 30, with clear decreases in notochord diameter in each myotomal segment (Figure 3.5i, j). Hemal spines remain as a continuous mesenchymal condensation that appears discontinuous with the hemal arches (Figure 3.5e-h). Dorsal root ganglia and spinal nerves remain broadly spaced, in contrast to their close precaudal positioning (Figure 3.5d, e).

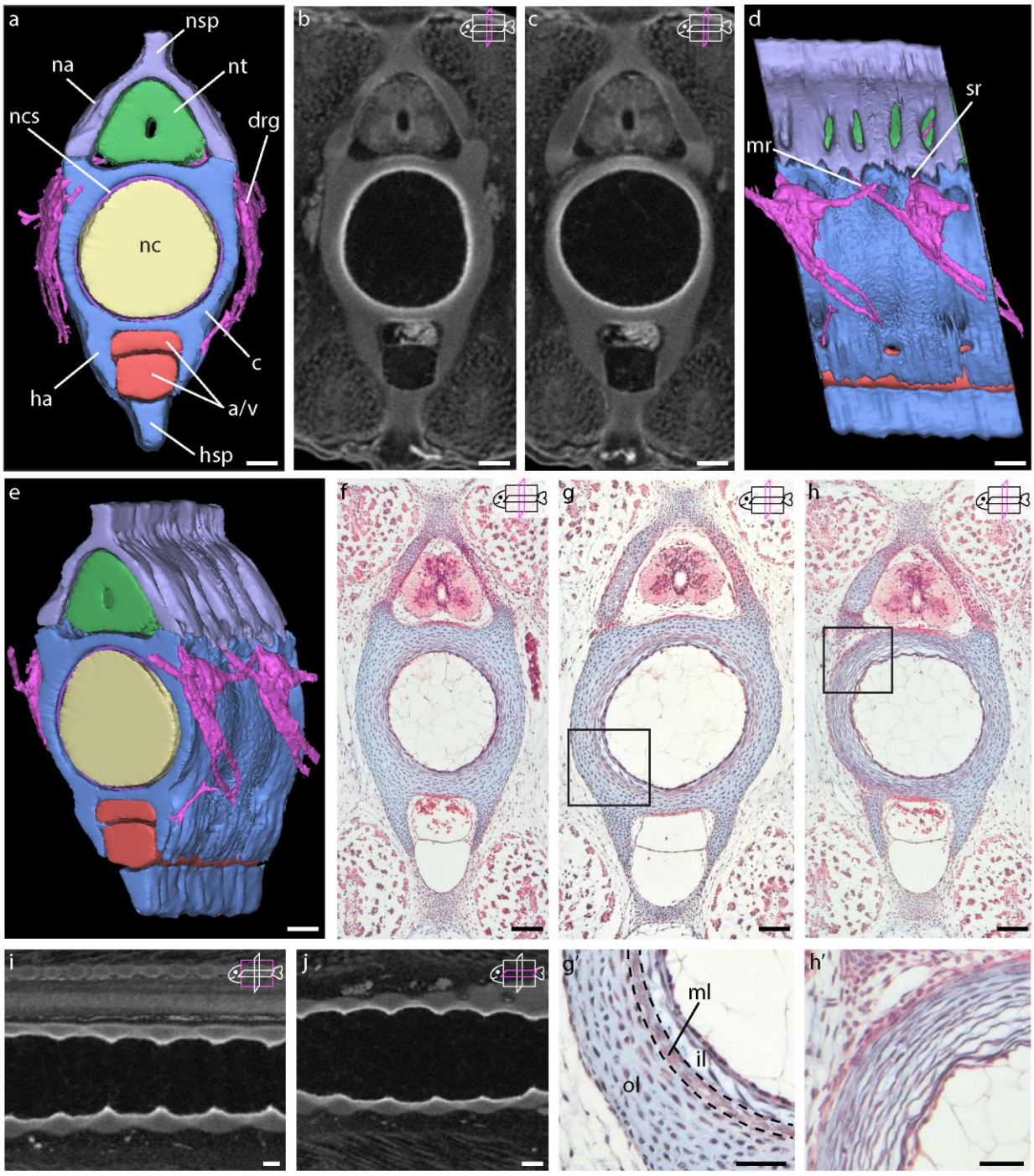

Figure 3.5. Caudal embryonic vertebral morphology in stage 31 skate embryos. a, anterior view of a CT reconstruction of the caudal vertebrae; b, transverse section through the PMA-stained CT scan showing the widest part of the vertebrae; c, transverse section through a CT scan showing the narrowest portion, where the continuous cartilage will eventually subdivide; d, lateral view of the CT reconstruction; e, anterolateral view of the CT reconstruction; f, transverse

Figure 3.5 continued. section stained with HEA, showing the thickened continuous cartilage; g, transverse section showing the early formation of the middle layer of tissue that will eventually form the areolar calcification; g', 20x magnification showing the incipient centrum; h, transverse oblique section showing the fibrous nature of the intervertebral tissue; h', 20x magnification of the fibrous intervertebral ring; i, sagittal section through the CT scan showing segmental constriction of the notochord; and j, horizontal section through the CT scan showing segmental thickening and constriction of the vertebral cartilage surrounding the notochord. a/v, caudal artery and vein, c, cartilage, drg, dorsal root ganglion, ha, hemal arch, hsp, hemal spine, il, inner layer of cartilage, ml, middle layer of centrum/areolar calcification, mr, motor nerve root, na, neural arch, nc, notochord, ncs, notochord sheath, nsp, neural spine, nt, neural tube, ol, outer layer of hyaline cartilage, sr, spinal nerve root. Scale bars represent 100 μm for most images; scale bars represent 50 μm for g' and h'.

Stage 32-33

All components of the vertebral column are present by stage 32, and neural arches, intercalary arches, and centra have all completely segmented (Figures 3.6 and 3.7). The arch cartilages now consist of clearly defined neural arches, which are long and thin in the precaudal region, and more substantial intercalary arches that contain spinal nerve foramina (Figure 3.6a-d, g). The neural spines have also begun to segment, but remain connected at their bases (Figure 3.6d, e). The transverse processes on the centrum cartilages are clearly pronounced, and extend both anteriorly at a slight ventral angle, and posterodorsally. The posterior portion of the transverse process overlaps the anterior portion of the subsequent transverse process (Figure 3.6d-g).

The developing areolar tissue, stained with eosin in section, is clearly visible in CT scans, in HEA-stained sections, and in whole mount skeletal preparations. In sagittal and transverse CT sections the areolar tissue begins to substantially constrict the notochord (Figure 3.6h, i). The middle layer of areolar tissue forms within the layer of spindle-shaped cells and is separate from the outer hyaline cartilage that envelops the notochord (Figure 3.6c, c'', j, j', k). Interestingly, this areolar calcification first forms just external to the notochord sheath in stage 32 (Figure 3.6c,

c’’), but in slightly older, stage 33, embryos, a layer of chondrocytes sparsely embedded in Alcian blue-stained matrix (the “inner zone of vertebral development” of (Ridewood, 1921) separates the centrum and the outer layer, suggesting that cartilage is differentiating on the inside of this mineralized tissue as well as on the outside (Figure 3.6j, j’). These segmented centra, along with the inner layer of cartilage, have increased in size from stage 31 and now substantially constrict the notochord in the center of each vertebral unit (Figure 3.6h, i, j, j’). In the intervertebral regions, the fibrous rings have enlarged dramatically and surround the persistent notochord (Figure 3.6a, c, c’, d, e, f, f’, g). The outer cartilage is no longer continuous, but is now present in the form of rectangle-shaped boxes that surround the centrum and notochord. The dorsolateral corners slant slightly posteriorly and contain spinal nerve foramina (Figure 3.6d).

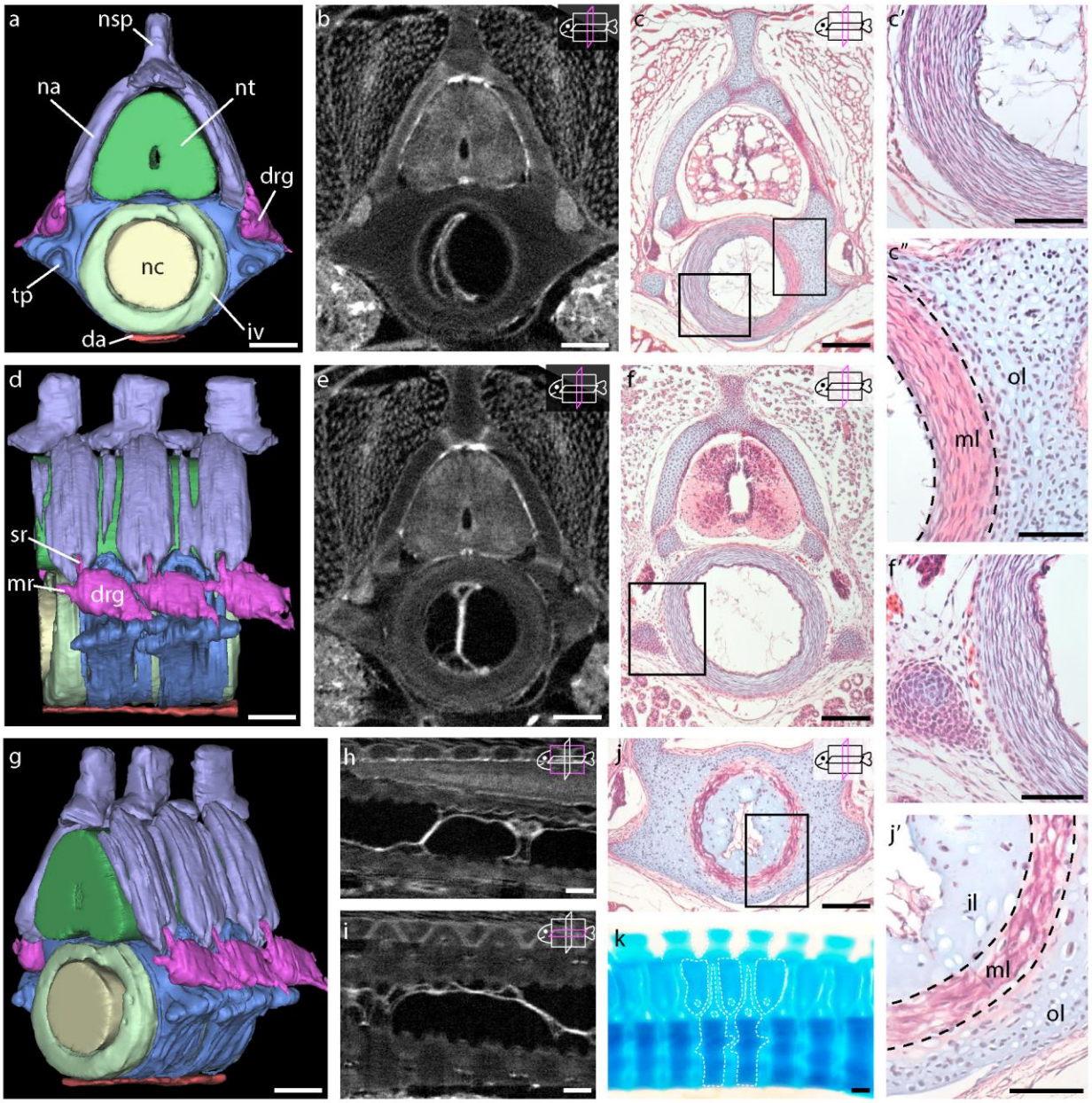

Figure 3.6. Precaudal embryonic vertebral morphology in stage 32 skate embryos. a, anterior view of a CT reconstruction of the precaudal vertebrae; b, transverse section through the IKI-stained CT scan showing the widest part of the vertebrae; c, transverse oblique section stained with HEA; c', 20x magnification of the fibrous ring shown in c; c'', 20x magnification of the mineralizing centrum and outer layer of cartilage shown in c, dashed lines indicate middle layer/areolar calcification; d, lateral view of the CT scan of the precaudal vertebrae; e, transverse section through the intervertebral region of the CT scan; f, transverse section through the intervertebral region stained with HEA; f', 20x magnification of the fibrous ring and transverse process shown in f; g, anterolateral view of the CT reconstruction; h, sagittal section of the CT

Figure 3.6 continued. scan; i, horizontal section of the CT scan; j, transverse section through a slightly older embryo showing the early areolar calcification of the centrum; j' 20x magnification of the developing centrum, dashed lines indicate middle layer/areolar calcification; k, skeletal preparation of precaudal vertebrae in lateral view showing well developed transverse processes. da, dorsal aorta, drg, dorsal root ganglion, il, inner layer of cartilage, iv, intervertebral region, ml, middle layer of centrum/areolar calcification, mr, motor nerve root, na, neural arch, nsp, neural spine, nt, neural tube, ol, outer layer of hyaline cartilage, sr, spinal nerve root, tp, transverse process. Icons in upper right corner indicate plane of section. Scale bars represent 200 μm for most images; scale bars represent 100 μm for c', c'', f', and j'.

During stage 32 several changes in vertebral morphology through the precaudal to caudal transition become more striking than in younger embryos. The same population of mesenchyme that condenses to form the transverse processes precaudally forms the hemal arches in the caudal region. Throughout the precaudal-caudal transition, in each successive vertebra, the transverse processes extend more and more ventrally until they are no longer transverse processes, but hemal arches (Figure 3.7a; see Daniel (1922) for a nice figure of this in *Rhinobatis*). The caudal artery and vein are surrounded by the hemal arches laterally and dorsally, and are protected ventrally by hemal spines (Figure 3.7a-e). The first hemal spine possesses two anterior prongs that cup the caudal artery and vein, as well as a median keel projecting ventrally (Figure 3.7e). More posterior hemal spines are not as well developed and extend as a single rod of ventral cartilage throughout the tail. At this point, the hemal arches and spines are not continuous with each other as they were in previous stages. The fibrous rings, mineralized centrum, and matrix deposited medial to the centrum, are visible in both CT and histological section (Figure 3.7b-d', f, g).

Another visible difference between the caudal and precaudal regions includes a transition to the diplospondylic condition seen across elasmobranchs, in which two vertebrae are present in each myotomal segment. This change is visible in the spacing out of spinal nerve foramina, with

one set of spinal nerves corresponding to each vertebral unit precaudally, but corresponding with two vertebral units in the caudal region (Figure 3.7h-j). Related to the spinal nerve spacing is the change in the shape of the neural and intercalary arches. Precaudally the neural arches are slender and articulate to the dorsal margin of the vertebral cartilage, while the intercalary arches are much wider and support spinal nerve foramina ventrally. In the caudal region, however, both neural and intercalary arches take on largely the same shape, with the only differences in morphology being a slight expansion of the apex in the intercalary arches and the base in the neural arches (Figure 3.6k and 3.7h). One neural spine is present for each set of neural and intercalary arches. The CT reconstructions in Figure 3.7(a, e, i, j) show that the anterior-posterior transition to caudal diplospondyly does not occur at the first appearance of hemal arches, but rather several vertebral segments posterior. The first several caudal vertebrae have hemal arches and spines, but both the relationship of spinal nerve foramina to vertebral cartilages and the neural arch morphology show the same pattern as the precaudal region. The whole mount, cleared and stained embryo (Figure 3.7h) shows the more typical morphology of the arches in caudal vertebrae.

In transverse oblique HEA-stained sections of slightly older (stage 33) embryos, all layers of the developing centrum are visible, including the inner layer, middle layer of areolar calcification, and outer layer of hyaline cartilage (Figure 3.7k). The layer of fibrous, spindle-shaped cells that persist in the space between vertebral cartilages can also be seen in the intervertebral regions in oblique sections.

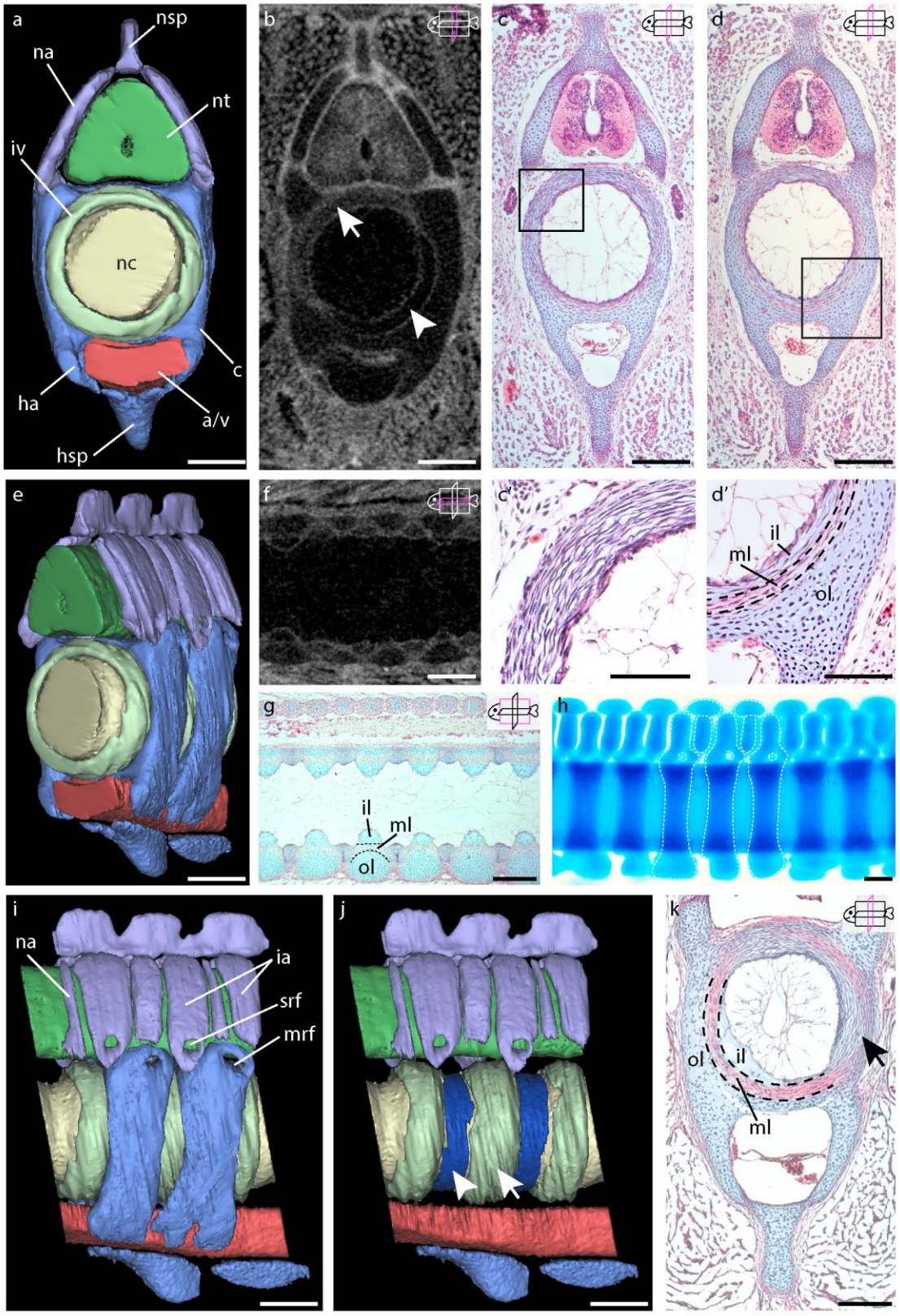

Figure 3.7. Caudal embryonic vertebral morphology in stage 32 skate embryos. a, anterior view

Figure 3. 7 continued. of a CT reconstruction of the caudal vertebrae; b, transverse section through the IKI-stained CT scan, arrow indicates fibrous ring and arrowhead indicates mineralizing centrum; c, transverse section stained with HEA; c', 20x magnification of the fibrous ring shown in c; d, transverse section stained with HEA and showing the mineralizing centrum; d', 20x magnification of the incipient areolar calcification, indicated by the dashed lines; e, anterolateral view of the CT reconstruction; f, horizontal section through the CT scan; g, sagittal section stained with HEA and showing the early areolar calcifications and inner layer of cartilage; h, skeletal preparation of caudal vertebrae; i, lateral view of a CT scan of the caudal vertebrae; j, lateral view of a CT scan of the caudal vertebrae with outer cartilage removed to show the inner layer (arrowhead) and intervertebral region (arrow); k, transverse oblique section of a slightly older embryo showing both the mineralizing centrum and fibrous ring (arrow). a/v, caudal artery and vein, ca, cartilage, ha, hemal arch, hsp, hemal spine, ia, intercalary arch, il, inner layer of cartilage, iv, intervertebral region, ml, middle layer of the centrum/areolar calcification, mrf, motor nerve root foramen, na, neural arch, nsp, neural spine, nt, neural tube, ol, outer layer of hyaline cartilage, srf, sensory nerve root foramen. Icons in upper right corner indicate plane of section. Scale bars represent 200 μm for most images; scale bars represent 100 μm for c' and d'.

Stage 34+

By stage 34 the vertebrae have taken on an adult-like morphology, with more sharply defined vertebral boundaries, mineralized centra, and a greatly reduced notochord (Figures 3.8 and 3.9). The outer edges of the cartilage have begun to calcify as dense blocks of tesserae, which are easily visible in the slices of the microCT scans (Figure 3.8b, e, h; Figure 3.9b, d, e, g), and the mineralized centrum has dramatically increased in both length and width.

The arches in the precaudal region are well developed, and the large intercalary arches envelop most of the spinal cord (Figure 3.8a-g). The sensory nerve roots exit the vertebral column through the foramina in the intercalary arches, while motor nerve roots exit through the dorsal portion of the outer hyaline cartilage (Figure 3.8d, g). The neural arches are present as small slivers of cartilage that extend dorsally around the neural tube and expand at their bases to provide foramina for the exiting motor nerve roots. Neural spines are fully separated now, with

expanded bases that articulate to the intercalary arches and wide dorsal margins, forming an elongate hourglass in cross section (Figure 3.8e). Histological sections show a fibrous perichondrium surrounding the hyaline cartilage of the arches and neural spines (Figure 3.8c, c', f, f'). Both sensory and motor nerve roots are large by this stage, to provide innervation to the anteroposteriorly-expanded pectoral fins.

Centra consist of boxes of outer, hyaline cartilage surrounding a middle layer of densely mineralized rings of areolar calcification (Figure 3.8b, c, c'', e, f, f'', h, i). The inner layer of the centrum, situated between the notochord and the areolar calcification, has almost completely constricted the notochord in the center of each vertebra, leaving only a small notochordal canal in the center of these centra (Figure 3.8f, f''). In section, these three layers stain differentially, with the outer cartilage staining light pink, the mineralized centrum staining a bright pink, and the third, inner layer remaining white or staining light blue (Figure 3.8f'').

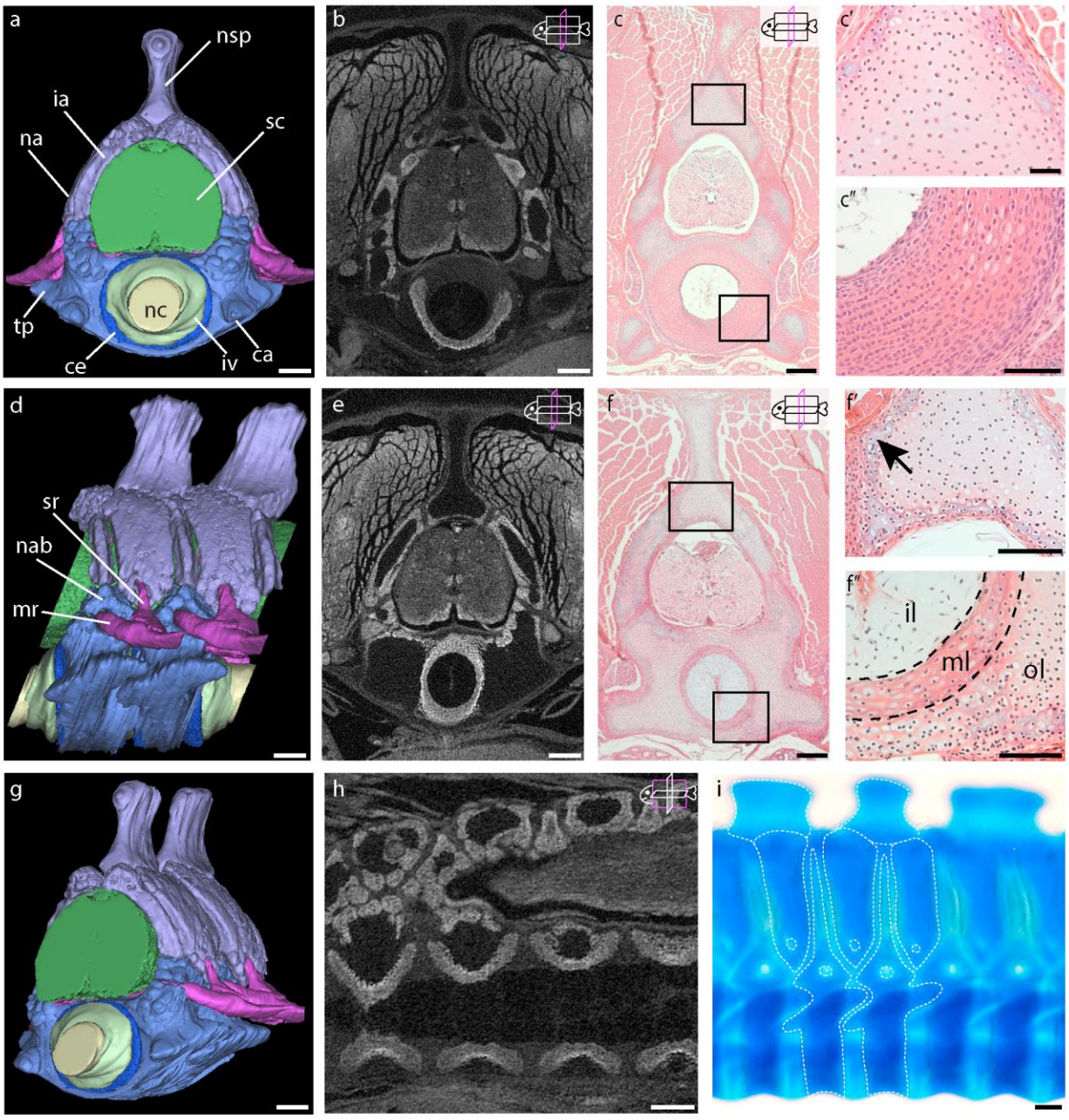

Figure 3.8. Precaudal embryonic vertebral morphology in stage 34 skates. a, anterior view of a CT reconstruction of the vertebrae; b, transverse section through the IKI-stained CT scan showing the mineralizing centrum; c, transverse section stained with HEA; c', 20x magnification of the neural spine cartilage; c'', 20x magnification of the areolar calcification of the centrum; d, lateral view of a CT reconstruction; e, transverse section through the CT scan showing the narrowest part of the centrum; f, transverse section stained with HEA and showing the narrowest part of the centrum; f', 20x magnification of the neural spine cartilage, arrow indicates developing tesserae; f'' 20x magnification of the areolar calcification of the centrum; g, anterolateral view of the CT reconstruction; h, sagittal section of the CT scan; i, skeletal

Figure 3.8 continued. preparation of precaudal vertebrae showing transverse processes, neural arches, and intercalary arches. ca, outer cartilage, ce, centrum, ia, intercalary arch, il, inner layer of cartilage, iv, intervertebral region, ml, middle layer of cartilage/areolar calcification, mr, motor nerve root, na, neural arch, nab, neural arch base, nc, notochord, nsp, neural spine, nt, neural tube, ol, outer layer of hyaline cartilage, sr, sensory nerve root, tp, transverse process. Icons in upper right corner indicate plane of section. Scale bars represent 200 μm for most images; scale bars represent 100 μm for c', c'', f', and c''.

Similar to stage 32 and 33 embryos, there are several differences in morphology between precaudal and caudal vertebrae in stage 34 embryos. The neural spines are anteroposteriorly longer caudally than in the precaudal region, and have a more rectangular and block-like appearance with laterally expanding bases that articulate to both the neural and intercalary arches (Figure 3.9a-e, h-j). The arches and outer cartilage of the centrum consist of hyaline cartilage with a peripheral layer of tesserae (Figure 3.9c, c', f-g).

The hemal arches have extended ventrally to fully enclose the caudal artery and vein (Figure 3.9a), and individual vertebrae are completely separated from one another in the caudal region (Figure 3.9h). Hemal arches and spines are fused together to form a single structure, but boundaries in the cartilages can still be seen in section (Figure 3.9b, c, e, f). The hemal spines are offset slightly posteriorly from the hemal arches, and the most posterior portion of each hemal spine rests ventral to the anterior portion of the next set of hemal arches (Figure 3.9h). The caudal mineralized centra are very similar to those in the precaudal region, showing a thin ring of areolar calcification in the center of each vertebral segment that thickens considerably near the anterior and posterior margins of each vertebra (Figure 3.9c, c'', d, g, f, f'', i, j). The duplication of caudal vertebrae results in the presence of two vertebrae for each myotomal segment and in the increased spacing of spinal nerves (Figure 3.9h). The neural and intercalary arches are similar

in thickness in the caudal region, with the base of the neural arches articulating to the outer centrum cartilage to form spinal nerve foramina (Figure 3.9h, i).

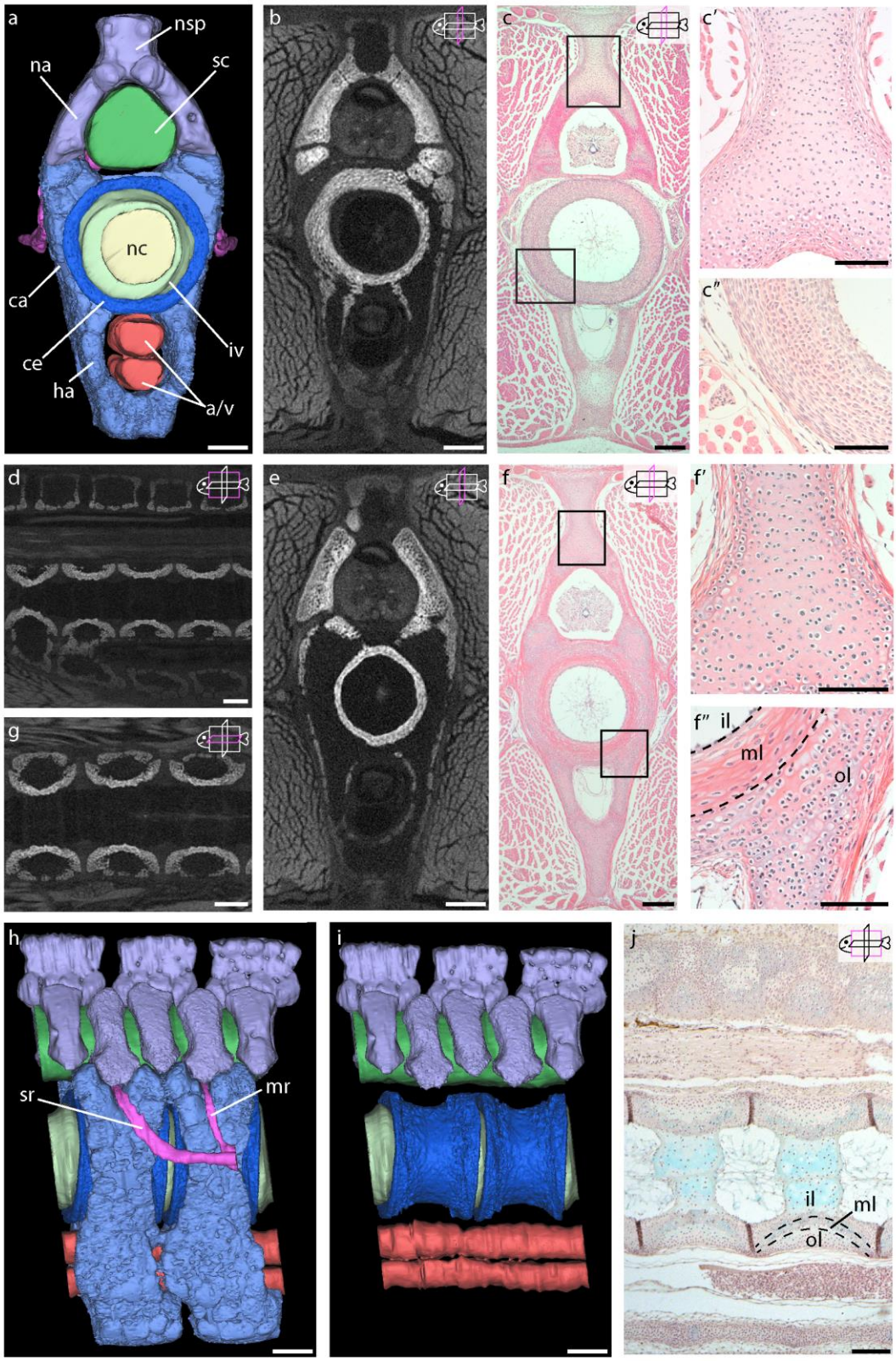

Figure 3.9. Caudal embryonic vertebral morphology in stage 34 skates. a, anterior view of a CT

Figure 3.9 continued. reconstruction of the caudal vertebrae; b, transverse section through the IKI-stained CT scan showing the mineralizing centrum; c, transverse section stained with HEA; c', 20x magnification of the neural spine cartilage; c'', 20x magnification of the areolar calcification of the centrum; d, sagittal section of the CT scan; e, transverse section of the CT scan showing the narrowest part of the centrum; f, transverse section stained with HEA and showing the narrowest part of the centrum; f', 20x magnification of the neural spine cartilage; f'' 20x magnification of f, dashed lines indicate middle layer/areolar calcification of the centrum; g, horizontal section through the CT scan; h, lateral view of a CT reconstruction; i, lateral view of the CT scan with outer cartilage removed; j, sagittal section stained with HEA, dashed lines indicate middle layer/areolar calcification. a/v, caudal artery and vein, ca, outer cartilage, ce, centrum, ha, hemal arch, il, inner layer of cartilage, iv, intervertebral region, ml, middle layer of the centrum/areolar calcification, mr, motor nerve root, na, neural arch, nc, notochord, nsp, neural spine, nt, neural tube, ol, outer layer of hyaline cartilage, sr, sensory nerve root. Icons in upper right corner indicate plane of section. Scale bars represent 200 μm for most images; scale bars represent 100 μm for c', c'', f', and c''.

Summary of vertebral development in Leucoraja erinacea

The computed tomographic and histological analyses in this study provide a comprehensive view of vertebral development in the little skate. We show that a continuous layer of mesenchyme condenses around the notochord at stage 27 and persists through vertebral development as a layer of spindle-shaped cells until it differentiates into the fibrous intervertebral rings and the areolar tissue in stage 31 (Figure 3.10). Beginning at stage 28, mesenchymal cells condense around the neural tube and caudal artery and vein to form continuous neural arch and hemal arch tissues that extend the length of the axial column. During stage 31 the neural and hemal arch mesenchyme differentiates into hyaline cartilage and surrounds the areolar tissue, where it will remain into adulthood. In stage 32 arch cartilages subdivide into intercalary and neural arches and spines dorsally, and hemal arches and spines ventrally. An inner layer of cartilage forms medial to the areolar calcification, and substantially constricts the notochord. By stage 34, the areolar calcification of the centrum is large and hourglass-shaped, and the inner layer of cartilage almost completely constricts the notochord in

the middle of each vertebral segment. In the intervertebral regions, the notochord persists into adulthood and is surrounded by the thickened ring of fibrous cells.

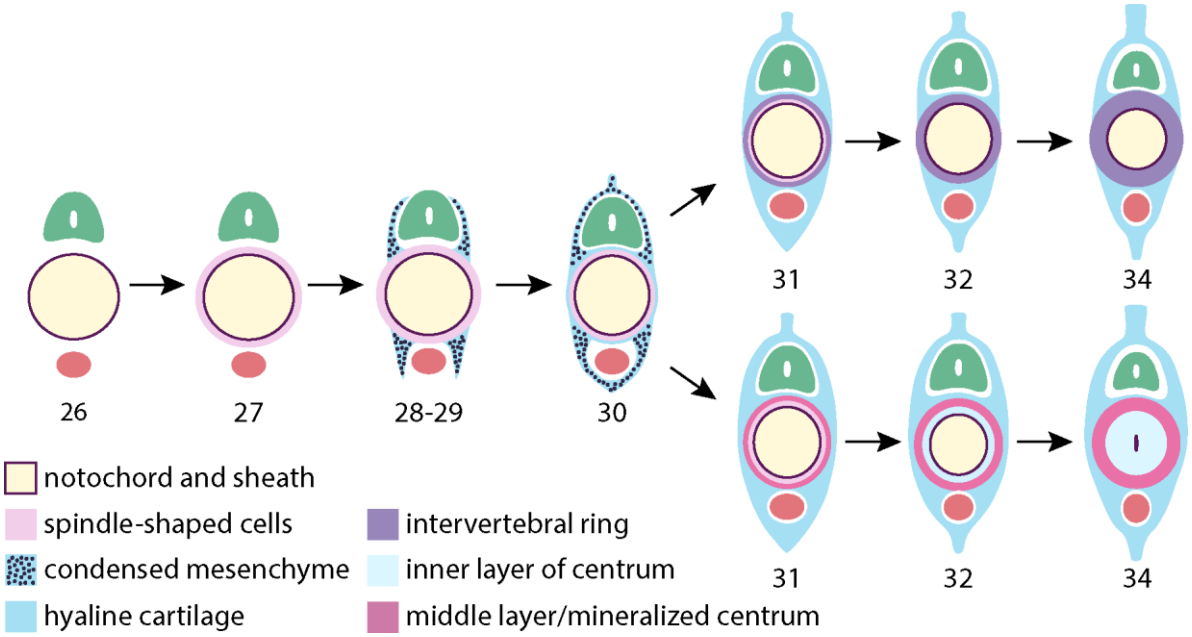

Figure 3.10. Schematic showing the stages of vertebral development in the little skate, from stage 27 to stage 34. The top row after the schematic splits shows cross sections of the intervertebral region (top) and the middle of a vertebra (bottom). Green = neural tube/spinal cord and red = caudal artery and vein.

Discussion

The fibrous sheath and perichordal tube

Several notable features were identified in the little skate in this study, including the initial formation of a continuous layer of spindle-shaped cells surrounding the notochord. This layer of cells subsequently differentiates into the areolar calcifications of the centra and the fibrous rings of the intervertebral regions. The spindle-shaped cells were first described as the thickened 'fibrous sheath' of the notochord in several shark species, including *Squalus acanthias*, *Mustelus vulgaris*, and *Scyliorhinus canicula*, and this sheath was widely accepted as a derivative of the

notochord epithelium (Gegenbaur, 1862; Gadow and Abbott, 1895), although some researchers believed it to be sclerotome-derived, along with the rest of the vertebral elements (Hasse, 1879; Klaatsch, 1893b). In sharks, the fibrous sheath is bounded externally by the elastica externa, a thin membrane of intercrossing elastic fibers. The fibrous sheath is thought to be invaded in large numbers by sclerotomal cells that perforate the elastica externa at the bases of the neural and hemal arches and then divide and differentiate into cartilage within the sheath (Gadow and Abbott, 1895; Goodrich, 1930). Cross sections of stage 27 skate embryos show mesenchymal cells condensing around the notochord prior to taking on an elongate spindle shape (Figure 3.1), suggesting that the cells of the fibrous sheath are mesenchymal in origin. In sections of stage 29 and 30 skate embryos, we were not able to easily identify the elastica externa or any cells that were in the process of migrating into the fibrous layer of spindle-shaped cells. Additionally, this layer of spindle-shaped cells is morphologically different than those described previously in sharks, with the cells having more irregular shapes and the layer including more extracellular matrix (Figure 3.1c', i'; Figure 3.2c', j'; compare to Eames (2007) Figure 6.). These differences imply that the fibrous sheath, previously identified to be a derivative of the notochord epithelium in sharks, develops from mesenchymal cells that have condensed around the notochord sheath in batoids. If this is the case, then the areolar calcifications in skates do not form through sclerotomal cells invading a notochord-derived fibrous sheath (the process described in sharks by Gadow and Abbott, 1895), but rather through mesenchymal cells first differentiating into concentric layers of elongate cells and then calcifying.

Similar continuous condensations of tissue surrounding the notochord have been described in several other vertebrate taxa, such as salamander, chick, and mouse, in which they have been termed the perichordal tube (Williams, 1942, 1959; Wake and Lawson, 1973; Christ

and Wilting, 1992). However, despite superficial similarities, there are important differences between the perichordal tube of tetrapods and the fibrous sheath of elasmobranchs. For example, in skate, the cells of the fibrous sheath become elongate and thin throughout the length of the axial column, running parallel to the notochord epithelium. The cells of the perichordal tube in chick, however, have the characteristic appearance of mesenchymal cells, and flatten into fibrous rings only at the intervertebral boundaries, early in vertebral development (Williams, 1942; Christ et al., 2000). This segmental thickening in chick occurs before the neural arches are fully developed. Similarly, in a plethodontid salamander, *Eurycea bislineata*, the perichordal tube is not consistent in diameter throughout the axial column, but rather forms thickened rings of elongate cells at incipient vertebral boundaries and thins to just one or two cells in the middle of each vertebral segment (Wake and Lawson, 1973). This unevenness contrasts with the fibrous sheath and the continuous cartilage of skates, which remains a constant thickness for several weeks of development, and does not subdivide until the neural and hemal arch mesenchyme has condensed and differentiated into cartilage.

It is unclear how widespread the perichordal tube is among vertebrates. Recent studies of the Japanese medaka (*Oryzias latipes*), a teleost fish, do not mention any layer of continuous tissue, but instead report that mesenchyme invades the notochord sheath at segmental intervals (Inohaya et al., 2007) and studies on vertebral development in other teleosts, such as zebrafish, do not discuss the condensation of sclerotomal mesenchyme in great detail (Morin-Kensicki et al., 2002; Fleming et al., 2004). However, there is some evidence of a thin tube of continuous mesenchyme in some teleost fishes. A thin layer of undifferentiated mesenchyme surrounding the notochord prior to centrum formation has been documented in Atlantic salmon, but by the

time centra begin to mineralize, neural and hemal arch cartilages are already well formed (Grotmol et al., 2003).

In addition to the notochord, mesenchyme also surrounds the neural tube in the form of unsegmented, nascent neural and intercalary arches in skate that differentiate into cartilage and later separate. We have found no evidence in the literature describing this continuous arch tissue in vertebrates outside sharks. Van Wijhe (1922) and De Beer (1924) documented the continuous early condensation of the neural arch mesenchyme in *Squalus acanthias* and *Heterodontus francisci*, respectively, but these observations were later dismissed by Goodrich (1930) and "better ascribed to a temporary fusion of rudiments set very close together than to the arcualia having been evolved from an originally continuous cartilaginous band" (p. 16). My observations, in the present work taken from microCT scans of the little skate and in previous works observed in several species of sharks (van Wijhe, 1922; de Beer, 1924), are inconsistent with Gadow and Abbott's (1895) model of vertebral development in which pairs of basidorsal and interdorsal cartilages form the building blocks of the neural and intercalary arches. I have shown here using microCT scans and histology that the earliest condensations of mesenchyme around the neural tube and caudal artery and vein in skate are indeed continuous throughout the length of the vertebral column.

Subdivision of initially continuous vertebral cartilage

The mode of vertebral segmentation described in this study, in which segmented paraxial mesoderm migrates to condense around the notochord and neural tube, forms a continuous sleeve of cartilage that extends the entire length of the body, and then secondarily subdivides into discrete, repeating vertebral elements, has not received much attention in the literature. Studies

describing vertebral development in chick, mouse, and human mention a perichordal tube of condensed mesenchyme, but no mechanism to explain the secondary subdivision of this structure is proposed (Christ and Wilting, 1992; Wallin et al., 1994; Christ et al., 2000). Development of the intersegmental blood vessels and spinal nerves is directed by interactions between the somites and the migrating neural crest cells (Stern and Keynes, 1987), and it is possible that these segmented structures are driving perichordal tube subdivision, but little functional evidence exists to support this. Segmentation of the perichordal tube in chick seems to take place when the incipient intervertebral discs begin to develop within the perichordal mesenchyme and replace the notochord (Christ and Wilting, 1992). These discs provide boundaries for developing vertebral centra, which later fuse to neural arch rudiments. In mammals, this process is similar; the notochord is not completely replaced, but instead becomes the nucleus pulposus at the center of each intervertebral disc (Lefebvre and Bhattaram, 2010). In skate, cells within the fibrous sheath first differentiate into hyaline cartilage, which thickens substantially, before secondarily subdividing into vertebrae late in stage 31.

Another question that arises with reference to the secondary subdivision of the continuous cartilage is the eventual fate of the notochord during vertebral development. The notochord persists in the intervertebral regions in stage 34 skate embryos, but it is unclear whether there is an overall reduction in the number of notochord cells or simply a reduction in cell size. It seems more likely that, rather than notochord cell death, the remaining notochord cells are simply squeezed out of the center of each vertebra as the centra constrict the notochord. Comparing sagittal sections of stage 31 and 32 embryos (Figure 3.4d and 3.7g) to stage 34 embryos (Figure 3.9j) shows a reduction in intervertebral notochord cell size, supporting this hypothesis. Additionally, more notochord cell nuclei are visible just peripheral to the inner layer

of centrum cartilage in stage 34 embryos than in stage 31 and 32 embryos, suggesting that these cells were indeed displaced from their prior positions and are now compacted into a smaller space.

The small bands of tissue that surround the notochord and correspond to nascent vertebral boundaries, as observed in one late stage 31 skate embryo (Figure 3.4b, j), may relate to the segmentation of the continuous vertebral cartilage in skate. The location of the bands at the widest part of the notochord, and just medial to the grooves in the dividing cartilage, is intriguing, and we speculate that these bands could represent iterative signaling centers that direct the subdivision of the tube of hyaline cartilage. Notochord segmentation has been proposed as a driver of centrum development in chick and in some teleost fishes (Stern, 1990; Grotmol et al., 2003). For example, in Atlantic salmon, calcification of the centrum seems to be initiated by the segmental organization of a layer of "chordoblast" cells located in the notochord sheath (Grotmol et al., 2005; Nordvik et al., 2005). In each vertebral segment these cells transition from an anteroposterior orientation to circular bands perpendicular to the AP axis. Subsequently, chordacentra begin to calcify in the notochord sheath at the position of these chordoblast bands, and sclerotomally-derived osteoblasts begin to deposit bone on the surface of the chordacentra (Grotmol et al., 2003). However, beyond these morphological observations, the phenomenon of notochord segmentation is controversial: it has not been documented outside of a small number of teleost species (Grotmol et al., 2003, 2005; Haga et al., 2009), and an underlying molecular mechanism remains elusive.

The composite nature of the axial skeleton in gnathostomes

Previous studies of skeletogenesis in sharks have identified three tissue layers early in the formation of the centrum, which is similar to what is documented in skate in this study (Daniel, 1922; Eames et al., 2007; Enault et al., 2015). These three layers, or zones of deposition, include an inner layer consisting of mostly extracellular matrix located superficial to the notochord, a middle layer of areolar calcification that forms the double cone of the centrum, and an outer layer of hyaline cartilage that is continuous with the arches and is covered with tesserae in adults. These layers stain differentially in later stage swell shark embryos (9 cm total length) (Eames et al., 2007) with the inner and outer layers staining with Safranin O and Alcian blue, indicating the presence of proteoglycans in the cartilage matrix, and the middle layer staining with Aniline blue, denoting the presence of collagen fibrils. Both the inner and middle layer, as well as the inner-most margin of the outer layer, showed alkaline phosphatase activity, which is indicative of mineralization. I recover the same three layers in the vertebrae of the little skate (Figure 3.8f, f''), suggesting that centrum construction is similar across many elasmobranchs. As noted previously, however, in some sharks and batoids (the porbeagle shark *Lamna nasus*, the hammerhead *Sphyrna blochii*, the basking shark *Cetorhinus maximus*, and the guitarfish *Rhinobatos productus*) there is no outer layer of hyaline cartilage around the centrum, but rather it is restricted to the arches and possibly just never migrates to surround the centrum (Ridewood, 1921; Daniel, 1922; Goodrich, 1930).

Multiple-part centra are known in many kinds of fishes. In most of these, the dual centrum complex consists of a chordacentral layer formed within the notochord sheath and an autocentrum consisting of a layer of bone deposited on the outside of the sheath and independent of the neural and hemal arches (Arratia et al., 2001). For example, the centrum of the fossil

holostean *Ophiopsis* is formed from an autocentrous deposition of smooth and compact bone on the outside of the notochord sheath, as well as an inner chordacentrum containing one or two rings of small tubes (Bartram, 1975). The Jurassic teleost *Leptolepis* also has an inner chordacentrum with a smooth outer autocentrum (Arratia and Hikuroa, 2010). Similarly, centra in Atlantic salmon have been documented to form from an inner layer of cells located within the notochord sheath and an outer layer of bone that is deposited by mesenchymal cells (Nordvik et al., 2005). In the little skate, however, the outer centrum cartilage does not develop independently of the neural and hemal arches, but is continuous with them and forms via the same mesenchymal cell population. These various examples provide evidence that centrum development is often complex and difficult to document. Centra are not merely formed through a single process, but can develop through a combination of mineralization within the notochord sheath, as well as condensation of sclerotomal cells around the notochord and neural tube.

This variation in centrum construction raises questions about the embryonic origins of these different centrum components. As mentioned previously, fate mapping experiments in axolotl and chick have shown that tetrapod centra, along with the remainder of the vertebral skeleton, are derived from cells of the ventral somites (Bagnall et al., 1988; Piekarski and Olsson, 2014). However, the same does not seem to be entirely true for teleost fishes. The notochord appears to play a significant role in centrum development in Japanese medaka and Atlantic salmon, with a separate layer of centrum bone developing within the notochord sheath, independent of the sclerotome-derived skeletal tissue (Ekanayake and Hall, 1987; Fleming et al., 2004; Nordvik et al., 2005). Even more compelling is the evidence from zebrafish, in which notochords have been shown to secrete bone matrix, and laser ablations of notochord cells result in the loss of centra (Fleming et al., 2004).

Conclusions

This study has comprehensively described the embryonic morphology and histology of the vertebral column in a skate for the first time. Histological and, in particular, 3D microtomographic data have helped to elucidate the process of early mesenchymal and condensation and differentiation. The antero-posteriorly continuous layer of cells that surrounds the notochord early in vertebral development appears to be mesenchymal in origin (likely derived from the sclerotome), and not derived from the notochord epithelium, as has been previously described in shark. It is possible that the notochord epithelium does play some role in inducing the formation of the layer of spindle-shaped cells, but additional experiments are necessary to determine this relationship. Additionally, rather than being separate structures at their genesis, neural arches initially condense continuously throughout the anterior-posterior axis before separating into neural and intercalary arches. Centra have evolved independently in several clades of vertebrates (Arratia et al., 2001), and those separate origins are evident when comparing centrum development across taxa. Skate centrum construction is markedly differently from that of osteichthyans (e.g. zebrafish and chick), in that the centrum consists of three layers of tissue: the inner layer of cartilage that constricts the notochord, the areolar calcification that makes up the double cone of the centrum, and an outer layer of hyaline cartilage. Zebrafish and chick centra both consist of one type of bone: acellular bone in the former and cellular bone in the latter (Hall, 2005).

While I have provided critical information on the morphology and tissues present throughout skate vertebral development, many aspects remain unclear, including the phylogenetic distributions of structures like the perichordal tube and composite centra, the embryonic origins of the centrum, and the mechanism driving the subdivision of the

cartilaginous tube in elasmobranchs. This lack of information can be remedied with contrast-enhanced microCT scans documenting axial column development across a broader range of taxa. Fate-mapping experiments to track the progeny of both the somites and the notochord in elasmobranchs will be crucial in determining if the notochord plays a substantial and general (perhaps ancestral) role in centrum development for gnathostomes, or whether the notochord-derived centra of teleosts are unique. Additional morphological studies aimed at identifying segmental features of the notochord (such as segmentally expressed genes or variations in notochord thickness) in other embryos, and experiments to identify and investigate the function of genes expressed segmentally along the notochord, will further test the role of the notochord in axial column segmentation.

When comparing vertebral development across gnathostomes, it becomes clear that this process is complex and variable within major taxa, and that Gadow's (1895) 'Arcualia Theory' of vertebral development does not apply to all elasmobranchs, let alone all vertebrates. Features that were clearly defined in several different species of shark, including the elastica externa, seem to be absent in the little skate. These differences again underscore the fact that shark anatomy and development are not general for vertebrates. Rather, as the sister group to osteichthyans, developmental data from elasmobranchs can help to polarize character transformations and determine primitive conditions across the gnathostome tree. As vertebrae represent such a fundamental feature of the vertebrate body plan, their complex construction and independent evolutionary histories underpinning vertebral skeletal diversity provide an opportunity to study variation in the mechanisms of axial segmentation and the developmental basis of convergent evolution.

Chapter 4: The embryonic origin of the axial skeleton in the little skate, *Leucoraja erinacea*

Summary

Vertebral anatomy and development vary across jawed vertebrates (gnathostomes). Centra, in particular, have independent phylogenetic origins in numerous gnathostome clades, such as the elasmobranchs, holocephalans, tetrapodomorphs, teleosts and holosteans, and there is evidence that the embryonic tissues contributing to the vertebrae may differ among gnathostome taxa. In chick and mouse, all parts of the vertebrae are derived from cells of the ventral portions of the somites (sclerotome), but in teleosts, vertebrae are derived from more diverse sources, with layers of acellular bone within centra apparently deposited by the notochord. Data from chondrichthyans can provide a test of whether sclerotomal or notochordal contributions to the centra are primitive for gnathostomes. In this chapter, I test the embryonic origins of the different components of the vertebral skeleton in the little skate, *Leucoraja erinacea*, using somite and notochord fate mapping experiments. CM-DiI injected into the ventral somite of early skate embryos is later recovered in the neural arches, hemal arches, inner layer of cartilage, areolar calcification of the centrum, and outer layer of hyaline cartilage (see chapter three). I demonstrate that the layer of spindle-shaped cells surrounding the notochord, previously thought to be notochord-derived in elasmobranchs, actually derive from sclerotome. Long-term fate mapping of notochord progenitor cells shows a contribution of labeled cells only to the vacuolated notochord cells and notochord epithelium, with no contribution to the vertebral skeleton. These experiments demonstrate that a sclerotomal origin of the vertebral skeleton is a general feature of gnathostomes, and that the teleost condition, in which the notochord

contributes to the centrum, is probably a specialized exception. Additionally, these findings contradict the assumption that fish, namely teleosts, show a primitive condition relative to tetrapods. Significantly, despite having evolved these structures independently, tetrapods and elasmobranchs employ the same tissues to build centra, suggesting some evolutionary polarity within the shared underlying morphogenetic processes.

Introduction

Vertebrae are the exemplary anatomical character of vertebrates, and for this reason, it is sometimes inferred that all vertebral constituent parts are homologous (Fleming et al., 2015) and are built using the same developmental mechanisms. However, vertebrae of the earliest vertebrates are relatively simple compared to their later jawed relatives. Indeed, both the earliest vertebrates and the earliest gnathostomes completely lacked centra, as do several extant taxa, signaling that many instances of centra in the vertebrate evolutionary tree were independent derivations. As I have shown in chapter two of this dissertation, centra have evolved independently in many different subgroups of vertebrates, including tetrapods, teleosts, and elasmobranchs, and vertebral morphology varies accordingly. Such apparent independence and variety in the evolutionary history of vertebral construction, raises important questions about instances of homoplasy, and especially about the developmental processes at work in each major clade. This works seeks to determine whether clades that have independently evolved centra have done so using conserved or divergent developmental mechanisms – and, in particular, common or distinct pools of skeletogenic progenitor cells.

At its most basic, the vertebral column consists of a series of paired neural arches that cover the spinal cord, paired hemal arches that enclose the caudal artery and vein, and, in many

gnathostomes, a series of centra that replace the notochord. In elasmobranchs each vertebra comprises a dorsal neural spine, two sets of cartilages dorsally that enclose the spinal cord (neural and intercalary arches), a single hemal arch enveloping the caudal artery and vein (unique to the caudal vertebrae), a hemal spine extending ventrally, and an outer layer of hyaline cartilage enclosing the centrum (Figure 4.1). Medial to the outer layer of hyaline cartilage is an areolar calcification (in the shape of an hourglass, along the rostro-caudal axis) and an inner layer of cartilage that constricts the notochord. In the intervertebral regions a ring of fibrous, spindle-shaped cells surrounds the remnants of the notochord.

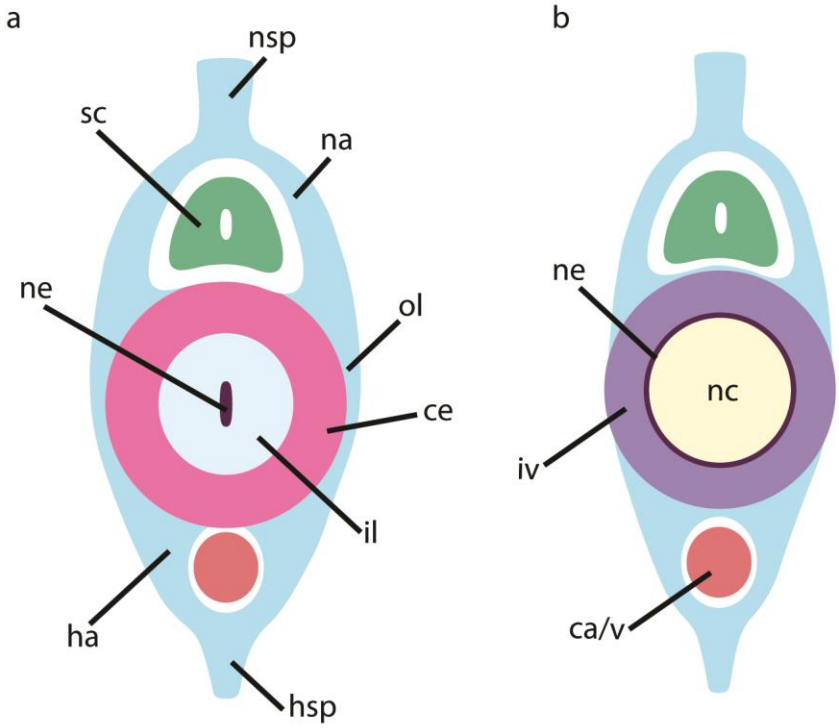

Figure 4.1. Schematic showing the individual components that make up a vertebra in adult skates. a, cross section through center of vertebra; b, cross section through intervertebral region. ca/v, caudal artery and vein; ce, centrum; ha, hemal arch; hsp, hemal spine; il, inner layer; iv, intervertebral ring; na, neural arch; nc, notochord; ne, notochord epithelium; nsp, neural spine; ol, outer layer; sc, spinal cord.

Somitic and notochordal contributions to the centra in osteichthyans

The two main embryonic tissues involved in vertebral development are the somites, segmented blocks of embryonic paraxial mesoderm, and the notochord, a stiff but flexible rod of vacuolated cells extending down the center of the body axis. Both of these cell populations have been shown to give rise to centra in different gnathostome taxa. A ventral subpopulation of the somites (the sclerotome) provides the embryonic source of centra in tetrapods (axolotl, a lissamphibian, and chicken, an amniote) and the notochord contributes chordoblast cells or bone matrix to centra in teleost ray finned fishes (salmon and zebrafish) (Bagnall et al., 1988; Fleming et al., 2004; Grotmol et al., 2005; Wang et al., 2013; Piekarski and Olsson, 2014; Ward et al., 2016).

In salmon no fate mapping experiments have been undertaken, but detailed morphological studies of vertebral column anatomy throughout development suggest that a small layer of chordoblast cells, derived from the notochord sheath, contribute the first layer of tissue to the developing centrum (Grotmol et al., 2003; Nordvik et al., 2005). These cells form within the notochord sheath, and it is clear from images taken of embryonic salmon vertebrae that the centrum bone consists of several distinct layers. As the centrum grows, layers of sclerotome-derived mesenchyme condense around the outside of the chordacentra (centra that form within the notochord sheath), forming a multi-part centrum (Wang et al., 2013). By adulthood, the inner layer of chordoblast cells makes up only a small portion of the overall centrum.

Several experiments in zebrafish have highlighted the substantial role of the notochord in vertebral development, including the contribution of notochord-secreted bone to the developing centrum. Sclerotome fate mapping experiments using injections of fluorescein-dextran have

shown that somite cells are incorporated into the vertebrae, although it is unclear whether those cells give rise to the centrum, or just the arches (Morin-Kensicki et al., 2002). When a single notochord cell is ablated, the corresponding centrum fails to form in that myotomal segment (Fleming et al., 2004). Notochord tissue was also found to produce bone matrix both *in vivo*, and when excised and cultured *in vitro*, in a segmental pattern (Fleming et al., 2001, 2004). Additionally, when the function of the *Tbx24* gene is blocked, resulting in the *fused somites* mutant, paraxial mesoderm fails to form regularly segmented somites early in development (Eeden et al., 1996). This mutation results in severe patterning defects in the neural and hemal arches, but the centra retain their characteristic wild-type morphology. This evidence suggests that in zebrafish, the notochord is responsible for building some of the bony tissue of the centra and that changes in somite boundaries seem to have little impact on centrum morphology.

In the axolotl, anterior somites were fate mapped using injections of fluorescein-dextran, as well as tissue grafting from transgenic green fluorescent protein-expressing (GFP+) donors (Piekarski and Olsson, 2014). When somites from GFP+ donors were transplanted into a wild type hosts, somite-derived cells were recovered surrounding the notochord and in the fibrous sheath early in development. Fluorescein-dextran experiments revealed numerous somite-derived cells in the developing neural arches. Labeled cells were also recovered in the developing cartilage of the centra, just lateral to the notochord, as well as in the fibrous cells making up the intervertebral rings (Piekarski and Olsson, 2014). Neither set of fate mapping experiments reared embryos until the centra were fully developed, so it cannot be said with complete certainty that the somites contribute to all vertebral components, but dye-labeled cells were present in early tissue condensations around the notochord, suggesting that those cells will eventually give rise to the centra of the adult vertebrae.

Numerous fate-mapping experiments in chick, using quail-chick chimaeras have shown that all components of the chick vertebral column, including the proximal portions of the ribs, are derived from migrating sclerotomal cells (Stern and Keynes, 1987; Bagnall et al., 1988; Aoyama and Asamoto, 2000). Furthermore, cell lineage tracing experiments within the somite have revealed that, the dorsal-most cells of the sclerotome give rise to the neural spines, the intermediate sclerotome gives rise to the neural arches and ribs, and the medial-most sclerotome gives rise to the centrum (Christ et al., 2000).

The notochord is known to play an important role in providing signals that regulate vertebral development, apart from its contribution to the centra of teleosts. Early notochord excision experiments in chick and salamander embryos show that the notochord is necessary for centrum development; when removed centra fail to segment and instead a solid rod of cartilage develops where the centra would usually form (Kitchin, 1949; Holtzer, 1952; Strudel, 1955). Some notochord-induced signals have been identified. The notochord expresses *Shh* in chick and mouse, which induces *Pax1* and *Mfh1* expression and maintains sclerotome proliferation (Fan and Tessier-Lavigne, 1994; Watanabe et al., 1998). These experiments testing the role of the notochord in centrum development have provided information on the signals involved in sclerotome proliferation, but other important signaling molecules are unknown and later vertebral development remains largely unstudied.

Does the sclerotome primitively give rise to the entire gnathostome vertebral skeleton?

When taken together, the previous studies on the contributions of the somites and notochord to vertebral development suggest a pattern: across tetrapods, somites give rise to all components of the vertebral skeleton, whereas in teleost fishes, the notochord gives rise to much

of the bone matrix of the developing centra. It is plausible, given the often-assumed primitive nature of fish when compared to tetrapods, that the potential of the notochord to contribute tissue to the centra is ancestral for gnathostomes. To determine whether a notochord contribution to vertebral centra is a teleost-specific feature of the axial skeleton, or a general feature for gnathostomes (that has been lost in tetrapods), data on the embryonic origin of vertebral skeletal elements in an osteichthyan outgroup – i.e. chondrichthyans – are needed.

Previous data on vertebral development in chondrichthyans derive largely from histological studies of a small number of shark species (Hasse, 1879; Klaatsch, 1893a; Gadow and Abbott, 1895; Goodrich, 1930). The most influential papers have posited that sclerotomal cells migrate from the somites to surround the notochord and neural tube, and perforate a notochord epithelium-derived fibrous sheath to then condense into vertebral cartilage (Gadow and Abbott, 1895; Goodrich, 1930). However, I have shown what seem to be mesenchymal cells condensing around the notochord in skate to form the spindle-shaped cells that are later referred to as the fibrous sheath of the notochord (Figure 3.1). Additionally, it is unclear whether the inner layer of cartilage (medial to the areolar calcification) is somite-derived, or whether the notochord is perhaps supplying cells for this tissue. To test whether the spindle-shaped cells of the fibrous sheath and inner layer cartilage are, indeed, derived from the paraxial mesoderm, and to determine if there is any notochordal component to the vertebrae in elasmobranchs, sclerotome and notochord long-term fate mapping data are needed. Here I present the results of such experiments, performed in embryos of the little skate, *Leucoraja erinacea*.

Materials and Methods

Animal collection, husbandry, and fixation

Collection and husbandry for *Leucoraja erinacea* embryos was performed as described in chapter three.

Gene cloning and riboprobe synthesis

Embryonic *L. erinacea* cDNA was provided by Joyce Pieretti (Shubin lab). A *Pax1* orthologue was first identified by searching Pubmed for *Scyliorhinus torazame Pax1* sequences and using those to BLAST against skate transcriptomic data through skatebase.org (Wyffels et al., 2014). Two sets of primers for *Pax1* were designed using Primer3 Plus: forward: 5'-CATACCCCAACCACATGTCA-3'; reverse: 5'-ACCGGACACCTATTCTGTGC-3'; and forward: 5'-CAACCTTCCCCTCAACTCAA-3'; reverse: 5'-TCTACGCGTTAGCCAGGTTT-3'. The probe sequences were PCR amplified using the selected primers and DNA was extracted and purified using a GeneJET gel extraction kit. The PCR products were ligated into a pGem-T easy cloning vector and then transformed into DH5 alpha competent cells. Minipreps and midipreps were performed using Qiagen kits and sequences were confirmed at the University of Chicago Comprehensive Cancer Center Sequencing and Genotyping Facility. Sequences were transcribed in a standard in vitro transcription reaction using SP6 and T7 RNA polymerases (one for each probe).

Whole mount mRNA *in situ* hybridization

L. erinacea embryos were rehydrated from 100% methanol (MeOH) (five minutes each at 75%, 50%, and 25% MeOH in PBS + 0.1% tween20 (PBT) and permeabilized in proteinase-K

(10µg/ml in PBT) for 15 minutes at room temperature. Embryos were then refixed with 4% paraformaldehyde at room temperature for 20 minutes and then rinsed 3 x 5 minutes with PBT. Prehybridization solution (5 ml formamide, 2.5 ml 20X SSC Ph 4.5, 1 ml 10% SDS, 250 µl tRNA, 5 µl Heparin, and 1.5 ml water) was added to the vial until embryos sank to the bottom. The solution was then removed and over 1 ml of prehybridization solution was replaced and the embryos were incubated for at least 60 minutes in a 70ºC water bath with gentle shaking. The prehybridization solution was then removed and 2 ml of hybridization mixture plus the riboprobe (7 µl/ml) were added and left to hybridize overnight at 70ºC.

Following hybridization embryos were rinsed 2 x 60 minutes with prewarmed solution 1 (20ml formamide, 8 ml 20X SSC pH 4.5, 4 ml 10% SDS, and 8 ml water) at 70ºC and then rinsed 2 x 30 minutes with another prewarmed solution (20 ml formamide, 4 ml 20X SSC pH 4.5, and 16 ml water) at 70ºC. Embryos were then rinsed 3 x 10 minutes in MABT and blocked with 20% heat inactivated sheep serum plus 1% Roche blocking agent for over 2.5 hours on a horizontal shaker. The block was then removed and placed with prewarmed block plus Roche anti-Dig antibody at a 1:2000 dilution and the tissue was incubated overnight at 4ºC with gentle shaking.

Following antibody detection the embryos were rinsed 3 x 5 minutes in MABT at room temperature and then rinsed 5 x6 0 minutes in MABT at room temperature and left in MABT for at least two days at 4ºC. The embryos were then rinsed 3 x 10 minutes in NTMT (2 ml 5M NaCL, 5 ml 2M Tris/HCL pH 9.5, 5 ml 1M MgCl2, 0.2 ml 50% Tween20, and water to 100 ml) and incubated in BM Purple and monitored for signal. Upon completion of the reaction embryos were rinsed 2 x 30 minutes in PBT and then fixed in 4% PFA at room temperature for one hour.

They were then rinsed 3 x 5 minutes in PBS and cleared in glycerol at 25%, 50%, and 75% glycerol in PBS for imaging and long term storage.

Vibratome sectioning

Following whole mount *in situ* hybridization, pieces of trunk in 75% glycerol in PBS and embedded in 15% gelatin in PBS. Gelatin blocks were post-fixed in 2% PFA overnight at 4ºC, trimmed and sectioned with a Leica VT1000s vibratome at a 40 µm thickness. Sections were mounted with fluoromout with DAPI to visualize morphological structures that were not readily apparent with light imaging. Slides were imaged under bright field and fluorescence with a Zeiss Axioscope.

Fate mapping experiments

Somite injections

L. erinacea embryos were obtained from the Marine Biological Laboratory in Woods Hole, MA and kept in a flow-through sea table between 15º and 18ºC until stage 24. A flap was cut in the egg case using a razor blade and the embryo and yolk were transferred to a Petri dish. Embryos were anesthetized in a solution of MS-2222 (Ethyl 3-aminobenzoate methanesulfonate – Sigma-Aldrich) in seawater. CellTracker CM-DiI (Thermofisher) (5 µg/µl in ethanol) was diluted 1:10 in 0.3 M sucrose and injected into the ventral somites (2-4 injections per embryo) using a pulled glass capillary needle and a Picospritzer pressure injector (Figure 4.2a). Embryos were returned to their egg cases and to the sea table to recover for 7 or 12 weeks.

"Notochord triangle" injections

In elasmobranch fishes the notochord derives from a small triangular region of progenitor cells (the "notochord triangle") that develops, beginning at stage 12, at the posterior margin of the blastodic during gastrulation (Ballard et al., 1993). At stage 14 a small window was cut in the egg case at the position of the embryo and CM-DiI was injected through the albumin layer into the notochord triangle (Figure 4.2b). The window was then sealed with donor eggshell and Krazy Glue™ gel and eggs were returned to the sea table to develop for an additional 16-18 weeks (Figure 4.2c).

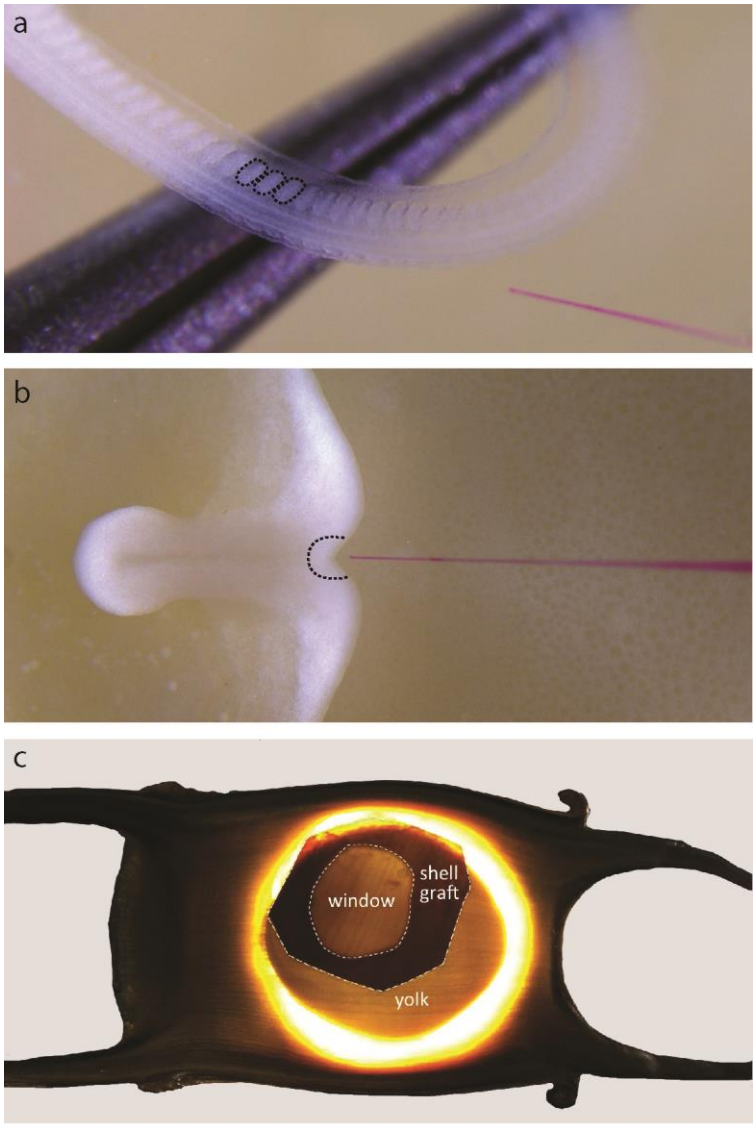

Figure 4.2. CM-DiI injections in the somites and notochord. a, pulled capillary needle loaded with CM-DiI and stage 24 embryo, with three somites highlighted using dashed lines; b, stage 13 embryo and CM-DiI needle showing notochord progenitor cells highlighted using a dashed line; c, the egg case of a notochord-injected embryo subsequent to windowing, injecting, and egg grafting.

Validation of fate mapping injection placement

To verify the correct placement of DiI injections, three somite-injected embryos were fixed immediately post-injection, and three notochord-injected embryos were fixed five days post-injection in 4% paraformaldehyde in PBS overnight at 4ºC, rinsed 3X15 min in PBS, and

stained with DAPI at a 1:1000 concentration and phalloidin at a 1:300 overnight at room tempterature. Somite-injected embryos were imaged on a Zeiss lightsheet microscope and notochord-injected embryos were imaged on Zeiss lightsheet or LSM 780 confocal microscopes.

Results

Conservation of sclerotome gene expression in the little skate

The transcription factor *Pax1* is expressed in the migrating sclerotome in chick, mouse, zebrafish, and medaka, and is therefore regarded as a sclerotome marker (Balling et al., 1996; Christ et al., 2004; Mise et al., 2008).To verify that the cells being targeted in skate somite fate mapping experiments are homologous with the source of sclerotome in osteichthyans, I characterized expression of *Pax1* in skate embryos at stages 22, 24, and 26 by whole mount mRNA *in situ* hybridization (WMISH), during which it is assumed that the cells of the sclerotome are migrating away from the somites and towards the notochord.

DAPI staining of cell nuclei and *Pax1* color inversion for tissue in section allowed for visualization of the extent of *Pax1* expression in relation to somite morphology. In stage 22 *Pax1* is expressed throughout the migrating sclerotome and is beginning to diffuse antero-posteriorly as these cells undergo EMT (Figure 4.3a, b, b'). In cross section, *Pax1* expression is strong from the medial margin of the somite to the lateral border of the notochord (Figure 4.3h, h'). Expression in stage 24 embryos is similar to stage 22, with staining throughout the sclerotome, in a pattern consistent with sclerotome emigrating from the ventral somite (Figure 4.3c, d, d'). By stage 26, *Pax1* expression is restricted slightly to the posterior margin of each somite in lateral view and sagittal section (Figure 4.3e, f, f'), and remains strongly expressed medially in cross section (Figure 4.3g, g').

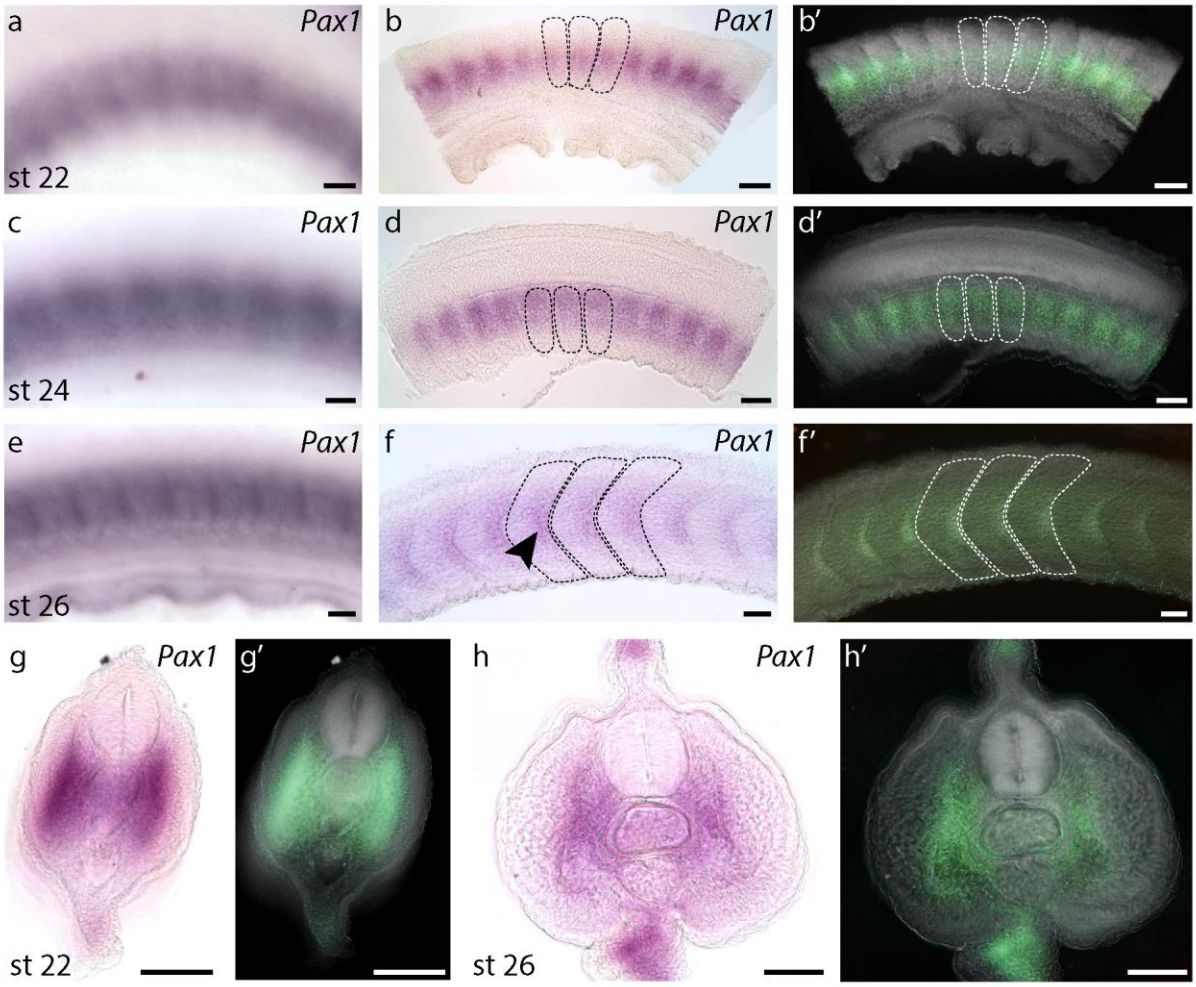

Figure 4.3. *Pax1* expression patterns in stages 22, 24, and 26 in the little skate. a, WMISH of **Figure 4.3 continued.** *Pax1* for stage a 22 embryo, in lateral view; b, sagittal section showing *Pax1* expression in a stage 22 embryo; b', sagittal section of a stage 22 embryo, showing *Pax1* expression, with color inverted and stained with DAPI; c, WMISH of *Pax1* for stage a 24 embryo, in lateral view; d, sagittal section showing *Pax1* expression in a stage 24 embryo; d', sagittal section of a stage 24 embryo, showing *Pax1* expression, with color inverted and stained with DAPI; e, WMISH of *Pax1* for stage a 26 embryo, in lateral view; f, sagittal section showing *Pax1* expression in a stage 26 embryo; f', sagittal section of a stage 26 embryo, showing *Pax1* expression, with color **Figure 4.3 continued.** inverted and stained with DAPI; g, cross section of a stage 22 embryo showing *Pax1* expression; g', cross section of a stage 22 embryo showing *Pax1* expression, with color inverted and stained with DAPI; h, cross section of a stage 26 embryo showing *Pax1* expression; h', cross section of a stage 26 embryo showing *Pax1* expression, with color inverted and stained with DAPI. Scale bars = 100 µm.

Sclerotome contributes to all components of the skate vertebral skeleton

CM-DiI was focally microinjected into the ventral somite, as confirmed by light sheet microscopy of embryos immediately post-injection (n=3). By 50-52 days post-injection (dpi) (approximately stage 31), the fibrous sheath had formed around the notochord, and mesenchyme had condensed around the neural tube and caudal artery and vein, but had not yet differentiated into cartilage (see chapter three). In all embryos analyzed at this stage (n=5), CM-DiI labeled cells were recovered in the outer layer of spindle-shaped cells of the fibrous sheath in the little skate throughout the axial column (Figure 4.4e-f). These cells seemed to be concentrated in the ventral half of each vertebral unit. CM-DiI-positive cells were identified throughout the layer of spindle-shaped cells (including amongst the inner-most layer of cells – Figure 4.4g), providing evidence that the entirety of this layer of tissue is derived from sclerotome cells, and not from the notochord epithelium, as was proposed by Gadow and Abbott (1895).

By 110dpi (approximately stage 34), vertebrae are fully developed, with completely segmented cartilages and a centrum consisting of three layers (Figure 4.1, and see chapter three). These three layers include the inner layer of hyaline cartilage that constricts the notochord, the areolar calcification, and an outer layer of hyaline cartilage, with the notochord persisting in the intervertebral regions. In this set of embryos, CM-DiI-positive cells were identified in every component of the vertebral skeleton, with the exception of the neural spines. Dorsally, CM-DiI was present in the chondrocytes of the neural arches, from their bases, near the areolar calcification, to more dorsal positions (n=2) (Figure 4.4h). CM-DiI also was recovered in all components of the centrum, including the inner layer of cartilage located medial to the centrum (n=1) (Figure 4.4l), the areolar calcifications (n=3) (Figure 4.4i), and chondrocytes of the outer centrum cartilage (n=2) (Figure 4.4k). As in embryos at 49dpi, the majority of CM-DiI was

recovered in the ventral half of each vertebra, though several instances of dorsally-localized dye were identified (Figure 4.4h, k). No CM-DiI was found in the remaining notochord, but in numerous sections CM-DiI was located in the nervous system, particularly in the dorsal root ganglia as they exit the spinal cord, which may be a result of contamination of neural crest cells during somite labeling, as dorsal root ganglia are neural-crest derived (Teillet et al., 1987) (data not shown).

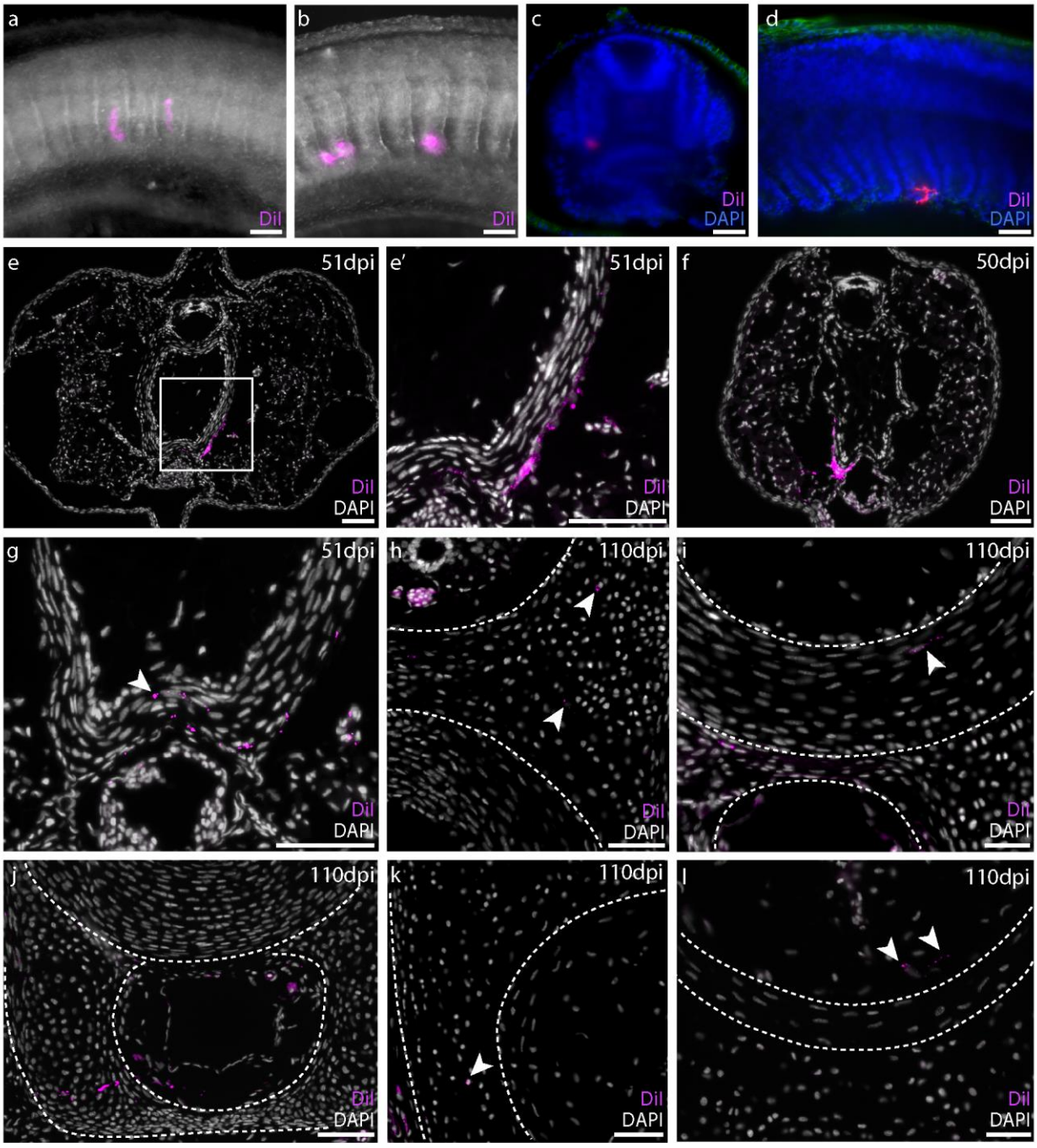

Figure 4.4. Somite fate mapping experiments. a-b, two embryos showing CM-DiI injections in the ventral somites; c-d, confocal images confirming the placement of the dye immediately post injection in cross section (c) and in sagittal section (d); e, CM-DiI labeled cells surrounding the fibrous sheath of the notochord 7 weeks post-injection; e', 20x zoom of the CM-DiI labeled cells in e; f, CM-DiI labeled mesenchymal cells condensing around the notochord in the caudal region 7 weeks post-injection; g, CM-DiI labeled cells present throughout the layer of spindle-shaped cells 7 weeks post-injection; h, CM-DiI labeled chondrocytes in the neural arch of a late-stage embryo 16 weeks post-injection; i, CM-DiI labeled cells in the areolar cartilage of the

Figure 4.4 continued. centrum 16 weeks post-injection; j, many CM-DiI labeled cells in the hemal arch of an embryo 16 weeks post-injection; k, CM-DiI labeled cells in the outer layer of hyaline cartilage surrounding the centrum 16 weeks post-injection; l, CM-DiI labeled cells in the inner layer of cartilage constricting the notochord 16 weeks post-injection. Scale bars = 100 μm.

The notochord does not contribute to the skate vertebral skeleton

Presumptive notochord cells of the early embryo (the notochordal triangles of Ballard et al. (1993)) were injected with CM-DiI in stage 12-14 embryos (Figure 4.5a, b). At 5dpi, (approximately stage 17), embryos (n=3) were fixed and imaged to confirm the accuracy and precision of injections. In these embryos, CM-DiI was found either only in the notochord (n=2) or in the notochord and neural tissue (n=1) (Figure 4.5c, d). CM-DiI was not located in the paraxial mesoderm in any embryos imaged at 5dpi, suggesting that notochordal triangle injections successfully labeled notochord progenitors without contamination of paraxial mesoderm.

At 116-129dpi (stage 34), CM-DiI was recovered in the anterior portion of the notochord in five of five individuals examined. In five embryos, CM-DiI was recovered in notochord cells (Figure 4.5e-f) or notochord epithelium (Figure 4.5h) of the intervertebral regions of the axial column. In three embryos, CM-DiI-positive cells were recovered in the remnants of notochord epithelium that persist in the center of the centrum, where the notochord is almost completely replaced by inner layer cartilage (Figure 4.5g), though no CM-DiI-positive chondrocytes were recovered in the inner layer of cartilage itself. No CM-DiI labeled chondrocytes were observed in any other components of the axial skeleton.

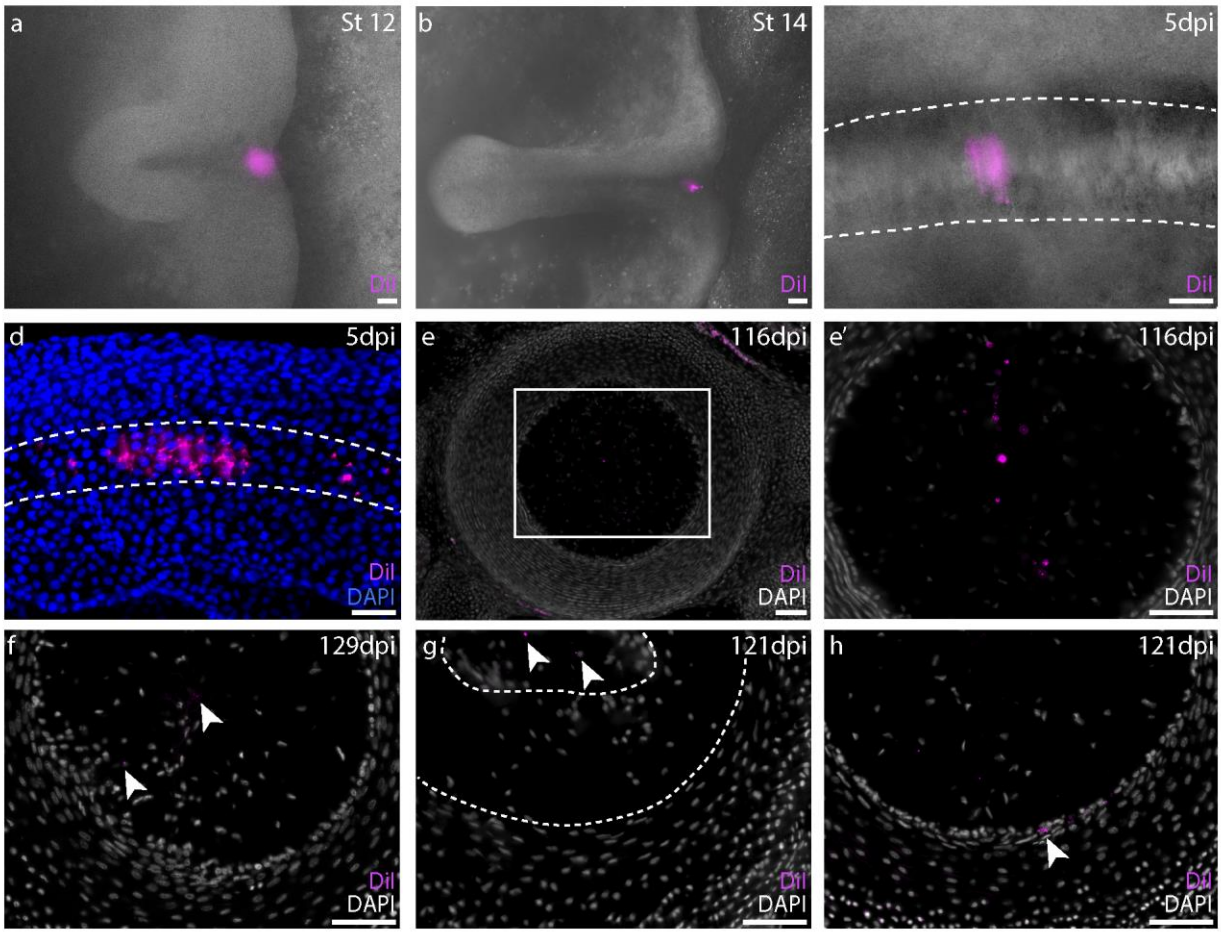

Figure 4.5. Notochord triangle fate mapping experiments. a, CM-DiI injection placement in the notochord triangle of a stage 12 skate embryo; b, CM-DiI injection placement in at stage 14 skate embryo; c, brightfield image of a skate embryo 5 days post-injection showing CM-DiI located only within the notochord; d, confocal image of a skate embryo 5 days post-injection showing a strip of CM-DiI throughout the notochord; e, a thin section of the notochord in an embryo 16 weeks post-injection showing CM-DiI positive notochord cells at 10x; e', 20x view of the indicated region in e, showing many DiI positive notochord cells; f, CM-DiI positive notochord cells in an embryo 18 weeks post-injection; g, CM-DiI postivie cells in the remnants of the notochord epithelium at the center of the inner layer of cartilage; h, the notochord epithelium showing CM-DiI labeled cells. Scale bars = 100 µm.

Discussion

The axial skeleton in gnathostomes is primitively somite-derived

The long-term somite fate mapping experiments reported here demonstrate that cells of the ventral somite contribute to all components of the vertebrae in skate, including the neural arches, hemal arches and spines, the inner layer of centrum cartilage, the areolar calcification of the centrum, and the hyaline cartilage surrounding the centrum. I also show that the somites give rise to the spindle-shaped cells that makes up the fibrous sheath described in chapter three. CM-DiI labeling of notochord progenitor cells resulted exclusively in labeling of the notochord itself and the notochord epithelium, with no contribution to the cartilage or mineralized tissues of the axial skeleton.

In all tetrapods studied to date (mouse, chick, and axolotl; thus covering amniotes and lissamphibians), vertebral elements are derived from the somites, although complementary notochord fate mapping experiments have not been undertaken (Figure 4.6) (Dalgleish, 1985; Bagnall et al., 1988; Piekarski and Olsson, 2014). Within the teleosts, there is evidence that the centra of both salmon and zebrafish form at least in part from notochord, either from cells in the notochord sheath or by notochord-secreted bone matrix (Fleming et al., 2004; Nordvik et al., 2005; Wang et al., 2013). Medaka, conversely, seem to derive their entire centrum skeleton from the sclerotome (Ekanayake and Hall, 1987). My demonstration that the axial skeleton of skates likely derives exclusively from sclerotome, along with available data from tetrapods and medaka, suggest that this tissue was likely the sole, primitive source of axial skeletal elements in jawed vertebrates. The notochord contribution to the centra in zebrafish and salmon is therefore likely a derived condition of teleost fishes. However, because teleosts are so diverse (over 26,000 living species (Nelson, 2006)) and vertebral development has only been studied in a small proportion of

these (cyprinids and salmonids), it remains to be determined whether a notochord contribution to the centrum is general for teleosts, or rather is an autapomorphic feature of a subset of teleost taxa. Additionally, because centra are likely independently derived in numerous non-teleost actinopterygians, such as gars and bichirs, it is unclear how deeply nested the notochord contribution to the centra is on the actinopterygian tree. Additional somite fate mapping experiments in actinopterygians such as gars (*Lepisosteus*), bichirs (*Polypterus*), and possibly a teleost taxon that is sister to the majority of teleosts, such as the osteoglossomorph butterflyfish (*Pantodon*), would provide a clearer picture of the evolution of centrum development across gnathostomes.

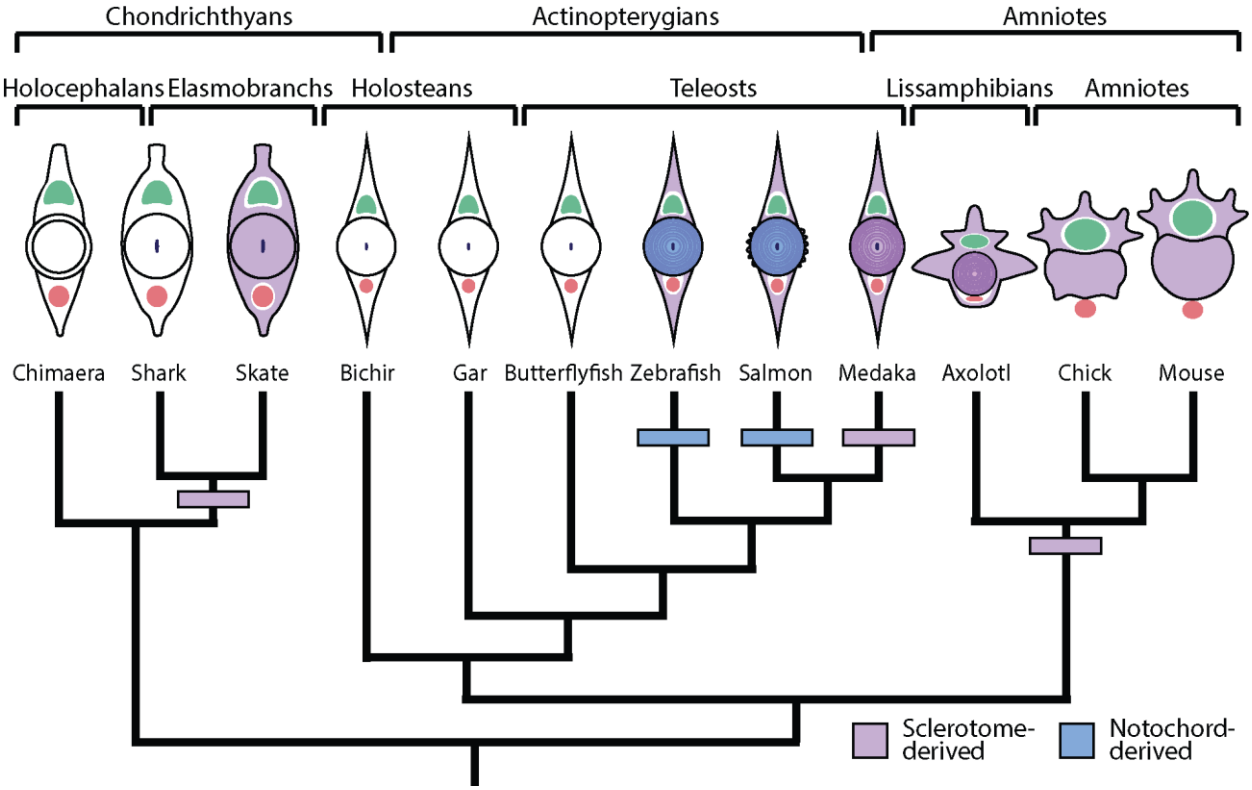

Figure 4.6. Schematic showing centrum evolution along with embryonic origins of vertebral elements. Boxes indicate independent originations of centra. Purple = somite-derived elements, blue = notochord-derived elements. White vertebrae indicate taxa for which no fate mapping studies have been done.

Although these experiments in skate show no cellular contribution from the notochord to the centra, it is still possible that the notochord epithelium provides some extracellular matrix (ECM) to one of the layers of the centrum, such as the inner cartilage layer or the areolar calcification. Importantly in zebrafish, the bone matrix secreted from the notochord is acellular, suggesting that contributions to the centra from the notochord need not be cells themselves, but rather can be bone or bone-like matrix (Fleming et al., 2004). An acellular contribution would not be obvious with the experiments undertaken in skate to date, but could be tested for using analyses of the expression of various ECM proteins in paraffin section throughout centrum development. For example, a recent study in fugu (*Takifugu rubripes*) showed that the two tissue layers bounding the acellular bone of the developing centrum - notochord basal cells (lining the inner surface of the notochord sheath) medially and osteoblasts peripherally – express known ECM-producing genes. The notochord basal cells and osteoblasts both expressed *Sparc* and *Col2a1*, while the osteoblasts that function to deposit acellular bone matrix also express *Col1a1*, suggesting that in fugu Sparc and Col2 might be synthesized by notochord basal cells to produce the matrix of the notochord sheath (Kaneko et al., 2016). In skate, if the notochord epithelium secretes an acellular matrix that envelopes the cells of the centrum, I would expect to see presence of these proteins first in the outer layer of the notochord epithelium and then at the location of the spindle-shaped cells that form the areolar calcification. Enault et al. (2015) examined collagen gene expression in two embryonic stages of the catshark *Scyliorhinus canicula*, and found that *Col2a1* was localized to the developing centrum in 6 cm-long embryos and was expressed both in the inner layer of the centrum and the hyaline cartilage in 9 cm-long embryos. However, the series of *Scyliorhinus* embryos was not complete, and few other potential genes or proteins involved in ECM deposition have been studied in chondrichthyans.

Experiments to examine of a wider array of genes and proteins involved in ECM formation throughout the entirely of vertebral development would provide a clearer picture of the potential notochord contribution of acellular tissue to the centrum in chondrichthyans.

It is interesting to note that CM-DiI was located most commonly in the ventral portions of the developing vertebrae, with instances of dorsally positioned dye being rare. Several factors could contribute to this result, including placement of the CM-DiI injections as well as the timing of injection. In chick, specific subpopulations of the sclerotome have been mapped to different components of the vertebrae, with dorsal-most, intermediate, and ventromedial cells giving rise to the neural spines, neural arches and ribs, and centra, respectively (Christ et al., 2000). It is possible that most of the dye injections were placed too far ventral to contribute to the neural spines. Given my gene expression data, it is also likely that sclerotomal cells had already begun their migration by the time I injected the dye into each embryo, resulting in biased labeling of later migrating subpopulations of sclerotome.

Embryonic origin of the fibrous sheath

The layer of spindle-shaped cells that surrounds the notochord early in elasmobranch vertebral development (also referred to as the fibrous sheath) was shown in chapter three to give rise to the areolar calcification of the centrum in the little skate. Many authors in the historical literature (Gegenbaur, 1872; Gadow and Abbott, 1895; Goodrich, 1930) state that this layer of elongate, spindle-shaped cells is derived from the notochord epithelium, and is later invaded by sclerotomal cells. Despite the suggestions of a somitic origin of the fibrous sheath by contemporary embryologists Hasse (1879) and Klaatsch (1893), the idea became entrenched, and the concept of notochordal origin of this tissue has prevailed to this day. Histological sections

described in chapter three of this dissertation show mesenchymal cells condensing around the notochord prior to the appearance of the elongate spindle-shaped cells that constitute the fibrous sheath. This study demonstrates that the notochord does not contribute cells to any component of the vertebral skeleton or the rings of spindle-shaped cells persisting in the intervertebral regions, and that conversely, the fibrous sheath is a derivative of the sclerotome in skates (Figure 4.4e-g).

Is somite resegmentation ancestral for gnathostomes?

Although the embryonic origins of the cells contributing to the vertebrae are now known in skate, it remains unclear whether each somite contributes to a single vertebra, or whether the somites and vertebrae are offset, with each somite contributing cells to two vertebrae, referred to as resegmentation (Remak, 1855; Christ et al., 2000). This frameshift causes the vertebrae to align with the myosepta, allowing myomeres to bridge two successive vertebrae and provide greater control over axial movement (Keynes and Stern, 1988). For many years after Remak's (1855) observations, the notion of resegmentation was rejected, first for all vertebrates and then later for fishes (Lauder, 1980; Christ and Wilting, 1992; Christ et al., 2000).

Experiments to track this somite resegmentation have been undertaken in the osteichthyans zebrafish, axolotl, and chick, with all taxa showing that a single somite gives rise to two vertebrae. In chick the somites are thought to recombine strictly, with the posterior half of the one somite and the anterior half of the next posterior somite forming a single vertebra (Bagnall et al., 1988; Huang et al., 2000). Recent experiments have confirmed that strict resegmentation occurs in chick, and also have documented a slight rostral shift in the alignment of the dorsoventral sclerotomal cells, accounting for a tilt in the neural arches of the lumbosacral region (Ward et al., 2016). Resegmentation in axolotl seems to follow the pattern of chick and

zebrafish, with one somite contributing to two vertebrae. However, because the anterior and posterior portions of each somite were not precisely labeled, it is unclear whether the resegmentation is strict, or whether some anterior somite cells end up in the anterior, as well as the posterior, portions of vertebrae (Piekarski and Olsson, 2014). In zebrafish, the anterior third of each somite contributes not only to the posterior third of each vertebra, but cells seem to leak into the anterior third as well, a process termed "leaky resegmentation" (Morin-Kensicki et al., 2002).

To determine whether resegmentation is an ancestral process for jawed vertebrates, and if so, whether the ancestral pattern is strict or leaky, experiments labeling adjacent somites with two different fluorescent dyes in skates would be ideal. Recovering both red and green dye-labeled cells as evenly mixed throughout the late-stage vertebrae would provide evidence that vertebral segments bear no correspondence to the original somite boundaries. Single vertebrae comprising only red- or green-labeled cells would indicate that individual somites correspond 1:1 with somite boundaries, and that no resegmentation has occurred. Lastly, somite boundaries may be maintained throughout vertebral segmentation, but shifted slightly. This scenario would result in a single vertebra that is found to consist of red-labeled cells anteriorly and green-labeled cells posteriorly. The question of the phylogenetic distribution of resegmentation becomes particularly interesting for chondrichthyans with caudal diplospondyly, like the little skate, because nothing is known about how a single somites contributes to two caudal vertebrae that are contained within one myotomal segment. Two-color fate mapping experiments focused on the caudal region would determine whether, for each myotomal segment, both vertebrae are formed from two somites, or whether one vertebra develops entirely from one somite while the other receives cells from two.

Conclusions

In this chapter I have demonstrated that in an elasmobranch chondrichthyan, the little skate, the entire vertebral skeleton likely derives from the somites. Dye-labeled cells derived from the somites were recovered in almost all parts of the vertebrae, including the neural and hemal arches, hemal spines, and all layers of the centrum. The findings of my experiments challenge the long-accepted developmental scenario proposed by Gadow and Abbott (1895) in which the fibrous sheath is proposed to be derived from the notochord and invaded by sclerotomal cells. The present work uses fate mapping experiments to show that notochord progenitor cells only give rise to the notochord and its enveloping epithelium. These results, combined with experimental data from several other gnathostome taxa, suggest that a sclerotomal origin of the vertebral skeleton is the general condition of gnathostomes, and that the notochord contribution seen in some teleosts, is likely a specialized condition. This finding is significant because each of the major gnathostome clades studied to date - elasmobranchs, teleosts, and tetrapods - all evolved centra independently. This raises questions about the genes and pathways at work in each group, the possible conservation of these molecular mechanisms, and provides a means of exploring homoplasy in the evolution and development of this fundamental feature of vertebrate morphology.

Chapter 5: Conclusions and future directions: centrum homology, vertebral segmentation, and the 'Arcualia Theory' reconsidered

In this dissertation I have analyzed the evolution and development of the vertebral column across gnathostomes using a combination of comparative morphological data, evolutionary analyses, descriptive embryology, and experimental manipulations. In chapter two I surveyed gnathostome vertebral morphology and examined the evolutionary patterns of vertebral modifications, focusing on centra. I concluded that centra, as well as several other vertebral structures, have originated independently numerous times in gnathostomes. Chapter three sought to determine how vertebral development in an insufficiently studied group, the cartilaginous fishes, differs from other gnathostomes, by utilizing microCT scans and histological sections of the little skate. I observed that skate centra begin as a layer of spindle-shaped cells surrounded by an unsegmented tube of cartilage that eventually segments and differentiates into three layers of tissue. Additionally, neural arches develop from strips of continuous mesenchyme that condense along the anterior-posterior axis. In chapter four I tested whether the embryonic source tissue for skate centra was the somites, which would correspond with tetrapods (Bagnall et al., 1988), or the notochord, which is what has been observed in some teleosts (Fleming et al., 2004; Nordvik et al., 2005). I found that all parts of the vertebrae in the little skate develop from the somites, providing evidence that a completely somite-derived vertebral skeleton is primitive for jawed vertebrates and that a notochord contribution is specialized for teleosts. Several key issues have emerged from the results of this dissertation, including homoplasy of portions of the vertebral skeleton, the process of vertebral segmentation, and relevance of these new findings to the

historical and accepted model of vertebral development and system of nomenclature proposed by Gadow and Abbott (1895) and reinforced by Goodrich (1930), Janvier (1996), Arratia et al. (2001), and Fleming et al. (2015). Here I will explore the implications of my dissertation research findings on these topics as well as the future research directions they suggest.

Homoplasy and homology in the vertebral column

This dissertation centers on the homoplasy of the vertebral column in several respects, including the multiple independent originations of centra throughout the evolution of jawed vertebrates and the question of whether these occurrences of centra are built in the same ways and using the same embryonic source tissues. It is clear that centra are highly homoplastic - the elasmobranchs, teleosts, and tetrapods (at the very least) represent three unambiguous centrum originations. However, parallels in centrum development among some groups, such as the contributions of the somites to the vertebral skeleton, hint at similar underlying mechanisms. Therefore, these mechanisms either evolved once and were deployed in numerous different lineages to build centra, or were assembled convergently. Here I explore homology at different levels in the morphology and development of centra, a key homoplastic feature of the vertebral column, and propose additional experiments necessary to further test the homology of the developmental mechanisms that build centra. Because detailed developmental data are only available for a limited number of gnathostomes, I will focus largely on centra in tetrapods (chick, mouse, and axolotl), teleosts (zebrafish, salmon, and medaka), and elasmobranchs (the little skate), although centra in other groups (non-teleost actinopterygians and lungfish) are likely also convergently evolved.

Debates and discussions on homology have been commonplace in the evolutionary biology literature for many years (Patterson, 1982, 1988; Van Valen, 1982; Roth, 1984; Wagner, 1989; Panchen, 1992). Homology was first defined in its current sense prior to acceptance of the evolution by natural selection by Owen (1843; pg. 379) as "the same organ in different animals under every variety of form and function." For Owen, the comparison of a taxon to an archetype provided the explanation of homology, and other early definitions of homology were similar, establishing correspondence in morphology, structure, and connectivity as criteria for homology (Patterson, 1982). For example, according to the early non-evolutionary definitions of homology, two bones could be considered homologous if they were located in the same position in the body, were built using the same tissue, and articulated to the same surrounding bones, regardless of the presence of that bone in the ancestor of the two taxa containing them. More recent, evolutionary-based definitions have referenced the importance of shared common ancestry as the key explanation of homology among morphological structures (Patterson, 1982).

Kinds of homology were aggregated and classified by Panchen (1992), based on a review by Patterson (1982), into two major categories, taxic and transformational, each containing a hierarchy of subcategories. The different ways of classifying taxic homology vary based on the position of the node in the phylogenetic hypothesis being considered, and represent characters that are used to unite groups of taxa at different phylogenetic levels. Taxic homology includes autapomorphies, which are features that characterize a single taxon, synapomorphies, which are present in and unite several taxa in a monophyletic group, and symplesiomorphies, which represent characters present at a phylogenetic level broader than that bring considered (Panchen, 1992). The same character can be considered to be an autapomorphy for one taxon but a synapomorphy of several taxa, or even a symplesiomorphy, when considering successively

deeper nodes in the tree. For example, jaws are an autapomorphy of gnathostomes, but a synapomorphy that unites chondrichthyans and osteichthyans, and a symplesiomorphy of more deeply nested groups such as birds and teleosts, that do not share the character to the exclusion of other taxa. Taxic homology in the form of apomorphies and plesiomorphies is referenced frequently in the current phylogenetic literature.

Transformational homology includes comparisons between two features that differ substantially but are thought to derive from a shared, and thus also developmental, ancestral condition (Patterson, 1982). Transformational homology can be further subdivided into singular, in which a structure in one taxon is compared directly to a similar structure in a different taxon, and iterative, which compares structures in a series. Examples of singular and iterative transformational homologues include the transformation of the forelimbs of tetrapods into the wings of birds, and the comparisons between cranial and caudal vertebrae in any gnathostome, respectively.

Within transformational homology are general homology, in which a structure is compared in reference to an ancestral or archetypal condition, and special homology, in which two corresponding structures are compared between two individual taxa (Owen, 1848; Panchen, 1992). Examples of general homology include comparisons between the archetypal vertebra of Owen (1848), mentioned in chapter one, with vertebrae observed in living and fossil gnathostomes. Comparisons between the centrum structure of individual taxa such as *Leucoraja* and *Danio* qualify as special, as well as taxic, homology. All taxic homology hypotheses must be made relative to a phylogenetic context.

Almost all classifications of homology listed above are applicable to vertebral column evolution. Most obviously, vertebrae represent a classic example of iterative homology, in which

a comparable structure is repeated multiple times throughout the body. Vertebrae provide an interesting case in which to study the elaboration of a common starting point for different functions throughout the body. This dissertation, however, focused 1) on centrum evolution across gnathostomes, and 2) on the similarities and differences in centrum development in tetrapods, teleosts, and elasmobranchs. The following sections will explore hypotheses of centrum homology in the context of phylogenetic relationships (taxic homologies) and Wagner's (1989) 'biological homology', which includes evolutionary developmental explanations of homology statements.

Centra in the context of phylogenetic homology

Different kinds homology hypotheses have been proposed to explain similarities in both morphology and development, and associated tests to determine whether certain structures are homologous according to each hypothesis have been devised. Cladistic (also called phylogenetic) homology was discussed by Patterson (1982) as characters that were present in the common ancestor of the taxa in which they are located, either in their current form or through an evolutionary transformation. Patterson (1982, 1988) proposed three tests of the relatedness of two conjectured homologues, including similarity, conjunction, and congruence. Similarity was originally used by Owen (1843) as the only criterion for determining the homology of two structures. To pass the similarity test two structures must be alike in form, which can include in morphology at the organ level, histology at the microscopic level, or sequence alignment at the molecular level. Rather than providing a strong test of a hypothesis of homology, similarity "validates it as worthy of testing or evaluates its internal consistency" (Patterson, 1982, page 38). The second test, conjunction, concerns the coexistence of the two proposed homologous

structures. If a single organism houses both, the test of conjunction is violated (although this test is not applicable for serially homologous structures which, by definition, are present multiple times within an organism). The third test, congruence, is related to the distribution of the character of interest on a phylogenetic tree, and whether the character can be considered a synapomorphy of the group to which it belongs. If the distribution pattern of the character on a tree requires more than one evolutionary origin the hypothesized homology fails and is revealed as homoplasy.

Centra have been hypothesized several times throughout the literature to be homoplastic, specifically among actinopterygians, tetrapods, elasmobranchs, and holocephalans (Schaeffer, 1967a; Laerm, 1979a, 1982; Arratia et al., 2001). I used supertrees and ancestral state reconstruction methods in chapter two of this dissertation to test these hypotheses, and found that centra were highly homoplastic within gnathostomes. When Patterson's (1982, 1988) tests are applied to the apparently independent originations of centra, each instance must be considered as a separate case. In each independent origination of centra, the centra themselves are not formed identical to those in other clades. When testing whether the centra are homologous in elasmobranchs and chimaeras, for example, the first criterion, similarity, can be rejected. The morphology of centra in these two groups is distinct enough to suggest that they are not homologous. Centra in chimaeroids consist only of calcified rings that surround a persistent notochord, while those in elasmobranchs constrict the notochord completely at the center of each vertebral unit and can be composed of up to three distinct layers of tissue (see chapter three). Additionally, the presence of centra is not a synapomorphy the group of chimaeras plus elasmobranchs, leading to the failure of the congruence test and therefore determining that centra are not homologous. The only test that the hypothesis of homologous centra passes in this case is

that of conjunction, because both kinds of centra are not found in one single organism. According to Patterson's (1988) table of categories, centra in chimaeras and elasmobranchs fall into the category of convergence. The same tests can be applied to centra in the tetrapodomorphs and actinopterygians, with similar results.

Existing source trees for evolutionary analyses are insufficient to represent the diversity of the fossil record of some gnathostome groups (e.g. early actinopterygians). To further test the homology of centra throughout gnathostomes, supertrees incorporating more well-resolved source phylogenetic trees including a wider taxonomic sample, particularly in the actinopterygian and chondrichthyan regions of the tree, are needed to make this a feasible aim. For example, the haplolepids actinopterygians mentioned in chapter two show clear evidence of centra, but are not currently included in phylogenetic analyses of early actinopterygians (see Gardiner, 2005). Inclusion of a wider range of taxa could drastically change the number of independent originations of centra inferred.

Centra in the context of biological homology

The term biological homology was put forward by Roth (1984) to include the developmental, or mechanistic, aspects of a character in a phylogenetic analysis. According to Roth (1984), shared developmental pathways provide a necessary explanation of a homology hypothesis. The same genes must be acting to recruit the same source tissue to build homologous structures. Building upon this argument, the biological homology concept, popularized by Wagner (1989), focuses more on the developmental constraints underlying a structure than the phylogenetic history of that structure. Wagner (1989) argues that putative homologues must share a set of developmental constraints, such as regulatory elements, that act to maintain the

morphology of the structure, because the development of phylogenetically homologous structures can be variable in their tissue of origin, sequence of development, and mode of induction. In order to reconstruct a transformational hypothesis for a character in the context of the biological homology concept, Wagner (1999) proposed a series of steps: 1) identify putative homologues, 2) determine a proper phylogeny for the taxa of interest, 3) describe patterns of variation across taxa, 4) analyze modes of development for each putative homologue, and 5) test whether differences in the modes of development affect differences in variational properties.

The many independent originations of centra across gnathostomes (i.e. the pattern of centrum morphology) raise questions about the similarities in the process of centrum development in these groups, and the possible underlying homology of those mechanisms. Because biological organization can be found at numerous levels within organisms (e.g. organ, tissue, gene, regulatory element), the homology of many different kinds of characters can be explored to determine how much of the process that leads to centrum development in skates is conserved across gnathostomes and how much has been invented independently in different lineages. In the remainder of this section I will evaluate the current evidence for the homology of the underlying developmental processes that build centra in amniotes, actinopterygians, and elasmobranchs to determine whether the same mechanism was invented once and then deployed numerous times in the independent originations of centra, or whether each mechanism evolved and was assembled separately.

When put in the context of Wagner's (1999) 'tests' of biological homology, the results of my dissertation chapters focusing on vertebral development show clear advances, but holes in the current knowledge of vertebral development also become evident. In this dissertation the putative homologues to be tested are the numerous, apparently independent, originations of

centra throughout gnathostomes. In chapter two of this dissertation I have provided both a phylogenetic hypothesis onto which to reconstruct ancestral states, and descriptions of the variation in centrum morphology seen among chondrichthyans, actinopterygians, and sarcopterygians. I determined that centrum morphology is highly variable in the taxa that evolve centra independently. In chapters three and four I have described the development of centra in an elasmobranch and concluded that there are some fundamental differences in the way certain teleost and tetrapod centra develop when compared with the little skate, as well as some similarities. In particular, these differences include the number, and potential, embryonic origins of the layers of tissue that combine to form a full centrum. Centra in tetrapods consist of cellular bone, while teleost centra are variable, comprising either a solid mass of acellular bone or, in some taxa, several layers of bone that seem to develop from different source tissues (Ekanayake and Hall, 1987; Fleming et al., 2004; Nordvik et al., 2005). Among the developmental similarities are the somitic origin of the centrum in elasmobranchs (the little skate), tetrapods (chick, mouse, and axolotl), and some teleosts (e.g. medaka).

Additional tests at the tissue level that would provide evidence for a common developmental ground plan for centra would be further fate mapping experiments of the somites in non-teleost actinopterygians such as gars (*Lepisosteus*) and bichirs (*Polypterus*), as well as a teleost with a known notochord contribution (zebrafish - *Danio*). To determine whether the somites are contributing any tissue to the centra, DiI-labeling of the somites to track the sclerotome contribution to the vertebrae in these groups would provide key data from a phylogenetic perspective. A somitic origin of the centra in gars and bichirs would reinforce my conclusions, based on the results from experiments in skate, that somite-derived centra are the general condition for gnathostomes. Furthermore, uncovering a somitic contribution to the

centra, in addition to the bone matrix deposited by the notochord, in zebrafish would suggest that the notochord is able to provide tissue to the centrum in some instances, but that the somites retain a role in centrum development across gnathostomes.

Because it is unclear whether the notochord contribution to the centrum seen in salmon and zebrafish is localized to teleosts, or is more widespread throughout actinopterygians, further experiments to elucidate notochord-derived tissues are necessary. It seems likely that that the notochord contributions to the centra in zebrafish and salmon consist of extracellular matrix, but not cells themselves. Therefore, studies of the expression of bone-like extracellular matrix proteins in the developing notochord and inner layer of the centrum in skate, as discussed in chapter four, could help to determine if similar processes are occurring outside teleosts, and whether the role of the notochord is more substantial than has been previously supposed.

Although this dissertation has begun to address the patterns of variation and modes of development in Wagner's (1999) tests of the biological homology concept, evidence from other biological units such as genes and regulatory networks remain incomplete. In addition to evidence from the tissue composition of and contributions to centra, homology can be tested at the level of gene expression and function, which provide an additional line of evidence, but alone do not prove homology. Many of the same genes are involved in sclerotome migration and potentially centrum development in all jawed vertebrates that have been studied to date (e.g. *Pax1, Twist, Pax9*), as they are expressed in migrating cells of the ventral portion of the somite (Wallin et al., 1994; Morin-Kensicki and Eisen, 1997; Christ et al., 2004; Fleming et al., 2004; and see chapter four). However, when *Pax1*and *Pax9* are knocked out or inhibited in different taxa, the resulting phenotypes vary, suggesting divergent roles in vertebral development. Double *Pax1/9* morpholino knockdowns in medaka show severe neural arch defects, but centra appear

mostly unchanged (Mise et al., 2008). Conversely, in mouse *Pax1/9* double knockouts, the medial-most vertebral components - the centra and intervertebral discs - do not develop, but neural arches experience only a minor decrease in size (Peters et al., 1999). These experiments provide a glimpse into the mechanisms underlying vertebral development, but much remains unknown. Examining the expression patterns of the sclerotome markers mentioned above, as well as notochord-secreted factors known to function in sclerotome migration, such as Shh and Noggin (Watanabe et al., 1998; Monsoro-Burq, 2005) in more gnathostome taxa would provide a good starting point. Finding the same genes expressed in the same tissues throughout centrum development would support a homologous underlying mechanism, even though centra themselves are homoplastic. Upon identifying gene expression patterns, the functions of these genes should be tested using pharmacological inhibitors where possible. Unfortunately, there currently is little available information for inhibitors of Pax or Twist proteins. However, the hedgehog signaling antagonist cyclopamine is used to block Shh protein function in chondrichthyans and could provide interesting data on the impact of a loss of sclerotome migration on vertebral segmentation (Nakamura et al., 2015; Gillis and Hall, 2016).

Experiments that would provide evidence for or against homologous developmental mechanisms include tests of the conservation and function of regulatory elements associated with vertebral development genes. As mentioned previously, *Pax1/9* double knockout mice show a complete lack of centra, indicating that these genes are crucial to centrum formation, at least in mammals (Peters et al., 1999). Numerous *Pax1* enhancers have been identified in mouse and human to be associated with vertebral column development, although their expression patterns and functions have not been thoroughly tested (Kokubu et al., 2009; Sharma et al., 2015). It would be interesting to determine whether these enhancers are present in both skate and

zebrafish by searching their respective genomes to identify conserved sequences. If skate *Pax1* enhancers are identified, the next steps would be performing assays of reporter expression using the skate sequences in both zebrafish and mouse. Skate enhancer sequences being able to reproduce endogenous *Pax1* expression in the sclerotome and vertebrae would indicate a shared ancestral developmental mechanism for gnathostome centra, rather than two sets of enhancers functioning in a similar manner.

Until more genetic and developmental data are available for the vertebral columns of a wider range of jawed vertebrates, it is difficult to say whether the processes that build centra are shared among the different gnathostome groups that evolved them. The criteria of shared phylogenetic history, embryonic origins, and common genetic components should not be considered in isolation, but rather in combination, to truly understand the evolutionary history of a character or trait. At present, it seems likely that the same genes are involved in vertebral development in teleosts, tetrapods, and elasmobranchs, but experiments testing the functions of these genes, and analyses of their regulatory elements, are lacking. More robust gnathostome phylogenies and further exploration of gene function and interactions in the developing centra and arches will determine just how much homoplasy exists in the vertebral column.

Future directions: uncovering axial regionalization

The vertebral column is also frequently used as an example of iterative or serial homology, in which the same structure is repeated one or more times within a single organism (Roth, 1984; Panchen, 1992). Based on its anterior-posterior location, a vertebra can develop particular characteristics specialized to its function in that region, such as transverse processes or hemal arches. Other vertebral modifications, like synarcuals and caudal diplospondyly, are also

dependent on the location of the vertebrae within the anterior-posterior axis. These differences in vertebral morphology constitute axial regionalization, which can be found in all jawed vertebrates, but is thought to be more pronounced in tetrapods (Goodrich, 1930; Ahlberg et al., 2005; Sallan, 2012).

This regionalization is well known to be controlled through anterior-posterior expression of *Hox* genes, which are a set of collinear genes with nested expression (Burke et al., 1995). The anterior-most boundaries of several *Hox* genes in particular (e.g. *Hoxc6, Hoxc11, Hoxd11*) seem to determine the regional boundaries of the axial column. Mammals, for instance, have five major axial regions, including the cervical, thoracic, lumbar, sacral, and caudal regions. These regions are defined by the presence of ribs or articulations with the pelvic girdle, which correspond quite well to *Hox* expression boundaries. Non-tetrapod gnathostomes, on the other hand, are generally considered to have only two vertebral regions, the precaudal and caudal (despite numerous exceptions) (Bird and Mabee, 2003). The only major difference between the precaudal and caudal vertebrae was thought to be the presence of either ribs or hemal arches and spines.

Experiments to determine the extent of axial regionalization in non-tetrapod gnathostomes are long overdue. Recent evidence from fossil and genetic data suggest that non-tetrapod gnathostomes have the potential to develop morphologically regionalized vertebrae, and that more axial regionalization may be present than is easily recognized by eye. For example, the vertebrae of the Carboniferous actinopterygian *Tarrasius* show five clear morphological regions (Sallan, 2012). New data from CT scans of the Carboniferous actinopterygian *Mesopoma* highlight a region of morphologically distinct vertebrae in the anterior portion of the vertebral column in which the first two hemal arches are fused at the midline. It is also clear that many

chondrichthyan vertebral columns include more than just the precaudal and caudal regions. The vertebrae in the Carboniferous shark *Tristychius* show considerable regional variation, with the neural and hemal arches of anterior-most vertebrae almost entirely enclosing the notochord (Dick, 1978). Near the first dorsal fin the neural spines are long and narrow and the ribs are long, with no hemal arches preserved, while in the region of the second dorsal fin the neural spines and ribs are much shorter. Within the batoids, the synarcual itself can be considered a region apart from the rest of the precaudal vertebrae. Additionally, precaudal ribs are common in the trunks of extant sharks, but in many taxa (e.g. *Heterodontus*) up to six or seven transitional vertebrae are present between the last rib-bearing vertebra and the first hemal arches and spines (Daniel, 1922).

In addition to these observable morphological changes, morphometric analyses of the shift in proportions of the vertebrae throughout the anterior-posterior axis could provide support for cryptic regionalization that has not yet been recognized. It has recently been shown that the vertebral skeleton in snakes, for which little axial regionalization was thought to exist, actually corresponds to mapped *Hox* boundaries when vertebrae along the A-P axis are measured and compared (Head and Polly, 2015). Many *Hox* expression boundaries in the somitic mesoderm of the catshark, *Scyliorhinus canicula*, show a close correlation with those of tetrapods, even though clear morphological changes in the vertebral skeleton at those boundaries are not obvious (and despite a HoxC cluster deletion) (Oulion et al., 2011). Therefore, it seems quite likely that a morphometric analysis of chondrichthyan vertebral proportions could yield evidence of similar axial regions.

Future directions: mechanisms of vertebral segmentation

The results from both the morphological study in chapter three and the experiments in chapter four have also generated questions about the process of vertebral segmentation in chondrichthyans, and its relation to segmentation in general across gnathostomes. Vertebral segmentation proceeds with the differentiation of somites as segmented embryonic structures, ensuing sclerotomal migration and condensation as a continuous envelope of tissue surrounding the notochord, and subsequent subdivision of this cartilage into vertebrae. No mechanism has been proposed to account for this series of developmental processes. In chapter three I identified segmented notochord bands that correspond in physical location to the incipient boundaries of the subdividing vertebrae. It is possible that these bands, or the tissues surrounding them, express certain genes that function to direct subdivision of the continuous cartilage. RNAseq experiments targeting these bands, or simply sampling the cartilage at the incipient vertebral boundaries, and comparing the expression profiles of these boundary tissues to cartilage from the center of each developing vertebra, would highlight differentially-expressed candidate genes that could then be considered for functional analysis.

In addition to identifying a mechanism for the secondary subdivision of the cartilaginous tube, I am interested in whether the somite cells maintain their segmental identity through this processes of segmentation, coalescence, and subdivision. As discussed previously, 'resegmentation' occurs when there is an anterior-posterior shift in the alignment of the somites with the myotomal segments, resulting in vertebrae that are formed in part from two adjacent somites and are positioned at myotomal boundaries (myosepta). Resegmentation has been documented in both tetrapods and teleosts (Bagnall et al., 1988; Morin-Kensicki et al., 2002; Piekarski and Olsson, 2014), but has not been investigated in cartilaginous fishes. Experiments to

track the cells of adjacent somites to their final destinations in vertebral cartilage would provide information on whether the vertebrae are 'prepatterned' by the somites.

Gadow's model of vertebral development and evolution reconsidered

I began this dissertation with a discussion of Gadow and Abbott's (1895) 'Arcualia Theory', which at its most basic states that vertebrae across all gnathostomes develop from four pairs of embryonic cartilages (basidorsals, basiventrals, interdorsals, and interventrals). Gadow and Abbott (1895) studied embryonic histological sections of several chondrichthyan and osteichthyan taxa (catsharks, dogfish, bowfins, gar, and lungfish) and despite the observations that interdorsals (e.g. gar, lungfish) and interventrals (e.g. lungfish, chimaeras) are not always present, chose to apply this model to all gnathostomes (Gadow, 1896). This theory has been rejected for tetrapods (Williams, 1959) and shown to be incompatible for osteichthyans and 'acanthodians' (Schaeffer, 1967a; Miles, 1970) based on comparisons of the neural and hemal arch patterns. Neither tetrapods nor 'acanthodians' have interdorsal or interventral arches, and although these structures are present in some osteichthyans fishes, they are absent in many others, suggesting that they are not representative of the general vertebral condition. Evidence reported here from chapter two also refutes portions of this model. Morphological data from early gnathostome fossils clearly show that the earliest versions of vertebrae included paired neural and hemal arches, but lacked those interdorsals and interventrals. Embryonic data collected from microCT scans in chapter three also provide evidence that despite the presence of both neural and intercalary arches (basidorsals and basiventrals) in skates, these cartilages do not form as independent condensations. Rather, mesenchyme condenses on either side of the neural tube as two unsegmented layers that extend the length of the anterior-posterior axis and later

subdivide into both sets of arches. Unfortunately, the continued use of Gadow and Abbott's (1895) model of vertebral construction and evolution has caused confusion in the developmental and paleontological literature, with researchers conflating the embryonic terms 'basidorsal' and 'basiventral' with the adult terms 'neural arch' and 'hemal arch'.

In addition to the four basic components of the vertebrae, Gadow and Abbott (1895) and Gadow (1933) posited that elasmobranch centra form through invasion of the thickened, fibrous notochord sheath by migrating sclerotomal cells. These cells were thought to first condense at neural and hemal arch positions (dorsolateral and ventrolateral to the notochord) and then perforate the elastica externa and differentiate into cartilage within the fibrous sheath. The sheath was described by several embryologists as derived from the notochord epithelium (Gegenbaur, 1872; Goodrich, 1930). Chapters three and four show that the process of centrum development in skate differs from this model. The "fibrous sheath" consists of condensed mesenchyme that differentiates into spindle-shaped cells around the notochord. Fate mapping experiments confirm that these cells are derived from the somites and not the notochord epithelium.

Gadow and Abbott's (1895) paper and Gadow's (1896) application to tetrapods serve as a cautionary tale against applying generalized models and hypotheses too broadly. The proposed model vertebra is an archetype, and as such is largely incongruent with the actual observed diversity of the vertebral column. Vertebrae are morphologically and developmentally diverse, with independent evolutionary origins for many of their observed components, and cannot be forced into narrow categories applicable to all vertebrates.

Appendix 1: Specimens examined and literature sources for chapter two

Table A1.1. List of specimen museum numbers and sources cited.

Acanthodes – Miles (1970)

Acanthostega – Coates (1996)

Achoania – Zhu et al. (2001) – no vertebrae known

Acipenser – Hilton et al. (2011)

Akmonistion – Coates and Sequeira (2001b)

Allenypterus – Lund and Lund (1984); FMNH PF 10025, PF 13511, PF 10942, PF 13512, PF 10940, PF 1093; CM 27255, 27284, 27288, 30627, 37509, 37698; MNHN ANP 104, 105

Amia – ANSP 3151, 5622, 5558, 8044, 78258

Amblyraja – Capetta (Cappetta, 1987); Personal Observation (should be *Leucoraja)*

Aphelodus – Kemp (1993), no vertebrae known

Archaeoceratodus – Kemp (1997a), no vertebrae known

Arganodus – Tabaste (1963); Kemp (1991), no vertebrae known

Ariguna – Kemp (1994)

Asiatoceratodus – Vorobyeva (1967)

Australosomus – Neilsen (1949)

Austroptyctodus – Johanson et al. (2013); MV P230240

Axelrodichthys - de Carvalho and Maisey (2008), no vertebrae known

Barameda – Long (1989); Garvey et al. (2005)

Beelarongia – no vertebrae known

Belonostomus – Brito et al. (1999); Bogan et al. (2011); CMNH 4776, 5001

Beltanodus – no vertebrae known

Table A1.1, continued. List of specimen museum numbers and sources cited.

Birgeria – Stensiö (1919); Sigogneau-Russel and Hahn (1994); NHM P19286; MNHN TRE 21

Boreosomus – Nielsen (1942); NHM P19866, P19867

Bothriolepis – Long (1983)

Brachyacanthus – no vertebrae known

Brindabellaspis – no vertebrae known

Brochoadmones – no vertebrae known

Buchanosteus – no vertebrae known

Callorhinchus – Didier (1995); ANSP 177805; 177826

Campbellodus – Johanson et al. (2013)

Caridosuctor – Lund and Lund (1984); FMNH PF 13505; PF 13508; PF 12920; MNHN ANP 106, 108, 111, 112, 113, 115, 116

Cassidiceps – no vertebrae known

Caturus – CM 869, 4697, 5000; MNHN 1882M CRN49, 1872-S14 CRN76, CRN501872-S14-3 CRN 4, 1913-9 CRN 63CRN 64-65

Ceratodus – no vertebrae known

Cheiracanthus – no vertebrae known

Cheirolepis – Arratia and Cloutier (1996)

Chimaera – Didier (1995)

Chinlea – Schaeffer (1967b)

Chirodipterus – Pridmore and Barwick (1993)

Chondrenchelys – Finarelli and Coates (2014); NMS 1998.35; 1891.53.33

Cladodoides – Maisey (2005)

Table A1.1, continued. List of specimen museum numbers and sources cited.

Cladoselache – Zangerl (1981)

Climatius – no vertebrae known

Cobelodus – Zangerl and Case (1976)

Coccoderma – Lambers (1996)

Coccosteus – Miles and Westoll (1968); NHM P20314, P42428, P59872, P59893, P59920, P59904, P59929, P60073, P60096, P61615, P61618, P61619, P61620; 1869.81.18, NMS 1882.60.3, 1888.61.29, 1890.91.21, 1893.107.27, 1893.107.28, 1895.190.1, 2002.26.1414, 2002.26.1729

Coelacanthus – Moy Thomas and Westoll (1935); MNHN 12904, MAE 119,

Compagopiscis – Gardiner and Miles (1994); Johanson et al. (2013)

Conchopoma – Marshall (1988); NHM P3336, P58467; CM 5151

Cowralepis – Ritchie (2005); Johanson et al. (2013)

Crassigyrinus – Panchen (1985)

Ctenurella – MNHN ARD 229, 230, 231, 232, 233, 237

Culmacanthus – no vertebrae known

Cyprinus – Backiel e al. (1984)

Dapedium – Woodward (1895); NHM P3508; P1556; P4420

Debeerius – Grogan and Lund (2000); CM 40627, 41030, 46101, 48510

Diabolepis – no vertebrae known

Dialipina – no vertebrae known

Dicksonosteus – no vertebrae known

Diplacanthus – Watson (1937); Miles (1970)

Table A1.1, continued. List of specimen museum numbers and sources cited.

Diplocercides – no vertebrae known

Diplurus – Schaeffer (1952); FMNH PF 10310, 10311, 10314

Dipnorhynchus – no vertebrae known

Dipterus – Ahlberg and Trewin (1994); NHM P618, P10613, P17637; AMNH 9141

Discoserra – CM 35547A2

Doliodus – no vertebrae known

Eastmanosteus – no vertebrae known

Egertonodus – check Maisey 1983; 1987

Elops – Schultze and Arratia 1988; Arratia et al. 2001

Elpistostege – Schultze and Arsenault (1985)

Entelognathus – no vertebrae known

Eurycaraspis – no vertebrae known

Eusthenopteron – Andrews and Westoll (1970a); Cote et al. (2002); NMS 1887.20.19, 1897.51.201, 1897.51.202, 1952.7,

Euthacanthus – no vertebrae known

Falcatus – CM 37529

Ferganoceratodus – no vertebrae known

Galeaspida – no vertebrae known

Garbergia – no vertebrae known

Gavinia – Long (1999)

Gemuendina – Gross (1963)

Gladiobranchus – no vertebrae known

Table A1.1, continued. List of specimen museum numbers and sources cited.

Glyptolepis – Andrews and Westoll (1970b); Ahlberg (1991); NMS 1898.120.49, 1898.120.50

Gnathorhiza – Dalquest et al. (1989); GM 26558, 26567, 38037

Gogodipterus – Long (1992)

Gogonasus – Long et al. (1997); MV 221807

Gosfordia – Ritchie (1981)

Griphognathus – Pridmore and Barwick (1993); NHM P52571; P52583

Groenlandaspis – no vertebrae known

Guiyu – no vertebrae known

Gyracanthides – no vertebrae known

Gyroptychius – Andrews and Westoll (1970b)

Hadronector – Lund and Lund (1984); CM 27307, 30712, 30713

Hamiltonichthys – Maisey (1989)

Harpacanthus – CM 46017, 48503

Harpagofututor – Lund (1982); CM 27326, 27330, 27331, 48760

Harriotta – Didier (1995); ANSP 174716, 177828

Helodus – Moy-Thomas (1936)

Heterodontus – Daniel (1922)

Hiodon – Schultze and Arratia (1988); Guo-Qing and Wilson (1994)

Holodipterus – MV P232055

Holonema – Miles (1971)

Holophagus –NMS 1950.38.77

Holopterygius – Jessen (1973); Friedman and Coates (2006)

Table A1.1, continued. List of specimen museum numbers and sources cited.

Holoptychius – no vertebrae known

Homalacanthus – no vertebrae known

Hopleacanthus – Schaumberg (1982)

Howidipterus – Long and Clement (2009)

Howqualepis – no vertebrae known

Hulettia – AMNH 10860, 10875, 10911

Hybodus – Woodward (1891); Maisey (1982)

Hydrolagus – Didier (1995); ANSP 174708, 177827

Ichthyostega – Ahlberg et al. (2005); Pierce et al. (2013)

Incisoscutum – Johanson et al. (2013); MV P230980

Iniopera – Zangerl and Case (1973)

Ionoscopus – Grande and Bemis (1998); CM 4036

Ischnacanthus – Dean (1907)

Jagorina – Stensiö (1969)

Janusiscus – no vertebrae known

Kathemacanthus – Gagnier and Wilson (1996)

Kawichthys – no vertebrae known

Kenichthys – no vertebrae known

Kentuckia – no vertebrae known

Kujdanowiaspis – Dupret (2010)

Latimeria – Arratia et al. (2001)

Latviacanthus – no vertebrae known

Table A1.1, continued. List of specimen museum numbers and sources cited.

Laugia – Stensiö (1932)

Lepidosiren – Arratia et al. (2001); Criswell (2015)

Lepisosteus – Grande (2010)

Leptolepis – MV P251203, P251221, P251233; CM 19067, 19070

Libys – Hauser and Martill (2013)

Ligulalepis – Basden and Young (2001)

Lissodus – Cappetta (1987)

Lochmocercus – Lund and Lund (1984)

Lonchidion – Cappetta (1987)

Lophosteus – no vertebrae known

Lunaspis – no vertebrae known

Lupopsyrus – no vertebrae known

Macropetalichthys – Denison (1978)

Macropoma – Lambers (1996)

Materpiscis – Long et al. (2008); Johanson et al. (2013)

Mawsonia – Woodward (1908); Carvalho (1982)

Meemannia – no vertebrae known

Megapleuron – Schultze (1977)

Mesacanthus – no vertebrae known

Mesopoma – NHM P11656

Metaceratodus – no vertebrae known

Microbrachius – no vertebrae known

Table A1.1, continued. List of specimen museum numbers and sources cited.

Microceratodus – no vertebrae known

Miguashaia – Cloutier (1996)

Mimipiscis – Gardiner (1984a); MV P221806; P228267

Mioceratodus – no vertebrae known

Moythomasia – Gardiner (1984a); MV 222915

Mustelus – Ridewood (1921)

Namatozodia – no vertebrae known

Neoceratodus – Arratia et al. (2001); Criswell (2015)

Notorynchus/*Hexanchus* – sharksrays.org

Obtusacanthus – no vertebrae known

Okameijei – Claeson (2011)

Onychodus – Andrews et al. (2005)

Onychoselache – Dick and Maisey (1980); Coates and Gess (2007)

Orlovichthys – no vertebrae known

Orthacanthus – Zidek (1993) NHM P24431

Osorioichthys – no vertebrae known

Osteolepis – Andrews and Westoll (1970b)

Osteostraci – Janvier et al. (2004)

Pachycormus – MNHN Millot STC 15, 33, 122

Palaeobates – no vertebrae known

Panderichthys – Vorobyeva and Schultze (1991)

Parabuchanosteus – no vertebrae known

Table A1.1, continued. List of specimen museum numbers and sources cited.

Paraceratodus – Arratia et al. (2001)

Parayunnanolepis – no vertebrae known

Parexus – Miles (1970)

Perleidus – no vertebrae known

Phanerosteon – Sallan (2012); AMNH 1151, 1152

Pholidophorus – Woodward (1895); Grande and Bemis (1998); CM 677, 4899, 4787

Phyllolepis – NHM P11912

Pillararhynchus – Barwick and Campbell (Barwick and Campbell, 1996)

Plesiobatis – no vertebrae known

Plourdosteus – MHNM 02-712, 02-901, 02-3375

Polyosteorhynchus – Lund and Lund (1984)

Polypterus – Bartsch and Gemballa (1992); ANSP 77997

Poracanthodes – no vertebrae known

Porolepis – no vertebrae known

Powichthys – no vertebrae known

Promesacanthus – no vertebrae known

Protopterus – Arratia et al. (2001); Criswell (2015)

Psarolepis – no vertebrae known

Pterichthyodes – no vertebrae known

Pteronisculus – Nielsen (1949); AMNH 1034, 1035, 1036, 2324

Ptomacanthus – no vertebrae known

Ptychoceratodus – no vertebrae known

Table A1.1, continued. List of specimen museum numbers and sources cited.

Pucapampella – no vertebrae known

Ramirosuarezia – no vertebrae known

Remigolepis – no vertebrae known

Rhabdoderma – Arratia et al. (2001)

Rhadinacanthus – no vertebrae known

Rhamphodopsis – Watson (1938)

Rhinobatos – NHM P2276

Rhinochimaera – Didier (1995); ANSP 174717

Romundina – Dupret et al. (2014)

Sagenodus – Schultze and Chorn (1997); CM 8517

Sassenia – no vertebrae known

Saurichthys – Maxwell (2013); Maxwell et al. (2015)

Scyliorhinus – Hasse (1879)

Semionotus – Grande (2010)

Serenichthys – Gess and Coates (2015)

Soederberghia – Ahlberg et al. (2001)

Sorbitorhynchus – no vertebrae known

Speonesydrion – no vertebrae known

Spermatodus – no vertebrae known

Squaloraja – NHM P2079, P2080, P2276, P3185, P4323, P43307; ANSP 6161

Squalus – Homberger and Walker (2004)

Stomiahykus – no vertebrae known

Table A1.1, continued. List of specimen museum numbers and sources cited.

Strepsodus – Andrews and Westoll (1970b)

Strunius – Gross (1956)

Styloichthys – no vertebrae known

Synechodus –Duffin (1993); NHM 49032; P4326; P 14223

Tamiobatis – no vertebrae known

Tarrasius – Sallan (2012); NMS 1885.54.13

Tetanopsyrus – no vertebrae known

Tribodus – no vertebrae known

Tristychius – NMS 1972.27.481D, E

Undina – Woodward (1917); MNHN 1900.16.7 SLN 53

Uranolophus – Campbell and Barwick (1988); Denison (1968)

Ventastega – no vertebrae known

Vernicomacanthus – no vertebrae known

Watsonulus – Grande and Bemis (1998)

Whiteia – Moy-Thomas (1935)

Wuttagoonaspis – no vertebrae known

Xenacanthus – NMS 1891.41.6

Youngolepis – no vertebrae known

Yunnanolepis – no vertebrae known

Appendix 2: MRP matrix used to generate supertree

Table A2.1. The matrix representation matrix used for supertree generation.

Mimipiscis	?	?	?	?	?	?	?	?	?	?	?	?	?	?	?	?	?	?	?	?	0	0	0	0	0	0	0	0	0	0
	0	0	0	0	0	0	0	?	?	?	?	?	?	?	?	?	?	?	?	?	?	?	?	?	?	1	0	0	1	0	1	0
	0	1	0	0	0	0	0	0	0	1	1	1	0	0	0	0	0	0	0	0	0	0	0	0	0	0	0	0	0	0	0	0
	0	0	0	0	0	0	1	1	1	1	1	0	0	0	0	0	0	0	0	?	?	?	?	?	?	?	?	?	?	?	?	?
	?	?	?	?	?	?	?	1	1	0	0	0	0	0	0	0	0	0	0	?	?	?	?	?	?	?	?	?	?	?	?	?
	?	?	?	?	?	?	?	?	?	?	?	?	?	?	?	?	?	?	?	?	?	?	?	?	?	?	?	?	?	?	?	?
	?																															
Debeerius	?	?	?	?	?	?	?	?	?	?	?	?	?	?	?	?	?	?	?	?	1	1	1	0	0	0	0	0	0	0	0
	0	0	0	0	0	0	?	?	?	?	?	?	?	?	?	?	?	?	?	?	?	?	?	1	0	0	1	0	1	0	0
	1	0	0	0	0	0	0	0	1	1	1	1	0	0	0	0	0	0	0	0	1	0	0	1	1	1	1	1	0	1	0	0
	1	0	0	1	1	0	0	0	0	0	0	0	0	0	0	0	0	?	?	?	?	?	?	?	?	?	?	?	?	?	?	?
	?	?	?	?	?	?	?	?	?	?	?	?	?	?	?	?	?	?	?	?	?	?	?	?	?	?	?	?	?	?	?	?
	?	?	?	?	?	?	?	?	?	?	?	?	?	?	?	?	?	?	?	?	?	?	?	?	?	?	?	?	?	?	?	?
Chimaera	?	?	?	?	?	?	?	?	?	?	?	?	?	?	?	?	?	?	?	?	1	1	1	1	0	0	0	0	0	0	0
	0	0	0	0	0	0	0	0	0	0	0	0	1	0	0	0	0	0	0	1	1	0	1	?	?	?	?	?	?	?	?	?
	?	?	?	?	?	?	?	?	?	?	?	?	?	?	?	?	?	?	?	?	?	?	?	?	?	?	?	?	?	?	?	?
	?	?	?	?	?	?	?	?	?	?	?	?	?	?	?	?	?	?	?	?	?	?	?	?	?	?	?	?	?	?	?	?
	?	?	?	?	?	?	?	?	?	?	?	?	?	?	?	?	?	?	?	?	?	?	?	?	?	?	?	?	?	?	?	?
	?	?	?	?	?	?	?	?	?	?	?	?	?	?	?	?	?	?	?	?	?	?	?	?	?	?	?	?	?	?	?	?
Helodus	?	?	?	?	?	?	?	?	?	?	?	?	?	?	?	?	?	?	?	?	1	1	1	1	1	0	0	0	0	0	0
	0	0	0	0	0	0	?	?	?	?	?	?	?	?	?	?	?	?	?	?	?	?	?	?	?	1	0	0	1	0	1	0	0
	1	0	0	0	0	0	0	0	1	1	1	1	0	0	0	0	0	0	0	0	1	0	0	1	1	1	1	1	0	1	0	0
	1	0	0	1	0	0	0	0	0	0	0	0	0	0	0	0	0	?	?	?	?	?	?	?	?	?	?	?	?	?	?	?
	?	?	?	?	?	?	?	?	?	?	?	?	?	?	?	?	?	?	?	?	?	?	?	?	?	?	?	?	?	?	?	?
	?	?	?	?	?	?	?	?	?	?	?	?	?	?	?	?	?	?	?	?	?	?	?	?	?	?	?	?	?	?	?	?
Iniopera	?	?	?	?	?	?	?	?	?	?	?	?	?	?	?	?	?	?	?	?	1	1	1	1	1	0	0	0	0	0	0
	0	0	0	0	0	0	?	?	?	?	?	?	?	?	?	?	?	?	?	?	?	?	?	?	?	?	?	?	?	?	?	?
	?	?	?	?	?	?	?	?	?	?	?	?	?	?	?	?	?	?	?	?	?	?	?	?	?	?	?	?	?	?	?	?
	?	?	?	?	?	?	?	?	?	?	?	?	?	?	?	?	?	?	?	?	?	?	?	?	?	?	?	?	?	?	?	?
	?	?	?	?	?	?	?	?	?	?	?	?	?	?	?	?	?	?	?	?	?	?	?	?	?	?	?	?	?	?	?	?
	?	?	?	?	?	?	?	?	?	?	?	?	?	?	?	?	?	?	?	?	?	?	?	?	?	?	?	?	?	?	?	?
Egertonodus	?	?	?	?	?	?	?	?	?	?	?	?	?	?	?	?	?	?	?	?	1	1	0	0	0	1	1	0	0	0
	0	0	0	0	0	0	0	?	?	?	?	?	?	?	?	?	?	?	?	?	?	?	?	?	?	?	?	?	?	?	?	?
	?	?	?	?	?	?	?	?	?	?	?	?	?	?	?	?	?	?	?	?	?	?	?	?	?	?	?	?	?	?	?	?
	?	?	?	?	?	?	?	?	?	?	?	?	?	?	?	?	?	?	?	?	?	?	?	?	?	?	?	?	?	?	?	?
	?	?	?	?	?	?	?	?	?	?	?	?	?	?	?	?	?	?	?	?	?	?	?	?	?	?	?	?	?	?	?	?
	?	?	?	?	?	?	?	?	?	?	?	?	?	?	?	?	?	?	?	?	?	?	?	?	?	?	?	?	?	?	?	?
	?																															
Tristychius	?	?	?	?	?	?	?	?	?	?	?	?	?	?	?	?	?	?	?	?	1	1	0	0	0	1	1	0	0	0
	0	0	0	0	0	0	0	?	?	?	?	?	?	?	?	?	?	?	?	?	?	?	?	?	?	1	0	0	1	0	1	0
	0	1	0	0	0	0	0	0	0	1	1	1	1	0	0	0	0	0	0	0	0	1	0	0	1	1	1	1	1	0	1	1
	0	0	0	0	0	0	0	0	0	0	0	0	0	0	0	0	0	0	?	?	?	?	?	?	?	?	?	?	?	?	?	?
	?	?	?	?	?	?	?	?	?	?	?	?	?	?	?	?	?	?	?	?	?	?	?	?	?	?	?	?	?	?	?	?
	?	?	?	?	?	?	?	?	?	?	?	?	?	?	?	?	?	?	?	?	?	?	?	?	?	?	?	?	?	?	?	?
	?																															
Synechodus	?	?	?	?	?	?	?	?	?	?	?	?	?	?	?	?	?	?	?	?	1	1	0	0	0	1	0	1	0	0
	0	0	0	0	0	0	0	?	?	?	?	?	?	?	?	?	?	?	?	?	?	?	?	?	?	?	?	?	?	?	?	?
	?	?	?	?	?	?	?	?	?	?	?	?	?	?	?	?	?	?	?	?	?	?	?	?	?	?	?	?	?	?	?	?
	?	?	?	?	?	?	?	?	?	?	?	?	?	?	?	?	?	?	?	?	?	?	?	?	?	?	?	?	?	?	?	?
	?	?	?	?	?	?	?	?	?	?	?	?	?	?	?	?	?	?	?	?	?	?	?	?	?	?	?	?	?	?	?	?

Table A2.1, continued. The matrix representation matrix used for supertree generation.

? ?
?
Notorhynchus ? ? ? ? ? ? ? ? ? ? ? ? ? ? ? ? ? ? ? 1 1 0 0 0 1 0 1 1 0
0 0 0 0 0 0 0 ?
? ?
? ?
? ?
? ?
?
Squalus ? ? ? ? ? ? ? ? ? ? ? ? ? ? ? ? ? ? ? 1 1 0 0 0 1 0 1 1 0 0
0 0 0 0 0 0 0 0 0 0 0 0 0 1 1 0 0 1 0 0 0 0 0 0 ? ? ? ? ? ? ? ?
? ?
? ?
? ?
? ?
Pucapampella ? ? ? ? ? ? ? ? ? ? ? ? ? ? ? ? ? ? ? 1 0 0 0 0 0 0 0 0
1 0 0 0 0 0 0 0 ? ? ? ? ? ? ? ? ? ? ? ? ? ? ? ? ? ? 1 0 0 1 0 1
0 0 1 0 0 0 0 0 0 0 1 1 1 1 0 0 0 0 0 0 0 0 1 0 0 1 1 1 0 0 0 0
0 0 0 0 0 0 0 0 0 0 0 0 0 0 0 0 0 0 0 ? ? ? ? ? ? ? ? ? ? ? ? ?
? ?
? ?
? ?
Doliodus ? ? ? ? ? ? ? ? ? ? ? ? ? ? ? ? ? ? ? 1 0 0 0 0 0 0 0 0 1 1
0 0 0 0 0 0 ? ? ? ? ? ? ? ? ? ? ? ? ? ? ? ? ? ? 1 0 0 1 0 1 0 0
1 0 0 0 0 0 0 0 1 1 1 1 0 0 0 0 0 0 0 0 1 0 0 1 1 1 1 0 0 0 0 0
0 0 0 0 0 0 0 0 0 0 0 0 0 0 0 0 0 ? ? ? ? ? ? ? ? ? ? ? ? ? ? ?
? ?
? ?
Cladodoides ? ? ? ? ? ? ? ? ? ? ? ? ? ? ? ? ? ? ? 1 0 0 0 0 0 0 0 0 1
1 1 1 0 0 0 0 ? ? ? ? ? ? ? ? ? ? ? ? ? ? ? ? ? ? 1 0 0 1 0 1 0
0 1 0 0 0 0 0 0 0 1 1 1 1 0 0 0 0 0 0 0 0 1 0 0 1 1 1 1 1 0 0 0
0 0 0 0 0 0 0 0 0 0 0 0 0 0 0 0 0 0 ? ? ? ? ? ? ? ? ? ? ? ? ? ?
? ?
? ?
?
Tamiobatis ? ? ? ? ? ? ? ? ? ? ? ? ? ? ? ? ? ? ? 1 0 0 0 0 0 0 0 0 1
1 1 1 1 0 0 0 ? ? ? ? ? ? ? ? ? ? ? ? ? ? ? ? ? ? 1 0 0 1 0 1 0
0 1 0 0 0 0 0 0 0 1 1 1 1 0 0 0 0 0 0 0 0 1 0 0 1 1 1 1 1 1 0 0
0 0 0 0 0 0 0 0 0 0 0 0 0 0 0 0 0 0 ? ? ? ? ? ? ? ? ? ? ? ? ? ?
? ?
? ?
?
Orthacanthus ? ? ? ? ? ? ? ? ? ? ? ? ? ? ? ? ? ? ? 1 0 0 0 0 0 0 0 0 1
1 1 1 1 0 0 0 ? ? ? ? ? ? ? ? ? ? ? ? ? ? ? ? ? ? 1 0 0 1 0 1 0
0 1 0 0 0 0 0 0 0 1 1 1 1 0 0 0 0 0 0 0 0 1 0 0 1 1 1 1 1 1 0 0
0 0 0 0 0 0 0 0 0 0 0 0 0 0 0 0 0 0 ? ? ? ? ? ? ? ? ? ? ? ? ? ?
? ?
? ?
?
Cladoselache ? ? ? ? ? ? ? ? ? ? ? ? ? ? ? ? ? ? ? 1 0 0 0 0 0 0 0 0 1
1 1 0 0 1 1 0 ? ? ? ? ? ? ? ? ? ? ? ? ? ? ? ? ? ? 1 0 0 1 0 1 0

Table A2.1, continued. The matrix representation matrix used for supertree generation.

0 1 0 0 0 0 0 0 0 1 1 1 1 0 0 0 0 0 0 0 0 1 0 0 1 1 1 1 1 0 1 0
0 1 1 0 0 0 0 0 0 0 0 0 0 0 0 0 0 0 ? ? ? ? ? ? ? ? ? ? ? ? ? ?
? ?
? ?
?

Cobelodus ? 1 0 0 0 0 0 0 0 0 1 1
1 0 0 1 1 0 ? 1 0 0 1 0 1 0 0
1 0 0 0 0 0 0 0 1 1 1 1 0 0 0 0 0 0 0 0 1 0 0 1 1 1 1 1 0 1 0 0
1 1 1 0 0 0 0 0 0 0 0 0 0 0 0 0 0 ? ? ? ? ? ? ? ? ? ? ? ? ? ? ?
? ?
? ?

Akmonistion ? 1 0 0 0 0 0 0 0 0 1
1 1 0 0 1 0 1 ? ? ? ? ? ? ? ? ? ? ? ? ? ? ? ? ? ? ? 1 0 0 1 0 1 0
0 1 0 0 0 0 0 0 0 1 1 1 1 0 0 0 0 0 0 0 0 1 0 0 1 1 1 1 1 0 1 0
0 1 1 1 0 0 0 0 0 0 0 0 0 0 0 0 0 0 ? ? ? ? ? ? ? ? ? ? ? ? ? ?
? ?
? ?
?

Kawichthys ? 1 0 0 0 0 0 0 0 0 1
1 1 0 0 1 0 1 ?
? ?
? ?
? ?
? ?
?

Cyprinus ?
? ? ? ? ? ? 1 1 0 0 0 0 0 0 0 0 0 0 0 0 0 0 0 0 0 ? ? ? ? ? ? ? ? ?
? ?
? ?
? ?
? ?

Tetraodon ?
? ? ? ? ? ? 1 1 1 0 0 0 0 0 0 0 0 0 0 0 0 0 0 0 0 ? ? ? ? ? ? ? ? ?
? ?
? ?
? ?
? ?

Polymixia ?
? ? ? ? ? ? 1 1 1 0 0 0 0 0 0 0 0 0 0 0 0 0 0 0 0 ? ? ? ? ? ? ? ? ?
? ?
? ?
? ?
? ?

Protopterus 1 1 0 1 0 1 0 1 0 0 0 0 0 1 1 1 1 0 1 ? ? ? ? ? ? ? ? ? ? ?
? ? ? ? ? ? ? 1 0 0 1 0 0 0 0 0 0 0 0 0 0 0 0 0 0 0 ? ? ? ? ? ? ? ? ?
? ?
? ?
? ?
? 1 1 1 1 1 0 1 1 1
0

Xenopus ?
? ? ? ? ? ? 1 0 0 1 1 0 0 0 0 0 0 0 0 0 0 0 0 0 0 ? ? ? ? ? ? ? ? ?

Table A2.1, continued. The matrix representation matrix used for supertree generation.

? ?
? ?
? ?
? ?

Struthio ?
? ? ? ? ? ? 1 0 0 1 1 1 0 0 0 0 0 0 0 0 0 0 0 0 ? ? ? ? ? ? ? ? ? ?
? ?
? ?
? ?
? ?
Ornithorhynchus ?
? ? ? ? ? ? ? 1 0 0 1 1 1 1 0 0 0 0 0 0 0 0 0 0 ? ? ? ? ? ? ? ? ? ?
? ?
? ?
? ?
? ?
? ?
Homo ?
? ? ? ? ? 1 0 0 1 1 1 1 0 0 0 0 0 0 0 0 0 0 ? ? ? ? ? ? ? ? ? ?
? ?
? ?
? ?
? ?
Plesiobatis ?
? ? ? ? ? ? ? 0 0 0 0 0 0 0 1 1 1 0 0 0 0 0 0 0 ? ? ? ? ? ? ? ? ? ?
? ?
? ?
? ?
? ?
?
Amblyraja? ?
? ? ? ? ? ? 0 0 0 0 0 0 0 1 1 1 1 0 0 0 0 0 0 0 ? ? ? ? ? ? ? ? ? ?
? ?
? ?
? ?
? ?
Okamejei ?
? ? ? ? ? ? 0 0 0 0 0 0 0 1 1 1 1 0 0 0 0 0 0 0 ? ? ? ? ? ? ? ? ? ?
? ?
? ?
? ?
? ?
Heterodontus ?
? ? ? ? ? ? ? 0 0 0 0 0 0 0 1 1 0 0 1 1 0 0 0 0 0 ? ? ? ? ? ? ? ? ? ?
? ?
? ?
? ?
? ?
?
Scyliorhinus ?
? ? ? ? ? ? ? 0 0 0 0 0 0 0 1 1 0 0 1 1 1 0 0 0 0 ? ? ? ? ? ? ? ? ? ?

Table A2.1, continued. The matrix representation matrix used for supertree generation.

? ?
? ?
? ?
? ?
?
Mustelus ?
? ? ? ? ? ? 0 0 0 0 0 0 0 1 1 0 0 1 1 1 0 0 0 0 ? ? ? ? ? ? ? ?
? ?
? ?
? ?
? ?
Callorhinchus? ?
? ? ? ? ? ? ? 0 0 0 0 0 0 0 1 0 0 0 0 0 0 1 0 0 0 ? ? ? ? ? ? ?
? ?
? ?
? ?
? ?
?
Rhinochimaera ?
? ? ? ? ? ? ? ? 0 0 0 0 0 0 0 1 0 0 0 0 0 0 1 1 1 0 ? ? ? ? ? ?
? ?
? ?
? ?
? ?
? ?
Hariotta ?
? ? ? ? ? ? 0 0 0 0 0 0 0 1 0 0 0 0 0 0 1 1 1 0 ? ? ? ? ? ? ? ?
? ?
? ?
? ?
? ?
Hydrolagus ?
? ? ? ? ? ? ? 0 0 0 0 0 0 0 1 0 0 0 0 0 0 1 1 0 1 ? ? ? ? ? ? ?
? ?
? ?
? ?
? ?
?
Galeaspida ?
? 0 0 0 0 0 0 0
0 0 0 0 0 0 0 0 0 0 0 0 0 0 0 0 0 0 0 0 0 0 0 0 0 0 0 0 0 0 0 0
0 0 0 0 0 0 0 0 0 0 0 0 0 0 0 0 0 0 ? ? ? ? ? ? ? ? ? ? ? ? ? ?
? ?
? ?
?
Osteostraci ?
? 0 0 0 0 0 0 0
0 0 0 0 0 0 0 0 0 0 0 0 0 0 0 0 0 0 0 0 0 0 0 0 0 0 0 0 0 0 0 0
0 0 0 0 0 0 0 0 0 0 0 0 0 0 0 0 0 0 ? ? ? ? ? ? ? ? ? ? ? ? ? ?
? ?
? ?
?

Table A2.1, continued. The matrix representation matrix used for supertree generation.

Brindabellaspis ?
? 1 0 0 0 0 0
0 0 0 0 0 0 0 0 0 0 0 0 0 0 0 0 0 0 0 0 0 0 0 0 0 0 0 0 0 0 0 0
0 0 0 0 0 0 0 0 0 0 0 0 0 0 0 0 0 0 0 ? ? ? ? ? ? ? ? ? ? ? ? ?
? ?
? ?
? ?
Parayunnanolepis ?
? 1 1 0 0 0
0 0 0 0 0 0 0 0 0 0 0 0 0 0 0 0 0 0 0 0 0 0 0 0 0 0 0 0 0 0 0 0
0 0 0 0 0 0 0 0 0 0 0 0 0 0 0 0 0 0 0 0 ? ? ? ? ? ? ? ? ? ? ? ?
? ?
? ?
? ? ?
Yunnanolepis ?
? 1 1 0 0 0 0 0
0 0 0 0 0 0 0 0 0 0 0 0 0 0 0 0 0 0 0 0 0 0 0 0 0 0 0 0 0 0 0 0
0 0 0 0 0 0 0 0 0 0 0 0 0 0 0 0 0 0 ? ? ? ? ? ? ? ? ? ? ? ? ? ?
? ?
? ?
?
Bothriolepis ?
? 1 1 1 0 0 0 0
0 0 0 0 0 0 0 0 0 0 0 0 0 0 0 0 0 0 0 0 0 0 0 0 0 0 0 0 0 0 0 0
0 0 0 0 0 0 0 0 0 0 0 0 0 0 0 0 0 0 ? ? ? ? ? ? ? ? ? ? ? ? ? ?
? ?
? ?
?
Pterichthyodes ?
? 1 1 1 0 0 0
0 0 0 0 0 0 0 0 0 0 0 0 0 0 0 0 0 0 0 0 0 0 0 0 0 0 0 0 0 0 0 0
0 0 0 0 0 0 0 0 0 0 0 0 0 0 0 0 0 0 0 ? ? ? ? ? ? ? ? ? ? ? ? ?
? ?
? ?
? ?
Lunaspis ?
? 1 0 0 1 1 0 0 0
0 0 0 0 0 0 0 0 0 0 0 0 0 0 0 0 0 0 0 0 0 0 0 0 0 0 0 0 0 0 0 0
0 0 0 0 0 0 0 0 0 0 0 0 0 0 0 0 0 ? ? ? ? ? ? ? ? ? ? ? ? ? ? ?
? ?
? ?
Macropetalichthys ?
? 1 0 0 1 1
0 0 0 0 0 0 0 0 0 0 0 0 0 0 0 0 0 0 0 0 0 0 0 0 0 0 0 0 0 0 0 0
0 0 0 0 0 0 0 0 0 0 0 0 0 0 0 0 0 0 0 0 ? ? ? ? ? ? ? ? ? ? ? ?
? ?
? ?
? ? ?
Romundina ?
? 1 0 0 1 0 1 0
0 0 0 0 0 0 0 0 0 0 0 0 0 0 0 0 0 0 0 0 0 0 0 0 0 0 0 0 0 0 0 0
0 0 0 0 0 0 0 0 0 0 0 0 0 0 0 0 0 0 ? ? ? ? ? ? ? ? ? ? ? ? ? ?

Table A2.1, continued. The matrix representation matrix used for supertree generation.

? ?
? ?
?

Rhamphodopsis ?
? 1 0 0 1 0 1
1 0 0 0 0 0 0 0 0 0 0 0 0 0 0 0 0 0 0 0 0 0 0 0 0 0 0 0 0 0
0 0 0 0 0 0 0 0 0 0 0 0 0 0 0 0 0 0 ? ? ? ? ? ? ? ? ? ? ? ?
? ?
? ?
? ?

Austroptyctodus ?
? 1 0 0 1 0 1
1 1 0 0 0 0 0 0 0 0 0 0 0 0 0 0 0 0 0 0 0 0 0 0 0 0 0 0 0 0
0 0 0 0 0 0 0 0 0 0 0 0 0 0 0 0 0 0 ? ? ? ? ? ? ? ? ? ? ? ?
? ?
? ?
? ?

Campbellodus ?
? 1 0 0 1 0 1
1 1 0 0 0 0 0 0 0 0 0 0 0 0 0 0 0 0 0 0 0 0 0 0 0 0 0 0 0 0
0 0 0 0 0 0 0 0 0 0 0 0 0 0 0 0 0 0 ? ? ? ? ? ? ? ? ? ? ? ?
? ?
? ?
? ?

Gemuendina ?
? 1 0 0 1 0 1 0
0 1 1 0 0 0 0 0 0 0 0 0 0 0 0 0 0 0 0 0 0 0 0 0 0 0 0 0 0 0 0
0 0 0 0 0 0 0 0 0 0 0 0 0 0 0 0 0 0 ? ? ? ? ? ? ? ? ? ? ? ?
? ?
? ?
?

Jagorina ?
? 1 0 0 1 0 1 0 0
1 1 0 0 0 0 0 0 0 0 0 0 0 0 0 0 0 0 0 0 0 0 0 0 0 0 0 0 0 0 0
0 0 0 0 0 0 0 0 0 0 0 0 0 0 0 0 0 0 ? ? ? ? ? ? ? ? ? ? ? ?
? ?
? ?

Kujdanowiaspis ?
? 1 0 0 1 0 1
0 0 1 0 1 0 0 0 0 0 0 0 0 0 0 0 0 0 0 0 0 0 0 0 0 0 0 0 0 0 0
0 0 0 0 0 0 0 0 0 0 0 0 0 0 0 0 0 0 ? ? ? ? ? ? ? ? ? ? ? ?
? ?
? ?
? ?

Dicksonosteus ?
? 1 0 0 1 0 1
0 0 1 0 1 1 0 0 0 0 0 0 0 0 0 0 0 0 0 0 0 0 0 0 0 0 0 0 0 0 0
0 0 0 0 0 0 0 0 0 0 0 0 0 0 0 0 0 0 ? ? ? ? ? ? ? ? ? ? ? ?
? ?
? ?
? ?

Table A2.1, continued. The matrix representation matrix used for supertree generation.

Buchanosteus ?
? 1 0 0 1 0 1 0
0 1 0 1 1 1 0 0 0 0 0 0 0 0 0 0 0 0 0 0 0 0 0 0 0 0 0 0 0 0 0
0 0 0 0 0 0 0 0 0 0 0 0 0 0 0 0 0 0 ? ? ? ? ? ? ? ? ? ? ? ? ?
? ?
? ?
?

Coccosteus ?
? 1 0 0 1 0 1 0
0 1 0 1 1 1 1 1 0 0 0 0 0 0 0 0 0 0 0 0 0 0 0 0 0 0 0 0 0 0 0
0 0 0 0 0 0 0 0 0 0 0 0 0 0 0 0 0 0 ? ? ? ? ? ? ? ? ? ? ? ? ?
? ?
? ?

Incisoscutum ?
? 1 0 0 1 0 1 0
0 1 0 1 1 1 1 1 0 0 0 0 0 0 0 0 0 0 0 0 0 0 0 0 0 0 0 0 0 0 0
0 0 0 0 0 0 0 0 0 0 0 0 0 0 0 0 0 0 ? ? ? ? ? ? ? ? ? ? ? ? ?
? ?
? ?
?

Cowralepis ?
? 1 0 0 1 0 1 0
0 1 0 1 1 1 1 0 1 0 0 0 0 0 0 0 0 0 0 0 0 0 0 0 0 0 0 0 0 0 0
0 0 0 0 0 0 0 0 0 0 0 0 0 0 0 0 0 0 ? ? ? ? ? ? ? ? ? ? ? ? ?
? ?
? ?

Eurycaraspis ?
? 1 0 0 1 0 1 0
0 1 0 1 1 1 1 0 1 0 0 0 0 0 0 0 0 0 0 0 0 0 0 0 0 0 0 0 0 0 0
0 0 0 0 0 0 0 0 0 0 0 0 0 0 0 0 0 0 ? ? ? ? ? ? ? ? ? ? ? ? ?
? ?
? ?

Entelognathus ?
? 1 0 0 1 0 1
0 0 1 0 0 0 0 0 0 0 1 0 0 0 0 0 0 0 0 0 0 0 0 0 0 0 0 0 0 0 0
0 0 0 0 0 0 0 0 0 0 0 0 0 0 0 0 0 0 ? ? ? ? ? ? ? ? ? ? ? ? ?
? ?
? ?
? ?

Janusiscus ?
? 1 0 0 1 0 1 0
0 1 0 0 0 0 0 0 0 1 1 0 0 0 0 0 0 0 0 0 0 0 0 0 0 0 0 0 0 0 0
0 0 0 0 0 0 0 0 0 0 0 0 0 0 0 0 0 0 ? ? ? ? ? ? ? ? ? ? ? ? ?
? ?
? ?
?

Ramirosuarezia ?
? 1 0 0 1 0 1
0 0 1 0 0 0 0 0 0 0 1 1 0 0 0 0 0 0 0 0 0 0 0 0 0 0 0 0 0 0 0

Table A2.1, continued. The matrix representation matrix used for supertree generation.

	0	0	0	0	0	0	0	0	0	0	0	0	0	0	0	0	0	0	0	?	?	?	?	?	?	?	?	?	?	?	?	?
	?	?	?	?	?	?	?	?	?	?	?	?	?	?	?	?	?	?	?	?	?	?	?	?	?	?	?	?	?	?	?	?
	?	?	?	?	?	?	?	?	?	?	?	?	?	?	?	?	?	?	?	?	?	?	?	?	?	?	?	?	?	?	?	?
	?	?																														
Dialipina	?	?	?	?	?	?	?	?	?	?	?	?	?	?	?	?	?	?	?	?	?	?	?	?	?	?	?	?	?	?	?	?
	?	?	?	?	?	?	?	?	?	?	?	?	?	?	?	?	?	?	?	?	?	?	?	?	1	0	0	1	0	1	0	0
	1	0	0	0	0	0	0	0	1	1	1	0	0	0	0	0	0	0	0	0	0	0	0	0	0	0	0	0	0	0	0	0
	0	0	0	0	0	1	0	0	0	0	0	0	0	0	0	0	0	?	?	?	?	?	?	?	?	?	?	?	?	?	?	?
	?	?	?	?	?	?	?	?	?	?	?	?	?	?	?	?	?	?	?	?	?	?	?	?	?	?	?	?	?	?	?	?
	?	?	?	?	?	?	?	?	?	?	?	?	?	?	?	?	?	?	?	?	?	?	?	?	?	?	?	?	?	?	?	?
Ligulalepis	?	?	?	?	?	?	?	?	?	?	?	?	?	?	?	?	?	?	?	?	?	?	?	?	?	?	?	?	?	?	?	?
	?	?	?	?	?	?	?	?	?	?	?	?	?	?	?	?	?	?	?	?	?	?	?	?	1	0	0	1	0	1	0	
	0	1	0	0	0	0	0	0	0	1	1	1	0	0	0	0	0	0	0	0	0	0	0	0	0	0	0	0	0	0	0	0
	0	0	0	0	0	0	1	1	0	0	0	0	0	0	0	0	0	?	?	?	?	?	?	?	?	?	?	?	?	?	?	?
	?	?	?	?	?	?	?	?	?	?	?	?	?	?	?	?	?	?	?	?	?	?	?	?	?	?	?	?	?	?	?	?
	?	?	?	?	?	?	?	?	?	?	?	?	?	?	?	?	?	?	?	?	?	?	?	?	?	?	?	?	?	?	?	?
	?																															
Cheirolepis	?	?	?	?	?	?	?	?	?	?	?	?	?	?	?	?	?	?	?	?	?	?	?	?	?	?	?	?	?	?	?	?
	?	?	?	?	?	?	?	?	?	?	?	?	?	?	?	?	?	?	?	?	?	?	?	?	1	0	0	1	0	1	0	
	0	1	0	0	0	0	0	0	0	1	1	1	0	0	0	0	0	0	0	0	0	0	0	0	0	0	0	0	0	0	0	0
	0	0	0	0	0	0	1	1	1	0	0	0	0	0	0	0	0	?	?	?	?	?	?	?	?	?	?	?	?	?	?	?
	?	?	?	?	?	?	?	0	0	0	0	0	0	0	0	0	0	0	?	?	?	?	?	?	?	?	?	?	?	?	?	?
	?	?	?	?	?	?	?	?	?	?	?	?	?	?	?	?	?	?	?	?	?	?	?	?	?	?	?	?	?	?	?	?
	?																															
Howqualepis	?	?	?	?	?	?	?	?	?	?	?	?	?	?	?	?	?	?	?	?	?	?	?	?	?	?	?	?	?	?	?	?
	?	?	?	?	?	?	?	?	?	?	?	?	?	?	?	?	?	?	?	?	?	?	?	?	1	0	0	1	0	1	0	
	0	1	0	0	0	0	0	0	0	1	1	1	0	0	0	0	0	0	0	0	0	0	0	0	0	0	0	0	0	0	0	0
	0	0	0	0	0	0	1	1	1	1	0	0	0	0	0	0	0	0	?	?	?	?	?	?	?	?	?	?	?	?	?	?
	?	?	?	?	?	?	?	1	1	1	0	0	0	0	0	0	0	0	?	?	?	?	?	?	?	?	?	?	?	?	?	?
	?	?	?	?	?	?	?	?	?	?	?	?	?	?	?	?	?	?	?	?	?	?	?	?	?	?	?	?	?	?	?	?
	?																															
Kentuckia	?	?	?	?	?	?	?	?	?	?	?	?	?	?	?	?	?	?	?	?	?	?	?	?	?	?	?	?	?	?	?	?
	?	?	?	?	?	?	?	?	?	?	?	?	?	?	?	?	?	?	?	?	?	?	?	?	1	0	0	1	0	1	0	
	1	0	0	0	0	0	0	0	1	1	1	0	0	0	0	0	0	0	0	0	0	0	0	0	0	0	0	0	0	0	0	0
	0	0	0	0	0	1	1	1	1	1	1	0	0	0	0	0	0	?	?	?	?	?	?	?	?	?	?	?	?	?	?	?
	?	?	?	?	?	?	1	1	1	1	1	0	0	0	0	0	0	0	?	?	?	?	?	?	?	?	?	?	?	?	?	?
	?	?	?	?	?	?	?	?	?	?	?	?	?	?	?	?	?	?	?	?	?	?	?	?	?	?	?	?	?	?	?	?
Moythomasia	?	?	?	?	?	?	?	?	?	?	?	?	?	?	?	?	?	?	?	?	?	?	?	?	?	?	?	?	?	?	?	?
	?	?	?	?	?	?	?	?	?	?	?	?	?	?	?	?	?	?	?	?	?	?	?	?	1	0	0	1	0	1	0	
	0	1	0	0	0	0	0	0	0	1	1	1	0	0	0	0	0	0	0	0	0	0	0	0	0	0	0	0	0	0	0	0
	0	0	0	0	0	0	1	1	1	1	1	1	0	0	0	0	0	0	?	?	?	?	?	?	?	?	?	?	?	?	?	?
	?	?	?	?	?	?	?	1	1	1	1	0	0	0	0	0	0	0	0	?	?	?	?	?	?	?	?	?	?	?	?	?
	?	?	?	?	?	?	?	?	?	?	?	?	?	?	?	?	?	?	?	?	?	?	?	?	?	?	?	?	?	?	?	?
	?																															
Guiyu	?	?	?	?	?	?	?	?	?	?	?	?	?	?	?	?	?	?	?	?	?	?	?	?	?	?	?	?	?	?	?	?
	?	?	?	?	?	?	?	?	?	?	?	?	?	?	?	?	?	?	?	?	?	?	?	?	1	0	0	1	0	1	0	0
	0	0	0	0	0	0	0	1	1	1	0	0	0	0	0	0	0	0	0	0	0	0	0	0	0	0	0	0	0	0	0	0
	0	0	0	0	1	1	0	0	0	0	1	0	0	0	0	0	?	?	?	?	?	?	?	?	?	?	?	?	?	?	?	?
	?	?	?	?	?	?	?	?	?	?	?	?	?	?	?	?	?	?	?	?	?	?	?	?	?	?	?	?	?	?	?	?
	?	?	?	?	?	?	?	?	?	?	?	?	?	?	?	?	?	?	?	?	?	?	?	?	?	?	?	?	?	?	?	
Psarolepis	?	?	?	?	?	?	?	?	?	?	?	?	?	?	?	?	?	?	?	?	?	?	?	?	?	?	?	?	?	?	?	?
	?	?	?	?	?	?	?	?	?	?	?	?	?	?	?	?	?	?	?	?	?	?	?	?	1	0	0	1	0	1	0	0

Table A2.1, continued. The matrix representation matrix used for supertree generation.

1 0 0 0 0 0 0 0 1 1 1 0 0 0 0 0 0 0 0 0 0 0 0 0 0 0 0 0 0 0 0 0
0 0 0 0 0 1 1 0 0 0 0 1 0 0 0 0 0 ? ? ? ? ? ? ? ? ? ? ? ? ? ? ?
? ? ? ? ? ? ? ? ? ? ? ? ? ? ? ? ? 0 0 0 0 0 0 0 0 0 0 0 0 0 0 0
0 0 ?
Onychodus ?
? 1 0 0 1 0 1 0
0 1 0 0 0 0 0 0 0 1 1 1 0 0 0 0 0 0 0 0 0 0 0 0 0 0 0 0 0 0 0 0
0 0 0 0 0 0 1 1 0 0 0 0 1 1 0 0 0 0 ? ? ? ? ? ? ? ? ? ? ? ? ? ?
? ?
? ? ? 0 0 0 0 0 0 1 1 0 0 0 0 0 0 0 0 0 0 0 0 ? ? ? ? ? ? ? ? ?
?
Styloichthys ?
? 1 0 0 1 0 1 0
0 1 0 0 0 0 0 0 0 1 1 1 0 0 0 0 0 0 0 0 0 0 0 0 0 0 0 0 0 0 0 0
0 0 0 0 0 0 1 1 0 0 0 0 1 1 1 0 0 0 0 1 1 0 0 0 0 0 0 0 0 0 0 0
0 0 0 0 0 0 0 ?
? ?
?
Eusthenopteron ?
? 1 0 0 1 0 1
0 0 1 0 0 0 0 0 0 0 1 1 1 0 0 0 0 0 0 0 0 0 0 0 0 0 0 0 0 0 0 0
0 0 0 0 0 0 0 1 1 0 0 0 0 1 1 1 1 1 0 ? ? ? ? ? ? ? ? ? ? ? ? ?
? 1 0 0 0 0 0 0 0 0 0 0
0 0 0 0 0 0 0 0 0 0 0 0 0 0 0 0 0 1 0 1 0 0 0 0 0 ? ? ? ? ? ? ? ?
? ?
Gogonasus ?
? 1 0 0 1 0 1 0
0 1 0 0 0 0 0 0 0 1 1 1 0 0 0 0 0 0 0 0 0 0 0 0 0 0 0 0 0 0 0 0
0 0 0 0 0 0 1 1 0 0 0 0 1 1 1 1 1 0 ? ? ? ? ? ? ? ? ? ? ? ? ? ?
? 1 0 0 0 0 0 0 0 0 0 0
0 0 0 ?
?
Glyptolepis ?
? 1 0 0 1 0 1 0
0 1 0 0 0 0 0 0 0 1 1 1 0 0 0 0 0 0 0 0 0 0 0 0 0 0 0 0 0 0 0 0
0 0 0 0 0 0 1 1 0 0 0 0 1 1 1 1 0 1 ? ? ? ? ? ? ? ? ? ? ? ? ? ?
? 0 1 0 0 0 0 0 0 0 0 0
0 0 0 0 0 0 0 0 0 0 0 0 0 0 1 1 0 0 0 0 0 0 0 0 ? ? ? ? ? ? ? ?
?
Porolepis ?
? 1 0 0 1 0 1 0 0
1 0 0 0 0 0 0 0 1 1 1 0 0 0 0 0 0 0 0 0 0 0 0 0 0 0 0 0 0 0 0 0
0 0 0 0 0 1 1 0 0 0 0 1 1 1 1 0 1 ? ? ? ? ? ? ? ? ? ? ? ? ? ? ?
? 0 1 0 0 0 0 0 0 0 0 0
0 0 0 0 0 0 0 0 0 0 0 0 0 1 0 0 0 0 0 0 0 0 0 ? ? ? ? ? ? ? ? ? ?
Culmacanthus ?
? 1 0 0 1 0 1
0 0 1 0 0 0 0 0 0 0 1 1 1 1 1 0 0 0 0 0 0 0 0 0 0 0 0 0 0 0 0 0
0 0 0 0 0 0 0 0 0 0 0 0 0 0 0 0 0 0 0 ? ? ? ? ? ? ? ? ? ? ? ? ?
? ?
? ?
? ?

Table A2.1, continued. The matrix representation matrix used for supertree generation.

Latviacanthus	?	?	?	?	?	?	?	?	?	?	?	?	?	?	?	?	?	?	?	?	?	?	?	?	?	?	?	?	?	?	?
	?	?	?	?	?	?	?	?	?	?	?	?	?	?	?	?	?	?	?	?	?	?	?	?	?	1	0	0	1	0	1	0
	0	1	0	0	0	0	0	0	0	1	1	1	1	1	0	0	0	0	0	0	0	0	0	0	0	0	0	0	0	0	0	0
	0	0	0	0	0	0	0	0	0	0	0	0	0	0	0	0	0	0	?	?	?	?	?	?	?	?	?	?	?	?	?	?
	?	?	?	?	?	?	?	?	?	?	?	?	?	?	?	?	?	?	?	?	?	?	?	?	?	?	?	?	?	?	?	?
	?	?	?	?	?	?	?	?	?	?	?	?	?	?	?	?	?	?	?	?	?	?	?	?	?	?	?	?	?	?	?	?
	?																															
Tetanopsyrus	?	?	?	?	?	?	?	?	?	?	?	?	?	?	?	?	?	?	?	?	?	?	?	?	?	?	?	?	?	?	?	?
	?	?	?	?	?	?	?	?	?	?	?	?	?	?	?	?	?	?	?	?	?	?	?	?	?	1	0	0	1	0	1	0
	0	1	0	0	0	0	0	0	0	1	1	1	1	1	1	0	0	0	0	0	0	0	0	0	0	0	0	0	0	0	0	0
	0	0	0	0	0	0	0	0	0	0	0	0	0	0	0	0	0	0	?	?	?	?	?	?	?	?	?	?	?	?	?	?
	?	?	?	?	?	?	?	?	?	?	?	?	?	?	?	?	?	?	?	?	?	?	?	?	?	?	?	?	?	?	?	?
	?	?	?	?	?	?	?	?	?	?	?	?	?	?	?	?	?	?	?	?	?	?	?	?	?	?	?	?	?	?	?	?
	?																															
Diplacanthus	?	?	?	?	?	?	?	?	?	?	?	?	?	?	?	?	?	?	?	?	?	?	?	?	?	?	?	?	?	?	?	?
	?	?	?	?	?	?	?	?	?	?	?	?	?	?	?	?	?	?	?	?	?	?	?	?	?	1	0	0	1	0	1	0
	0	1	0	0	0	0	0	0	0	1	1	1	1	1	1	1	0	0	0	0	0	0	0	0	0	0	0	0	0	0	0	0
	0	0	0	0	0	0	0	0	0	0	0	0	0	0	0	0	0	0	?	?	?	?	?	?	?	?	?	?	?	?	?	?
	?	?	?	?	?	?	?	?	?	?	?	?	?	?	?	?	?	?	?	?	?	?	?	?	?	?	?	?	?	?	?	?
	?	?	?	?	?	?	?	?	?	?	?	?	?	?	?	?	?	?	?	?	?	?	?	?	?	?	?	?	?	?	?	?
	?																															
Gladiobranchus	?	?	?	?	?	?	?	?	?	?	?	?	?	?	?	?	?	?	?	?	?	?	?	?	?	?	?	?	?	?	?	?
	?	?	?	?	?	?	?	?	?	?	?	?	?	?	?	?	?	?	?	?	?	?	?	?	?	1	0	0	1	0	1	
	0	0	1	0	0	0	0	0	0	0	1	1	1	1	1	1	1	0	0	0	0	0	0	0	0	0	0	0	0	0	0	0
	0	0	0	0	0	0	0	0	0	0	0	0	0	0	0	0	0	0	?	?	?	?	?	?	?	?	?	?	?	?	?	?
	?	?	?	?	?	?	?	?	?	?	?	?	?	?	?	?	?	?	?	?	?	?	?	?	?	?	?	?	?	?	?	?
	?	?	?	?	?	?	?	?	?	?	?	?	?	?	?	?	?	?	?	?	?	?	?	?	?	?	?	?	?	?	?	?
	?	?																														
Cassidiceps	?	?	?	?	?	?	?	?	?	?	?	?	?	?	?	?	?	?	?	?	?	?	?	?	?	?	?	?	?	?	?	?
	?	?	?	?	?	?	?	?	?	?	?	?	?	?	?	?	?	?	?	?	?	?	?	?	?	1	0	0	1	0	1	0
	0	1	0	0	0	0	0	0	0	1	1	1	1	1	1	0	1	0	0	0	0	0	0	0	0	0	0	0	0	0	0	0
	0	0	0	0	0	0	0	0	0	0	0	0	0	0	0	0	0	0	?	?	?	?	?	?	?	?	?	?	?	?	?	?
	?	?	?	?	?	?	?	?	?	?	?	?	?	?	?	?	?	?	?	?	?	?	?	?	?	?	?	?	?	?	?	?
	?	?	?	?	?	?	?	?	?	?	?	?	?	?	?	?	?	?	?	?	?	?	?	?	?	?	?	?	?	?	?	?
	?																															
Euthacanthus	?	?	?	?	?	?	?	?	?	?	?	?	?	?	?	?	?	?	?	?	?	?	?	?	?	?	?	?	?	?	?	?
	?	?	?	?	?	?	?	?	?	?	?	?	?	?	?	?	?	?	?	?	?	?	?	?	?	1	0	0	1	0	1	0
	0	1	0	0	0	0	0	0	0	1	1	1	1	1	1	0	1	0	0	0	0	0	0	0	0	0	0	0	0	0	0	0
	0	0	0	0	0	0	0	0	0	0	0	0	0	0	0	0	0	0	?	?	?	?	?	?	?	?	?	?	?	?	?	?
	?	?	?	?	?	?	?	?	?	?	?	?	?	?	?	?	?	?	?	?	?	?	?	?	?	?	?	?	?	?	?	?
	?	?	?	?	?	?	?	?	?	?	?	?	?	?	?	?	?	?	?	?	?	?	?	?	?	?	?	?	?	?	?	?
	?																															
Ischnacanthus	?	?	?	?	?	?	?	?	?	?	?	?	?	?	?	?	?	?	?	?	?	?	?	?	?	?	?	?	?	?	?	?
	?	?	?	?	?	?	?	?	?	?	?	?	?	?	?	?	?	?	?	?	?	?	?	?	?	1	0	0	1	0	1	
	0	0	1	0	0	0	0	0	0	0	1	1	1	1	1	1	0	1	1	0	0	0	0	0	0	0	0	0	0	0	0	0
	0	0	0	0	0	0	0	0	0	0	0	0	0	0	0	0	0	0	?	?	?	?	?	?	?	?	?	?	?	?	?	?
	?	?	?	?	?	?	?	?	?	?	?	?	?	?	?	?	?	?	?	?	?	?	?	?	?	?	?	?	?	?	?	?
	?	?	?	?	?	?	?	?	?	?	?	?	?	?	?	?	?	?	?	?	?	?	?	?	?	?	?	?	?	?	?	?
	?	?																														
Poracanthodes	?	?	?	?	?	?	?	?	?	?	?	?	?	?	?	?	?	?	?	?	?	?	?	?	?	?	?	?	?	?	?	?
	?	?	?	?	?	?	?	?	?	?	?	?	?	?	?	?	?	?	?	?	?	?	?	?	?	1	0	0	1	0	1	
	0	0	1	0	0	0	0	0	0	0	1	1	1	1	1	1	0	1	1	0	0	0	0	0	0	0	0	0	0	0	0	0

Table A2.1, continued. The matrix representation matrix used for supertree generation.

0 0 0 0 0 0 0 0 0 0 0 0 0 0 0 0 0 0 0 ? ? ? ? ? ? ? ? ? ? ? ? ?
? ?
? ?
? ?

Mesacanthus ?
? 1 0 0 1 0 1 0
0 1 0 0 0 0 0 0 0 1 1 1 1 1 1 0 1 0 1 0 0 0 0 0 0 0 0 0 0 0 0 0
0 0 0 0 0 0 0 0 0 0 0 0 0 0 0 0 0 0 ? ? ? ? ? ? ? ? ? ? ? ? ? ?
? ?
? ?
?

Promesacanthus ?
? 1 0 0 1 0 1
0 0 1 0 0 0 0 0 0 0 1 1 1 1 1 1 0 1 0 1 0 0 0 0 0 0 0 0 0 0 0 0
0 0 0 0 0 0 0 0 0 0 0 0 0 0 0 0 0 0 ? ? ? ? ? ? ? ? ? ? ? ? ? ?
? ?
? ?
? ?

Cheiracanthus ?
? 1 0 0 1 0 1
0 0 1 0 0 0 0 0 0 0 1 1 1 1 1 1 0 1 0 0 1 0 0 0 0 0 0 0 0 0 0 0
0 0 0 0 0 0 0 0 0 0 0 0 0 0 0 0 0 0 ? ? ? ? ? ? ? ? ? ? ? ? ? ?
? ?
? ?
?

Acanthodes ?
? 1 0 0 1 0 1 0
0 1 0 0 0 0 0 0 0 1 1 1 1 1 1 0 1 0 0 1 1 0 0 0 0 0 0 0 0 0 0 0
0 0 0 0 0 0 0 0 0 0 0 0 0 0 0 0 0 0 ? ? ? ? ? ? ? ? ? ? ? ? ? ?
? ?
? ?
?

Homalacanthus ?
? 1 0 0 1 0 1
0 0 1 0 0 0 0 0 0 0 1 1 1 1 1 1 0 1 0 0 1 1 0 0 0 0 0 0 0 0 0 0
0 0 0 0 0 0 0 0 0 0 0 0 0 0 0 0 0 0 ? ? ? ? ? ? ? ? ? ? ? ? ? ?
? ?
? ?
? ?

Climatius ?
? 1 0 0 1 0 1 0 0
1 0 0 0 0 0 0 0 1 1 1 1 0 0 0 0 0 0 0 0 1 0 0 0 0 0 0 0 0 0 0 0
0 0 0 0 0 0 0 0 0 0 0 0 0 0 0 0 0 0 ? ? ? ? ? ? ? ? ? ? ? ? ? ?
? ?
? ?

Ptomacanthus? ?
? 1 0 0 1 0 1 0
0 1 0 0 0 0 0 0 0 1 1 1 1 0 0 0 0 0 0 0 0 1 0 0 0 0 0 0 0 0 0 0
0 0 0 0 0 0 0 0 0 0 0 0 0 0 0 0 0 0 ? ? ? ? ? ? ? ? ? ? ? ? ? ?
? ?
? ?
?

Table A2.1, continued. The matrix representation matrix used for supertree generation.

Brochoadmones ?
? 1 0 0 1 0 1
0 0 1 0 0 0 0 0 0 0 1 1 1 1 0 0 0 0 0 0 0 0 1 1 0 0 0 0 0 0 0 0
0 0 0 0 0 0 0 0 0 0 0 0 0 0 0 0 0 0 0 ? ? ? ? ? ? ? ? ? ? ? ? ?
? ?
? ?
? ?
Kathemacanthus ?
? 1 0 0 1 0 1
0 0 1 0 0 0 0 0 0 0 1 1 1 1 0 0 0 0 0 0 0 0 1 1 0 0 0 0 0 0 0 0
0 0 0 0 0 0 0 0 0 0 0 0 0 0 0 0 0 0 0 ? ? ? ? ? ? ? ? ? ? ? ? ?
? ?
? ?
? ?
Brachyacanthus ?
? 1 0 0 1 0 1
0 0 1 0 0 0 0 0 0 0 1 1 1 1 0 0 0 0 0 0 0 0 1 0 1 0 0 0 0 0 0 0
0 0 0 0 0 0 0 0 0 0 0 0 0 0 0 0 0 0 0 ? ? ? ? ? ? ? ? ? ? ? ? ?
? ?
? ?
? ?

Parexus ?
? 1 0 0 1 0 1 0 0
1 0 0 0 0 0 0 0 1 1 1 1 0 0 0 0 0 0 0 0 1 0 1 0 0 0 0 0 0 0 0 0
0 0 0 0 0 0 0 0 0 0 0 0 0 0 0 0 0 0 ? ? ? ? ? ? ? ? ? ? ? ? ? ?
? ?
? ?
Vwaynensis ?
? 1 0 0 1 0 1 0
0 1 0 0 0 0 0 0 0 1 1 1 1 0 0 0 0 0 0 0 0 1 0 1 0 0 0 0 0 0 0 0
0 0 0 0 0 0 0 0 0 0 0 0 0 0 0 0 0 0 ? ? ? ? ? ? ? ? ? ? ? ? ? ?
? ?
? ?
?
Gyracanthides ?
? 1 0 0 1 0 1
0 0 1 0 0 0 0 0 0 0 1 1 1 1 0 0 0 0 0 0 0 0 1 0 0 1 0 0 0 0 0 0
0 0 0 0 0 0 0 0 0 0 0 0 0 0 0 0 0 0 0 ? ? ? ? ? ? ? ? ? ? ? ? ?
? ?
? ?
? ?
Lupopsyrus ?
? 1 0 0 1 0 1 0
0 1 0 0 0 0 0 0 0 1 1 1 1 0 0 0 0 0 0 0 0 1 0 0 1 0 0 0 0 0 0 0
0 0 0 0 0 0 0 0 0 0 0 0 0 0 0 0 0 0 ? ? ? ? ? ? ? ? ? ? ? ? ? ?
? ?
? ?
?
Obtusacanthus ?
? 1 0 0 1 0 1
0 0 1 0 0 0 0 0 0 0 1 1 1 1 0 0 0 0 0 0 0 0 1 0 0 1 1 0 0 0 0 0

Table A2.1, continued. The matrix representation matrix used for supertree generation.

0 0 0 0 0 0 0 0 0 0 0 0 0 0 0 0 0 0 0 ? ? ? ? ? ? ? ? ? ? ? ? ?
? ?
? ?
? ?

Hamiltonichthys ?
? 1 0 0 1 0 1
0 0 1 0 0 0 0 0 0 0 1 1 1 1 0 0 0 0 0 0 0 0 1 0 0 1 1 1 1 1 0 1
1 1 0 0 0 0 0 0 0 0 0 0 0 0 0 0 0 0 0 ? ? ? ? ? ? ? ? ? ? ? ? ?
? ?
? ?
? ?

Onychoselache ?
? 1 0 0 1 0 1
0 0 1 0 0 0 0 0 0 0 1 1 1 1 0 0 0 0 0 0 0 0 1 0 0 1 1 1 1 1 0 1
1 1 0 0 0 0 0 0 0 0 0 0 0 0 0 0 0 0 0 ? ? ? ? ? ? ? ? ? ? ? ? ?
? ?
? ?
? ?

Chondrenchelys ?
? 1 0 0 1 0 1
0 0 1 0 0 0 0 0 0 0 1 1 1 1 0 0 0 0 0 0 0 0 1 0 0 1 1 1 1 1 0 1
0 0 1 0 0 1 1 0 0 0 0 0 0 0 0 0 0 0 0 ? ? ? ? ? ? ? ? ? ? ? ? ?
? ?
? ?
? ?

Porolepiformes ?
? ?
? ?
? 1 0 0 0 0 0 0 0 0 0 0 0 0
0 0 0 0 0 0 0 0 ?
? ?
? ?

Actinopterygii ?
? ?
? ?
? 1 0 0 0 0 0 0 0 0 0 0 0 0
0 0 0 0 0 0 0 0 ?
? ?
? ?

Miguashaia ?
? ?
? ?
? 0 1 0 0 0 0 0 0 0 0 0 0 0
0 0 0 0 0 0 0 ?
? ? ? 0 0 0 0 0 0 1 0 1 0 0 0 0 0 0 0 0 0 0 0 ? ? ? ? ? ? ? ? ? ?
?

Gavinia ?
? ?
? ?
? 0 1 1 0 0 0 0 0 0 0 0 0 0 0
0 0 0 0 0 0 ?
? ?

Table A2.1, continued. The matrix representation matrix used for supertree generation.

Diplocercides ?
? ?
? ?
? ? ? ? ? ? ? ? ? ? ? ? ? ? ? ? ? ? 0 1 0 1 0 0 0 0 0 0 0 0 0 0
0 0 0 0 0 0 0 ? ? ? ? ? ? ? ? ? ? ? ? 0 0 0 0 0 0 0 0 0 0 0 0 0
0 0 0 0 0 0 0 0 0 1 0 1 1 0 0 0 0 0 0 0 0 0 0 ? ? ? ? ? ? ? ? ?
?
Serenichthys ?
? ?
? ?
? ? ? ? ? ? ? ? ? ? ? ? ? ? ? ? ? ? 0 1 0 1 1 0 0 0 0 0 0 0 0 0
0 0 0 0 0 0 0 ?
? ?
?
Allenypterus ?
? ?
? ?
? ? ? ? ? ? ? ? ? ? ? ? ? ? ? ? ? ? 0 1 0 1 1 1 1 0 0 0 0 0 0 0
0 0 0 0 0 0 0 ?
? ? ? 0 0 0 0 0 0 1 0 1 1 0 0 0 0 0 0 0 0 0 0 ? ? ? ? ? ? ? ? ?
?
Holopterygius ?
? ?
? ?
? ? ? ? ? ? ? ? ? ? ? ? ? ? ? ? ? ? 0 1 0 1 1 1 1 0 0 0 0 0 0 0
0 0 0 0 0 0 0 ?
? ?
?
Lochmocercus ?
? ?
? ?
? ? ? ? ? ? ? ? ? ? ? ? ? ? ? ? ? ? ? 0 1 0 1 1 1 0 1 0 0 0 0 0
0 0 0 0 0 0 0 0 ?
? ?
? ?
Polyosteorhynchus ?
? ?
? ?
? 0 1 0 1 1 1 0 1 1 0 0 0
0 0 0 0 0 0 0 0 0 ?
? ?
? ? ?
Hadronector ?
? ?
? ?
? ? ? ? ? ? ? ? ? ? ? ? ? ? ? ? ? ? 0 1 0 1 1 1 0 1 1 1 0 0 0 0
0 0 0 0 0 0 0 ?
? ?
?
Caridosuctor ?
? ?
? ?

Table A2.1, continued. The matrix representation matrix used for supertree generation.

? ? ? ? ? ? ? ? ? ? ? ? ? ? ? ? ? ? 0 1 0 1 1 1 0 1 1 1 1 0 0 0
0 0 0 0 0 0 0 ?
? ?
?

Rhabdoderma ?
? ?
? ?
? ? ? ? ? ? ? ? ? ? ? ? ? ? ? ? ? ? 0 1 0 1 1 1 0 1 1 1 1 0 0 0
0 0 0 0 0 0 0 ?
? ?
?

Sassenia ?
? ?
? ?
? ? ? ? ? ? ? ? ? ? ? ? ? ? ? ? ? 0 1 0 1 1 1 0 1 1 1 1 1 1 0 0
0 0 0 0 0 0 ?
? ?

Spermatodus ?
? ?
? ?
? ? ? ? ? ? ? ? ? ? ? ? ? ? ? ? ? ? 0 1 0 1 1 1 0 1 1 1 1 1 1 0
0 0 0 0 0 0 0 ?
? ?
?

Coccoderma ?
? ?
? ?
? ? ? ? ? ? ? ? ? ? ? ? ? ? ? ? ? ? 0 1 0 1 1 1 0 1 1 1 1 1 0 1
1 0 0 0 0 0 0 ?
? ?
?

Laugia ?
? ?
? ?
? ? ? ? ? ? ? ? ? ? ? ? ? ? ? ? ? 0 1 0 1 1 1 0 1 1 1 1 1 0 1 1 0
0 0 0 0 0 ?
? ?

Coelacanthus ?
? ?
? ?
? ? ? ? ? ? ? ? ? ? ? ? ? ? ? ? ? ? 0 1 0 1 1 1 0 1 1 1 1 1 0 1
0 1 0 0 0 0 0 ?
? ?
?

Whiteia ?
? ?
? ?
? ? ? ? ? ? ? ? ? ? ? ? ? ? ? ? ? 0 1 0 1 1 1 0 1 1 1 1 1 0 1 0
1 1 0 0 0 0 ?
? ?

Holophagus ?
? ?

Table A2.1, continued. The matrix representation matrix used for supertree generation.

? ?
? ? ? ? ? ? ? ? ? ? ? ? ? ? ? ? ? ? 0 1 0 1 1 1 0 1 1 1 1 1 0 1
0 1 1 1 0 0 0 ?
? ?
?

Udinia ?
? ?
? ?
? ? ? ? ? ? ? ? ? ? ? ? ? ? ? ? ? 0 1 0 1 1 1 0 1 1 1 1 1 0 1 0 1
1 1 0 0 0 ?
? ?

Latimeria ?
? ?
? ?
? ? ? ? ? ? ? ? ? ? ? ? ? ? ? ? ? 0 1 0 1 1 1 0 1 1 1 1 1 0 1 0 1
1 1 1 0 0 0 ?
? ?

Macropoma ?
? ?
? ?
? ? ? ? ? ? ? ? ? ? ? ? ? ? ? ? ? ? 0 1 0 1 1 1 0 1 1 1 1 1 0 1
0 1 1 1 0 0 0 ?
? ?
?

Garnbergia ?
? ?
? ?
? 0 1 0 1 1 1 0 1 1 1 1 1 0 1
0 1 1 1 0 0 0 ?
? ?
?

Libys ?
? ?
? ?
? ? ? ? ? ? ? ? ? ? ? ? ? ? ? ? ? 0 1 0 1 1 1 0 1 1 1 1 1 0 1 0 1
1 1 0 0 0 ?
? ?

Diplurus ?
? ?
? ?
? ? ? ? ? ? ? ? ? ? ? ? ? ? ? ? ? ? 0 1 0 1 1 1 0 1 1 1 1 1 0 1 0
1 1 1 1 0 0 ?
? ?

Chinlea ?
? ?
? ?
? ? ? ? ? ? ? ? ? ? ? ? ? ? ? ? ? ? 0 1 0 1 1 1 0 1 1 1 1 1 0 1 0
1 1 1 1 1 0 ?
? ?

Axelrodichthys ?
? ?
? ?

Table A2.1, continued. The matrix representation matrix used for supertree generation.

? ? ? ? ? ? ? ? ? ? ? ? ? ? ? ? ? ? ? 0 1 0 1 1 1 0 1 1 1 1 1 0
1 0 1 1 1 1 1 1 ?
? ?
? ?

Mawsonia ?
? ?
? ?
? ? ? ? ? ? ? ? ? ? ? ? ? ? ? ? ? 0 1 0 1 1 1 0 1 1 1 1 1 0 1 0
1 1 1 1 1 1 ?
? ?

Polypterus ?
? ?
? ?
? ?
? ? ? ? ? ? ? 1 0 0 0 0 0 0 0 0 0 0 0 ? ? ? ? ? ? ? ? ? ? ? ? ? ? ?
? ?
?

Birgeria ?
? ?
? ?
? ?
? ? ? ? ? ? 1 1 1 1 1 1 0 0 0 0 0 ? ? ? ? ? ? ? ? ? ? ? ? ? ? ? ? ?
? ?

Saurichthys ?
? ?
? ?
? ?
? ? ? ? ? ? ? 1 1 1 1 1 1 1 1 0 0 0 0 ? ? ? ? ? ? ? ? ? ? ? ? ? ? ?
? ?
?

Acipenser ?
? ?
? ?
? ?
? ? ? ? ? ? 1 1 1 1 1 1 1 0 0 0 0 ? ? ? ? ? ? ? ? ? ? ? ? ? ? ? ? ?
? ?

Pteronisculus ?
? ?
? ?
? ?
? ? ? ? ? ? ? 1 1 1 1 1 1 0 0 1 0 0 0 ? ? ? ? ? ? ? ? ? ? ? ? ? ? ?
? ?
?

Boreosomus ?
? ?
? ?
? ?
? ? ? ? ? ? ? 1 1 1 1 1 1 0 0 1 1 0 0 ? ? ? ? ? ? ? ? ? ? ? ? ? ? ?
? ?
?

Table A2.1, continued. The matrix representation matrix used for supertree generation.

Australosomus ?
? ?
? ?
? ?
? ? ? ? ? ? ? ? 1 1 1 1 1 1 0 0 1 1 1 0 ? ? ? ? ? ? ? ? ? ? ? ?
? ?
? ?

Perleidus ?
? ?
? ?
? ?
? ? ? ? ? ? 1 1 1 1 1 1 0 0 1 1 1 1 ? ? ? ? ? ? ? ? ? ? ? ? ?
? ?

Neopterygii ?
? ?
? ?
? ?
? ? ? ? ? ? ? 1 1 1 1 1 1 0 0 1 1 1 1 ? ? ? ? ? ? ? ? ? ? ? ? ?
? ?
?

Powichthys ?
? ?
? ?
? ?
? 0 0 1 0 0 0 0 0 0 0 0 0
0 0 0 1 0 0 0 0 0 0 0 0 0 0 0 0 0 0 0 0 0 0 ? ? ? ? ? ? ? ? ?
?

Youngolepis ?
? ?
? ?
? ?
? 0 0 1 1 0 0 0 0 0 0 0 0
0 0 0 1 1 0 0 0 0 0 0 0 0 0 0 0 0 0 0 0 0 0 ? ? ? ? ? ? ? ? ?
?

Diabolepis ?
? ?
? ?
? ?
? 0 0 1 1 1 0 0 0 0 0 0 0
0 0 0 1 1 1 0 0 0 0 0 0 0 0 0 0 0 0 0 0 0 0 ? ? ? ? ? ? ? ? ?
?

Dipnorhynchus ?
? ?
? ?
? ?
? 0 0 1 1 1 1 0 0 0 0 0 0
0 0 0 0 1 1 1 1 1 1 0 0 0 0 0 0 0 0 0 0 0 0 0 ? ? ? ? ? ? ? ? ?
? ?

Uranolophus ?
? ?
? ?

Table A2.1, continued. The matrix representation matrix used for supertree generation.

? ?
? ? ? ? ? ? ? ? ? ? ? ? ? ? ? ? ? ? ? 0 0 1 1 1 1 1 0 0 0 0 0 0
0 0 0 1 1 1 1 1 0 0 0 0 0 0 0 0 0 0 0 0 0 0 ? ? ? ? ? ? ? ? ? ?
?

Stomiahykus ?
? ?
? ?
? ?
? ? ? ? ? ? ? ? ? ? ? ? ? ? ? ? ? ? ? 0 0 1 1 1 1 1 0 0 0 0 0 0
0 0 0 ?
?

Chirodipterus1 ?
? ?
? ?
? ?
? 0 0 1 1 1 1 1 1 1 0 0 0
0 0 0 0 ?
? ?

Gogodipterus ?
? ?
? ?
? ?
? 0 0 1 1 1 1 1 1 1 0 0 0
0 0 0 ?
?

Pillararhynchus ?
? ?
? ?
? ?
? 0 0 1 1 1 1 1 1 0 1 0 0
0 0 0 0 ?
? ?

Sorbitorhynchus ?
? ?
? ?
? ?
? 0 0 1 1 1 1 1 1 0 1 1 0
0 0 0 0 ?
? ?

Dipterus ?
? ?
? ?
? ?
? 0 0 1 1 1 1 1 1 0 1 1 1 0 0
0 0 1 1 1 1 0 0 0 0 0 0 0 0 0 0 0 0 0 0 0 0 ? ? ? ? ? ? ? ? ? ?

Orlovichthys ?
? ?
? ?
? ?
? 0 0 1 1 1 1 1 1 0 1 1 1 1
0 0 0 ?
?

Table A2.1, continued. The matrix representation matrix used for supertree generation.

Chirodipterus2 ?
? ?
? ?
? ?
? 0 0 1 1 1 1 1 1 0 1 1 1
1 0 0 0 ?
? ?
Holodipterus ?
? ?
? ?
? ?
? ? ? ? ? ? ? ? ? ? ? ? ? ? ? ? ? ? ? 0 0 1 1 1 1 1 1 0 1 1 1 1
1 0 0 ?
?
Griphognathus1 ?
? ?
? ?
? ?
? 0 0 1 1 1 1 1 1 0 1 1 1
1 1 1 0 ?
? ?
Griphognathus2 ?
? ?
? ?
? ?
? 0 0 1 1 1 1 1 1 0 1 1 1
1 1 1 1 ?
? ?
Soederberghia ?
? ?
? ?
? ?
? 0 0 1 1 1 1 1 1 0 1 1 1
1 1 1 1 ?
? ?
Speonesydrion ?
? ?
? ?
? ?
? ?
? ? ? ? 1 1 1 1 1 1 0 0 0 0 0 0 0 0 0 0 0 0 0 0 ? ? ? ? ? ? ? ?
? ?
Holoptychius ?
? ?
? ?
? ?
? ?
? ? ? 0 0 0 0 0 0 0 0 0 0 1 1 0 0 0 0 0 0 0 0 ? ? ? ? ? ? ? ? ?
?
Strunius ?
? ?
? ?

Table A2.1, continued. The matrix representation matrix used for supertree generation.

? ?
? ?
? ? 0 0 0 0 0 0 1 1 0 0 0 0 0 0 0 0 0 0 0 0 ? ? ? ? ? ? ? ? ? ?
Barameda ?
? ?
? ?
? ?
? ?
? ? 0 0 0 0 0 0 0 0 0 0 0 0 1 1 0 0 0 0 0 0 ? ? ? ? ? ? ? ? ? ?
Strepsodus ?
? ?
? ?
? ?
? ?
? ? ? 0 0 0 0 0 0 0 0 0 0 0 0 1 1 0 0 0 0 0 0 ? ? ? ? ? ? ? ? ?
?
Osteolepis ?
? ?
? ?
? ?
? ?
? ? 0 0 0 0 0 0 0 0 0 0 0 0 1 0 1 1 0 0 0 0 ? ? ? ? ? ? ? ? ? ?
Gyroptychius ?
? ?
? ?
? ?
? ?
? ? ? 0 0 0 0 0 0 0 0 0 0 0 0 1 0 1 1 0 0 0 0 ? ? ? ? ? ? ? ? ?
?
Beelarongia ?
? ?
? ?
? ?
? ?
? ? ? 0 0 0 0 0 0 0 0 0 0 0 0 1 0 1 1 0 0 0 0 ? ? ? ? ? ? ? ? ?
?
Elpistostege ?
? ?
? ?
? ?
? ?
? ? ? 0 0 0 0 0 0 0 0 0 0 0 0 1 0 1 0 1 1 0 0 ? ? ? ? ? ? ? ? ?
?
Panderichthys ?
? ?
? ?
? ?
? ?
? ? ? ? 0 0 0 0 0 0 0 0 0 0 0 0 1 0 1 0 1 1 0 0 ? ? ? ? ? ? ? ?
? ?
Crassigyrinus ?
? ?

Table A2.1, continued. The matrix representation matrix used for supertree generation.

```
? ? ? ? ? ? ? ? ? ? ? ? ? ? ? ? ? ? ? ? ? ? ? ? ? ? ? ? ? ? ? ?
? ? ? ? ? ? ? ? ? ? ? ? ? ? ? ? ? ? ? ? ? ? ? ? ? ? ? ? ? ? ? ?
? ? ? ? ? ? ? ? ? ? ? ? ? ? ? ? ? ? ? ? ? ? ? ? ? ? ? ? ? ? ? ?
? ? ? 0 0 0 0 0 0 0 0 0 0 0 0 1 0 1 0 1 0 1 0 ? ? ? ? ? ? ? ? ?
?
Ventastega ? ? ? ? ? ? ? ? ? ? ? ? ? ? ? ? ? ? ? ? ? ? ? ? ? ? ? ? ?
? ? ? ? ? ? ? ? ? ? ? ? ? ? ? ? ? ? ? ? ? ? ? ? ? ? ? ? ? ? ? ?
? ? ? ? ? ? ? ? ? ? ? ? ? ? ? ? ? ? ? ? ? ? ? ? ? ? ? ? ? ? ? ?
? ? ? ? ? ? ? ? ? ? ? ? ? ? ? ? ? ? ? ? ? ? ? ? ? ? ? ? ? ? ? ?
? ? ? ? ? ? ? ? ? ? ? ? ? ? ? ? ? ? ? ? ? ? ? ? ? ? ? ? ? ? ? ?
? ? ? 0 0 0 0 0 0 0 0 0 0 0 0 1 0 1 0 1 0 1 1 ? ? ? ? ? ? ? ? ?
?
Acanthostega ? ? ? ? ? ? ? ? ? ? ? ? ? ? ? ? ? ? ? ? ? ? ? ? ? ? ? ? ?
? ? ? ? ? ? ? ? ? ? ? ? ? ? ? ? ? ? ? ? ? ? ? ? ? ? ? ? ? ? ? ?
? ? ? ? ? ? ? ? ? ? ? ? ? ? ? ? ? ? ? ? ? ? ? ? ? ? ? ? ? ? ? ?
? ? ? ? ? ? ? ? ? ? ? ? ? ? ? ? ? ? ? ? ? ? ? ? ? ? ? ? ? ? ? ?
? ? ? ? ? ? ? ? ? ? ? ? ? ? ? ? ? ? ? ? ? ? ? ? ? ? ? ? ? ? ? ?
? ? ? 0 0 0 0 0 0 0 0 0 0 0 0 1 0 1 0 1 0 1 1 ? ? ? ? ? ? ? ? ?
?
Ichthyostega ? ? ? ? ? ? ? ? ? ? ? ? ? ? ? ? ? ? ? ? ? ? ? ? ? ? ? ? ?
? ? ? ? ? ? ? ? ? ? ? ? ? ? ? ? ? ? ? ? ? ? ? ? ? ? ? ? ? ? ? ?
? ? ? ? ? ? ? ? ? ? ? ? ? ? ? ? ? ? ? ? ? ? ? ? ? ? ? ? ? ? ? ?
? ? ? ? ? ? ? ? ? ? ? ? ? ? ? ? ? ? ? ? ? ? ? ? ? ? ? ? ? ? ? ?
? ? ? ? ? ? ? ? ? ? ? ? ? ? ? ? ? ? ? ? ? ? ? ? ? ? ? ? ? ? ? ?
? ? ? 0 0 0 0 0 0 0 0 0 0 0 0 1 0 1 0 1 0 1 1 ? ? ? ? ? ? ? ? ?
?
Sagenodus ? ? ? ? ? ? ? ? ? ? ? ? ? ? ? ? ? ? ? ? ? ? ? ? ? ? ? ? ?
? ? ? ? ? ? ? ? ? ? ? ? ? ? ? ? ? ? ? ? ? ? ? ? ? ? ? ? ? ? ? ?
? ? ? ? ? ? ? ? ? ? ? ? ? ? ? ? ? ? ? ? ? ? ? ? ? ? ? ? ? ? ? ?
? ? ? ? ? ? ? ? ? ? ? ? ? ? ? ? ? ? ? ? ? ? ? ? ? ? ? ? ? ? ? ?
? ? ? ? ? ? ? ? ? ? ? ? ? ? ? ? ? ? ? ? ? ? ? ? ? ? ? ? ? ? ? ?
? ? ? ? ? ? ? ? ? ? ? ? ? ? ? ? ? ? ? ? ? ? ? 0 0 0 0 0 0 0 0 0
0
Gnathorhiza 1 1 0 1 1 0 0 0 0 0 0 0 0 0 0 0 0 0 0 ? ? ? ? ? ? ? ? ? ?
? ? ? ? ? ? ? ? ? ? ? ? ? ? ? ? ? ? ? ? ? ? ? ? ? ? ? ? ? ? ? ?
? ? ? ? ? ? ? ? ? ? ? ? ? ? ? ? ? ? ? ? ? ? ? ? ? ? ? ? ? ? ? ?
? ? ? ? ? ? ? ? ? ? ? ? ? ? ? ? ? ? ? ? ? ? ? ? ? ? ? ? ? ? ? ?
? ? ? ? ? ? ? ? ? ? ? ? ? ? ? ? ? ? ? ? ? ? ? ? ? ? ? ? ? ? ? ?
? ? ? ? ? ? ? ? ? ? ? ? ? ? ? ? ? ? ? ? ? ? ? 1 0 0 0 0 0 0 0 0
0
Beltanodus 1 1 0 1 1 0 0 0 0 0 0 0 0 0 0 0 0 0 0 ? ? ? ? ? ? ? ? ? ?
? ? ? ? ? ? ? ? ? ? ? ? ? ? ? ? ? ? ? ? ? ? ? ? ? ? ? ? ? ? ? ?
? ? ? ? ? ? ? ? ? ? ? ? ? ? ? ? ? ? ? ? ? ? ? ? ? ? ? ? ? ? ? ?
? ? ? ? ? ? ? ? ? ? ? ? ? ? ? ? ? ? ? ? ? ? ? ? ? ? ? ? ? ? ? ?
? ? ? ? ? ? ? ? ? ? ? ? ? ? ? ? ? ? ? ? ? ? ? ? ? ? ? ? ? ? ? ?
? ? ? ? ? ? ? ? ? ? ? ? ? ? ? ? ? ? ? ? ? ? ? 1 0 0 0 0 0 0 0 0
0
Microceratodus 1 1 0 1 0 1 0 1 1 0 0 0 1 0 0 0 0 0 0 ? ? ? ? ? ? ? ? ?
? ? ? ? ? ? ? ? ? ? ? ? ? ? ? ? ? ? ? ? ? ? ? ? ? ? ? ? ? ? ? ?
? ? ? ? ? ? ? ? ? ? ? ? ? ? ? ? ? ? ? ? ? ? ? ? ? ? ? ? ? ? ? ?
? ? ? ? ? ? ? ? ? ? ? ? ? ? ? ? ? ? ? ? ? ? ? ? ? ? ? ? ? ? ? ?
? ? ? ? ? ? ? ? ? ? ? ? ? ? ? ? ? ? ? ? ? ? ? ? ? ? ? ? ? ? ? ?
```

Table A2.1, continued. The matrix representation matrix used for supertree generation.

```
 ? ? ? ? ? ? ? ? ? ? ? ? ? ? ? ? ? ? ? ? ? ? ? ? 1 1 0 0 0 0 0 0
 0 0
Neoceratodus 1 1 0 1 0 1 0 1 0 0 0 0 0 1 1 1 1 1 0 ? ? ? ? ? ? ? ? ? ?
 ? ? ? ? ? ? ? ? ? ? ? ? ? ? ? ? ? ? ? ? ? ? ? ? ? ? ? ? ? ? ? ?
 ? ? ? ? ? ? ? ? ? ? ? ? ? ? ? ? ? ? ? ? ? ? ? ? ? ? ? ? ? ? ? ?
 ? ? ? ? ? ? ? ? ? ? ? ? ? ? ? ? ? ? ? ? ? ? ? ? ? ? ? ? ? ? ? ?
 ? ? ? ? ? ? ? ? ? ? ? ? ? ? ? ? ? ? ? ? ? ? ? ? ? ? ? ? ? ? ? ?
 ? ? ? ? ? ? ? ? ? ? ? ? ? ? ? ? ? ? ? ? ? ? ? 1 1 1 0 0 0 0 0 0
 0
Ferganoceratodus 1 1 0 1 0 1 1 0 0 0 0 0 0 0 0 0 0 0 0 ? ? ? ? ? ? ? ?
 ? ? ? ? ? ? ? ? ? ? ? ? ? ? ? ? ? ? ? ? ? ? ? ? ? ? ? ? ? ? ? ?
 ? ? ? ? ? ? ? ? ? ? ? ? ? ? ? ? ? ? ? ? ? ? ? ? ? ? ? ? ? ? ? ?
 ? ? ? ? ? ? ? ? ? ? ? ? ? ? ? ? ? ? ? ? ? ? ? ? ? ? ? ? ? ? ? ?
 ? ? ? ? ? ? ? ? ? ? ? ? ? ? ? ? ? ? ? ? ? ? ? ? ? ? ? ? ? ? ? ?
 ? ? ? ? ? ? ? ? ? ? ? ? ? ? ? ? ? ? ? ? ? ? ? ? ? 1 1 1 1 0 0 0
 0 0 0
Ceratodus 1 1 0 1 0 1 0 1 1 1 1 0 0 0 0 0 0 0 0 ? ? ? ? ? ? ? ? ? ? ?
 ? ? ? ? ? ? ? ? ? ? ? ? ? ? ? ? ? ? ? ? ? ? ? ? ? ? ? ? ? ? ? ?
 ? ? ? ? ? ? ? ? ? ? ? ? ? ? ? ? ? ? ? ? ? ? ? ? ? ? ? ? ? ? ? ?
 ? ? ? ? ? ? ? ? ? ? ? ? ? ? ? ? ? ? ? ? ? ? ? ? ? ? ? ? ? ? ? ?
 ? ? ? ? ? ? ? ? ? ? ? ? ? ? ? ? ? ? ? ? ? ? ? ? ? ? ? ? ? ? ? ?
 ? ? ? ? ? ? ? ? ? ? ? ? ? ? ? ? ? ? ? ? ? ? 1 1 1 1 1 0 0 0 0 0
Paraceratodus 1 0 0 0 0 0 0 0 0 0 0 0 0 0 0 0 0 0 0 ? ? ? ? ? ? ? ? ?
 ? ? ? ? ? ? ? ? ? ? ? ? ? ? ? ? ? ? ? ? ? ? ? ? ? ? ? ? ? ? ? ?
 ? ? ? ? ? ? ? ? ? ? ? ? ? ? ? ? ? ? ? ? ? ? ? ? ? ? ? ? ? ? ? ?
 ? ? ? ? ? ? ? ? ? ? ? ? ? ? ? ? ? ? ? ? ? ? ? ? ? ? ? ? ? ? ? ?
 ? ? ? ? ? ? ? ? ? ? ? ? ? ? ? ? ? ? ? ? ? ? ? ? ? ? ? ? ? ? ? ?
 ? ? ? ? ? ? ? ? ? ? ? ? ? ? ? ? ? ? ? ? ? ? ? ? 1 1 1 1 1 1 0 0
 0 0
Asiatoceratodus 1 1 0 1 0 1 0 1 0 0 0 0 0 1 1 0 0 0 0 ? ? ? ? ? ? ? ? ?
 ? ? ? ? ? ? ? ? ? ? ? ? ? ? ? ? ? ? ? ? ? ? ? ? ? ? ? ? ? ? ? ?
 ? ? ? ? ? ? ? ? ? ? ? ? ? ? ? ? ? ? ? ? ? ? ? ? ? ? ? ? ? ? ? ?
 ? ? ? ? ? ? ? ? ? ? ? ? ? ? ? ? ? ? ? ? ? ? ? ? ? ? ? ? ? ? ? ?
 ? ? ? ? ? ? ? ? ? ? ? ? ? ? ? ? ? ? ? ? ? ? ? ? ? ? ? ? ? ? ? ?
 ? ? ? ? ? ? ? ? ? ? ? ? ? ? ? ? ? ? ? ? ? ? ? ? 1 1 1 1 1 1 0 0
 0 0
Ptychoceratodusp ? ? ? ? ? ? ? ? ? ? ? ? ? ? ? ? ? ? ? ? ? ? ? ? ? ? ?
 ? ? ? ? ? ? ? ? ? ? ? ? ? ? ? ? ? ? ? ? ? ? ? ? ? ? ? ? ? ? ? ?
 ? ? ? ? ? ? ? ? ? ? ? ? ? ? ? ? ? ? ? ? ? ? ? ? ? ? ? ? ? ? ? ?
 ? ? ? ? ? ? ? ? ? ? ? ? ? ? ? ? ? ? ? ? ? ? ? ? ? ? ? ? ? ? ? ?
 ? ? ? ? ? ? ? ? ? ? ? ? ? ? ? ? ? ? ? ? ? ? ? ? ? ? ? ? ? ? ? ?
 ? ? ? ? ? ? ? ? ? ? ? ? ? ? ? ? ? ? ? ? ? ? ? ? ? 1 1 1 1 1 0 1
 0 0 0
Arganodus 1 1 0 1 0 1 1 0 0 0 0 0 0 0 0 0 0 0 0 ? ? ? ? ? ? ? ? ? ?
 ? ? ? ? ? ? ? ? ? ? ? ? ? ? ? ? ? ? ? ? ? ? ? ? ? ? ? ? ? ? ? ?
 ? ? ? ? ? ? ? ? ? ? ? ? ? ? ? ? ? ? ? ? ? ? ? ? ? ? ? ? ? ? ? ?
 ? ? ? ? ? ? ? ? ? ? ? ? ? ? ? ? ? ? ? ? ? ? ? ? ? ? ? ? ? ? ? ?
 ? ? ? ? ? ? ? ? ? ? ? ? ? ? ? ? ? ? ? ? ? ? ? ? ? ? ? ? ? ? ? ?
 ? ? ? ? ? ? ? ? ? ? ? ? ? ? ? ? ? ? ? ? ? ? ? 1 1 1 1 1 0 1 1 0
 0
Ptychoceratodus 1 1 0 1 0 1 0 1 1 0 0 0 1 0 0 0 0 0 0 ? ? ? ? ? ? ? ? ?
 ? ? ? ? ? ? ? ? ? ? ? ? ? ? ? ? ? ? ? ? ? ? ? ? ? ? ? ? ? ? ? ?
```

Table A2.1, continued. The matrix representation matrix used for supertree generation.

? ?
? ?
? ?
? 1 1 1 1 1 0 1 1
1 1
Gosfordia 1 1 0 1 0 1 0 1 0 0 0 0 0 1 0 0 0 0 0 ? ? ? ? ? ? ? ? ? ? ?
? ?
? ?
? ?
? ?
? 1 1 1 1 1 0 1 1 1 1
Conchopoma 0 0 0 0 0 0 0 0 0 0 0 0 0 0 0 0 0 0 0 ? ? ? ? ? ? ? ? ? ?
? ?
? ?
? ?
? ?
? ?
?
Megapleuron 1 1 1 0 0 0 0 0 0 0 0 0 0 0 0 0 0 0 0 ? ? ? ? ? ? ? ? ? ?
? ?
? ?
? ?
? ?
? ?
?
Aphelodus 1 1 1 0 0 0 0 0 0 0 0 0 0 0 0 0 0 0 0 ? ? ? ? ? ? ? ? ? ? ?
? ?
? ?
? ?
? ?
? ?
Metaceratodus 1 1 0 1 0 1 0 1 1 1 1 0 0 0 0 0 0 0 0 ? ? ? ? ? ? ? ? ?
? ?
? ?
? ?
? ?
? ?
? ?
Namatozodia 1 1 0 1 0 1 0 1 1 1 0 1 0 0 0 0 0 0 0 ? ? ? ? ? ? ? ? ? ?
? ?
? ?
? ?
? ?
? ?
?
Ariguna 1 1 0 1 0 1 0 1 1 1 0 1 0 0 0 0 0 0 0 ? ? ? ? ? ? ? ? ? ? ?
? ?
? ?
? ?
? ?
? ?

Table A2.1, continued. The matrix representation matrix used for supertree generation.

Archaeoceratodus 1 1 0 1 0 1 0 1 0 0 0 0 0 1 1 1 0 0 0 ? ? ? ? ? ? ? ?
? ?
? ?
? ?
? ?
? ?
? ? ?
Mioceratodus 1 1 0 1 0 1 0 1 0 0 0 0 0 1 1 1 1 1 0 ? ? ? ? ? ? ? ? ? ?
? ?
? ?
? ?
? ?
? ?
?
Lepidosiren 1 1 0 1 0 1 0 1 0 0 0 0 0 1 1 1 1 0 1 ? ? ? ? ? ? ? ? ? ?
? ?
? ?
? ?
? ?
? ?
?

Appendix 3: Timescaling figures and tables

Table A3.1. Table of taxon age ranges and references for dates.

Taxon	First	Last	Source	Stage
Acanthodes	359	290	Davis et al. (2012)	Tournaisian - Sakmarian
Acanthostega	372	359	Clack (1988)	Famennian
Achoania	419	411	Zhu et al. (2001)	Lochkovian
Acipenser	83.6	0	Gardiner (1984b)	Campanian - Recent
Acrodus	252	83.6	Stensö (1921); Cappetta (1987)	Induan - Santonian
Akmonistion	330.9	323.2	Coates and Sequeira (2001b)	Serpukhovian
Allenypterus	331	323	Lund and Lund (1984)	Serpukhovian
Amblyraja	86.3	0	Cappetta (1987)	Santonian - Recent
Amia	59.2	0	Grande and Bemis (1998)	Thanetian - Recent
Aphelodus	252	247	Kemp (1993)	Induan - Olenekian
Archaeoceratodus	247	11.6	Kemp (1997a)	Anisian - Serravallian
Arganodus	252	100	Tabaste (1963); Kemp (1991)	Induan - Albian
Ariguna	252	247	Kemp (1994)	Induan - Olenekian
Asiatoceratodus	252	247	Vorobyeva (1967)	Induan - Olenekian
Asteracanthus	247	66	Rieppel (1981); Tabaste (1963)	Anisian - Maastrichtian
Australosomus	252	250	Nielson (1942)	Induan - Olenekian
Austroptyctodus	384	380	Long et al. (2015)	Frasnian
Axelrodichthys	126	86.3	De Carvalho and Maisey (2008)	Aptian - Coniacian
Barameda	359	347	Garvey et al. (2005)	Tournaisian
Beelarongia	383	372	Long (1987)	Frasnian
Belonostomus	168	56	Bryant (1987)	Bathonian - Thanetian
Beltanodus	252	247	Schultze (1981)	Induan - Olenekian
Birgeria	252	201	Stensiö (1921); Sigogneau-Russel and Hahn (1994)	Induan - Rhaetian
Boreosomus	252	237	Nielson (1942)	Induan - Ladinian
Bothriolepis	388	359	Young (1989); Denison (1978)	Givetian - Famennian
Brachyacanthus	419	411	Watson (1937)	Lochkovian
Brindabellaspis	410.8	407.6	Burrow et al. (2015)	Pragian
Brochoadmones	419	411	Hanke and Wilson (2006)	Lochkovian
Buchanosteus	408	393	Chapman (1916); Young (1979)	Lochkovian
Callorhinchus	170	0	Brown (1946)	Bajocian - Recent
Campbellodus	384	380	Long (1997)	Frasnian
Caridosuctor	331	323	Lund and Lund (1984)	Serpukhovian
Cassidiceps	419	411	Gagnier and Wilson (1996)	Lockhovian
Caturus	200	125	Schaeffer and Patterson (1984)	Rhaetian - Barremian

Table A3.1, continued. Table of taxon age ranges and references for dates.

Ceratodus	252	23	Schultze (2004)	Induan - Chattian
Cheiracanthus	408	359	Trinajstic (2001); Traquair (1893)	Emsian - Frasnian
Cheirolepis	398	372	Arratia et al. (2004)	Eifelian - Frasnian
Chimaera	56	0	Ward (1973)	Ypresian - Recent
Chinlea	228	209	Elliott (1987)	Norian
Chirodipterus	385	374	Gross (1933)	Late Frasnian
Chondrenchelys	347	331	Coates and Finarelli (2014)	Visean/Holkerian
Cladodoides	385	374	Maisey (2005)	Late Frasnian
Cladoselache	374	359	Maisey (2007)	Famennian
Climatius	419	411	Burrow et al. (2015)	Lochkovian
Cobelodus	313	304	Zangerl and Case (1976)	Westphalian
Coccoderma	152	139	Cloutier and Forey (1991)	Tithonian - Berriasian
Coccosteus	393	383	Miller (1841); Denison (1978)	Eifelian - Givetian
Coelacanthus	279	250	Cloutier and Forey (1991)	Kungurian - Induan
Compagopiscis	384	380	Gardiner and Miles (1994)	Frasnian
Conchopoma	315	290	Denison (1969)	Moscovian - Sakmarian
Cowralepis	385	377.5	Ritchie (2005)	Late Givetian - Early Fransian
Crassigyrinus	347	323	Panchen (1985)	Visean - Serpukhovian
Ctenurella	384	380	Miles and Young (1977)	Frasnian
Culmacanthus	393	372	Long (1983); Burrow and Young (2012)	Eifelian - Fransian
Cyprinus	41	0	Liu (1957)	Bartonian - Recent
Dapedium	209	174	Woodward (1895)	Rhaetian - Toarcian
Debeerius	331	323	Grogan and Lund (2000)	Serpukhovian
Diabolepis	411	408	Chang (1984)	Pragian
Dialipina	416	414	Schultze and Cumbaa (2001); Basden & Young (2001)	Lochkovian
Dicksonosteus	411	407	Goujet (1975)	Siegenian/ragian
Diplacanthus	393	372	Luksevics et al. (2010); Woodward (1891)	Frasnian
Diplocercides	383	331	Cloutier and Forey (1991)	Frasnian - Visean
Diplurus	237	199	Cloutier and Forey (1991)	Carnian - Hettangian
Dipnorhynchus	408	393	Clack et al. (2011)	Emsian
Dipterus	393	359	Eastman (1907)	Eifelian - Famennian
Discoserra	331	323	Lund (2000)	Serpukhovian
Doliodus	408	400.5	Miller et al. (2003)	Early Emsian
Eastmanosteus	393	372	Dennis-Bryan (1987); Hanke et al. (2001)	Eifelian - Frasnian
Egertonodus	145	110	Egerton (1845); Maisey (1983)	Berriasian - Albian
Elops	0	0	Nelson (2006)	Recent
Elpistostege	383	372	Schultze and Arsenault (1985)	Frasnian
Entelognathus	426	423	Zhu et al. (2013)	Ludlow

Table A3.1, continued. Table of taxon age ranges and references for dates.

Eurycaraspis	388	383	Liu (1991)	Givetian
Eusthenopteron	388	372	Zupins (2008)	Givetian - Frasnian
Euthacanthus	419	411	Powrie (1864); Paton (1976)	Lochkovian
Falcatus	331	323	Lund (1985)	Serpukhovian
Ferganoceratodus	174	134	Cavin et al. (2007)	Aalenian - Valanginian
Galeaspida	439	372	Janvier (1996)	Telychian - Givetian
Garnbergia	241	237	Martin and Wenz (1984)	Ladinian
Gavinia	383	372	Long (1999)	Frasnian
Gemuendina	408	393	Gross (1963)	Emsian
Gladiobranchus	419	411	Hanke and Davis (2008)	Lochkovian
Glyptolepis	393	372	Cloutier and Ahlberg (1996)	Eifelian - Frasnian
Gnathorhiza	299	247	Berman (1976); Minikh (1977)	Asselian - Olenekian
Gogodipterus	384	380	Long (1992)	Frasnian
Gogonasus	384	380	Long et al. (2006)	Frasnian
Gosfordia	252	247	Ritchie (1981)	Induan - Olenekian
Griphognathus	388	380	Schultze (1969); Miles (1977)	Givetian - Frasnian
Groenlandaspis	388	359	Janvier and Ritchie (1977); Long (1995)	Givetian - Famennian
Guiyu	426	423	Zhu et al. (2009)	Late Ludlow
Gyracanthides	408	331	Anderson et al. (1999); Turner et al. (2005)	Emsian - Visean
Gyroptychius	393	383	Newman et al. (2015)	Eifelian - Givetian
Hadronector	331	323	Lund and Lund (1984)	Serpukhovian
Hamiltonichthys	305	299	Maisey (1989)	Late Virgilian
Harpacanthus	331	323	Traquair (1886)	Serpukhovian
Harpagofututor	331	323	Lund (1982)	Serpukhovian
Harriotta	86.3	0	Werdelin (1986)	Santonian - Recent
Helodus	359	323	Moy-Thomas (1936); Stahl (1999)	Tournaisian - Serpukhovian
Heterodontus	174	0	Thies (1983)	Aalenian - Recent
Hiodon	41.2	0	Li and Wilson (1994)	Bartonian - Recent
Holodipterus	384	380	Miles (1977)	Frasnian
Holonema	384	380	Miles (1971)	Frasnian
Holophagus	201	199	Woodward (1890)	Hettangian -
Holopterygius	384	382	Friedman and Coates (2006)	Givetian - Frasnian
Holoptychius	383	347	Blom et al. (2007)	Frasnian - Tournaisian
Homalacanthus	383	372	Gagnier (1996)	Frasnian
Hopleacanthus	260	252	Schaumberg (1982)	Wuchiapingian - Changhsingian
Howidipterus	383	372	Long and Clement (2009)	Frasnian
Howqualepis	383	372	Long (1988)	Frasnian
Hulettia	168	164	Schaeffer and Patterson (1984)	Bathonian - Callovian

Table A3.1, continued. Table of taxon age ranges and references for dates.

Hybodus	247	66	(1987)	Anisian - Maastrichtian
Hydrolagus	0	0	Dean (1906)	Recent
Ichthyostega	372	359	Blom (2005)	Famennian
Incisoscutum	384	380	Dennis and Miles (1981)	Frasnian
Iniopera	313	299	Zangerl and Case (1973); Pradel et al. (2010)	Westphalian - Virgilian
Ionoscopus	164	100	Grande and Bemis (1998)	Oxfordian - Albian
Ischnacanthus	419	411	Watson (1937)	Lochkovian
Jagorina	385	374	Jaekel (1921)	Late Frasnian
Janusiscus	416	414	Giles et al. (2015)	Lochkovian
Kathemacanthus	419	411	Gagnier and Wilson (1996)	Lochkovian
Kawichthys	305	299	Pradel et al. (2011)	Late Virgilian
Kenichthys	408	393	Zhu and Ahlberg (2004)	Emsian
Kentuckia	359	347	Rayner (1952)	Tournaisian
Kujdanowiaspis	419	408	Dupret (2010)	Lochkovian - Pragian
Latimeria	0	0	Smith (1953)	Recent
Latviacanthus	419	393	Schultze and Zidek (1982)	Lochkovian - Emsian
Laugia	252	247	Stensiö (1932)	Induan - Olenekian
Lepidosiren	72.1	0	Schultze (1991)	Maastrichtian - Recent
Lepisosteus	120	0	Cavin (2010)	Aptian - Recent
Leptolepis	247	139	Woodward (1895)	Anisian - Berriasian
Libys	152	145	Munster (1842)	Tithonian
Ligulalepis	411	393	Basden and Young (2001)	Pragian - Emsian
Lissodus	252	100	Rees and Underwood (2002)	Induan - Albian
Lochmocercus	331	323	Lund and Lund (1984)	Serpukhovian
Lonchidion	241	66	Rees and Underwood (2002)	Ladinian - Maastrichtian
Lophosteus	427	408	Schultze and Märss (2004)	Ludlow - Pragian
Lunaspis	408	393	Macadie (2007)	Emsian
Lupopsyrus	419	411	Bernacsek & Dineley (1977); Hanke and Davis (2012)	Lochkovian
Macropetalichthys	408	383	Woodward (1941)	Emsian - Givetian
Macropoma	113	83.6	Cloutier and Forey (1991)	Albian - Santonian
Materpiscis	384	380	Long et al. (2008)	Frasnian
Mawsonia	145	93.9	De Carvalho and Maisey (2008)	Berriasian - Cenomanian
Meemannia	419	411	Zhu et al. (2009)	Lochkovian
Megapleuron	315	295	Schultze (1977)	Moscovian - Autunian
Mesacanthus	419	411	Watson (1937)	Lochkovian
Mesopoma	347	307	Coates (1999)	Visean - Moscovian
Metaceratodus	72.1	0.01	Kemp (1997b)	Maastrichtian - Pleistocene
Microbrachius	408	383	Traquair (1888); Wang and Zhang (1999)	Emsian - Givetian

Table A3.1, continued. Table of taxon age ranges and references for dates.

Microceratodus	252	247	Schultze (1981)	Early Triassic
Miguashaia	388	372	Schultze (1973); Forey et al. (2000);	Givetian - Frasnian
Mimipiscis	384	380	Choo (2011)	Frasnian
Mioceratodus	47.8	2.6	Kemp (1991); Kemp (1998)	Middle Eocene - Pliocene
Moythomasia	388	372	Gardiner (1984a); Choo (2015)	Frasnian
Mustelus	56	0	Cappetta (1976)	Ypresian - Recent
Namatozodia	252	247	Kemp (1993)	Induan - Olenekian
Neoceratodus	126	0	Kemp (1997a)	Aptian - Recent
Notorynchus	126	0	Cappetta (1975)	Aptian - Recent
Obtusacanthus	419	411	Hanke and Wilson (2004)	Lockhovian
Okamejei	0	0	Nelson (2006)	Recent
Onychodus	393	359	Newberry (1857)	Eifelian - Famennian
Onychoselache	347	331	Dick and Maisey (1980)	Visean
Orlovichthys	372	359	Krupina et al. (2001)	Famennian
Orthacanthus	323	273	Zangerl (1981)	Upper Carboniferous - Lower Permian
Osorioichthys	372	259	Taverne (1997)	Famennian
Osteolepis	388	383	Thomson (1965)	Givetian
Osteostraci	433	372	Janvier (1996)	Wenlock - Frasnian
Pachycormus	183	174	Arratia and Schultze (2013)	Toarcian
Palaeobates	250	201	Romano and Brinkmann (2010)	Olenekian - Rhaetian
Panderichthys	388	383	Ahlberg et al. (1996)	Givetian - Frasnian
Parabuchanosteus	408	393	White and Toombs (1972)	Emsian
Paraceratodus	252	247	Martin (1981); Schultze (1981)	Induan - Olenekian
Parayunnanolepis	419	411	Zhu et al. (2012)	Lochkovian
Parexus	419	411	Watson (1937); Miles (1973)	Lochkovian
Perleidus	247	237	Lombardo et al. (2011)	Anisian - Ladinian
Phanerosteon	359	331	Moy-Thomas and Miles (1971); Smithson et al. (2012)	Tournaisian - Visean
Pholidophorus	247	126	Woodward (1890)	Anisian - Barremian
Pillararhynchus	384	380	Barwick and Campbell (1996)	Frasnian
Plesiobatis	0	0	Nelson (2006)	Recent
Plourdosteus	383	372	Cloutier et al. (1996)	Frasnian
Polymixia	0	0	Farias et al. (2008)	Recent
Polyosteorhynchus	331	323	Lund and Lund (1984)	Serpukhovian
Polypterus	7.2	0	Otero et al. (2006)	Messinian - Recent
Poracanthodes	419	411	Valiukevičius (1992)	Lochkovian
Porolepis	411	383	Gross (1936)	Pragian - Givetian
Powichthys	419	408	Cloutier and Ahlberg (1996)	Lochkovian - Pragian
Promesacanthus	419	411	Hanke (2008)	Lochkovian

Table A3.1, continued. Table of taxon age ranges and references for dates.

Protopterus	100	0	Werner (1994)	Cenomanian - Recent
Psarolepis	419	393	Yu (1998); Zhu et al. (1999)	Lochkovian - Emsian
Pterichthyodes	408	383	Young (1974); Hemmings (1978)	Emisan - Givetian
Pteronisculus	252	237	Schaeffer and Mangus (1976)	Induan - Ladinian
Ptomacanthus	418	412	Brazeau (2009)	Lochkovian
Ptychoceratodus	252	237	Schultze (1981); Kemp (1996)	Induan - Ladinian
Pucapampella	408	383	Maisey (2001); Maisey and Anderson (2001)	Emsian - Givetian
Ramirosuarezia	393	388	Pradel et al. (2009)	Eifelian
Remigolepis	383	359	Young (1974); Alekseev et al. (1994)	Frasnian - Famennian
Rhabdoderma	347	299	Cloutier and Forey (1991)	Visean - Gzhelian
Rhadinacanthus	393	383	Miles (1973)	Emsian - Givetian
Rhamphodopsis	393	383	Watson (1934); Miles (1967)	Eifelian - Givetian
Rhinochimaera	0	0	Didier (1995)	Recent
Romundina	419	410	Dupret et al. (2014)	Lochkovian
Sagenodus	359	272	Schultze and Chorn (1997); Carpenter et al. (2014)	Tournaisian - Kungurian
Sassenia	250	247	Stensiö (1921)	Olenekian
Saurichthys	252	181	Maxwell et al. (2015)	Induan - Toarcian
Scyliorhinus	100	0	Underwood and Ward (2008)	Cenomanian - Recent
Semionotus	247	183	McCune (1996)	Anisian - Pliensbachian
Serenichthys	372	359	Gess and Coates (2015)	Famennian
Soederberghia	388	359	Schultze (1992); Ahlberg et al. (2001); Schultze (2010)	Givetian - Famennian
Sorbitorhynchus	408	393	Clack et al. (2011)	Emsian
Speonesydrion	408	393	Campbell and Barwick (1984)	Emsian
Spermatodus	299	272	Cope (1894)	Lower Permian
Squaloraja	199	191	Agassiz (1836)	Sinemurian
Squalus	83.6	0	Cappetta (1987)	Campanian - Recent
Stomiahykus	393	388	Bernacsek (1977)	Eifelian
Strepsodus	372	323	Janvier et al. (1984); Johanson et al. (2000)	Famennian - Serpukhovian
Strunius	383	359	Upeniece (1995); Lebedev (1995)	Frasnian - Famennian
Styloichthys	419	411	Zhu and Yu (2002); Friedman (2007b)	Lochkovian
Synechodus	247	56	Yamagushi (2004); Casier (1943)	Tithonian - Thanetian
Tamiobatis	372	347	Schaeffer (1981); Williams (1998)	Famennian - Tournaisian
Tarrasius	359	318	Sallan (2012)	Tournaisian - Bashkirian
Tetanopsyrus	419	411	Hanke et al. (2001)	Lochkovian
Tetraodon	7.2	0	Stewart (2003)	Messinian - Recent
Tribodus	113	93.9	Lane and Maisey (2012)	Albian - Cenomanian
Tristychius	347	331	Dick (1978); Coates and Gess (2007)	Visean

Table A3.1, continued. Table of taxon age ranges and references for dates.

Undina	241	145	Cloutier and Forey (1991)	Ladinian - Tithonian
Uranolophus	411	408	Denison (1968)	Pragian
Ventastega	372	359	Ahlberg et al. (2008)	Famennian
Vernicomacanthus	419	411	Powrie (1864); Miles (Miles, 1973); Paton (1976)	Lochkovian
Watsonulus	252	247	Grande and Bemis (1998)	Induan - Olenekian
Whiteia	252	247	Moy-Thomas (1935)	Induan - Olenekian
Wuttagoonaspis	393	388	Ritchie (1973)	Eifelian
Youngolepis	411	408	Zhu and Fan (1995)	Pragian
Yunnanolepis	419	411	Wang et al. (2010)	Lochkovian

Table A3.2. Geologic interval times in millions of years.

	start_time	end_time			
Telychian	439	433	Aalenian	174	170
Wenlock	433	427	Bajocian	170	168
Ludlow	427	423	Bathonian	168	166
Pridoli	423	419	Callovian	166	164
Lochkovian	419	411	Oxfordian	164	157
Pragian	411	408	Kimmeridgian	157	152
Emsian	408	393	Tithonian	152	145
Eifelian	393	388	Berriasian	145	139
Givetian	388	383	Valanginian	139	134
Gogo	384	380	Hauterivian	134	131
Frasnian	383	372	Barremian	131	126
Famennian	372	359	Aptian	126	113
Tournaisian	359	347	Albian	113	100
Visean	347	331	Cenomanian	100	93.9
Serpukhovian	331	323	Turonian	93.9	89.8
Bashkirian	323	315	Coniacian	89.8	86.3
Moscovian	315	307	Santonian	86.3	83.6
Kasimovian	307	304	Campanian	83.6	72.1
Gzhelian	304	299	Maastrichtian	72.1	66
Asselian	299	296	Danian	66	61.1
Sakmarian	296	290	Selandian	61.1	59.2
Artinskian	290	279	Thanetian	59.2	56
Kungurian	279	272	Ypresian	56	47.8
Roadian	272	269	Lutetian	47.8	41.2
Wordian	269	265	Bartonian	41.2	37.8
Capitanian	265	260	Priabonian	37.8	33.9
Wuchiapingian	260	254	Rupelian	33.9	28.1
Changhsingian	254	252	Chattian	28.1	23
Induan	252	250	Aquitanian	23	20.4
Olenekian	250	247	Burdigalian	20.4	16
Anisian	247	241	Langhian	16	13.8
Ladinian	241	237	Serravallian	13.8	11.6
Carnian	237	228	Tortonian	11.6	7.2
Norian	228	209	Messinian	7.2	5.3
Rhaetian	209	201	Zanglean	5.3	3.6
Hettangian	201	199	Piacenzian	3.6	2.6
Sinemurian	199	191	Gelasian	2.6	1.8
Pliensbachian	191	183	Calabrian	1.8	0.01
Toarcian	183	174	Holocene	0.01	0

Table A3.3. Geologic intervals for which each taxon is present.

	first_int	last_int			
Acanthodes	13	21	*Chinlea*	34	34
Acanthostega	12	12	*Chirodipterus*	11	11
Achoania	5	5	*Chondrenchelys*	14	14
Acipenser	57	78	*Cladodoides*	11	11
Acrodus	29	56	*Cladoselache*	12	12
Akmonistion	15	15	*Climatius*	5	5
Allenypterus	15	15	*Cobelodus*	17	17
Amblyraja	56	78	*Coccoderma*	46	47
Amia	61	78	*Coccosteus*	8	9
Aphelodus	29	30	*Coelacanthus*	23	29
Archaeoceratodus	31	71	*Compagopiscis*	10	10
Arganodus	29	52	*Conchopoma*	17	21
Ariguna	29	29	*Cowralepis*	9	11
Asiatoceratodus	29	30	*Crassigyrinus*	14	15
Asteracanthus	31	58	*Ctenurella*	11	11
Australosomus	29	30	*Culmacanthus*	8	11
Austroptyctodus	10	10	*Cyprinus*	64	78
Axelrodichthys	51	55	*Dapedium*	35	39
Barameda	13	13	*Debeerius*	15	15
Beelarongia	11	11	*Diabolepis*	6	6
Belonostomus	42	61	*Dialipina*	5	5
Beltanodus	28	30	*Dicksonosteus*	6	6
Birgeria	29	35	*Diplacanthus*	11	11
Boreosomus	29	32	*Diplocercides*	11	14
Bothriolepis	9	12	*Diplurus*	33	36
Brachyacanthus	5	5	*Dipnorhynchus*	7	7
Brindabellaspis	6	6	*Dipterus*	8	12
Brochoadmones	5	5	*Discoserra*	15	15
Buchanosteus	5	5	*Doliodus*	7	7
Callorhinchus	41	78	*Eastmanosteus*	8	11
Campbellodus	10	10	*Egertonodus*	47	52
Caridosuctor	15	15	*Elops*	78	78
Cassidiceps	5	5	*Elpistostege*	11	11
Caturus	35	50	*Entelognathus*	3	3
Ceratodus	28	67	*Eurycaraspis*	9	9
Cheiracanthus	7	10	*Eusthenopteron*	9	11
Cheirolepis	8	11	*Euthacanthus*	5	5
Chimaera	62	78	*Falcatus*	15	15
			Ferganoceratodus	40	48

Table A3.3, continued. Geologic intervals for which each taxon is present.

Galeaspida	1	9	*Jagorina*	10	10
Garnbergia	32	32	*Janusiscus*	5	5
Gavinia	11	11	*Kathemacanthus*	5	5
Gemuendina	7	7	*Kawichthys*	19	19
Gladiobranchus	5	5	*Kenichthys*	7	7
Glyptolepis	8	11	*Kentuckia*	13	13
Gnathorhiza	20	30	*Kujdanowiaspis*	5	6
Gogodipterus	10	10	*Latimeria*	78	78
Gogonasus	10	10	*Latviacanthus*	5	7
Gosfordia	29	30	*Laugia*	29	30
Griphognathus	9	11	*Lepidosiren*	58	78
Groenlandaspis	9	12	*Lepisosteus*	51	78
Guiyu	3	3	*Leptolepis*	31	47
Gyracanthides	7	14	*Libys*	46	46
Gyroptychius	8	9	*Ligulalepis*	6	7
Hadronector	15	15	*Lissodus*	29	52
Hamiltonichthys	19	19	*Lochmocercus*	15	15
Harpacanthus	15	15	*Lonchidion*	32	58
Harpagofututor	15	15	*Lophosteus*	3	6
Harriotta	56	78	*Lunaspis*	7	7
Helodus	13	15	*Lupopsyrus*	5	5
Heterodontus	40	78	*Macropetalichthys*	7	9
Hiodon	64	78	*Macropoma*	52	56
Holodipterus	10	10	*Materpiscis*	10	10
Holonema	10	10	*Mawsonia*	47	53
Holophagus	36	36	*Meemannia*	5	5
Holopterygius	9	11	*Megapleuron*	17	20
Holoptychius	11	13	*Mesacanthus*	5	5
Homalacanthus	11	11	*Mesopoma*	14	17
Hopleacanthus	27	28	*Metaceratodus*	58	77
Howidipterus	11	11	*Microbrachius*	7	9
Howqualepis	11	11	*Microceratodus*	29	30
Hulettia	42	43	*Miguashaia*	9	11
Hybodus	31	58	*Mimipiscis*	10	10
Hydrolagus	78	78	*Mioceratodus*	63	75
Ichthyostega	12	12	*Moythomasia*	10	10
Incisoscutum	10	10	*Mustelus*	62	78
Iniopera	16	18	*Namatozodia*	29	30
Ionoscopus	44	52	*Neoceratodus*	51	78
Ischnacanthus	5	5	*Notorynchus*	51	78

Table A3.3, continued. Geologic intervals for which each taxon is present.

Obtusacanthus	5	5	*Rhabdoderma*	13	19
Okamejei	78	78	*Rhadinacanthus*	7	9
Onychodus	8	12	*Rhamphodopsis*	8	9
Onychoselache	14	14	*Rhinochimaera*	78	78
Orlovichthys	12	12	*Romundina*	5	5
Orthacanthus	16	23	*Sagenodus*	13	23
Osorioichthys	12	12	*Sassenia*	30	30
Osteolepis	9	9	*Saurichthys*	28	38
Osteostraci	2	11	*Scyliorhinus*	52	78
Pachycormus	39	39	*Semionotus*	31	38
Palaeobates	30	35	*Serenichthys*	12	12
Panderichthys	9	11	*Soederberghia*	9	12
Parabuchanosteus	7	7	*Sorbitorhynchus*	7	7
Paraceratodus	29	30	*Speonesydrion*	7	7
Parayunnanolepis	5	5	*Spermatodus*	20	23
Parexus	5	5	*Squaloraja*	37	37
Perleidus	31	32	*Squalus*	57	78
Phanerosteon	13	14	*Stomiahykus*	8	8
Pholidophorus	31	50	*Strepsodus*	12	15
Pillararhynchus	10	10	*Strunius*	11	12
Plesiobatis	78	78	*Styloichthys*	5	5
Plourdosteus	11	11	*Synechodus*	46	61
Polymixia	78	78	*Tamiobatis*	12	13
Polyosteorhynchus	15	15	*Tarrasius*	13	16
Polypterus	73	78	*Tetanopsyrus*	5	5
Poracanthodes	5	5	*Tetraodon*	73	78
Porolepis	6	9	*Tribodus*	52	53
Powichthys	5	6	*Tristychius*	14	14
Promesacanthus	5	5	*Undina*	32	46
Protopterus	53	78	*Uranolophus*	6	6
Psarolepis	5	7	*Ventastega*	12	12
Pterichthyodes	7	9	*Vernicomacanthus*	5	5
Pteronisculus	29	30	*Watsonulus*	29	30
Ptomacanthus	5	5	*Whiteia*	29	30
Ptychoceratodus	29	32	*Wuttagoonaspis*	8	8
Pucapampella	7	9	*Youngolepis*	6	6
Ramirosuarezia	8	8	*Yunnanolepis*	5	5
Remigolepis	11	12			

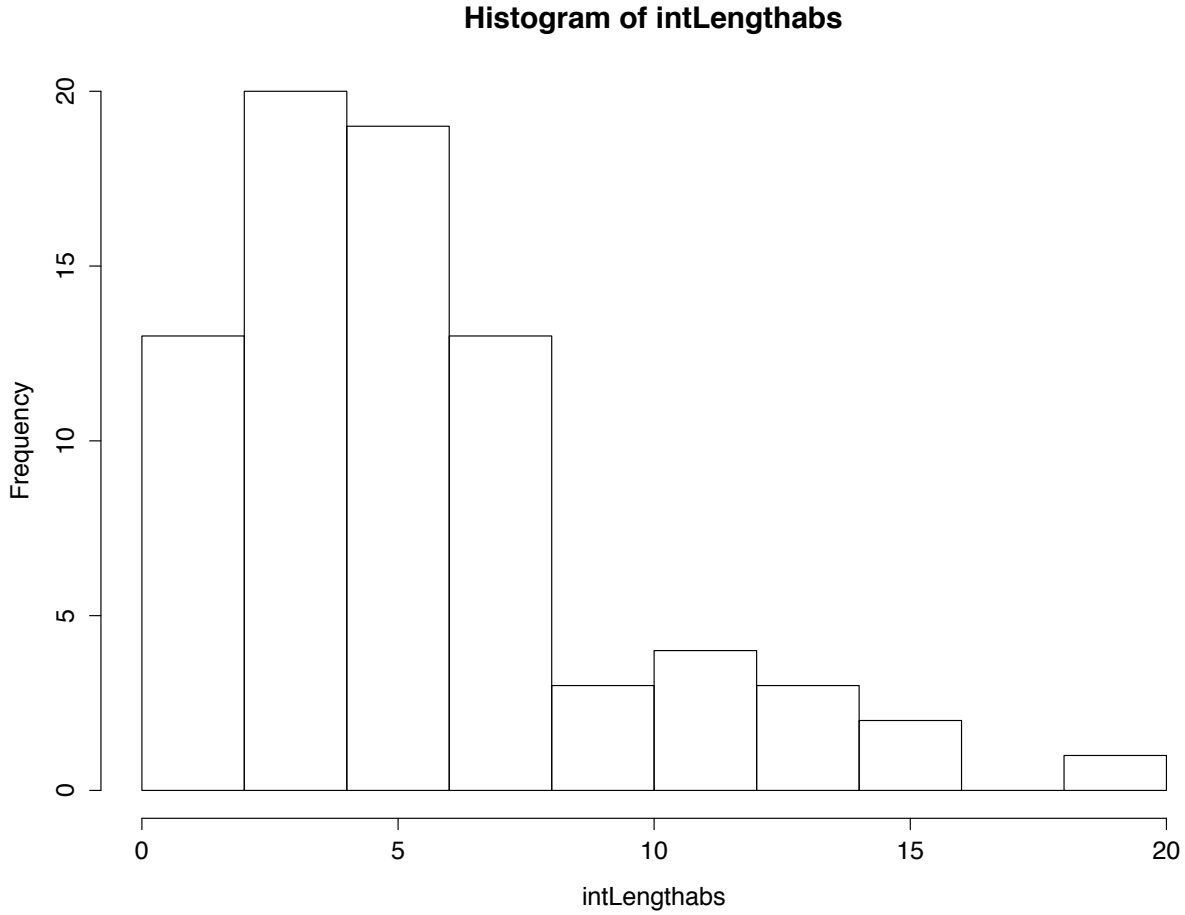

Figure A3.1. Histogram of geologic interval lengths used for time scaling. This histogram shows the frequency of taxon sampling for time intervals based on interval length, with the duration of each interval plotted on the x axis.

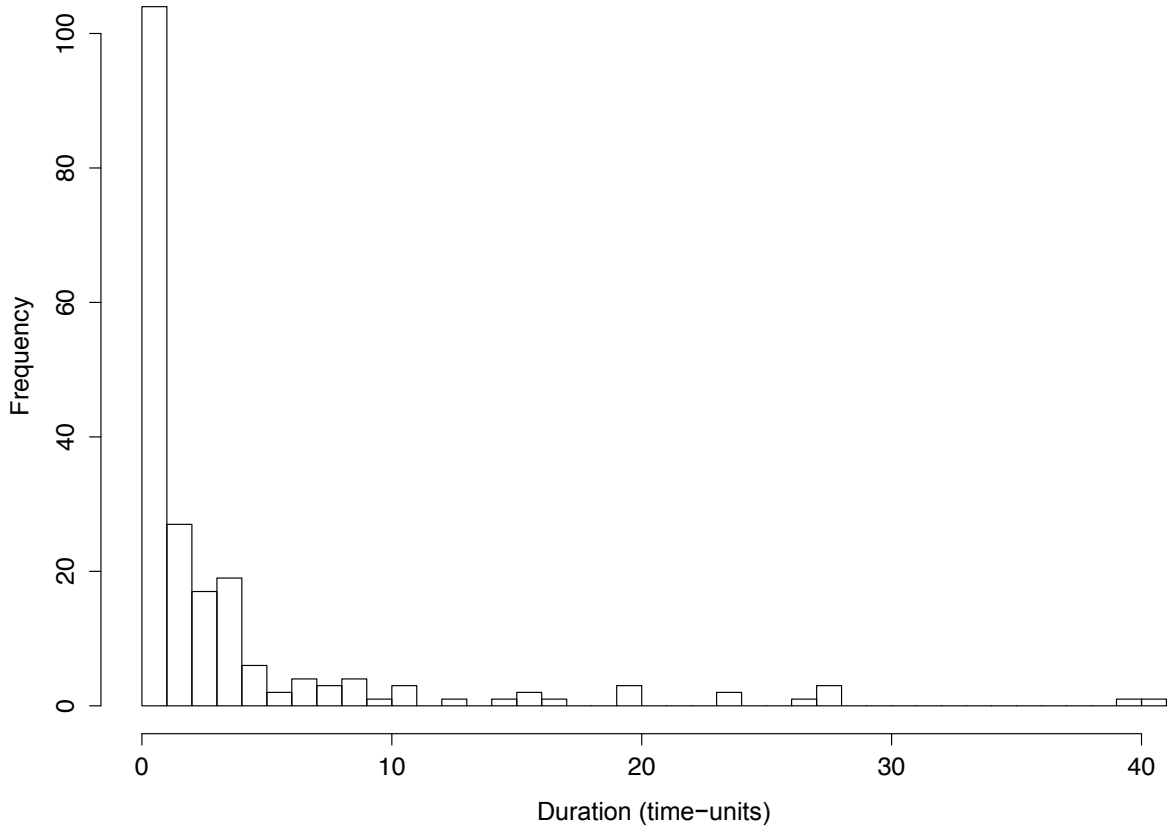

Figure A3.2. Frequency of taxon sampling for supertree. This histogram shows the number of taxa grouped by the number of intervals they span. Many genera included in the supertree (over 100) fall only within one interval (geologic stage), while approximately 65 are known from 2-4 intervals and relatively few have ranges extending through more than four intervals.

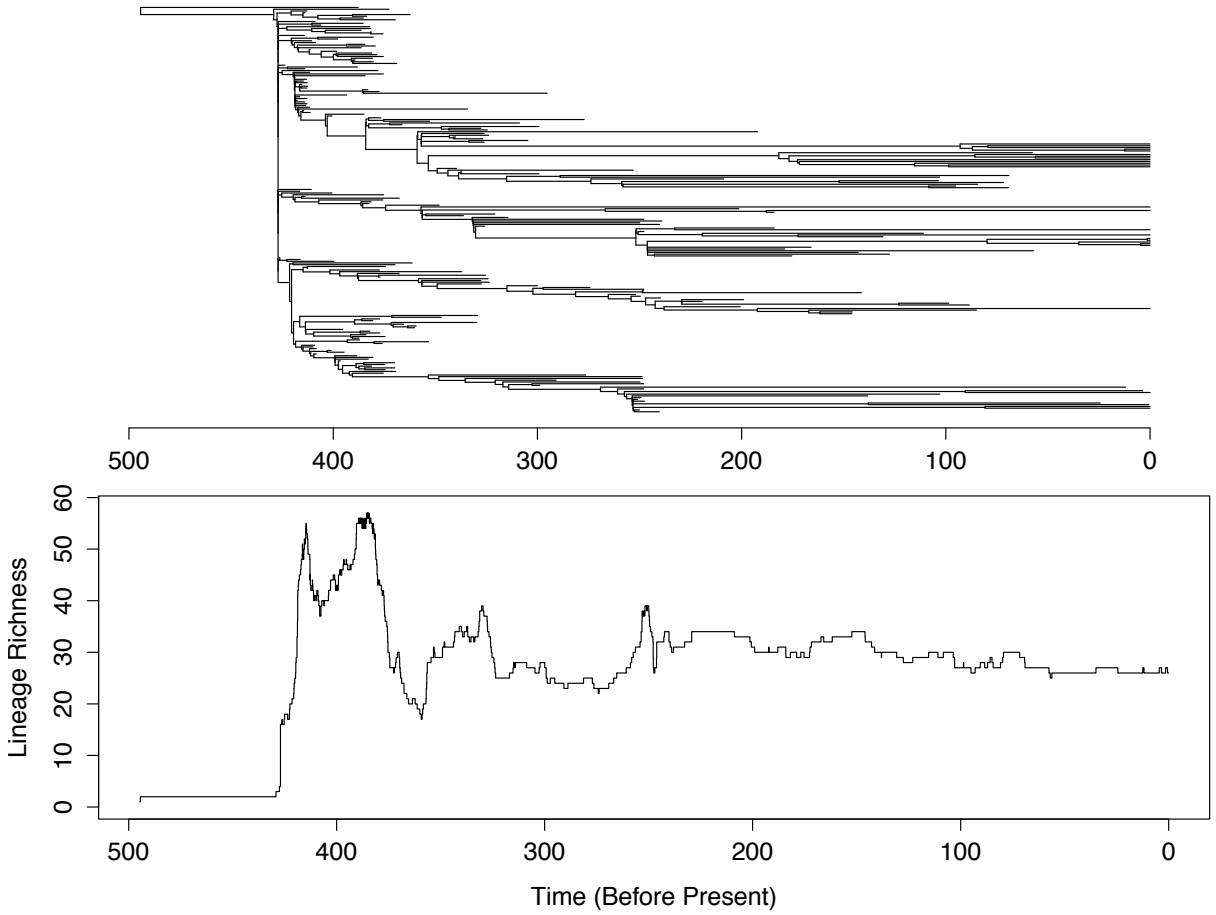

Figure A3.3. Diversity curve for time scaled supertree. This figure shows the diversity curve for taxa reperesented in the time-scaled supertree plotted alongside the supertree itself. The curve shows that taxa from the Paleozoic are more highly represented in this tree than Mesozoic and Cenozoic taxa.

Appendix 4: Vertebral character matrix

Table A4.1. Vertebral character states coded for each taxon.

	Centra	Anterior Fusions	Polyspondyly	NA fusion	Intercalaries
Acanthodes	0	0	0	0	0
Acanthostega	1	0	0	2	0
Achoania	?	?	?	?	?
Acipenser	0	0	0	1	1
Acrodus	?	?	?	?	?
Akmonistion	0	0	0	1	0
Allenypterus	0	0	0	2	0
Amblyraja	2	1	1	2	1
Amia	2	0	1	0	3
Aphelodus	?	?	?	?	?
Archaeoceratodus	?	?	?	?	?
Arganodus	?	?	?	?	?
Ariguna	0	0	0	?	0
Asiatoceratodus	0	0	0	?	0
Asteracanthus	?	?	?	?	?
Australosomus	1	0	1	0	1
Austroptyctodus	0	1	?	0	0
Axelrodichthys	0	0	0	?	0
Barameda	1	0	?	?	?
Beelarongia	?	?	?	?	?
Belonostomus	2	0	?	2	0
Beltanodus	?	?	?	?	?
Birgeria	0	?	0	0	0
Boreosomus	0	0	?	0	?
Bothriolepis	0	0	0	0	?
Brachyacanthus	?	?	?	?	?
Brindabellaspis	?	?	?	?	?
Brochoadmones	?	?	?	?	?
Buchanosteus	?	?	?	?	?
Callorhinchus	0	1	?	0	2
Campbellodus	0	1	?	0	0
Caridosuctor	0	0	0	2	0
Cassidiceps	?	?	?	?	?
Caturus	0/1	0	1	2	?
Ceratodus	0	0	?	?	?
Cheiracanthus	?	?	?	?	?
Cheirolepis	0	?	?	0	?

Table A4.1, continued. Vertebral character states coded for each taxon.

Chimaera	1	1	2	0	2
Chinlea	0	0	0	2	0
Chirodipterus	?	?	?	?	?
Chondrenchelys	1	0	1	2	0
Cladodoides	?	?	?	?	?
Cladoselache	0	0	0	0	0
Climatius	?	?	?	?	?
Cobelodus	0	0	0	0	0
Coccoderma	0	0	0	2	0
Coccosteus	0	0	0	0	0
Coelacanthus	0	0	0	2	0
Compagopiscis	0	1	0	2	0
Conchopoma	0	0	0	1	0
Cowralepis	0	1	0	2	0
Crassigyrinus	1	0	?	0	0
Ctenurella	0	0	0	?	0
Culmacanthus	?	?	?	?	?
Cyprinus	2	1	0	2	0
Dapedium	0	0	0	?	0
Debeerius	0	0	0	0	0
Diabolepis	?	?	?	?	?
Dialipina	?	?	?	?	?
Dicksonosteus	?	1	?	?	?
Diplacanthus	0	0	0	0	0
Diplocercides	?	?	?	?	?
Diplurus	0	0	0	2	0
Dipnorhynchus	?	?	?	?	?
Dipterus	0	0	0	0/1	0
Discoserra	0	0	0	1	0
Doliodus	?	?	?	?	?
Eastmanosteus	?	?	?	?	?
Egertonodus	?	?	?	?	?
Elops	2	0	0	2	0
Elpistostege	1	0	0	0	?
Entelognathus	?	?	?	?	?
Eurycaraspis	?	?	?	?	?
Eusthenopteron	1	0	0	2	0
Euthacanthus	?	?	?	?	?
Falcatus	0	0	0	0	0
Ferganoceratodus	?	?	?	?	?

Table A4.1, continued. Vertebral character states coded for each taxon.

Galeaspida	?	?	?	?	?
Garnbergia	?	?	?	?	?
Gavinia	?	?	?	?	?
Gemuendina	1	1	?	?	?
Gladiobranchus	?	?	?	?	?
Glyptolepis	1	0	0	2	0
Gnathorhiza	0	0	0	2	0
Gogodipterus	?	?	?	?	?
Gogonasus	1	?	?	?	?
Gosfordia	0	0	0	?	0
Griphognathus	2	?	0	0	?
Groenlandaspis	?	?	?	?	?
Guiyu	?	?	?	?	?
Gyracanthides	?	?	?	?	?
Gyroptychius	1	?	?	?	?
Hadronector	0	0	0	2	0
Hamiltonichthys	0	0	0	1	?
Harpacanthus	1	0	0	?	0
Harpagofututor	1	0	1	0	2
Harriotta	1	1	2	0	2
Helodus	0	1	?	?	?
Heterodontus	2	0	1	2	1
Hiodon	2	0	0	2	0
Holodipterus	?	?	?	?	?
Holonema	0	?	?	?	?
Holophagus	0	0	0	2	0
Holopterygius	0	0	0	1	0
Holoptychius	?	?	?	?	?
Homalacanthus	?	?	?	?	?
Hopleacanthus	2	0	?	?	?
Howidipterus	0	0	?	?	?
Howqualepis	0	0	?	0	0
Hulettia	1	0	1	0	1
Hybodus	0	0	0	0	?
Hydrolagus	1	1	2	0	2
Ichthyostega	1	0	0	2	0
Incisoscutum	0	1	0	2	0
Iniopera	0	0	0	0	0
Ionoscopus	2	0	0	2	?
Ischnacanthus	0	?	?	?	0

Table A4.1, continued. Vertebral character states coded for each taxon.

Jagorina	2	1	?	?	?
Janusiscus	?	?	?	?	?
Kathemacanthus	0	0	0	0	0
Kawichthys	?	?	?	?	?
Kenichthys	?	?	?	?	?
Kentuckia	?	?	?	?	?
Kujdanowiaspis	?	1	?	?	?
Latimeria	0	0	0	2	0
Latviacanthus	?	?	?	?	?
Laugia	0	0	?	?	?
Lepidosiren	0	0	0	0	0
Lepisosteus	2	0	0	1	0
Leptolepis	2	0	0	2	0
Libys	?	?	?	?	?
Ligulalepis	?	?	?	?	?
Lissodus	0	?	?	?	?
Lochmocercus	0	0	0	2	0
Lonchidion	?	?	?	?	?
Lophosteus	?	?	?	?	?
Lunaspis	?	?	?	?	?
Lupopsyrus	?	?	?	?	?
Macropetalichthys	?	?	?	?	?
Macropoma	0	0	0	2	0
Materpiscis	0	1	0	0	0
Mawsonia	0	0	0	2	0
Meemannia	?	?	?	?	?
Megapleuron	0	0	?	?	?
Mesacanthus	?	?	?	?	?
Mesopoma	0	0	?	0	2
Metaceratodus	?	?	?	?	?
Microbrachius	?	?	?	?	?
Microceratodus	?	?	?	?	?
Miguashaia	0	0	?	?	?
Mimipiscis	0	0	0	0	0
Mioceratodus	?	?	?	?	?
Moythomasia	0	0	0	0	0
Mustelus	2	0	1	?	?
Namatozodia	?	?	?	?	?
Neoceratodus	0	0	0	0	2
Notorynchus	1	0	?	?	?

Table A4.1, continued. Vertebral character states coded for each taxon.

Obtusacanthus	?	?	?	?	?
Okamejei	2	1	1	2	2
Onychodus	1	0	0	0	0
Onychoselache	0	0	0	0	2
Orlovichthys	?	?	?	?	?
Orthacanthus	0	0	0	0	0
Osorioichthys	?	?	?	?	?
Osteolepis	1	0	0	0	0
Osteostraci	0	0	?	?	?
Pachychormus	0	0	0	0	?
Palaeobates	?	?	?	?	?
Panderichthys	1	0	0	0	0
Parabuchanosteus	?	?	?	?	?
Paraceratodus	0	0	0	0	0
Parayunnanolepis	?	?	?	?	?
Parexus	0	0	?	0	?
Perleidus	?	?	?	?	?
Phanerosteon	1	0	0	0	0
Pholidophorus	1	0	1	2	?
Pillararhynchus	?	?	?	?	?
Plesiobatis	?	?	?	?	?
Plourdosteus	0	?	0	0	0
Polymixia	2	0	0	?	?
Polyosteorhynchus	0	0	0	2	0
Polypterus	2	0	0	1	0
Poracanthodes	?	?	?	?	?
Porolepis	?	?	?	?	?
Powichthys	?	?	?	?	?
Promesacanthus	?	?	?	?	?
Protopterus	0	0	0	0	0
Psarolepis	?	?	?	?	?
Pterichthyodes	0	?	?	0	?
Pteronisculus	0	0	0	0	1
Ptomacanthus	?	?	?	?	?
Ptychoceratodus	?	?	?	?	?
Pucapampella	?	?	?	?	?
Ramirosuarezia	?	?	?	?	?
Remigolepis	?	?	?	?	?
Rhabdoderma	0	?	0	2	0
Rhadinacanthus	?	?	?	?	?

Table A4.1, continued. Vertebral character states coded for each taxon.

Rhamphodopsis	0	?	0	0	0
Rhinochimaera	1	1	2	?	2
Romundina	?	?	?	?	?
Sagenodus	0	0	0	0	0
Sassenia	?	?	?	?	?
Saurichthys	0	0	0	1	1
Scyliorhinus	2	0	1	0	1
Semionotus	0	0	0	1	0
Serenichthys	0	?	?	?	?
Soederberghia	2	0	0	?	?
Sorbitorhynchus	?	?	?	?	?
Speonesydrion	?	?	?	?	?
Spermatodus	?	?	?	?	?
Squaloraja	2	1	2	?	2
Squalus	2	0	1	?	?
Stomiahykus	?	?	?	?	?
Strepsodus	2	0	?	2	0
Strunius	?	?	?	?	?
Styloichthys	?	?	?	?	?
Synechodus	2	0	?	?	?
Tamiobatis	?	?	?	?	?
Tarrasius	1/2	0	0	?	?
Tetanopsyrus	?	?	?	?	?
Tetraodon	2	0	0	?	?
Tribodus	?	?	?	?	?
Tristychius	0	0	?	1	?
Undina	0	0	0	2	0
Uranolophus	0	0	0	1	0
Ventastega	?	?	?	?	?
Vernicomacanthus	?	?	?	?	?
Watsonulus	0	0	0	0	0
Whiteia	0	0	?	?	0
Wuttagoonaspis	?	?	?	?	?
Youngolepis	?	?	?	?	?
Yunnanolepis	?	?	?	?	?

Appendix 5: Tables of prior probabilities for threshold model analyses

Table A5.1. Prior probabilities for threshold model analysis for centra.

	Absent	Ring	Full
Acanthodes	1	0	0
Acanthostega	0	0	1
Achoania	0.33	0.33	0.33
Acipenser	1	0	0
Acrodus	0.33	0.33	0.33
Akmonistion	1	0	0
Allenypterus	1	0	0
Amblyraja	0	0	1
Amia	0	0	1
Aphelodus	0.33	0.33	0.33
Archaeoceratodus	0.33	0.33	0.33
Arganodus	0.33	0.33	0.33
Ariguna	1	0	0
Asiatoceratodus	1	0	0
Asteracanthus	0.33	0.33	0.33
Australosomus	0	1	0
Austroptyctodus	1	0	0
Axelrodichthys	1	0	0
Barameda	0	1	0
Beelarongia	0.33	0.33	0.33
Belonostomus	0	0	1
Beltanodus	0.33	0.33	0.33
Birgeria	1	0	0
Boreosomus	1	0	0
Bothriolepis	1	0	0
Brachyacanthus	0.33	0.33	0.33
Brindabellaspis	0.33	0.33	0.33
Brochoadmones	0.33	0.33	0.33
Buchanosteus	0.33	0.33	0.33
Callorhinchus	1	0	0
Campbellodus	1	0	0
Caridosuctor	1	0	0
Cassidiceps	0.33	0.33	0.33
Caturus	0.5	0.5	0
Ceratodus	1	0	0
Cheiracanthus	0.33	0.33	0.33
Cheirolepis	0.33	0.33	0.33
Chimaera	0	1	0
Chinlea	1	0	0
Chirodipterus	0.33	0.33	0.33
Chondrenchelys	0	1	0
Cladodoides	0.33	0.33	0.33
Cladoselache	1	0	0
Climatius	0.33	0.33	0.33
Cobelodus	1	0	0
Coccoderma	1	0	0
Coccosteus	1	0	0
Coelacanthus	1	0	0
Compagopiscis	1	0	0
Conchopoma	1	0	0
Cowralepis	1	0	0
Crassigyrinus	0	1	0
Ctenurella	1	0	0
Culmacanthus	0.33	0.33	0.33
Cyprinus	0	0	1
Dapedium	1	0	0
Debeerius	1	0	0
Diabolepis	0.33	0.33	0.33
Dialipina	0.33	0.33	0.33
Dicksonosteus	0.33	0.33	0.33
Diplacanthus	1	0	0
Diplocercides	0.33	0.33	0.33
Diplurus	1	0	0
Dipnorhynchus	0.33	0.33	0.33
Dipterus	1	0	0
Discoserra	1	0	0
Doliodus	0.33	0.33	0.33
Eastmanosteus	0.33	0.33	0.33
Egertonodus	1	0	0
Elops	0	0	1
Elpistostege	0	1	0
Entelognathus	0.33	0.33	0.33
Eurycaraspis	0.33	0.33	0.33
Eusthenopteron	0	1	0
Euthacanthus	0.33	0.33	0.33

Table A5.1, continued. Prior probabilities for threshold model analysis for centra.

Falcatus	1	0	0	*Ionoscopus*	0	0	1
Ferganoceratodus	0.33	0.33	0.33	*Ischnacanthus*	1	0	0
Galeaspida	0.33	0.33	0.33	*Jagorina*	0	1	0
Garnbergia	0.33	0.33	0.33	*Janusiscus*	0.33	0.33	0.33
Gavinia	0.33	0.33	0.33	*Kathemacanthus*	1	0	0
Gemuendina	0	1	0	*Kawichthys*	0.33	0.33	0.33
Gladiobranchus	0.33	0.33	0.33	*Kenichthys*	0.33	0.33	0.33
Glyptolepis	0	1	0	*Kentuckia*	0.33	0.33	0.33
Gnathorhiza	1	0	0	*Kujdanowiaspis*	0.33	0.33	0.33
Gogodipterus	0.33	0.33	0.33	*Latimeria*	1	0	0
Gogonasus	0	1	0	*Latviacanthus*	0.33	0.33	0.33
Gosfordia	1	0	0	*Laugia*	1	0	0
Griphognathus	0	0	1	*Lepidosiren*	1	0	0
Groenlandaspis	0.33	0.33	0.33	*Lepisosteus*	0	0	1
Guiyu	0.33	0.33	0.33	*Leptolepis*	0	0	1
Gyracanthides	0.33	0.33	0.33	*Libys*	0.33	0.33	0.33
Gyroptychius	0	1	0	*Ligulalepis*	0.33	0.33	0.33
Hadronector	1	0	0	*Lissodus*	1	0	0
Hamiltonichthys	1	0	0	*Lochmocercus*	1	0	0
Harpacanthus	0	1	0	*Lonchidion*	0.33	0.33	0.33
Harpagofututor	0	1	0	*Lophosteus*	0.33	0.33	0.33
Harriotta	0	1	0	*Lunaspis*	0.33	0.33	0.33
Helodus	1	0	0	*Lupopsyrus*	0.33	0.33	0.33
Heterodontus	0	0	1	*Macropetalichthys*	0.33	0.33	0.33
Hiodon	0	0	1	*Macropoma*	1	0	0
Holodipterus	0.33	0.33	0.33	*Materpiscis*	1	0	0
Holonema	1	0	0	*Mawsonia*	1	0	0
Holophagus	1	0	0	*Meemannia*	0.33	0.33	0.33
Holopterygius	1	0	0	*Megapleuron*	1	0	0
Holoptychius	0.33	0.33	0.33	*Mesacanthus*	0.33	0.33	0.33
Homalacanthus	0.33	0.33	0.33	*Mesopoma*	1	0	0
Hopleacanthus	0	0	1	*Metaceratodus*	0.33	0.33	0.33
Howidipterus	1	0	0	*Microbrachius*	0.33	0.33	0.33
Howqualepis	0.33	0.33	0.33	*Microceratodus*	0.33	0.33	0.33
Hulettia	0	1	0	*Miguashaia*	0	1	0
Hybodus	1	0	0	*Mimipiscis*	1	0	0
Hydrolagus	0	1	0	*Mioceratodus*	0.33	0.33	0.33
Ichthyostega	0	1	0	*Moythomasia*	1	0	0
Incisoscutum	1	0	0	*Mustelus*	0	0	1
Iniopera	1	0	0	*Namatozodia*	0.33	0.33	0.33

Table A5.1, continued. Prior probabilities for threshold model analysis for centra.

Neoceratodus	1	0	0	*Remigolepis*	0.33	0.33	0.33
Notorynchus	0.33	0.33	0.33	*Rhabdoderma*	1	0	0
Obtusacanthus	0.33	0.33	0.33	*Rhadinacanthus*	0.33	0.33	0.33
Okamejei	0	0	1	*Rhamphodopsis*	1	0	0
Onychodus	0	1	0	*Rhinochimaera*	0	1	0
Onychoselache	1	0	0	*Romundina*	0.33	0.33	0.33
Orlovichthys	0.33	0.33	0.33	*Sagenodus*	1	0	0
Orthacanthus	1	0	0	*Sassenia*	0.33	0.33	0.33
Osorioichthys	0.33	0.33	0.33	*Saurichthys*	1	0	0
Osteolepis	0	1	0	*Scyliorhinus*	0	0	1
Osteostraci	1	0	0	*Semionotus*	1	0	0
Pachycormus	1	0	0	*Serenichthys*	1	0	0
Palaeobates	0.33	0.33	0.33	*Soederberghia*	0	0	1
Panderichthys	0	1	0	*Sorbitorhynchus*	0.33	0.33	0.33
Parabuchanosteus	0.33	0.33	0.33	*Speonesydrion*	0.33	0.33	0.33
Paraceratodus	1	0	0	*Spermatodus*	0.33	0.33	0.33
Parayunnanolepis	0.33	0.33	0.33	*Squaloraja*	0	0	1
Parexus	1	0	0	*Squalus*	0	0	1
Perleidus	0.33	0.33	0.33	*Stomiahykus*	0.33	0.33	0.33
Phanerosteon	0	1	0	*Strepsodus*	0	0	1
Pholidophorus	0	1	0	*Strunius*	0.33	0.33	0.33
Pillararhynchus	0.33	0.33	0.33	*Styloichthys*	0.33	0.33	0.33
Plesiobatis	0.33	0.33	0.33	*Synechodus*	0	0	1
Plourdosteus	1	0	0	*Tamiobatis*	0.33	0.33	0.33
Polymixia	0	0	1	*Tarrasius*	0	0.5	0.5
Polyosteorhynchus	1	0	0	*Tetanopsyrus*	0.33	0.33	0.33
Polypterus	0	1	0	*Tetraodon*	0	0	1
Poracanthodes	0.33	0.33	0.33	*Tribodus*	0.33	0.33	0.33
Porolepis	0.33	0.33	0.33	*Tristychius*	1	0	0
Powichthys	0.33	0.33	0.33	*Undina*	1	0	0
Promesacanthus	0.33	0.33	0.33	*Uranolophus*	1	0	0
Protopterus	1	0	0	*Ventastega*	0.33	0.33	0.33
Psarolepis	0.33	0.33	0.33	*Vernicomacanthus*	0.33	0.33	0.33
Pterichthyodes	1	0	0	*Watsonulus*	1	0	0
Pteronisculus	1	0	0	*Whiteia*	1	0	0
Ptomacanthus	0.33	0.33	0.33	*Wuttagoonaspis*	0.33	0.33	0.33
Ptychoceratodus	0.33	0.33	0.33	*Youngolepis*	0.33	0.33	0.33
Pucapampella	0.33	0.33	0.33	*Yunnanolepis*	0.33	0.33	0.33
Ramirosuarezia	0.33	0.33	0.33				

Table A5.2. Prior probabilities for threshold model analysis for anterior vertebral fusions.

	Absent	Present
Acanthodes	1	0
Acanthostega	1	0
Achoania	0.5	0.5
Acipenser	1	0
Acrodus	0.5	0.5
Akmonistion	1	0
Allenypterus	1	0
Amblyraja	0	1
Amia	1	0
Aphelodus	0.5	0.5
Archaeoceratodus	0.5	0.5
Arganodus	0.5	0.5
Ariguna	1	0
Asiatoceratodus	1	0
Asteracanthus	0.5	0.5
Australosomus	1	0
Austroptyctodus	0	1
Axelrodichthys	1	0
Barameda	1	0
Beelarongia	0.5	0.5
Belonostomus	1	0
Beltanodus	0.5	0.5
Birgeria	0.5	0.5
Boreosomus	1	0
Bothriolepis	1	0
Brachyacanthus	0.5	0.5
Brindabellaspis	0.5	0.5
Brochoadmones	0.5	0.5
Buchanosteus	0.5	0.5
Callorhinchus	0	1
Campbellodus	0	1
Caridosuctor	1	0
Cassidiceps	0.5	0.5
Caturus	1	0
Ceratodus	1	0
Cheiracanthus	0.5	0.5
Cheirolepis	0.5	0.5
Chimaera	0	1
Chinlea	1	0
Chirodipterus	0.5	0.5
Chondrenchelys	1	0
Cladodoides	0.5	0.5
Cladoselache	1	0
Climatius	0.5	0.5
Cobelodus	1	0
Coccoderma	1	0
Coccosteus	1	0
Coelacanthus	1	0
Compagopiscis	0	1
Conchopoma	1	0
Cowralepis	0	1
Crassigyrinus	1	0
Ctenurella	0	1
Culmacanthus	0.5	0.5
Cyprinus	0	1
Dapedium	1	0
Debeerius	1	0
Diabolepis	0.5	0.5
Dialipina	0.5	0.5
Dicksonosteus	0	1
Diplacanthus	1	0
Diplocercides	0.5	0.5
Diplurus	1	0
Dipnorhynchus	0.5	0.5
Dipterus	1	0
Discoserra	1	0
Doliodus	0.5	0.5
Eastmanosteus	0.5	0.5
Egertonodus	0.5	0.5
Elops	1	0
Elpistostege	1	0
Entelognathus	0.5	0.5
Eurycaraspis	0.5	0.5
Eusthenopteron	1	0
Euthacanthus	0.5	0.5
Falcatus	1	0
Ferganoceratodus	0.5	0.5
Galeaspida	0.5	0.5
Garnbergia	0.5	0.5

Table A5.2, continued. Prior probabilities for threshold model analysis for anterior vertebral fusions.

Gavinia	0.5	0.5	*Janusiscus*	0.5	0.5
Gemuendina	0	1	*Kathemacanthus*	1	0
Gladiobranchus	0.5	0.5	*Kawichthys*	0.5	0.5
Glyptolepis	1	0	*Kenichthys*	0.5	0.5
Gnathorhiza	1	0	*Kentuckia*	0.5	0.5
Gogodipterus	0.5	0.5	*Kujdanowiaspis*	0	1
Gogonasus	0.5	0.5	*Latimeria*	1	0
Gosfordia	1	0	*Latviacanthus*	0.5	0.5
Griphognathus	0.5	0.5	*Laugia*	1	0
Groenlandaspis	0.5	0.5	*Lepidosiren*	1	0
Guiyu	0.5	0.5	*Lepisosteus*	1	0
Gyracanthides	0.5	0.5	*Leptolepis*	1	0
Gyroptychius	0.5	0.5	*Libys*	0.5	0.5
Hadronector	1	0	*Ligulalepis*	0.5	0.5
Hamiltonichthys	1	0	*Lissodus*	1	0
Harpacanthus	1	0	*Lochmocercus*	1	0
Harpagofututor	1	0	*Lonchidion*	0.5	0.5
Harriotta	0	1	*Lophosteus*	0.5	0.5
Helodus	1	0	*Lunaspis*	0.5	0.5
Heterodontus	1	0	*Lupopsyrus*	0.5	0.5
Hiodon	1	0	*Macropetalichthys*	0.5	0.5
Holodipterus	0.5	0.5	*Macropoma*	1	0
Holonema	0.5	0.5	*Materpiscis*	0	1
Holophagus	1	0	*Mawsonia*	1	0
Holopterygius	1	0	*Meemannia*	0.5	0.5
Holoptychius	0.5	0.5	*Megapleuron*	1	0
Homalacanthus	0.5	0.5	*Mesacanthus*	0.5	0.5
Hopleacanthus	1	0	*Mesopoma*	1	0
Howidipterus	1	0	*Metaceratodus*	0.5	0.5
Howqualepis	1	0	*Microbrachius*	0.5	0.5
Hulettia	1	0	*Microceratodus*	0.5	0.5
Hybodus	1	0	*Miguashaia*	1	0
Hydrolagus	0	1	*Mimipiscis*	1	0
Ichthyostega	1	0	*Mioceratodus*	0.5	0.5
Incisoscutum	0	1	*Moythomasia*	1	0
Iniopera	1	0	*Mustelus*	1	0
Ionoscopus	1	0	*Namatozodia*	0.5	0.5
Ischnacanthus	0.5	0.5	*Neoceratodus*	1	0
Jagorina	0	1	*Notorynchus*	1	0

Table A5.2, continued. Prior probabilities for threshold model analysis for anterior vertebral fusions.

Obtusacanthus	0.5	0.5
Okamejei	0	1
Onychodus	1	0
Onychoselache	1	0
Orlovichthys	0.5	0.5
Orthacanthus	1	0
Osorioichthys	0.5	0.5
Osteolepis	1	0
Osteostraci	1	0
Pachycormus	1	0
Palaeobates	0.5	0.5
Panderichthys	1	0
Parabuchanosteus	0.5	0.5
Paraceratodus	1	0
Parayunnanolepis	0.5	0.5
Parexus	1	0
Perleidus	0.5	0.5
Phanerosteon	1	0
Pholidophorus	1	0
Pillararhynchus	0.5	0.5
Plesiobatis	0.5	0.5
Plourdosteus	0.5	0.5
Polymixia	1	0
Polyosteorhynchus	1	0
Polypterus	1	0
Poracanthodes	0.5	0.5
Porolepis	0.5	0.5
Powichthys	0.5	0.5
Promesacanthus	0.5	0.5
Protopterus	1	0
Psarolepis	0.5	0.5
Pterichthyodes	0.5	0.5
Pteronisculus	1	0
Ptomacanthus	0.5	0.5
Ptychoceratodus	0.5	0.5
Pucapampella	0.5	0.5
Ramirosuarezia	0.5	0.5
Remigolepis	0.5	0.5
Rhabdoderma	0.5	0.5
Rhadinacanthus	0.5	0.5
Rhamphodopsis	0.5	0.5
Rhinochimaera	0	1
Romundina	0.5	0.5
Sagenodus	1	0
Sassenia	0.5	0.5
Saurichthys	1	0
Scyliorhinus	1	0
Semionotus	1	0
Serenichthys	0.5	0.5
Soederberghia	1	0
Sorbitorhynchus	0.5	0.5
Speonesydrion	0.5	0.5
Spermatodus	0.5	0.5
Squaloraja	0	1
Squalus	1	0
Stomiahykus	0.5	0.5
Strepsodus	1	0
Strunius	0.5	0.5
Styloichthys	0.5	0.5
Synechodus	1	0
Tamiobatis	0.5	0.5
Tarrasius	1	0
Tetanopsyrus	0.5	0.5
Tetraodon	1	0
Tribodus	0.5	0.5
Tristychius	1	0
Undina	1	0
Uranolophus	1	0
Ventastega	0.5	0.5
Vernicomacanthus	0.5	0.5
Watsonulus	1	0
Whiteia	1	0
Wuttagoonaspis	0.5	0.5
Youngolepis	0.5	0.5
Yunnanolepis	0.5	0.5

Table A5.3. Prior probabilities for threshold model analysis for polyspondyly.

	None	Diplospond-yly in tail	Polyspondyly throughout
Acanthodes	1	0	0
Acanthostega	1	0	0
Achoania	0.33	0.33	0.33
Acipenser	1	0	0
Acrodus	0.33	0.33	0.33
Akmonistion	1	0	0
Allenypterus	1	0	0
Amblyraja	0	1	0
Amia	0	1	0
Aphelodus	0.33	0.33	0.33
Archaeoceratodus	0.33	0.33	0.33
Arganodus	0.33	0.33	0.33
Ariguna	1	0	0
Asiatoceratodus	1	0	0
Asteracanthus	0.33	0.33	0.33
Australosomus	0	1	0
Austroptyctodus	0.33	0.33	0.33
Axelrodichthys	1	0	0
Barameda	0.33	0.33	0.33
Beelarongia	0.33	0.33	0.33
Belonostomus	0.33	0.33	0.33
Beltanodus	0.33	0.33	0.33
Birgeria	1	0	0
Boreosomus	0.33	0.33	0.33
Bothriolepis	1	0	0
Brachyacanthus	0.33	0.33	0.33
Brindabellaspis	0.33	0.33	0.33
Brochoadmones	0.33	0.33	0.33
Buchanosteus	0.33	0.33	0.33
Callorhinchus	0.33	0.33	0.33
Campbellodus	0.33	0.33	0.33
Caridosuctor	1	0	0
Cassidiceps	0.33	0.33	0.33
Caturus	0	1	0
Ceratodus	0.33	0.33	0.33
Cheiracanthus	0.33	0.33	0.33
Cheirolepis	0.33	0.33	0.33
Chimaera	0	0	1
Chinlea	1	0	0
Chirodipterus	0.33	0.33	0.33
Chondrenchelys	1	0	0
Cladodoides	0.33	0.33	0.33
Cladoselache	1	0	0
Climatius	0.33	0.33	0.33
Cobelodus	1	0	0
Coccoderma	1	0	0
Coccosteus	1	0	0
Coelacanthus	1	0	0
Compagopiscis	1	0	0
Conchopoma	1	0	0
Cowralepis	1	0	0
Crassigyrinus	0.33	0.33	0.33
Ctenurella	1	0	0
Culmacanthus	0.33	0.33	0.33
Cyprinus	1	0	0
Dapedium	1	0	0
Debeerius	1	0	0
Diabolepis	0.33	0.33	0.33
Dialipina	0.33	0.33	0.33
Dicksonosteus	0.33	0.33	0.33
Diplacanthus	1	0	0
Diplocercides	0.33	0.33	0.33
Diplurus	1	0	0
Dipnorhynchus	0.33	0.33	0.33
Dipterus	1	0	0
Discoserra	1	0	0
Doliodus	0.33	0.33	0.33
Eastmanosteus	0.33	0.33	0.33
Egertonodus	0.33	0.33	0.33
Elops	1	0	0
Elpistostege	0.33	0.33	0.33
Entelognathus	0.33	0.33	0.33
Eurycaraspis	0.33	0.33	0.33
Eusthenopteron	1	0	0
Euthacanthus	0.33	0.33	0.33
Falcatus	1	0	0

Table A5.3, continued. Prior probabilities for threshold model analysis for polyspondyly.

Gemuendina	0.33	0.33	0.33
Gladiobranchus	0.33	0.33	0.33
Glyptolepis	1	0	0
Gnathorhiza	1	0	0
Gogodipterus	0.33	0.33	0.33
Gogonasus	0.33	0.33	0.33
Gosfordia	1	0	0
Griphognathus	1	0	0
Groenlandaspis	0.33	0.33	0.33
Guiyu	0.33	0.33	0.33
Gyracanthides	0.33	0.33	0.33
Gyroptychius	0.33	0.33	0.33
Hadronector	1	0	0
Hamiltonichthys	1	0	0
Harpacanthus	1	0	0
Harpagofututor	0	1	0
Harriotta	0	0	1
Helodus	0.33	0.33	0.33
Heterodontus	0	1	0
Hiodon	1	0	0
Holodipterus	0.33	0.33	0.33
Holonema	0.33	0.33	0.33
Holophagus	1	0	0
Holopterygius	1	0	0
Holoptychius	0.33	0.33	0.33
Homalacanthus	0.33	0.33	0.33
Hopleacanthus	0.33	0.33	0.33
Howidipterus	0.33	0.33	0.33
Howqualepis	0.33	0.33	0.33
Hulettia	0	1	0
Hybodus	1	0	0
Hydrolagus	0	0	1
Ichthyostega	1	0	0
Incisoscutum	1	0	0
Iniopera	1	0	0
Ionoscopus	1	0	0
Ischnacanthus	0.33	0.33	0.33
Jagorina	0.33	0.33	0.33
Janusiscus	0.33	0.33	0.33
Kathemacanthus	1	0	0
Kawichthys	0.33	0.33	0.33
Kenichthys	0.33	0.33	0.33
Kentuckia	0.33	0.33	0.33
Kujdanowiaspis	0.33	0.33	0.33
Latimeria	0.33	0.33	0.33
Latviacanthus	0.33	0.33	0.33
Laugia	0.33	0.33	0.33
Lepidosiren	1	0	0
Lepisosteus	1	0	0
Leptolepis	1	0	0
Libys	0.33	0.33	0.33
Ligulalepis	0.33	0.33	0.33
Lissodus	0.33	0.33	0.33
Lochmocercus	1	0	0
Lonchidion	0.33	0.33	0.33
Lophosteus	0.33	0.33	0.33
Lunaspis	0.33	0.33	0.33
Lupopsyrus	0.33	0.33	0.33
Macropetalichthys	0.33	0.33	0.33
Macropoma	1	0	0
Materpiscis	1	0	0
Mawsonia	1	0	0
Meemannia	0.33	0.33	0.33
Megapleuron	0.33	0.33	0.33
Mesacanthus	0.5	0.5	0
Mesopoma	0.33	0.33	0.33
Metaceratodus	0.33	0.33	0.33
Microbrachius	0.33	0.33	0.33
Microceratodus	0.33	0.33	0.33
Miguashaia	0.33	0.33	0.33
Mimipiscis	1	0	0
Mioceratodus	0.33	0.33	0.33
Moythomasia	1	0	0
Mustelus	0	1	0
Namatozodia	0.33	0.33	0.33
Neoceratodus	1	0	0
Notorynchus	0	1	0
Obtusacanthus	0.33	0.33	0.33
Okamejei	0	1	0

Table A5.3, continued. Prior probabilities for threshold model analysis for polyspondyly.

Onychodus	1	0	0	*Rhadinacanthus*	0.33	0.33	0.33
Onychoselache	1	0	0	*Rhamphodopsis*	1	0	0
Orlovichthys	0.33	0.33	0.33	*Rhinochimaera*	0	0	1
Orthacanthus	1	0	0	*Romundina*	0.33	0.33	0.33
Osorioichthys	0.33	0.33	0.33	*Sagenodus*	1	0	0
Osteolepis	1	0	0	*Sassenia*	0.33	0.33	0.33
Osteostraci	0.33	0.33	0.33	*Saurichthys*	1	0	0
Pachycormus	1	0	0	*Scyliorhinus*	0	1	0
Palaeobates	0.33	0.33	0.33	*Semionotus*	1	0	0
Panderichthys	1	0	0	*Serenichthys*	0.33	0.33	0.33
Parabuchanosteus	0.33	0.33	0.33	*Soederberghia*	1	0	0
Paraceratodus	1	0	0	*Sorbitorhynchus*	0.33	0.33	0.33
Parayunnanolepis	0.33	0.33	0.33	*Speonesydrion*	0.33	0.33	0.33
Parexus	0.33	0.33	0.33	*Spermatodus*	0.33	0.33	0.33
Perleidus	0.33	0.33	0.33	*Squaloraja*	0	0	1
Phanerosteon	1	0	0	*Squalus*	0	1	0
Pholidophorus	0	1	0	*Stomiahykus*	0.33	0.33	0.33
Pillararhynchus	0.33	0.33	0.33	*Strepsodus*	0.33	0.33	0.33
Plesiobatis	0.33	0.33	0.33	*Strunius*	0.33	0.33	0.33
Plourdosteus	1	0	0	*Styloichthys*	0.33	0.33	0.33
Polymixia	1	0	0	*Synechodus*	0.33	0.33	0.33
Polyosteorhynchus	1	0	0	*Tamiobatis*	0.33	0.33	0.33
Polypterus	1	0	0	*Tarrasius*	1	0	0
Poracanthodes	0.33	0.33	0.33	*Tetanopsyrus*	0.33	0.33	0.33
Porolepis	0.33	0.33	0.33	*Tetraodon*	1	0	0
Powichthys	0.33	0.33	0.33	*Tribodus*	0.33	0.33	0.33
Promesacanthus	0.33	0.33	0.33	*Tristychius*	0.33	0.33	0.33
Protopterus	1	0	0	*Undina*	1	0	0
Psarolepis	0.33	0.33	0.33	*Uranolophus*	1	0	0
Pterichthyodes	0.33	0.33	0.33	*Ventastega*	0.33	0.33	0.33
Pteronisculus	1	0	0	*Vernicomacanthus*	0.33	0.33	0.33
Ptomacanthus	0.33	0.33	0.33	*Watsonulus*	1	0	0
Ptychoceratodus	0.33	0.33	0.33	*Whiteia*	0.33	0.33	0.33
Pucapampella	0.33	0.33	0.33	*Wuttagoonaspis*	0.33	0.33	0.33
Ramirosuarezia	0.33	0.33	0.33	*Youngolepis*	0.33	0.33	0.33
Remigolepis	0.33	0.33	0.33	*Yunnanolepis*	0.33	0.33	0.33
Rhabdoderma	1	0	0				

Appendix 6: Posterior probabilities for threshold model analyses

Table A6.1. Posterior probabilities for the independent evolution of centra.

Taxon	Node	State	PP1	PP2	PP3	PP4	PP5	PP6	PP7	PP8	PP9	PP10
Antiarchs	459	Absent	0.6392	0.9625	0.8239	0.6117	0.9825	0.8764	0.5742	0.9900	0.5892	0.7652
		Ring	0.3158	0.0374	0.1672	0.3807	0.0174	0.1235	0.4182	0.0099	0.4107	0.2347
		Full	0.0449	0.0000	0.0087	0.0074	0.0000	0.0000	0.0074	0.0000	0.0000	0.0000
Ptytodonts	454	Absent	0.9126	1.0000	0.9712	0.9987	0.9900	0.9962	0.9650	0.9775	0.8689	0.7902
		Ring	0.0873	0.0000	0.0287	0.0012	0.0099	0.0037	0.0349	0.0224	0.1298	0.2097
		Full	0.0000	0.0000	0.0000	0.0000	0.0000	0.0000	0.0000	0.0000	0.0000	0.0000
Arthrodires + others	439	Absent	0.9975	0.4019	0.7053	0.5156	0.9500	0.7490	0.3645	0.7727	0.4731	0.6504
		Ring	0.0024	0.5967	0.2946	0.4843	0.0499	0.2509	0.6142	0.2272	0.5268	0.3420
		Full	0.0000	0.0012	0.0000	0.0000	0.0000	0.0000	0.0212	0.0000	0.0000	0.0074
All Chondrichthyans	371	Absent	0.8264	0.1235	0.5867	0.9525	0.7428	0.4794	0.8414	0.0112	0.3957	0.5568
		Ring	0.1735	0.8764	0.4132	0.0474	0.2571	0.5205	0.1585	0.6791	0.6042	0.4431
		Full	0.0000	0.0000	0.0000	0.0000	0.0000	0.0000	0.0000	0.3096	0.0000	0.0000
Chondrichthyans -acanthodians	384	Absent	0.9450	0.2534	0.7166	0.6716	0.8089	0.8089	0.9500	0.3570	0.5018	0.6591
		Ring	0.0549	0.7465	0.2784	0.3283	0.1910	0.1910	0.0486	0.6429	0.4194	0.3383
		Full	0.0000	0.0000	0.0049	0.0000	0.0000	0.0000	0.0012	0.0000	0.0786	0.0024
Hybodonts	404	Absent	0.9450	0.9176	1.0000	0.9700	1.0000	0.8988	0.9063	0.9413	0.8639	0.9176
		Ring	0.0461	0.0823	0.0000	0.0299	0.0000	0.1011	0.0923	0.0586	0.1161	0.0823
		Full	0.0087	0.0000	0.0000	0.0000	0.0000	0.0000	0.0012	0.0000	0.0199	0.0000
Elasmobranchs	399	Absent	0.9113	0.9176	0.8876	0.8764	0.7627	0.7390	0.9563	0.8651	0.6928	0.8589
		Ring	0.0886	0.0823	0.1123	0.1235	0.2372	0.2609	0.0424	0.1348	0.3071	0.1285
		Full	0.0000	0.0000	0.0000	0.0000	0.0000	0.0000	0.0012	0.0000	0.0000	0.0124
Holocephalans	388	Absent	0.7915	0.6754	0.6541	0.8988	0.7078	0.6741	0.7827	0.5605	0.4843	0.9488
		Ring	0.2084	0.3245	0.3458	0.1011	0.2921	0.3258	0.1697	0.4394	0.5156	0.0511
		Full	0.0000	0.0000	0.0000	0.0000	0.0000	0.0000	0.0474	0.0000	0.0000	0.0000
Symmoriiforms	419	Absent	1.0000	0.8639	0.9712	0.9263	0.9213	0.9912	0.9862	0.0012	0.9251	0.8639
		Ring	0.0000	0.1360	0.0287	0.0736	0.0786	0.0087	0.0049	0.0237	0.0749	0.1360
		Full	0.0000	0.0000	0.0000	0.0000	0.0000	0.0000	0.0087	0.9750	0.0000	0.0000
All Osteichthyans	244	Absent	0.9687	0.1485	0.4357	0.9238	0.6167	0.4307	0.7128	0.7103	0.6666	0.4494
		Ring	0.0312	0.8514	0.5642	0.0761	0.3832	0.5692	0.2871	0.2896	0.3333	0.5505
		Full	0.0000	0.0000	0.0000	0.0000	0.0000	0.0000	0.0000	0.0000	0.0000	0.0000
Tetrapodomorphs	358	Absent	0.2047	0.0124	0.0986	0.1235	0.0786	0.2446	0.0074	0.0736	0.7727	0.1910
		Ring	0.7915	0.9875	0.8951	0.8764	0.9113	0.7528	0.7677	0.8102	0.2272	0.8064
		Full	0.0037	0.0000	0.0062	0.0000	0.0099	0.0024	0.2247	0.1161	0.0000	0.0024
Coealacanths	289	Absent	0.4594	0.2858	0.4357	0.3183	0.6891	0.5405	0.3707	0.3995	0.9600	0.8676
		Ring	0.5405	0.7141	0.5642	0.6816	0.3108	0.4594	0.6292	0.6004	0.0399	0.1323
		Full	0.0000	0.0000	0.0000	0.0000	0.0000	0.0000	0.0000	0.0000	0.0000	0.0000
Porolepiforms	317	Absent	0.4694	0.3945	0.1985	0.3395	0.5792	0.4119	0.2808	0.3270	0.9438	0.5967
		Ring	0.5305	0.6054	0.8014	0.6604	0.4207	0.5880	0.7191	0.6729	0.0561	0.4032
		Full	0.0000	0.0000	0.0000	0.0000	0.0000	0.0000	0.0000	0.0000	0.0000	0.0000
Lungfish	325	Absent	0.8501	0.8014	0.5530	0.7166	0.8601	0.3458	0.6017	0.5218	0.8264	0.9275
		Ring	0.1498	0.1985	0.4469	0.2833	0.1398	0.6541	0.3870	0.4781	0.1735	0.0724
		Full	0.0000	0.0000	0.0000	0.0000	0.0000	0.0000	0.0112	0.0000	0.0000	0.0000
All actinopterygians	250	Absent	0.8426	0.5293	0.5480	0.9925	0.8764	0.7702	0.8639	0.4981	0.5930	0.8626
		Ring	0.1573	0.4332	0.4519	0.0074	0.1235	0.2297	0.1323	0.5018	0.3970	0.1360
		Full	0.0000	0.0374	0.0000	0.0000	0.0000	0.0000	0.0037	0.0000	0.0099	0.0012
Neopterygians	266	Absent	0.8876	0.2646	0.6167	0.7028	0.8801	0.9275	0.6779	1.0000	0.7478	0.9450
		Ring	0.1123	0.7353	0.3820	0.2971	0.1198	0.0724	0.3058	0.0000	0.2496	0.0549
		Full	0.0000	0.0000	0.0012	0.0000	0.0000	0.0000	0.0162	0.0000	0.0024	0.0000
Teleosts	267	Absent	0.7665	0.0299	0.1235	0.6017	0.7290	0.8526	0.0761	0.9450	0.6092	0.9063
		Ring	0.2334	0.9700	0.8764	0.3982	0.2709	0.1473	0.8539	0.0549	0.3745	0.0936
		Full	0.0000	0.0000	0.0000	0.0000	0.000	0.0000	0.0699	0.0000	0.0162	0.0000
Crown gnathostomes	243	Absent	0.9563	0.1098	0.5568	0.9850	0.8401	0.4119	0.7415	0.7877	0.5018	0.4831
		Ring	0.0436	0.8901	0.4431	0.0149	0.1598	0.5880	0.2584	0.2122	0.4981	0.5168
		Full	0.0000	0.0000	0.0000	0.0000	0.0000	0.0000	0.0000	0.0000	0.0000	0.0000
Stem gnathostomes	234	Absent	0.7203	0.4469	0.6566	0.8539	1.0000	0.7240	0.5430	0.9775	0.5168	0.4244
		Ring	0.2796	0.5530	0.3433	0.1460	0.0000	0.2759	0.4569	0.0224	0.4831	0.5755
		Full	0.0000	0.0000	0.0000	0.0000	0.0000	0.0000	0.0000	0.0000	0.0000	0.0000

Table A6.2. Posterior probabilities for anterior fusions.

Taxon	Node #	State	PP1	PP2	PP3	PP4	PP5	PP6	PP7	PP8	PP9	PP10
Antiarchs	459	Absent	0.9350	1.0000	0.5430	0.9700	0.9762	0.5131	0.9563	0.4007	0.8327	0.6392
		Present	0.0649	0.0000	0.4569	0.0299	0.0237	0.4868	0.0436	0.5992	0.1672	0.3607
Ptytodonts	454	Absent	0.3782	0.1672	0.1011	0.0124	0.0224	0.0911	0.0636	0.0299	0.1897	0.0836
		Present	0.6217	0.8327	0.8988	0.9875	0.9775	0.9088	0.9363	0.9700	0.8102	0.9163
Arthrodires + others	439	Absent	0.2521	0.4456	0.0274	0.1323	0.1672	0.1872	0.3183	0.0848	0.1473	0.0149
		Present	0.7478	0.5543	0.9725	0.8676	0.8327	0.8127	0.6816	0.9151	0.8526	0.9850
All Chondrichthyans	371	Absent	0.8564	0.8589	0.2833	0.5930	0.3408	0.9425	0.8813	0.9600	0.6229	0.3720
		Present	0.1435	0.1410	0.7166	0.4069	0.6591	0.0574	0.1186	0.0399	0.3770	0.6279
Chondrichthyans -acanthodians	384	Absent	1.0000	0.6254	0.8851	0.8714	0.7166	0.9825	0.9375	0.9962	0.9188	0.9488
		Present	0.0000	0.3745	0.1148	0.1285	0.2833	0.0174	0.0624	0.0037	0.0811	0.0511
Hybodonts	404	Absent	0.9013	0.1373	0.8751	0.8102	0.3046	0.9887	0.8002	0.9900	0.9912	0.7490
		Present	0.0986	0.8626	0.1248	0.1897	0.6953	0.0112	0.1997	0.0099	0.0087	0.2509
Elasmobranchs	399	Absent	0.9563	0.9950	1.0000	0.9800	0.9900	0.9750	0.9662	0.9525	0.9750	1.0000
		Present	0.0436	0.0049	0.0000	0.0199	0.0099	0.0249	0.0337	0.0474	0.0249	0.0000
Holocephalans	388	Absent	0.9238	0.8426	0.9900	0.7191	1.0000	0.9987	0.8689	0.9350	1.0000	1.0000
		Present	0.0761	0.1573	0.0099	0.2808	0.0000	0.0012	0.1310	0.0649	0.0000	0.0000
Symmoriiformes	419	Absent	0.9837	0.9026	1.0000	0.9900	0.9900	1.0000	0.9026	0.9775	1.0000	1.0000
		Present	0.0162	0.0973	0.0000	0.0099	0.0099	0.0000	0.0973	0.0224	0.0000	0.0000
All Osteichthyans	244	Absent	0.9800	0.7178	0.6641	0.5917	0.8114	0.6928	0.7877	0.7652	0.5742	0.3058
		Present	0.0199	0.2821	0.3358	0.4082	0.1885	0.3071	0.2122	0.2347	0.4257	0.6941
Tetrapodomorphs	358	Absent	0.9937	1.0000	0.9563	0.9450	1.0000	0.8751	0.9176	0.9225	0.9338	0.7153
		Present	0.0062	0.0000	0.0436	0.0549	0.0000	0.1248	0.0823	0.0774	0.0661	0.2846
Coealacanths	289	Absent	0.8963	0.9588	0.5580	0.7253	0.8227	0.9575	0.9026	0.8951	0.6579	0.5018
		Present	0.1036	0.0411	0.4419	0.2746	0.1772	0.0424	0.0973	0.1048	0.3420	0.4981
Porolepiforms	317	Absent	1.0000	0.9600	0.9176	0.8014	0.7315	0.8926	0.9238	0.9637	0.9225	0.6392
		Present	0.0000	0.0399	0.0823	0.1985	0.2684	0.1073	0.0761	0.0362	0.0774	0.3607
Lungfish	325	Absent	1.0000	0.9051	0.9762	0.9912	0.8264	0.9837	0.8888	0.9975	1.0000	0.8689
		Present	0.0000	0.0948	0.0237	0.0087	0.1735	0.0162	0.1111	0.0024	0.0000	0.1310
All actinopterygians	250	Absent	0.9600	0.6978	0.9637	0.8052	0.8676	1.0000	0.9937	0.8938	0.8776	0.8801
		Present	0.0399	0.3021	0.0362	0.1947	0.1323	0.0000	0.0062	0.1061	0.1223	0.1198
Neopterygians	266	Absent	0.9925	1.0000	0.9875	0.8626	0.9313	0.9912	0.9937	1.0000	0.9375	0.8252
		Present	0.0074	0.0000	0.0124	0.1373	0.0686	0.0087	0.0062	0.0000	0.0624	0.1747
Teleosts	267	Absent	0.9513	1.0000	0.9787	0.8339	0.9687	1.0000	1.0000	1.0000	0.8501	0.9013
		Present	0.0486	0.0000	0.0212	0.1660	0.0312	0.0000	0.0000	0.0000	0.1498	0.0986
Crown gnathostomes	243	Absent	0.9825	0.9575	0.3895	0.4868	0.6966	0.9088	0.9038	0.6953	0.7340	0.2022
		Present	0.0174	0.0424	0.6104	0.5131	0.3033	0.0911	0.0961	0.3046	0.2659	0.7977
Stem gnathostomes	234	Absent	1.0000	0.9675	0.2084	0.7790	1.0000	0.2958	0.9675	0.3570	0.5917	0.9563
		Present	0.0000	0.0324	0.7915	0.2209	0.0000	0.7041	0.0324	0.6429	0.4082	0.0436

Table A6.3. Posterior probabilities for polyspondyly.

Taxon	Node #	State	PP1	PP2	PP3	PP4	PP5	PP6	PP7	PP8	PP9	PP10
Antiarchs	459	None	0.5518	0.5280	0.4781	0.6029	0.9051	0.6292	0.3433	0.9038	0.4294	0.6941
		Diplo	0.4481	0.4719	0.5218	0.3970	0.0948	0.3695	0.6566	0.0961	0.5705	0.3058
		Poly	0.0000	0.0000	0.0000	0.0000	0.0000	0.0012	0.0000	0.0000	0.0000	0.0000
Ptytodonts	454	None	0.9850	0.8714	0.8913	0.9875	0.8152	0.9700	0.9388	0.9662	0.8476	0.8776
		Diplo	0.0149	0.1285	0.1086	0.0124	0.1847	0.0299	0.0611	0.0337	0.1523	0.1223
		Poly	0.0000	0.0000	0.0000	0.0000	0.0000	0.0000	0.0000	0.0000	0.0000	0.0000
Arthrodires + others	439	None	0.5455	1.0000	0.4244	0.3845	0.8264	0.6079	0.6679	0.9650	0.8714	0.5917
		Diplo	0.4544	0.0000	0.5755	0.6154	0.1735	0.3920	0.3320	0.0349	0.1285	0.4082
		Poly	0.0000	0.0000	0.0000	0.0000	0.0000	0.0000	0.0000	0.0000	0.0000	0.0000
All Chondrichthyans	371	None	0.4232	0.4319	0.5468	0.0387	0.9762	0.2808	0.6704	0.3720	0.9837	0.7265
		Diplo	0.5767	0.5680	0.4531	0.9612	0.0237	0.7191	0.3295	0.6229	0.0162	0.2734
		Poly	0.0000	0.0000	0.0000	0.0000	0.0000	0.0000	0.0000	0.0049	0.0000	0.0000
Chondrichthyans -acanthodians	384	None	0.5642	0.1360	0.6242	0.9450	0.8252	0.7652	0.7777	0.5593	0.6791	0.9737
		Diplo	0.4357	0.8639	0.3757	0.0549	0.1747	0.2347	0.2222	0.4406	0.3208	0.0262
		Poly	0.0000	0.0000	0.0000	0.0000	0.0000	0.0000	0.0000	0.0000	0.0000	0.0000
Hybodonts	404	None	0.5355	0.8089	0.7727	0.6392	0.3882	0.8414	0.5230	0.9563	0.6791	0.0000
		Diplo	0.4644	0.1910	0.2272	0.3607	0.6117	0.1585	0.4769	0.0436	0.3208	0.9962
		Poly	0.0000	0.0000	0.0000	0.0000	0.0000	0.0000	0.0000	0.0000	0.0000	0.0037
Elasmobranchs	399	None	0.2084	0.7128	0.7665	0.6267	0.7677	0.6117	0.9363	0.6878	0.9338	0.6304
		Diplo	0.7915	0.2871	0.2334	0.3732	0.2322	0.3882	0.0636	0.3121	0.0661	0.3695
		Poly	0.0000	0.0000	0.0000	0.0000	0.0000	0.0000	0.0000	0.0000	0.0000	0.0000
Holocephalans	388	None	0.0249	0.8277	0.7141	0.3707	0.5593	0.7203	0.9800	0.6267	1.0000	0.6204
		Diplo	0.9750	0.1722	0.2858	0.6292	0.4406	0.2796	0.0199	0.3732	0.0000	0.3795
		Poly	0.0000	0.0000	0.0000	0.0000	0.0000	0.0000	0.0000	0.0000	0.0000	0.0000
Symmoriiformes	419	None	0.7478	0.9987	0.8913	0.9975	1.0000	1.0000	0.9588	0.0274	0.9925	0.9762
		Diplo	0.2521	0.0012	0.1086	0.0024	0.0000	0.0000	0.0411	0.9563	0.0074	0.0237
		Poly	0.0000	0.0000	0.0000	0.0000	0.0000	0.0000	0.0000	0.0162	0.0000	0.0000
All Osteichthyans	244	None	0.7378	0.9350	0.7028	0.2259	0.9213	0.2671	0.5393	0.9812	0.9388	0.8401
		Diplo	0.2621	0.0649	0.2971	0.7740	0.0786	0.7328	0.4606	0.0187	0.0611	0.1598
		Poly	0.0000	0.0000	0.0000	0.0000	0.0000	0.0000	0.0000	0.0000	0.0000	0.0000
Tetrapodomorphs	358	None	0.8464	0.9612	0.9200	0.8426	0.9925	0.9051	0.9313	0.8014	0.6491	0.8789
		Diplo	0.1535	0.0387	0.0799	0.1573	0.0074	0.0948	0.0686	0.1985	0.3508	0.1210
		Poly	0.0000	0.0000	0.0000	0.0000	0.0000	0.0000	0.0000	0.0000	0.0000	0.0000
Coealacanths	289	None	0.3470	1.0000	0.4481	0.7802	0.8976	0.6479	0.8751	0.8339	0.6816	1.0000
		Diplo	0.6529	0.0000	0.5518	0.2197	0.1023	0.3520	0.1248	0.1660	0.3183	0.0000
		Poly	0.0000	0.0000	0.0000	0.0000	0.0000	0.0000	0.0000	0.0000	0.0000	0.0000
Porolepiforms	317	None	0.8164	0.9975	0.6916	0.8701	0.9313	0.9300	0.8414	0.7815	0.5680	0.9363
		Diplo	0.1835	0.0024	0.3083	0.1298	0.0686	0.0699	0.1585	0.2184	0.4319	0.0636
		Poly	0.0000	0.0000	0.0000	0.0000	0.0000	0.0000	0.0000	0.0000	0.0000	0.0000
Lungfish	325	None	0.9975	0.9200	0.8501	0.9288	0.8551	0.8764	0.9700	0.9488	0.8526	0.8701
		Diplo	0.0024	0.0799	0.1498	0.0711	0.1448	0.1235	0.0299	0.0511	0.1473	0.1298
		Poly	0.0000	0.0000	0.0000	0.0000	0.0000	0.0000	0.0000	0.0000	0.0000	0.0000
All actinopterygians	250	None	0.6641	0.7315	0.8988	1.0000	0.9962	0.9912	0.8726	0.5767	0.7840	0.9313
		Diplo	0.3358	0.2684	0.1011	0.0000	0.0037	0.0087	0.1273	0.4232	0.2159	0.0686
		Poly	0.0000	0.0000	0.0000	0.0000	0.0000	0.0000	0.0000	0.0000	0.0000	0.0000
Neopterygians	266	None	1.0000	1.0000	0.7428	0.9151	0.8214	0.8377	0.9350	1.0000	0.8139	0.8127
		Diplo	0.0000	0.0000	0.2571	0.0848	0.1785	0.1622	0.0649	0.0000	0.1860	0.1872
		Poly	0.0000	0.0000	0.0000	0.0000	0.0000	0.0000	0.0000	0.0000	0.0000	0.0000
Teleosts	267	None	1.0000	1.0000	0.6529	0.8776	0.9987	0.4756	0.9925	0.9950	0.5605	0.7003
		Diplo	0.0000	0.0000	0.3470	0.1223	0.0012	0.5243	0.0074	0.0049	0.4394	0.2996
		Poly	0.0000	0.0000	0.0000	0.0000	0.0000	0.0000	0.0000	0.0000	0.0000	0.0000
Crown gnathostomes	243	None	0.8064	0.8714	0.6092	0.1298	0.9151	0.3682	0.5205	0.9026	0.9563	0.8701
		Diplo	0.1935	0.1285	0.3907	0.8701	0.0848	0.6317	0.4794	0.0973	0.0436	0.1298
		Poly	0.0000	0.0000	0.0000	0.0000	0.0000	0.0000	0.0000	0.0000	0.0000	0.0000
Stem gnathostomes	234	None	0.7153	0.7640	0.3895	0.2996	0.9263	0.8327	0.2958	0.9213	0.8227	0.9925
		Diplo	0.2846	0.2359	0.6104	0.7003	0.0736	0.1672	0.7041	0.0786	0.1772	0.0074
		Poly	0.0000	0.0000	0.0000	0.0000	0.0000	0.0000	0.0000	0.0000	0.0000	0.0000

Appendix 7: Threshold model ancestral state reconstruction results plotted on supertrees

This appendix includes supertrees on which are plotted the results from threshold model ancestral state reconstruction analyses for centra, anterior fusions, and polyspondyly. Each tree represents a stochastically sampled time-scaled tree using the paleotree R package. Threshold model analyses were run ten times on each tree to provide an estimate of the confidence of the posterior probabilities recovered. Posterior probabilities for each analyes are listed in Appendix 6 (above). For centra, blue indicates absence, green indicates ring centra, and purple indicates full centra. For anterior fusions, blue indicates absence of fusion and red indicates fusion. For polyspondyly, blue indicates absence, orange indicates caudal diplospondyly, and green indicates full polyspondyly.

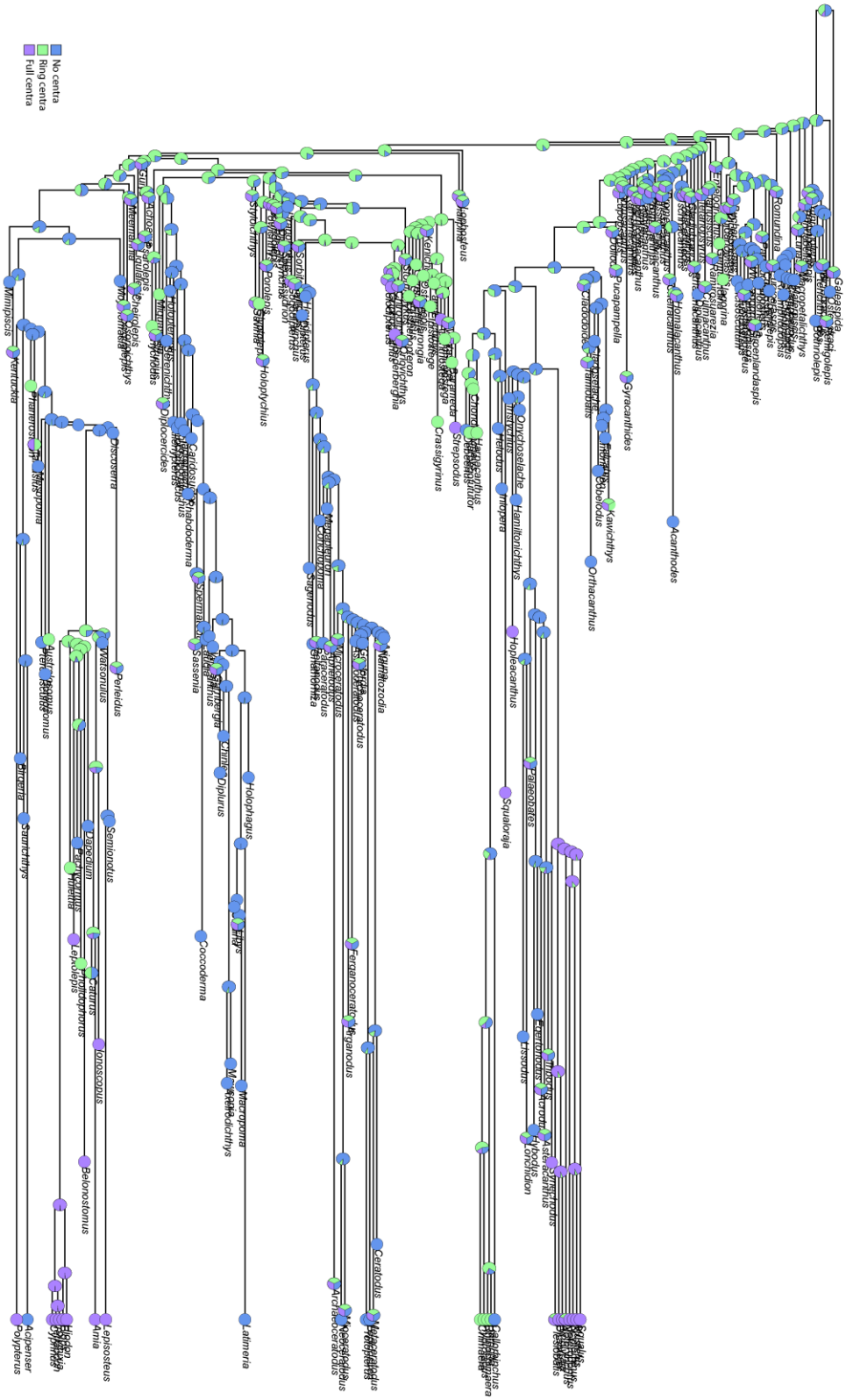

Figure A7.1. Threshold model ancestral state reconstruction for centra on tree 2.

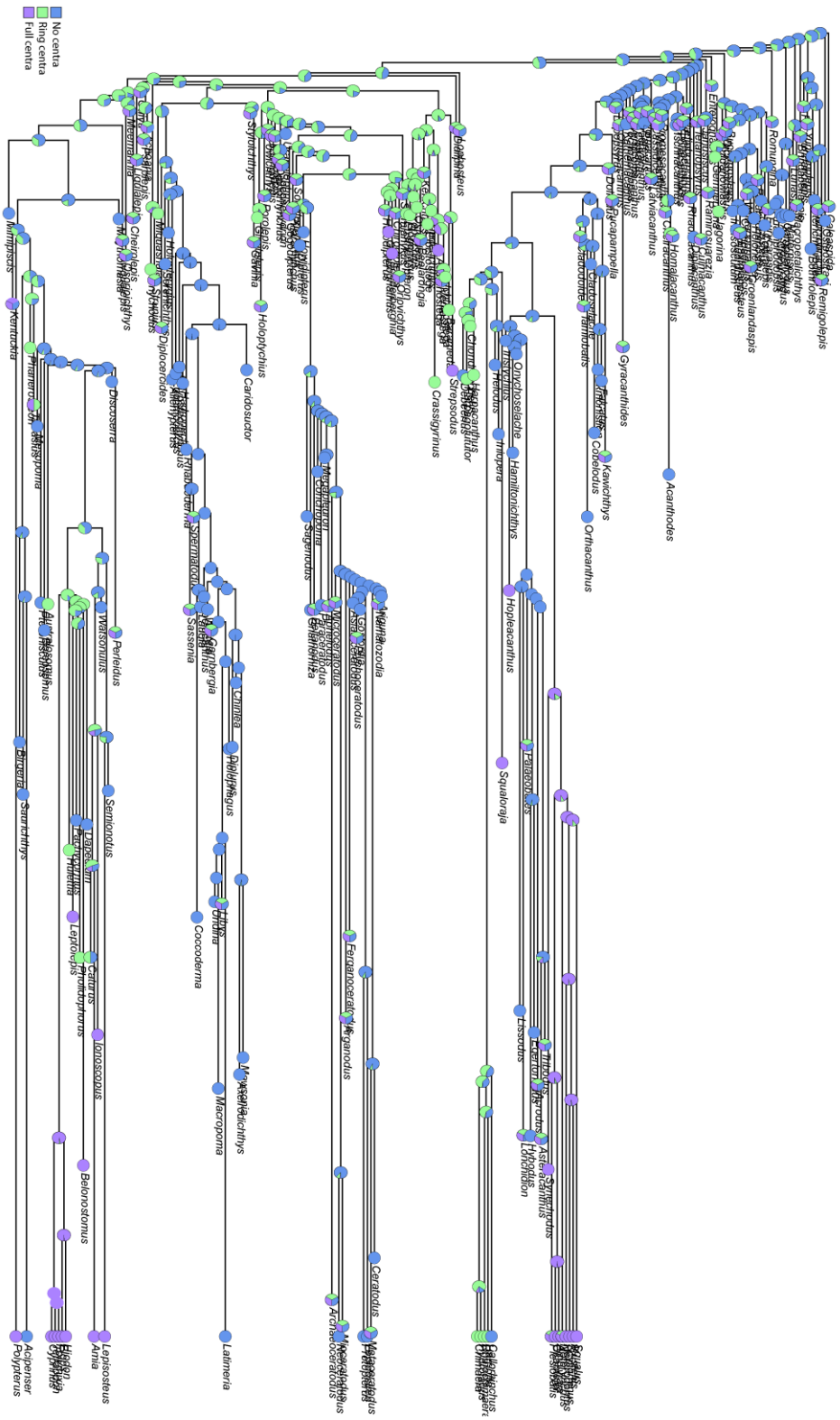

Figure A7.2. Threshold model ancestral state reconstruction for centra on tree 3.

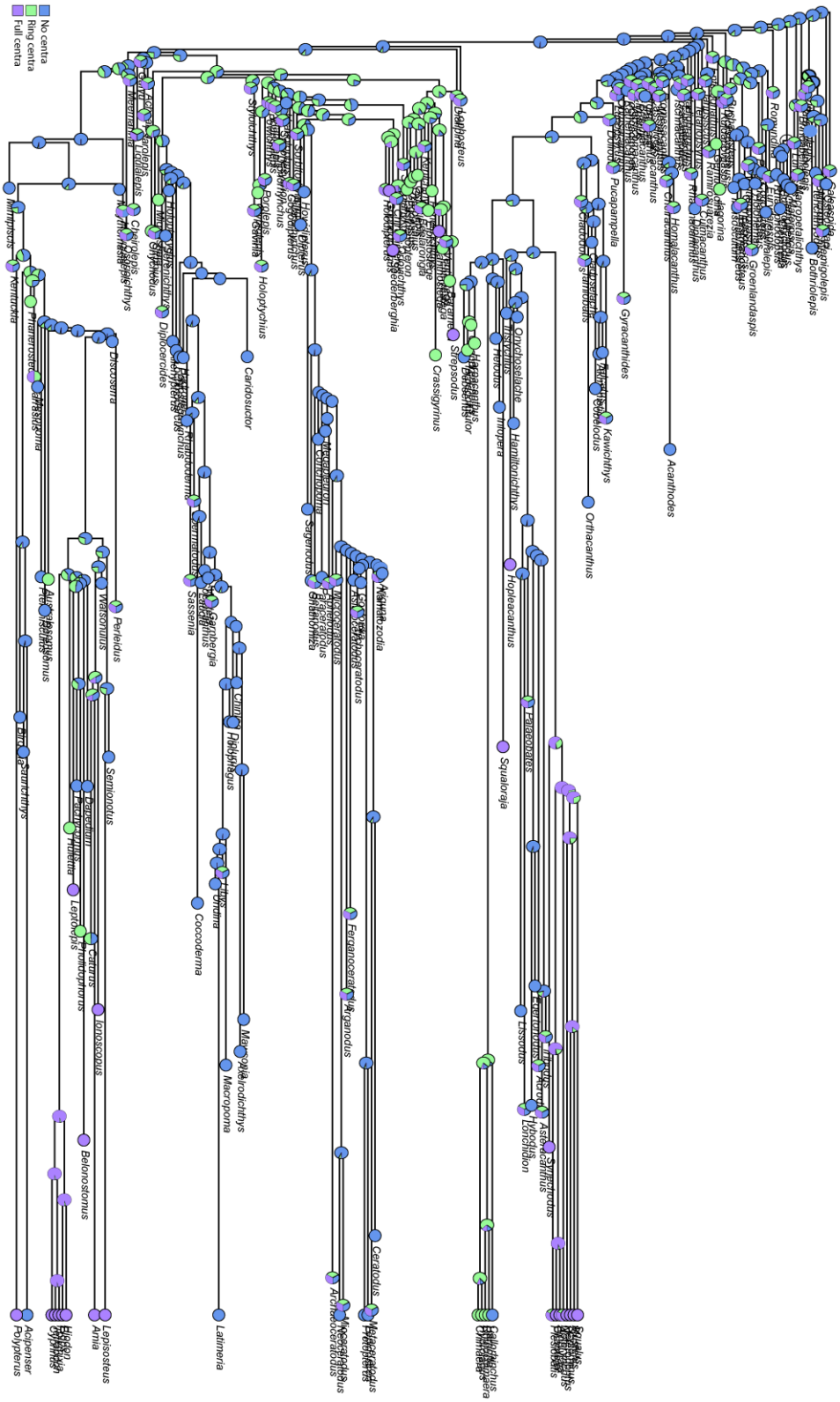

Figure A7.3. Threshold model ancestral state reconstruction for centra on tree 4.

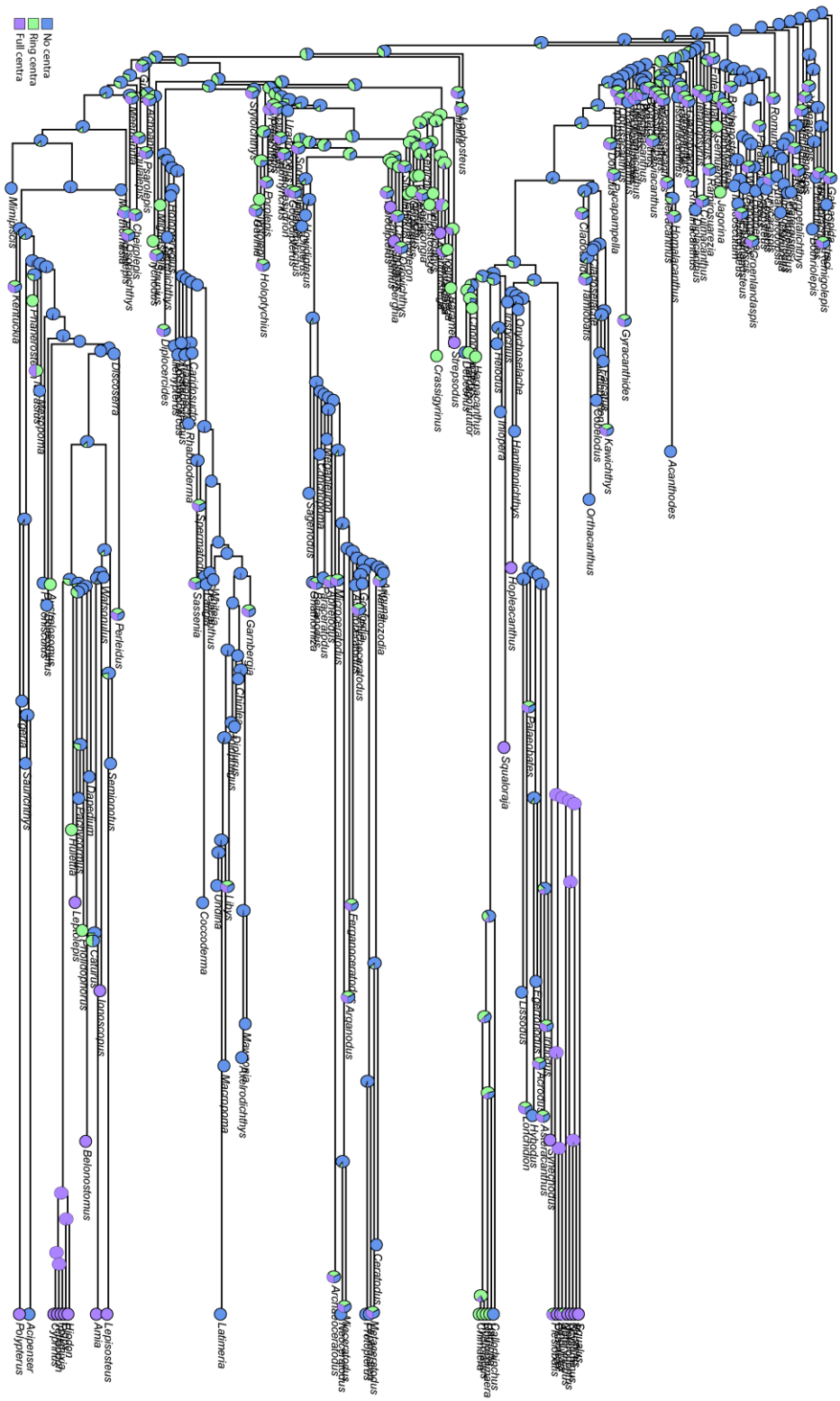

Figure A7.4. Threshold model ancestral state reconstruction for centra on tree 5.

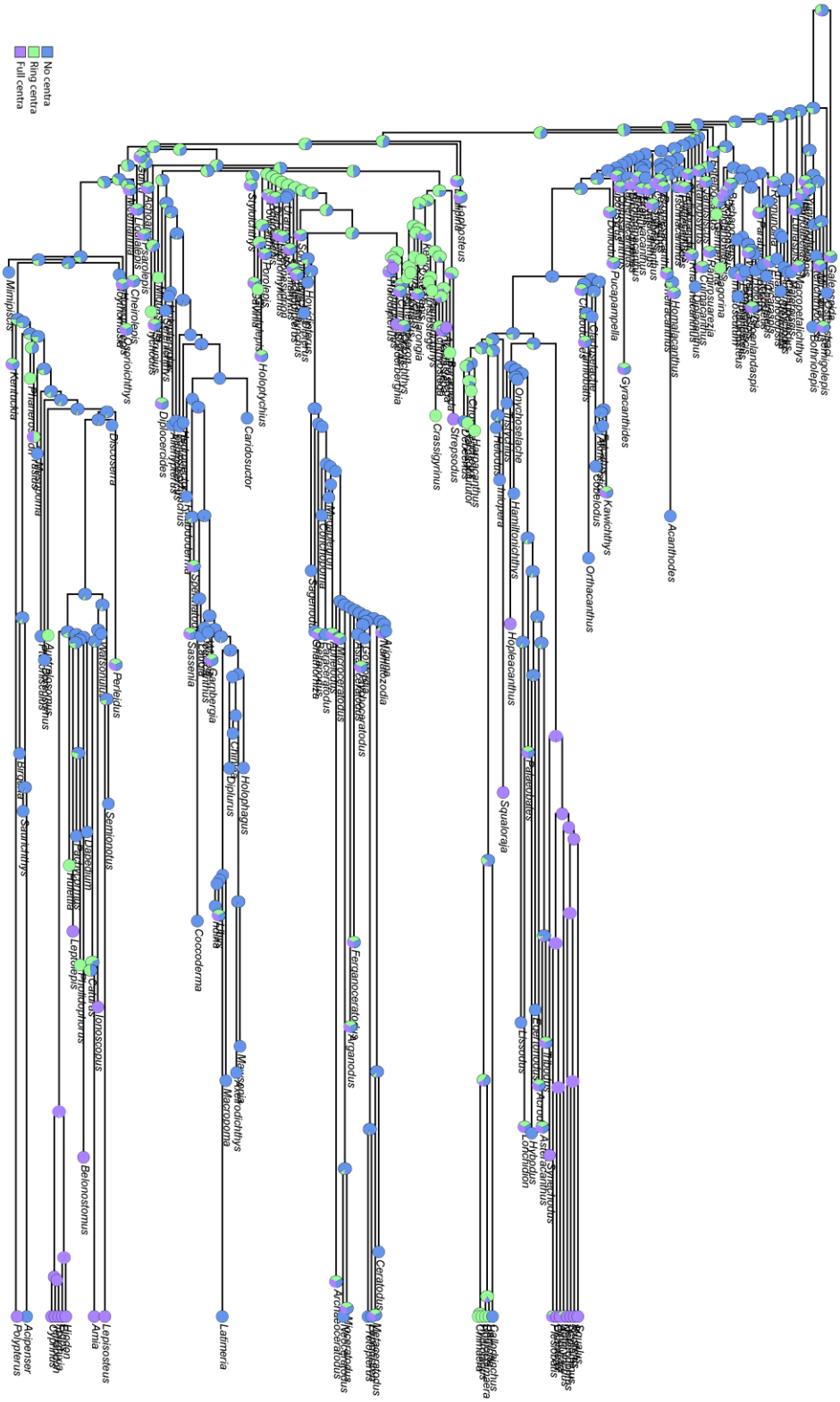

Figure A7.5. Threshold model ancestral state reconstruction for centra on tree 6.

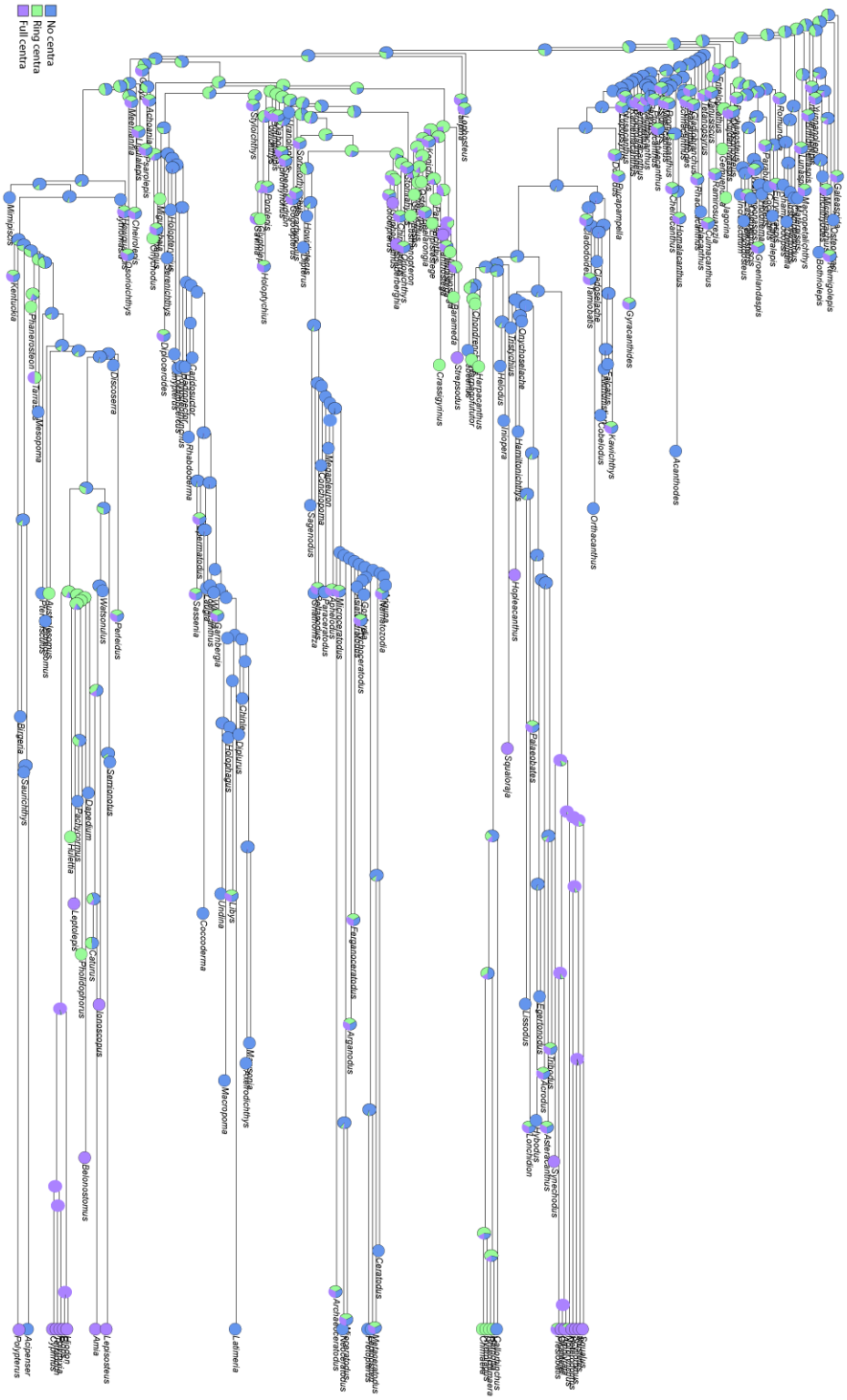

Figure A7.6. Threshold model ancestral state reconstruction for centra on tree 7.

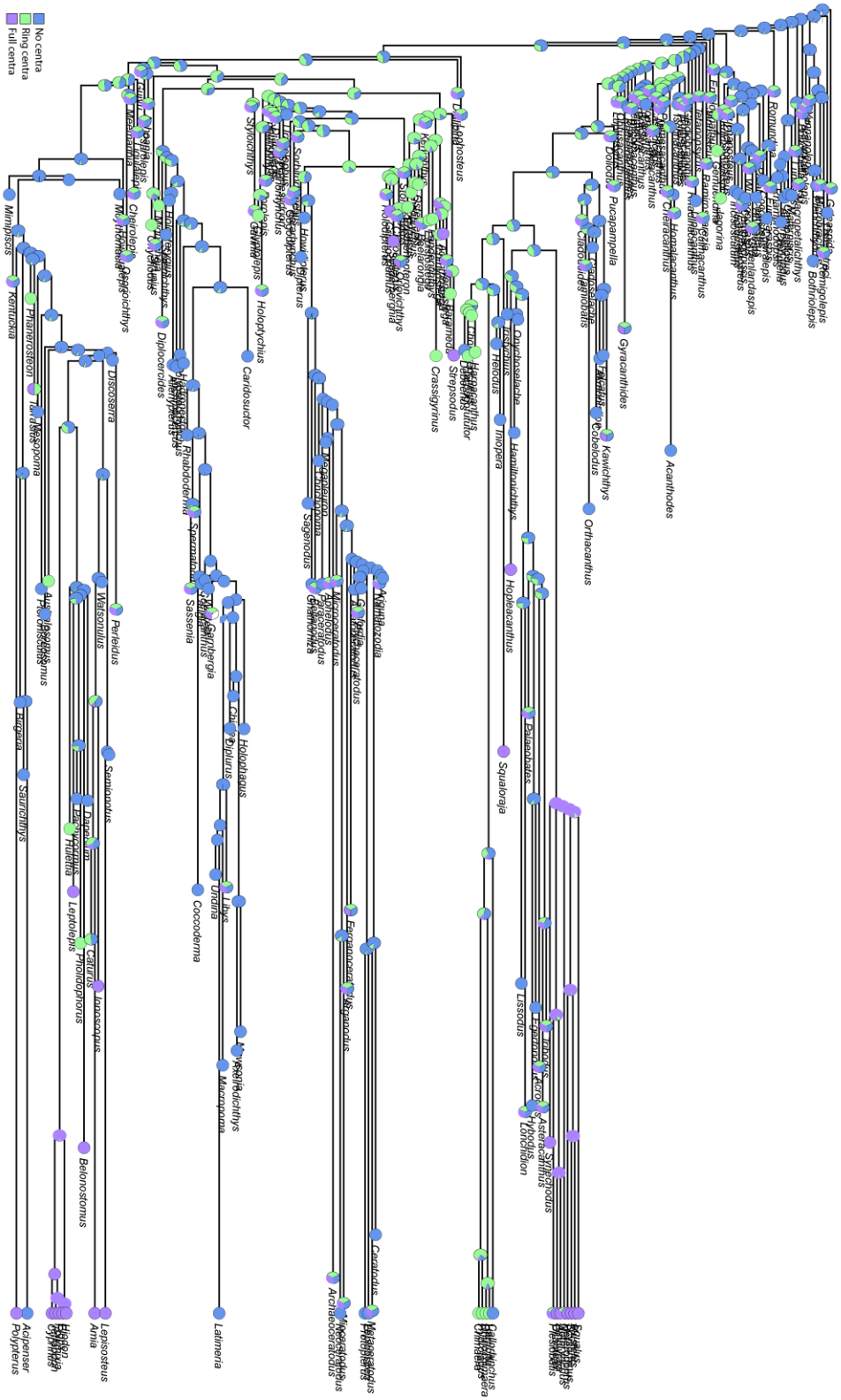

Figure A7.7. Threshold model ancestral state reconstruction for centra on tree 8.

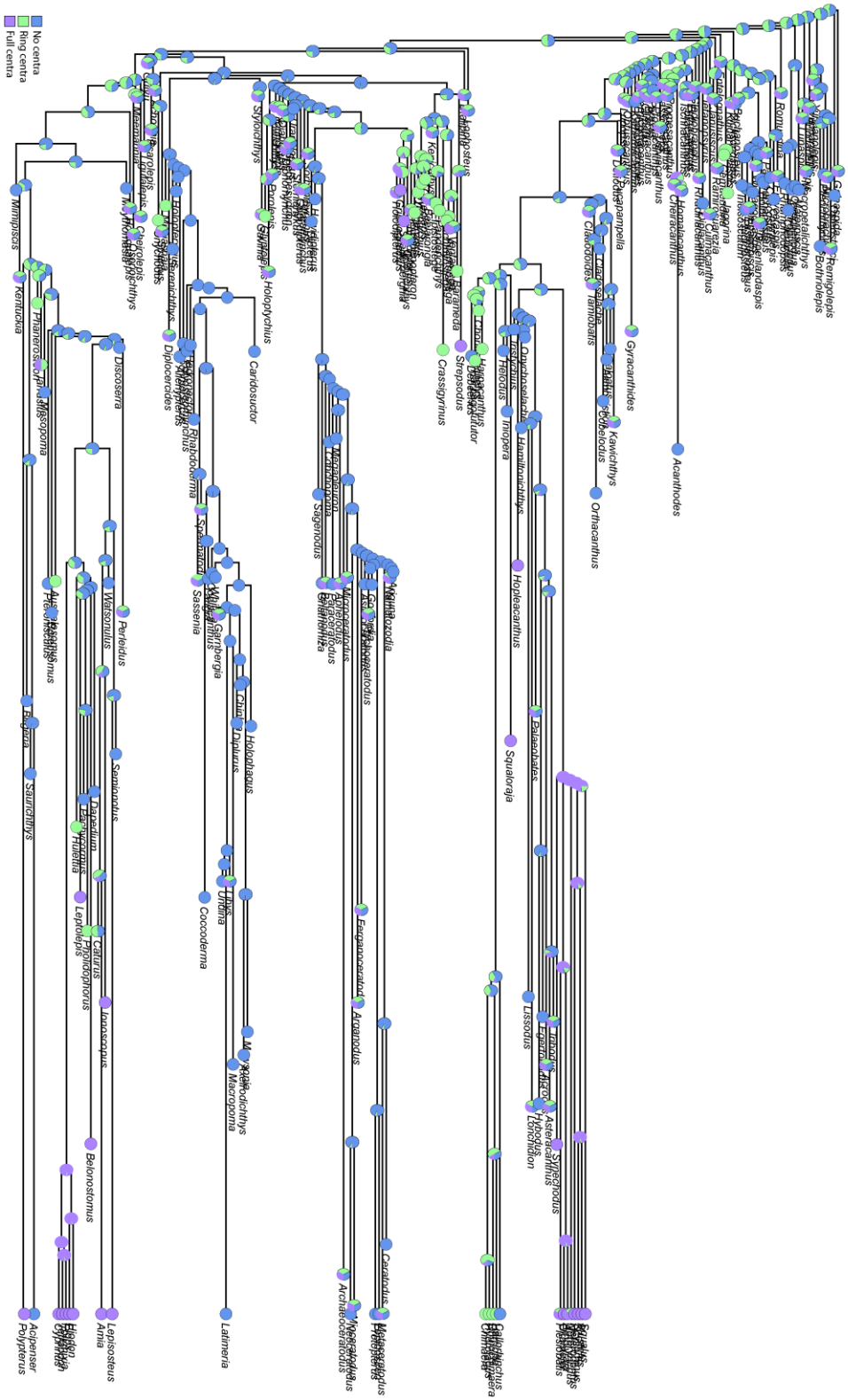

Figure A7.8. Threshold model ancestral state reconstruction for centra on tree 9.

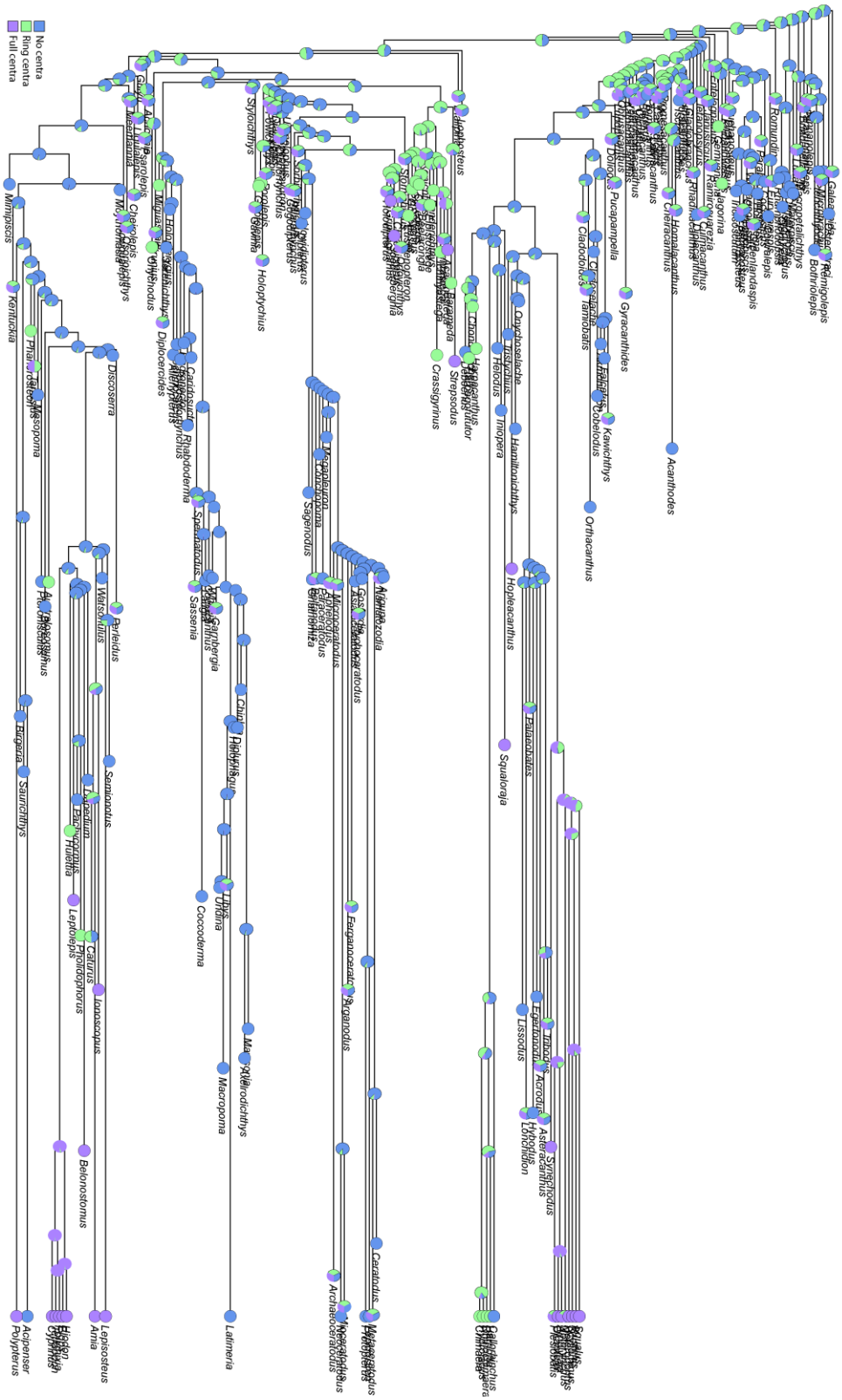

Figure A7.9. Threshold model ancestral state reconstruction for centra on tree 10.

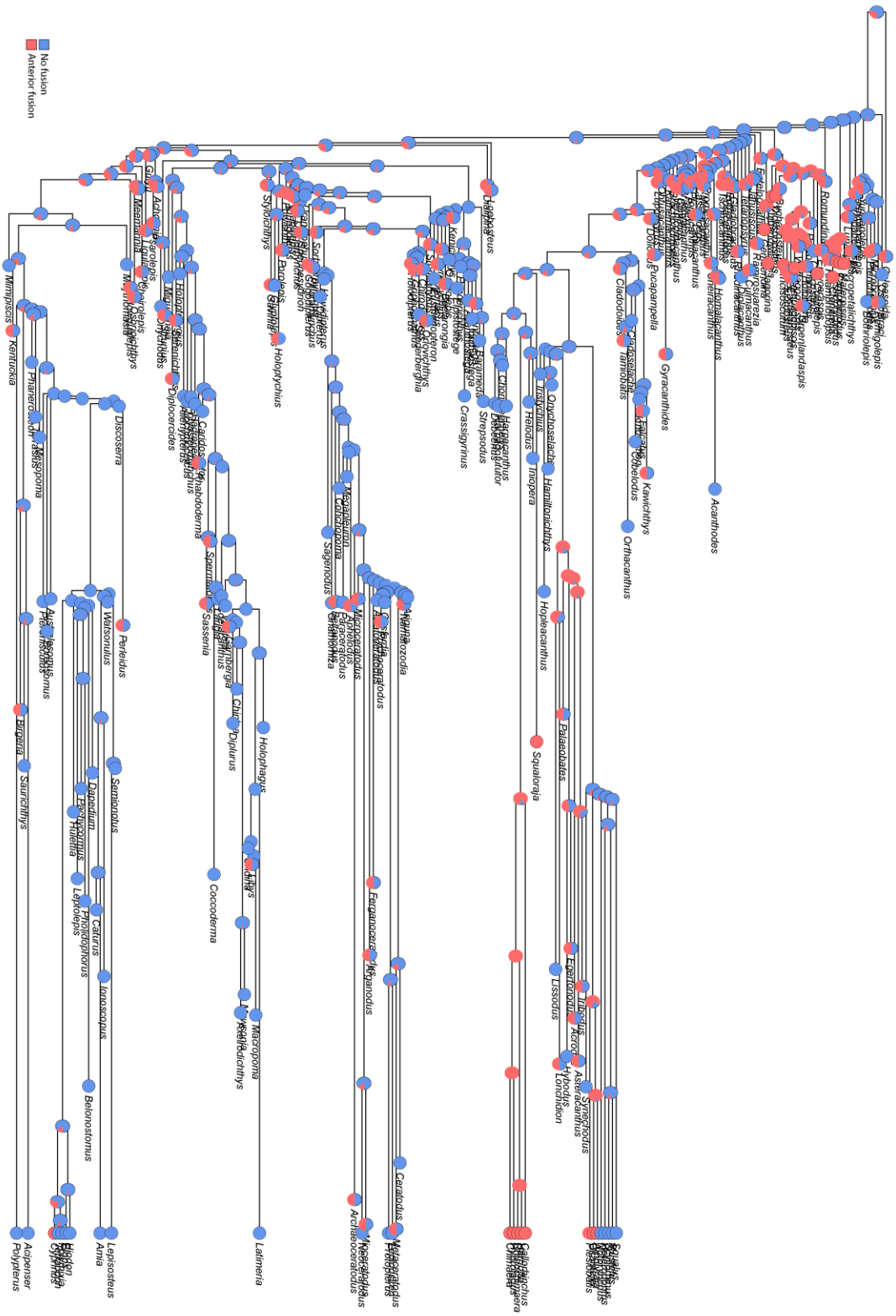

Figure A7.10. Threshold model ancestral state reconstruction for anterior fusions on tree 2.

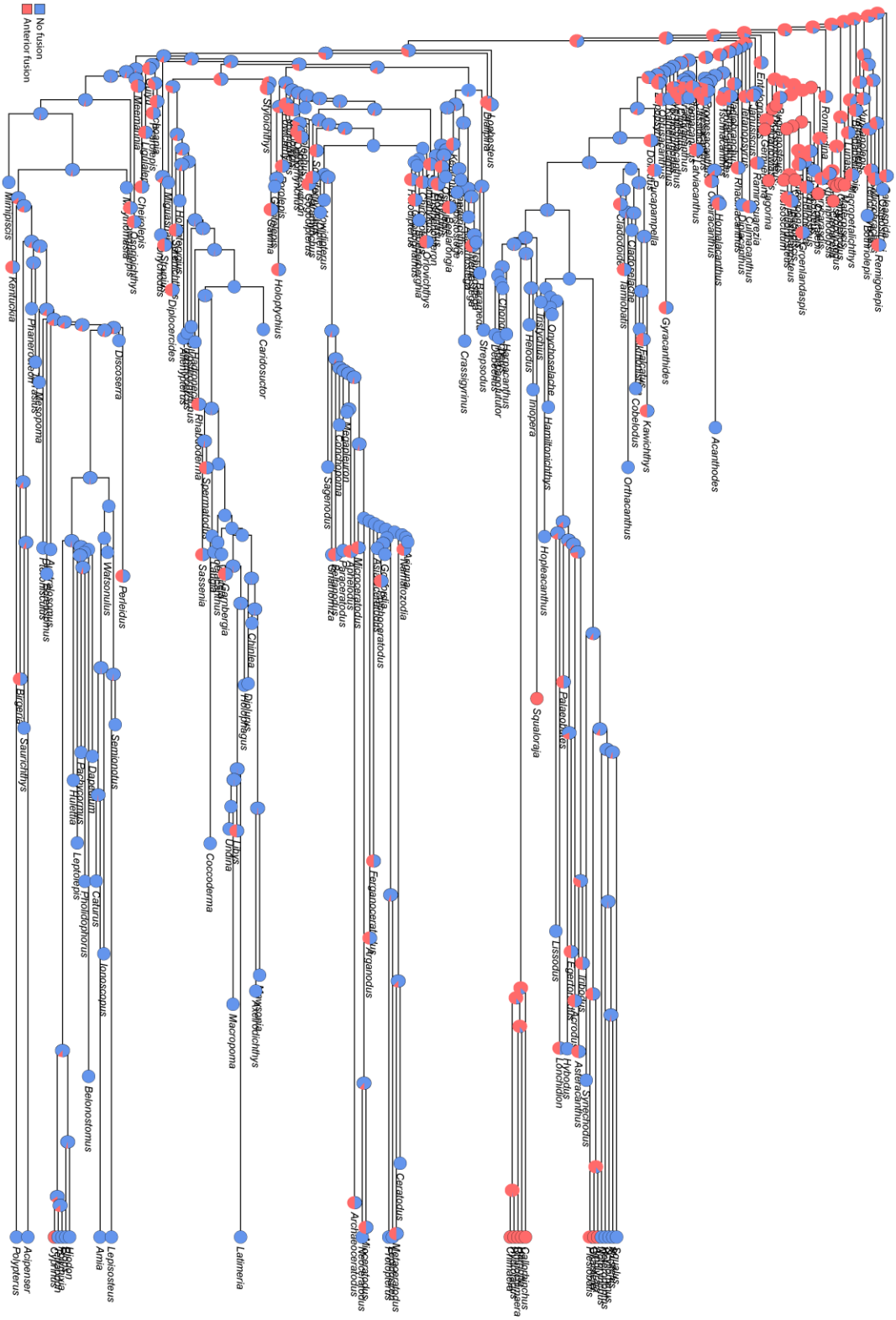

Figure A7.11. Threshold model ancestral state reconstruction for anterior fusions on tree 3.

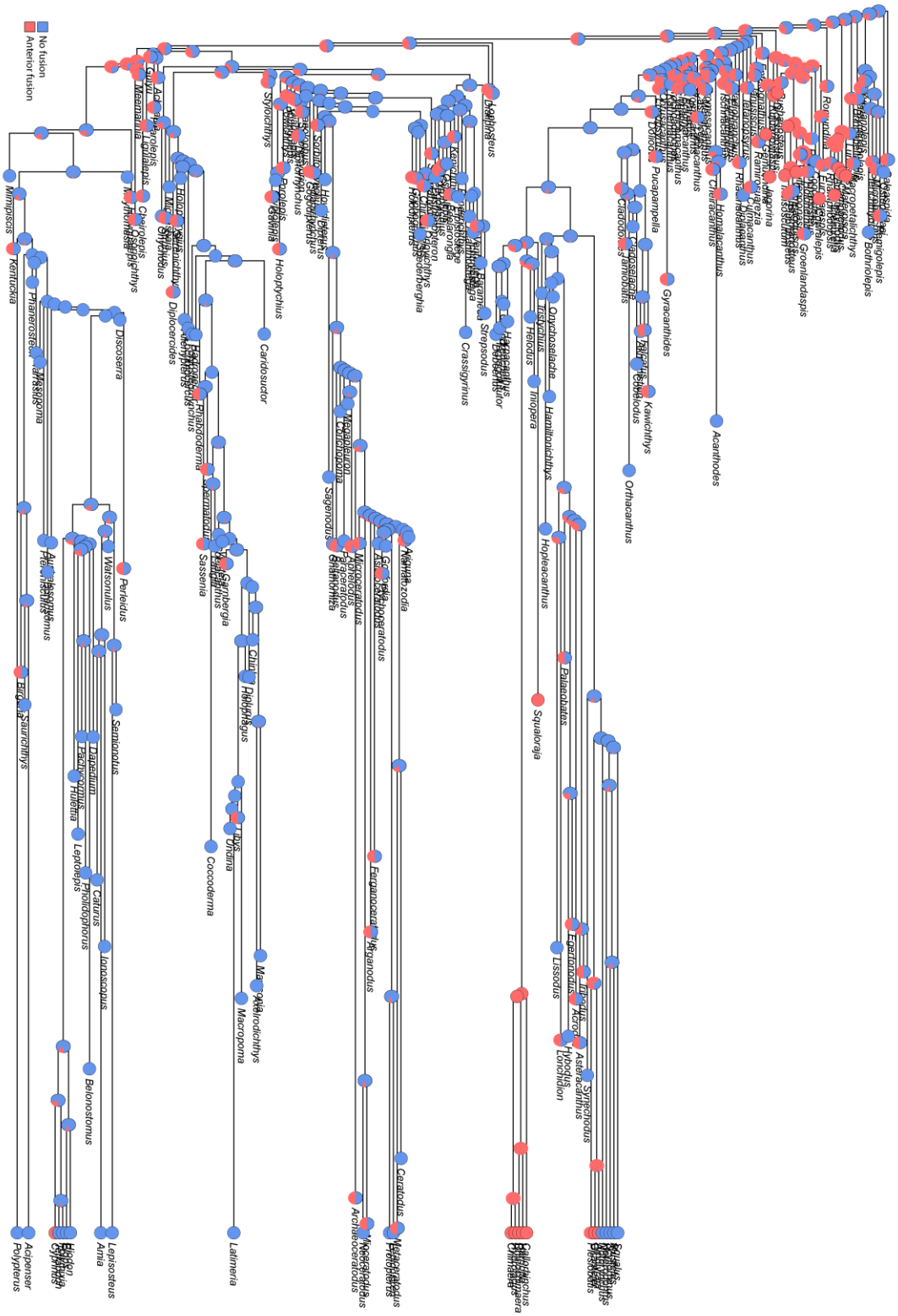

Figure A7.12. Threshold model ancestral state reconstruction for anterior fusions on tree 4.

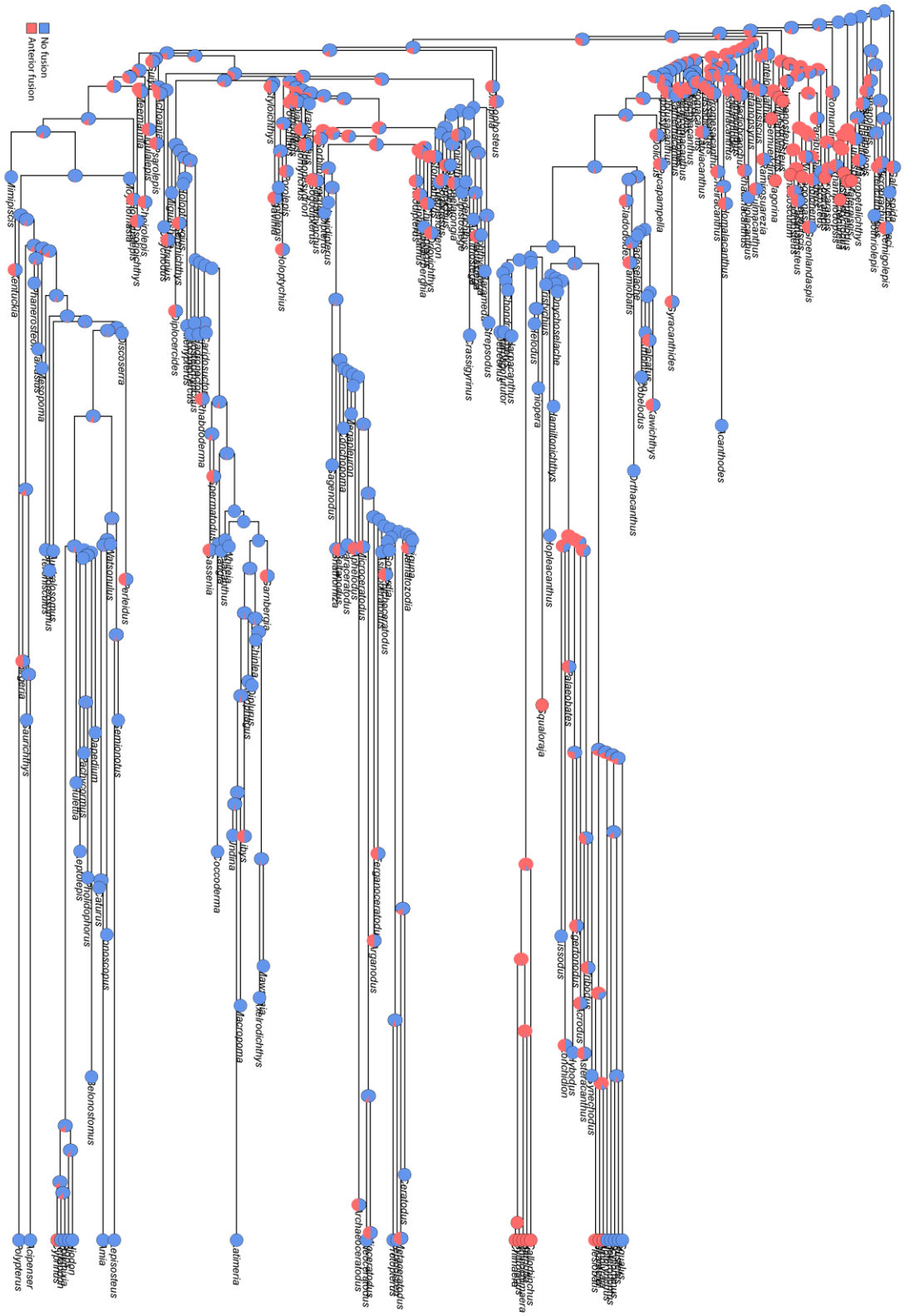

Figure A7.13. Threshold model ancestral state reconstruction for anterior fusions on tree 5.

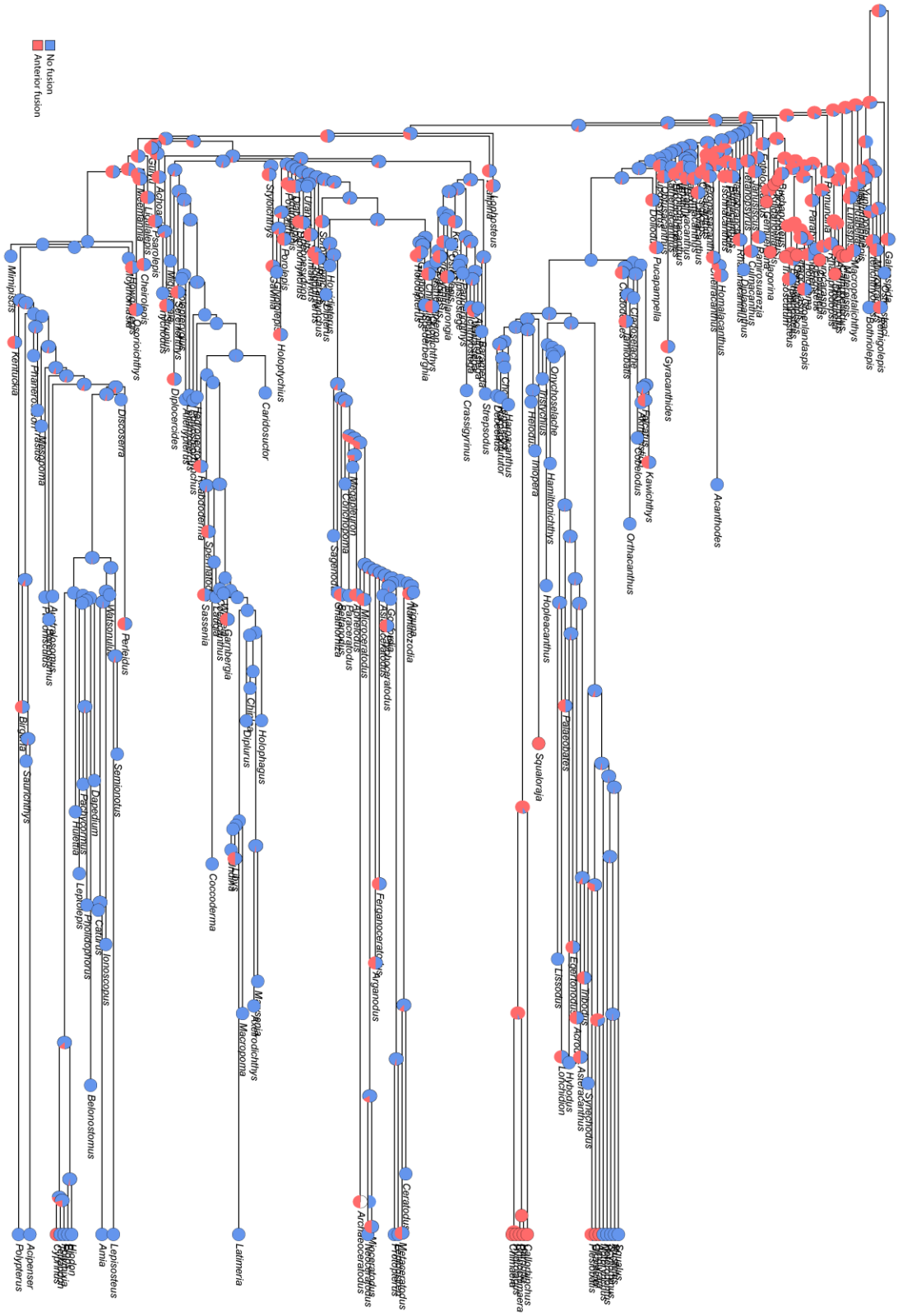

Figure A7.14. Threshold model ancestral state reconstruction for anterior fusions on tree 6.

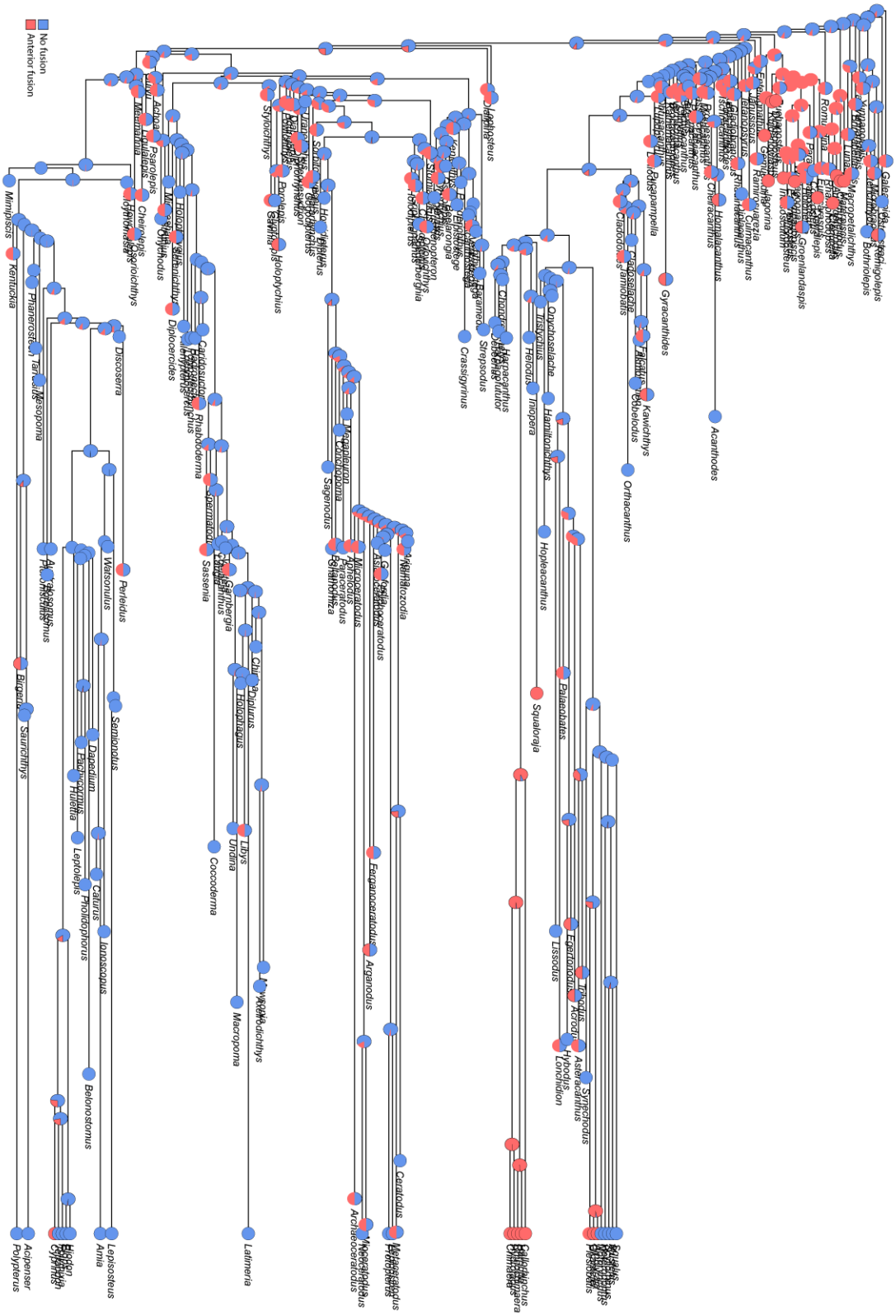

Figure A7.15. Threshold model ancestral state reconstruction for anterior fusions on tree 7.

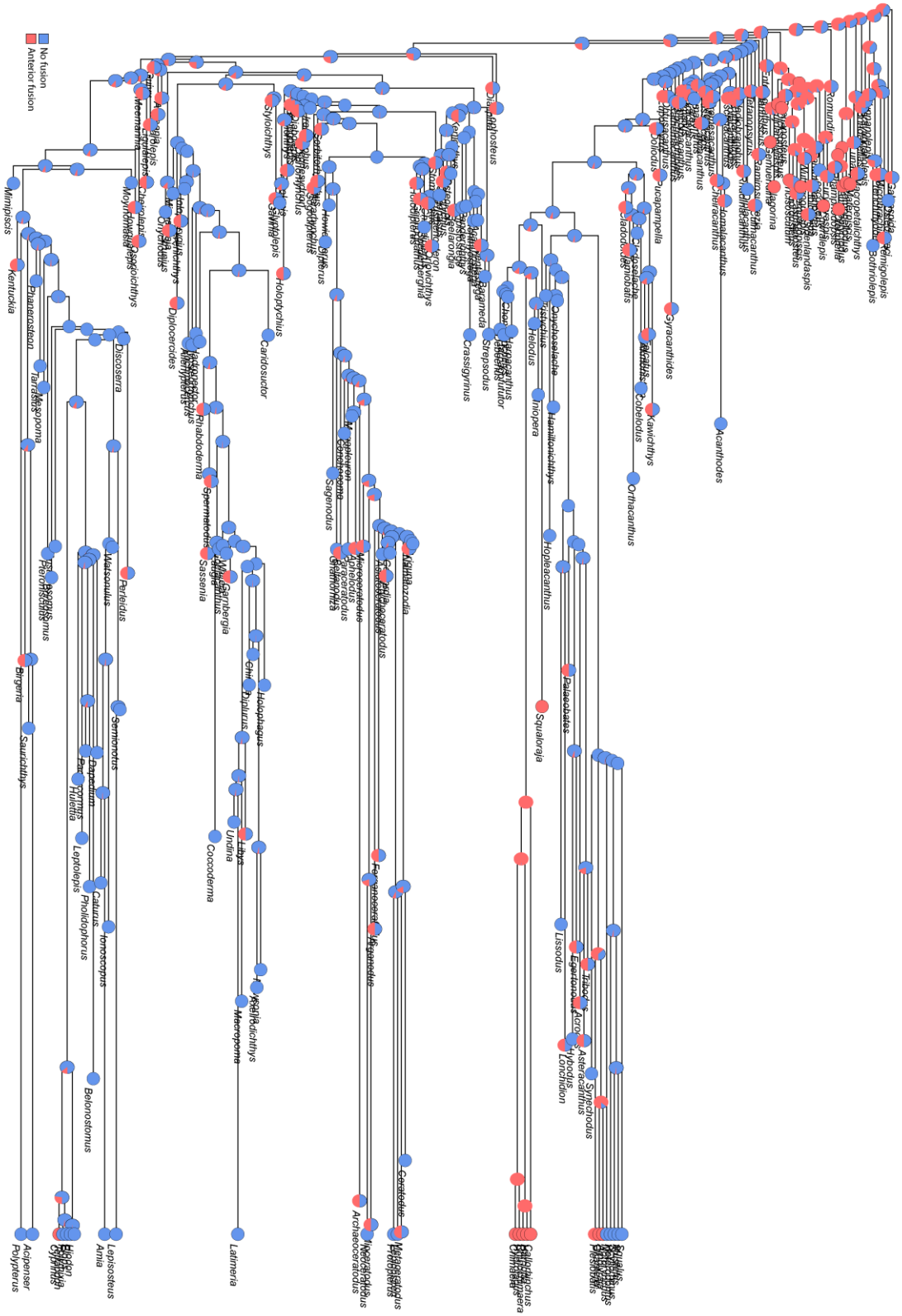

Figure A7.16. Threshold model ancestral state reconstruction for anterior fusions on tree 8.

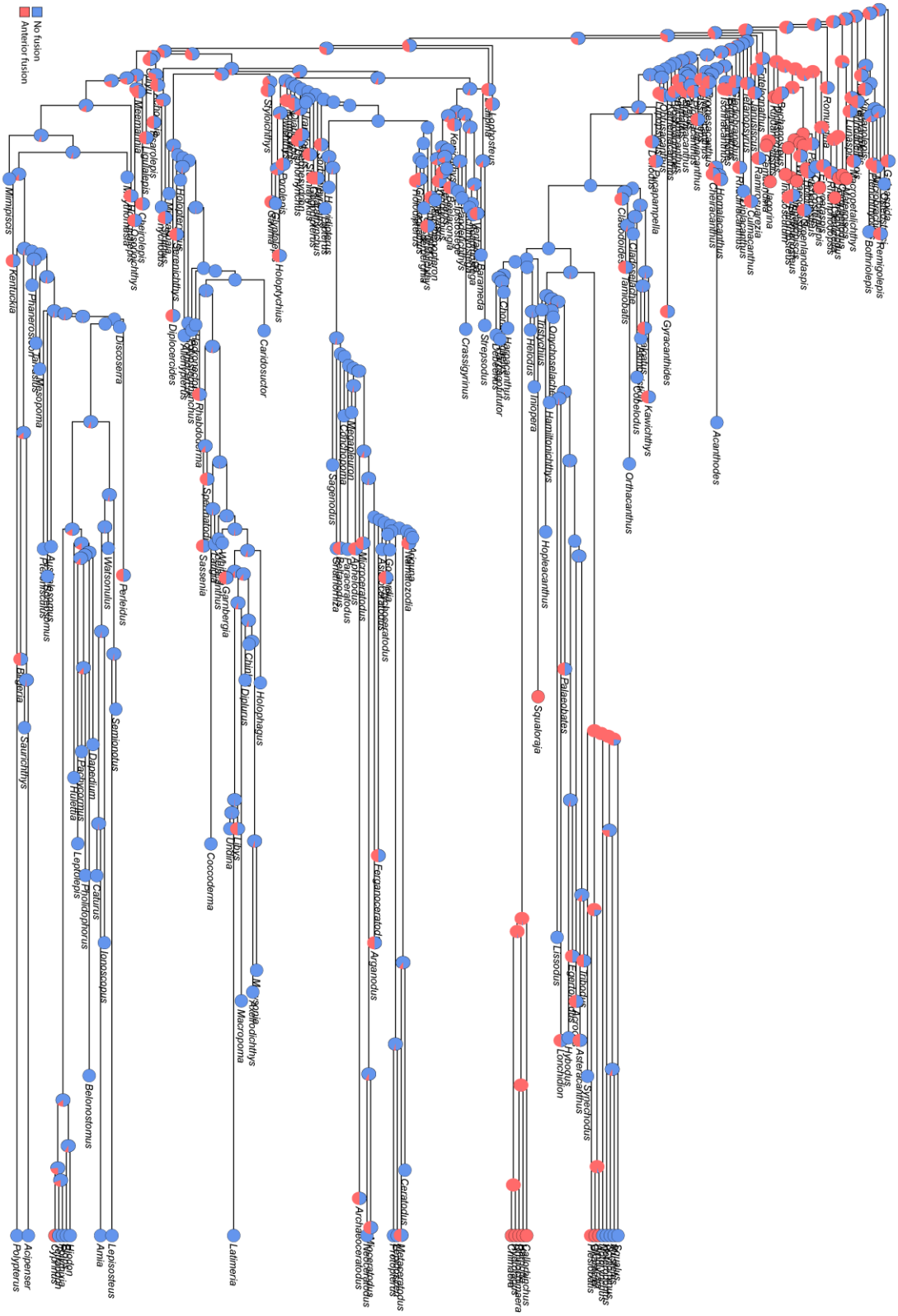

Figure A7.17. Threshold model ancestral state reconstruction for anterior fusions on tree 9.

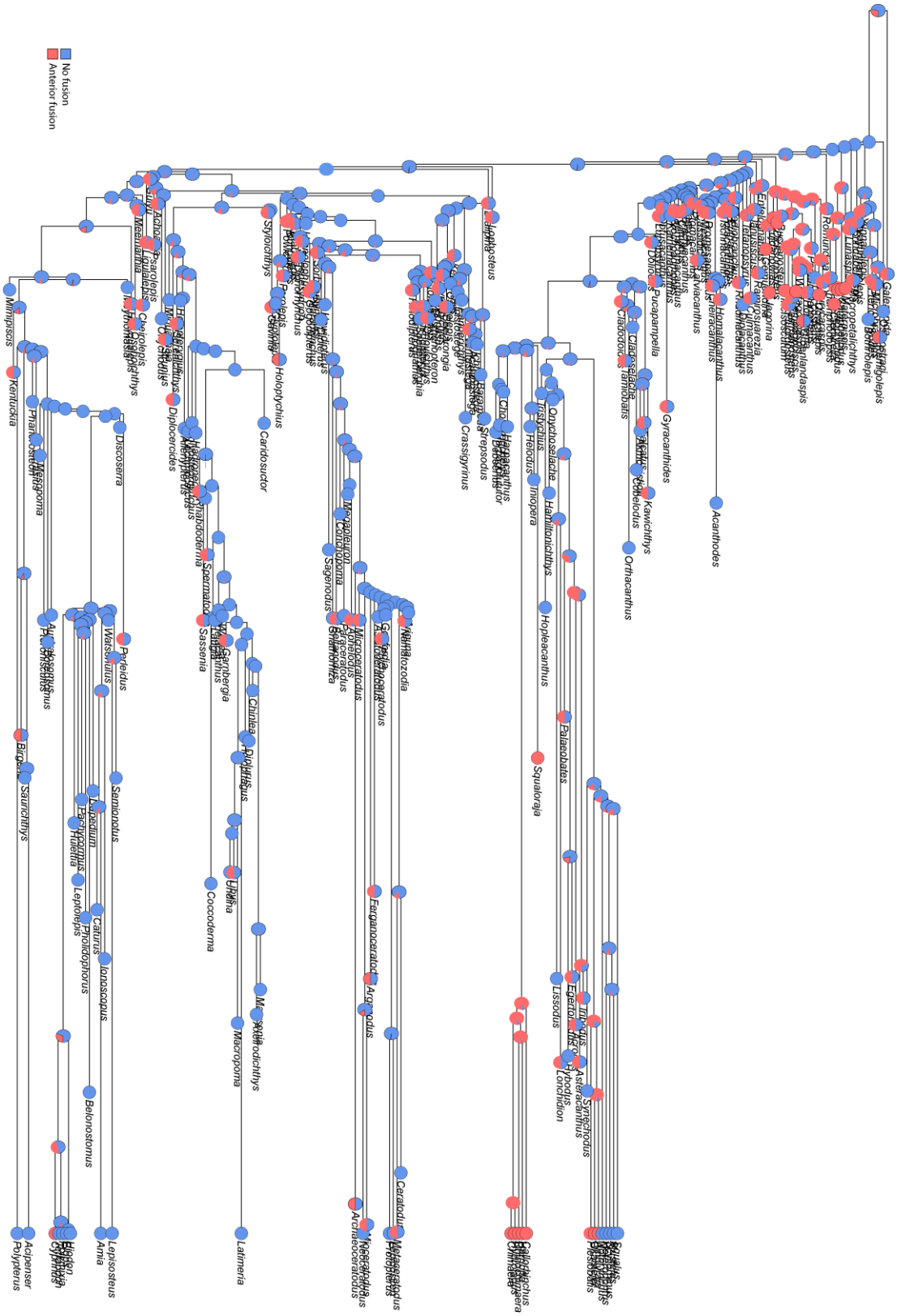

Figure A7.18. Threshold model ancestral state reconstruction for anterior fusions on tree 10.

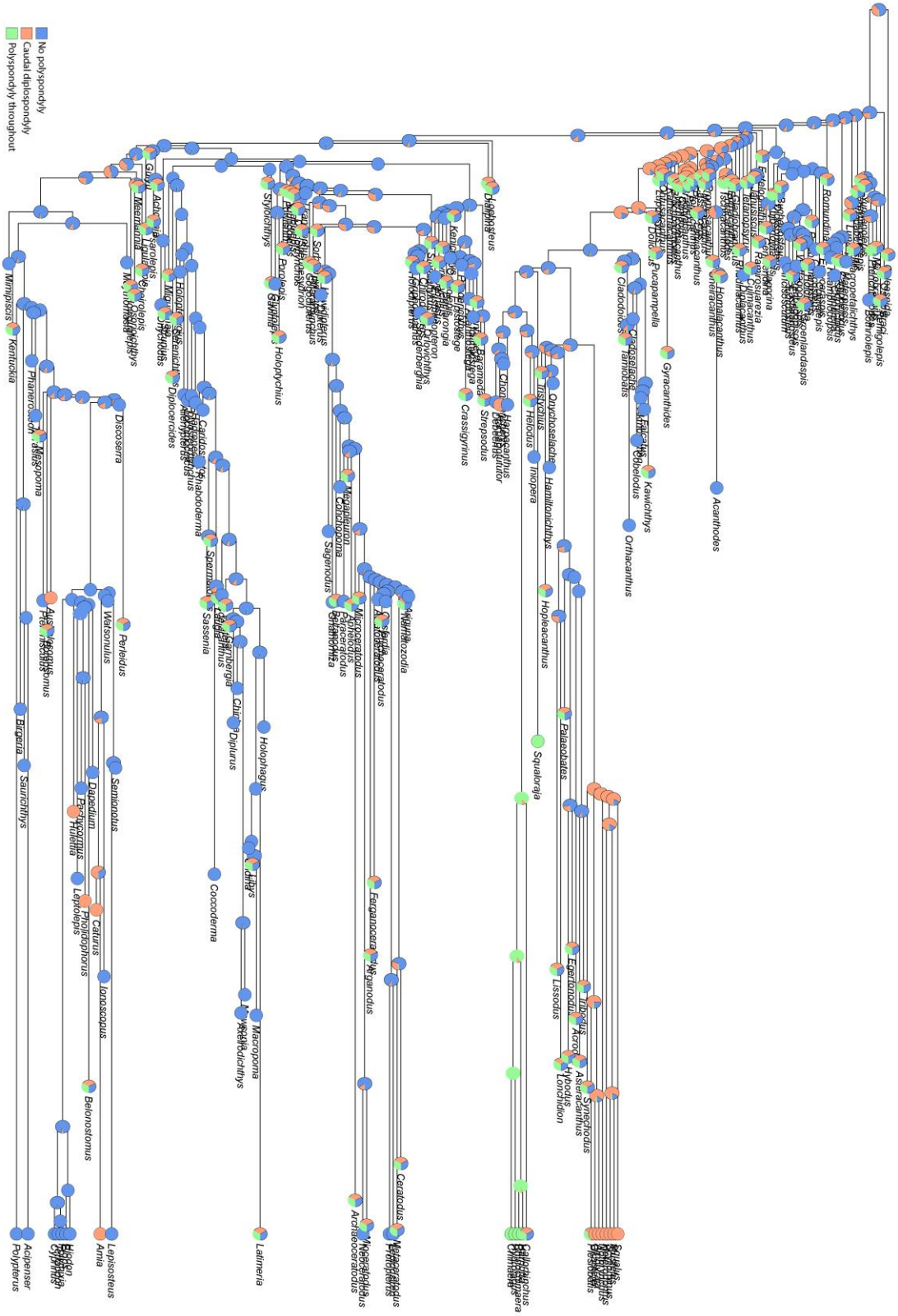

Figure A7.19. Threshold model ancestral state reconstruction for polyspondyly on tree 2.

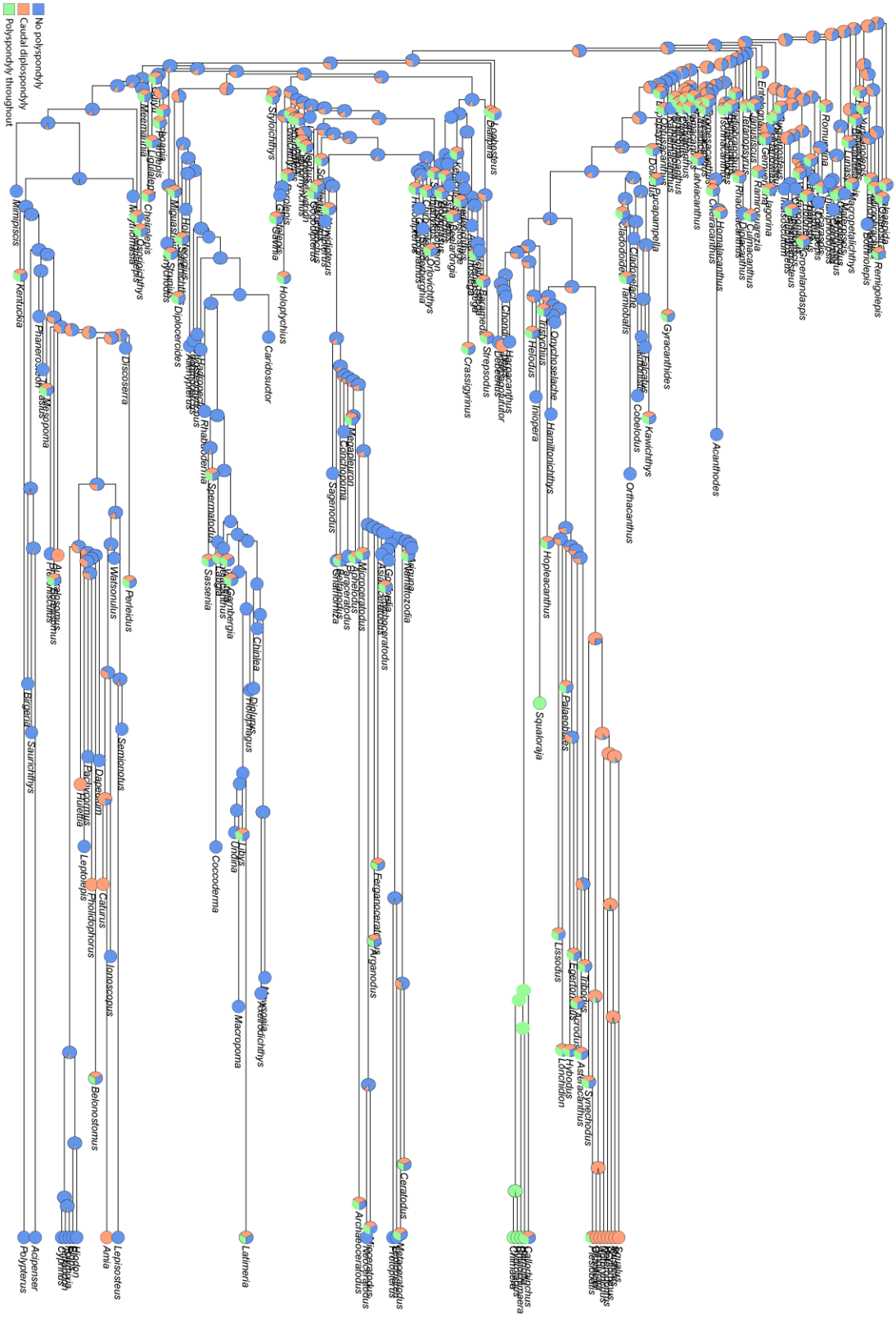

Figure A7.20. Threshold model ancestral state reconstruction for polyspondyly on tree 3.

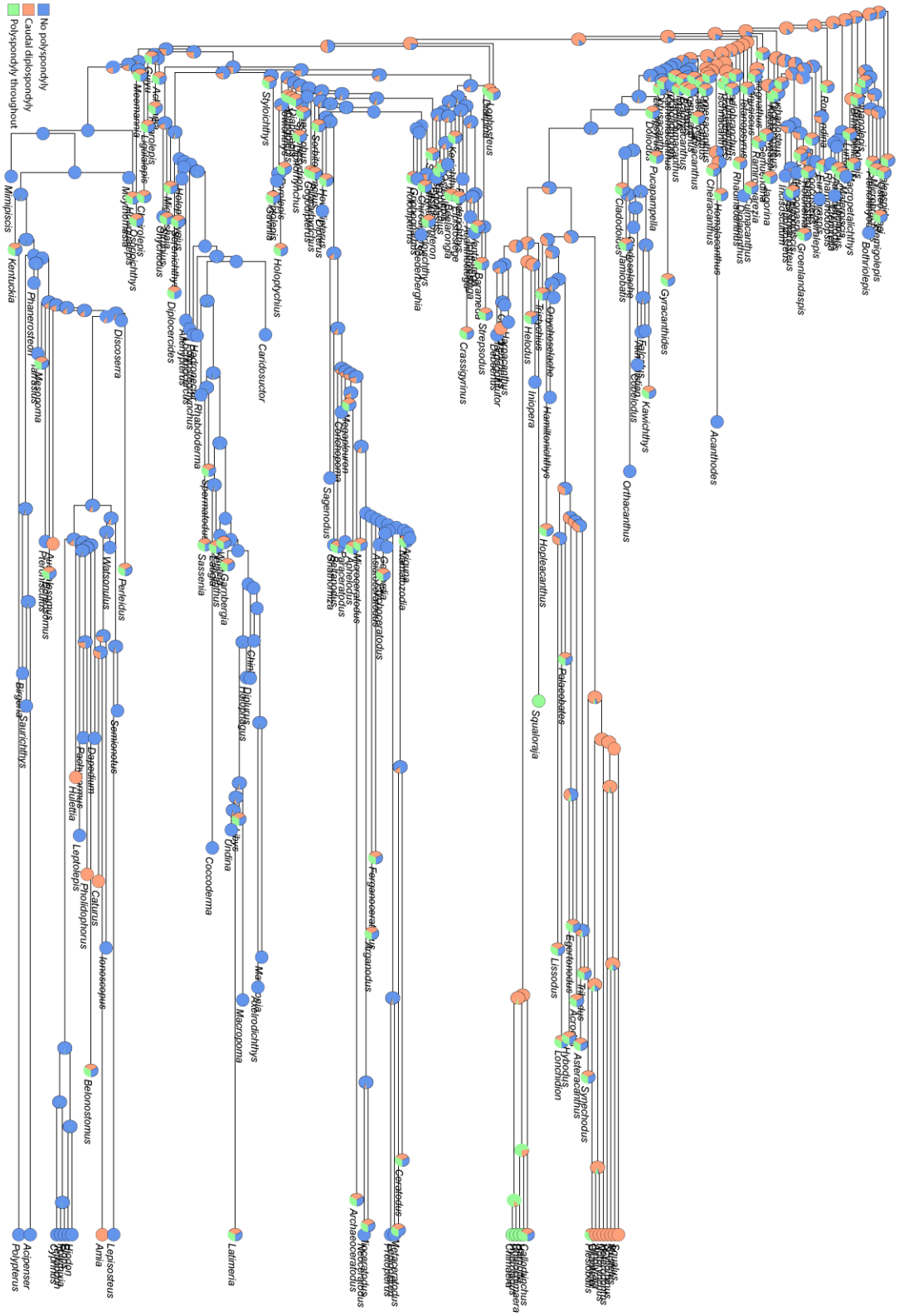

Figure A7.21. Threshold model ancestral state reconstruction for polyspondyly on tree 4.

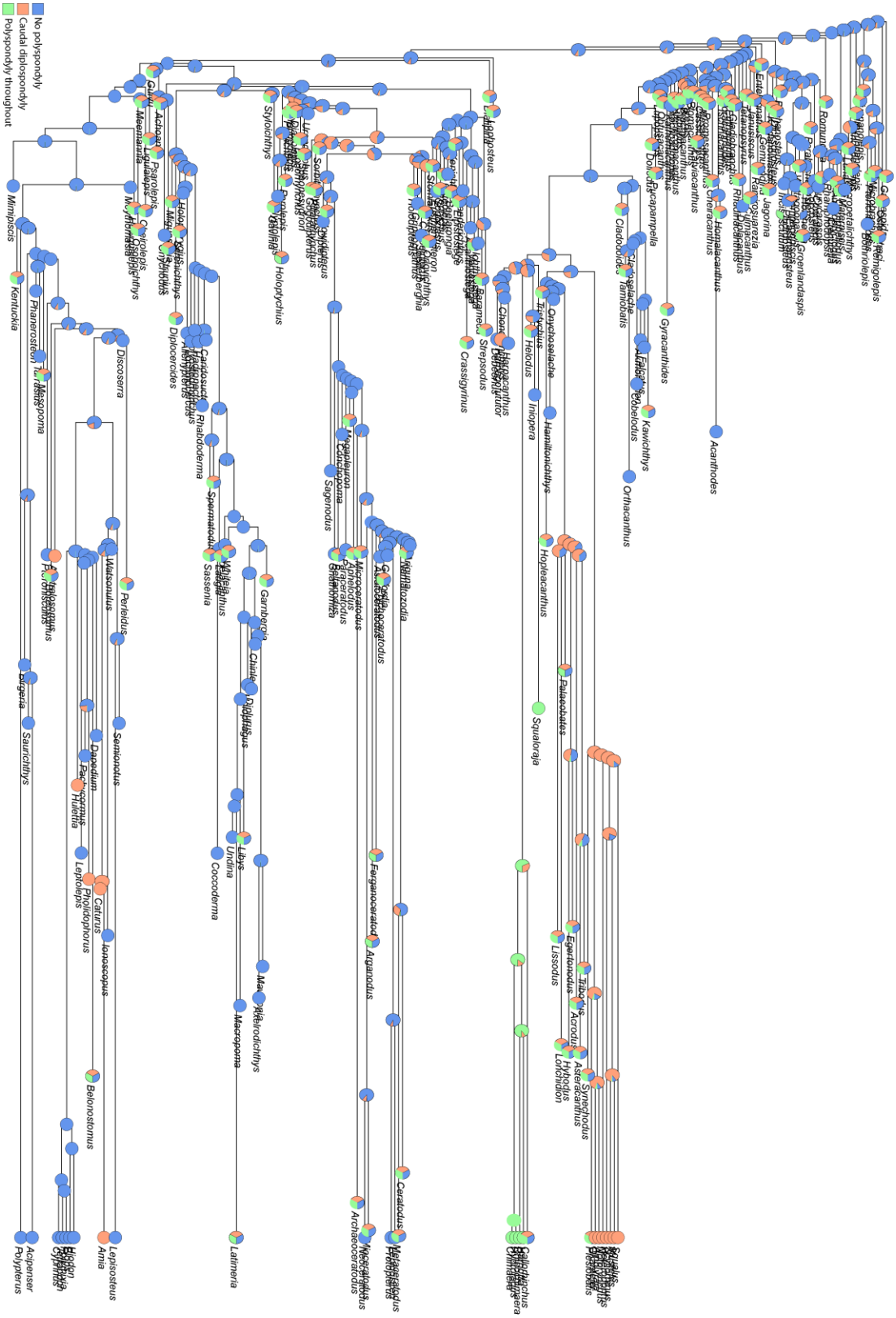

Figure A7.22. Threshold model ancestral state reconstruction for polyspondyly on tree 5.

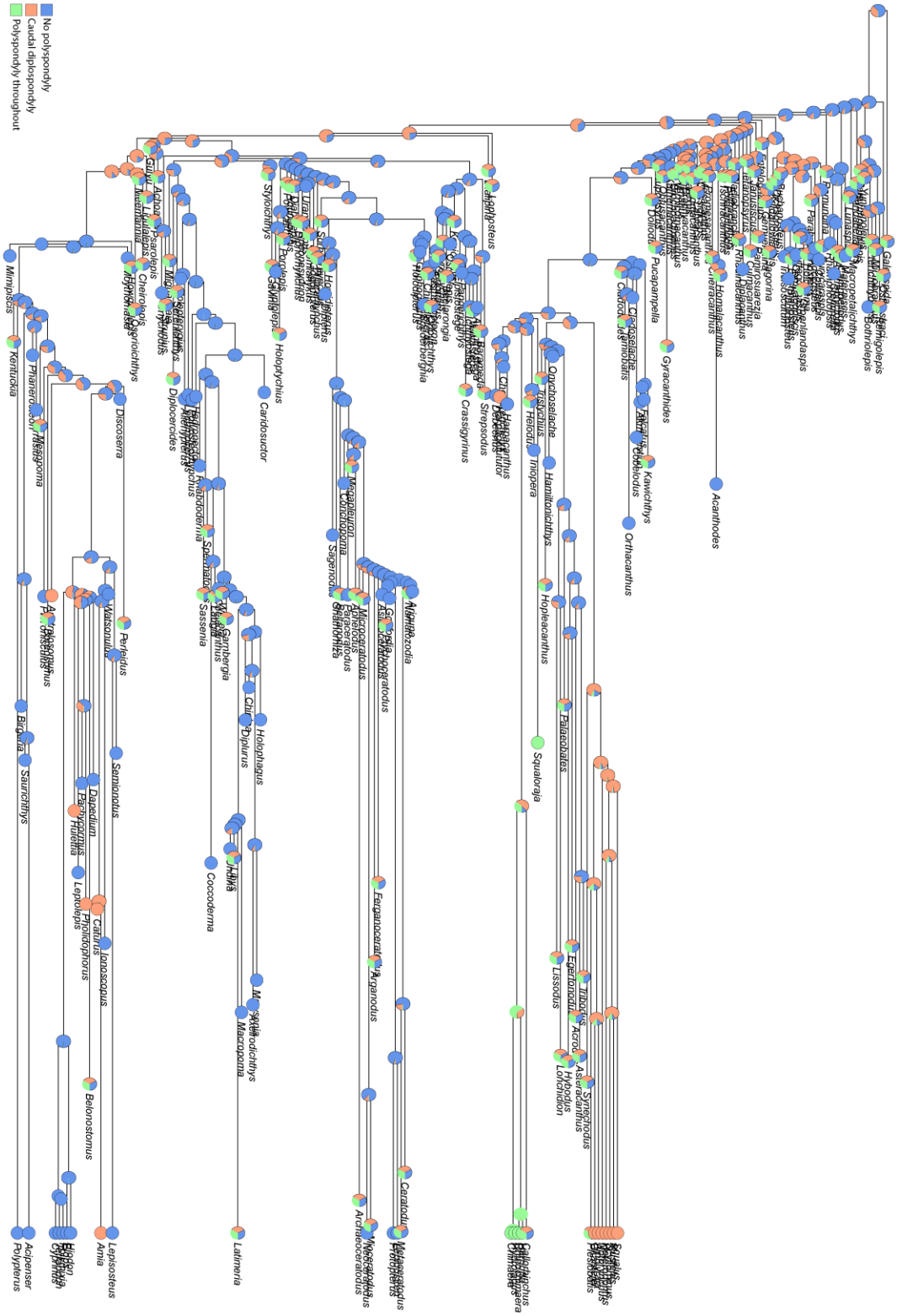

Figure A7.23. Threshold model ancestral state reconstruction for polyspondyly on tree 6.

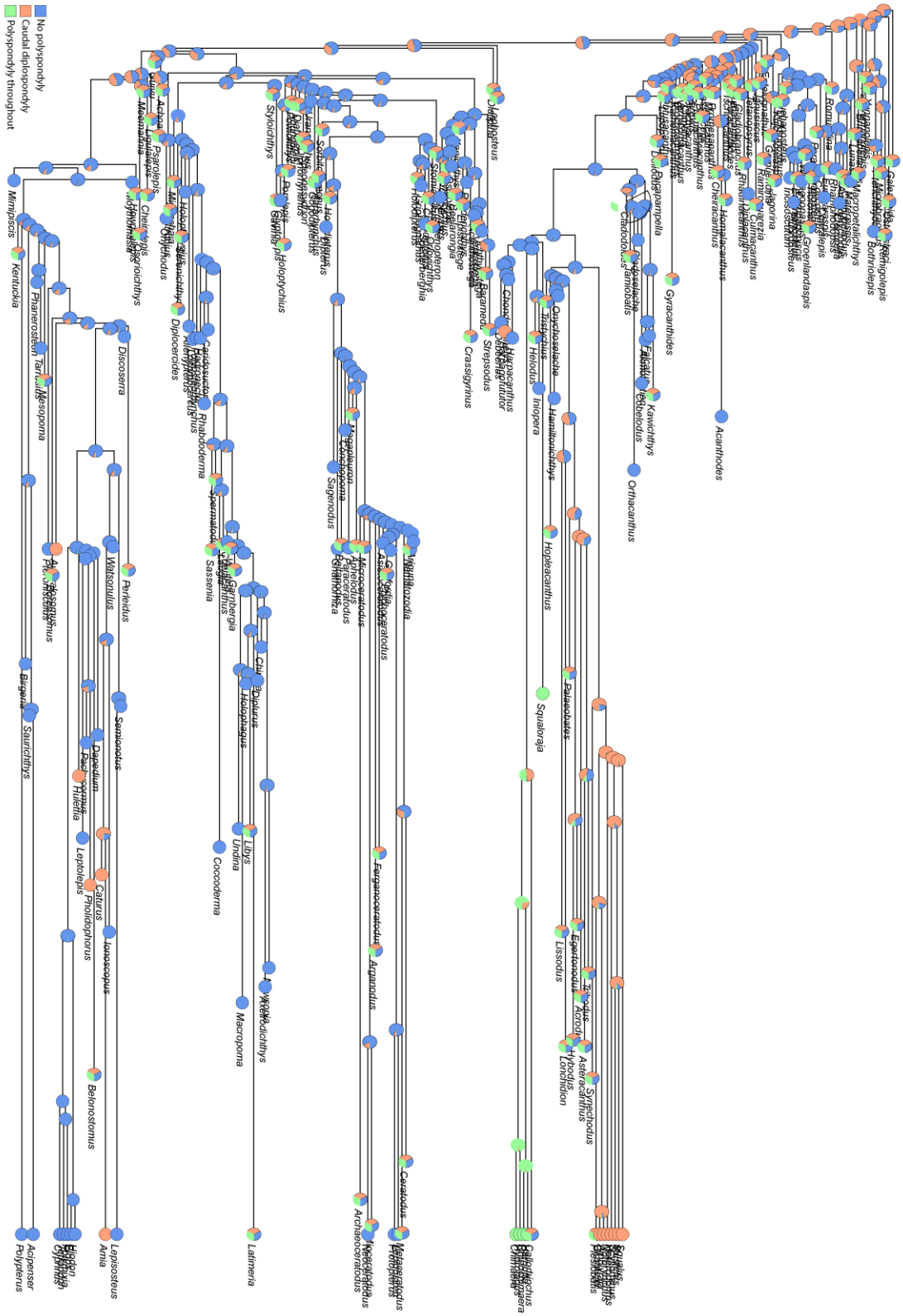

Figure A7.24. Threshold model ancestral state reconstruction for polyspondyly on tree 7.

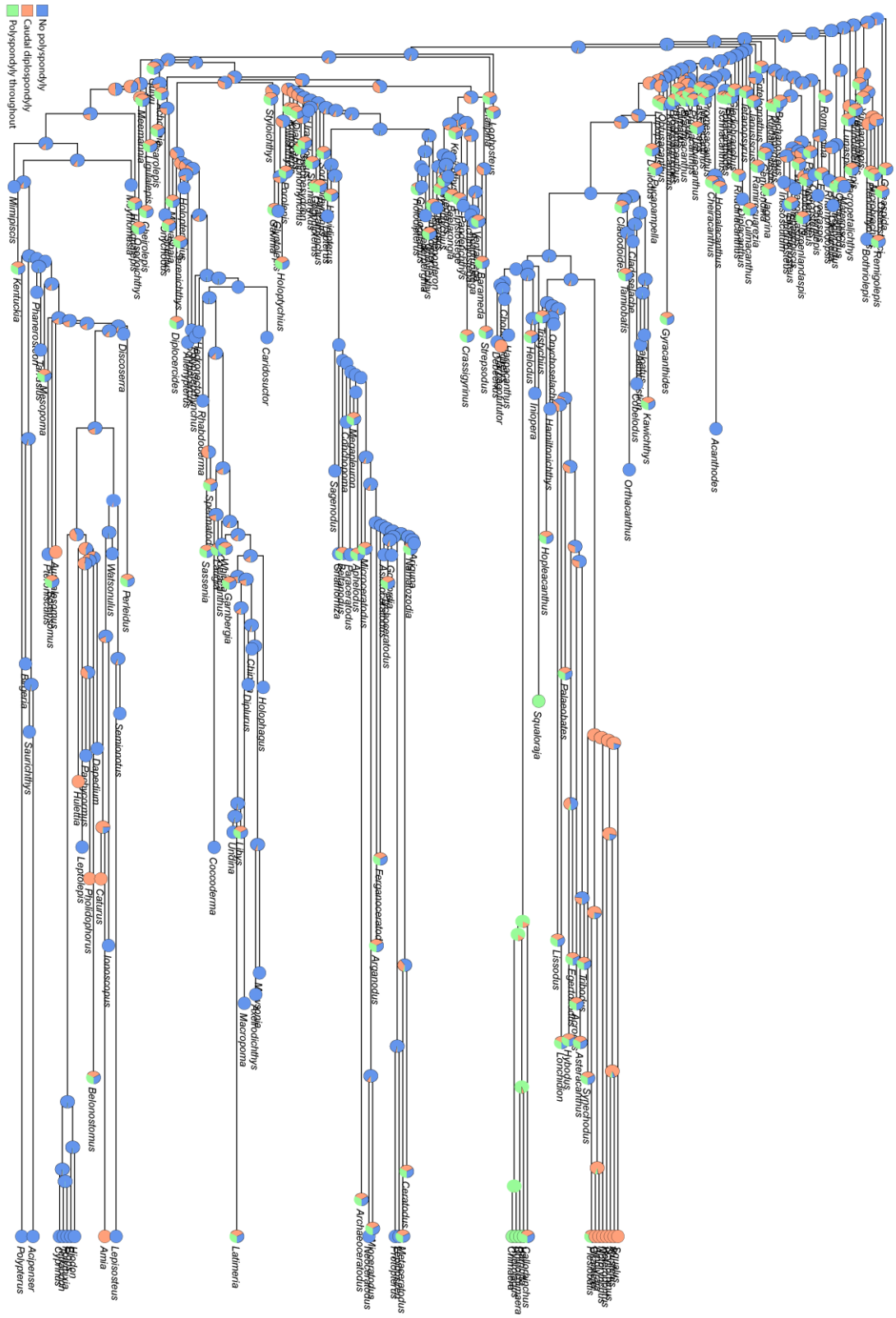

Figure A7.25. Threshold model ancestral state reconstruction for polyspondyly on tree 8.

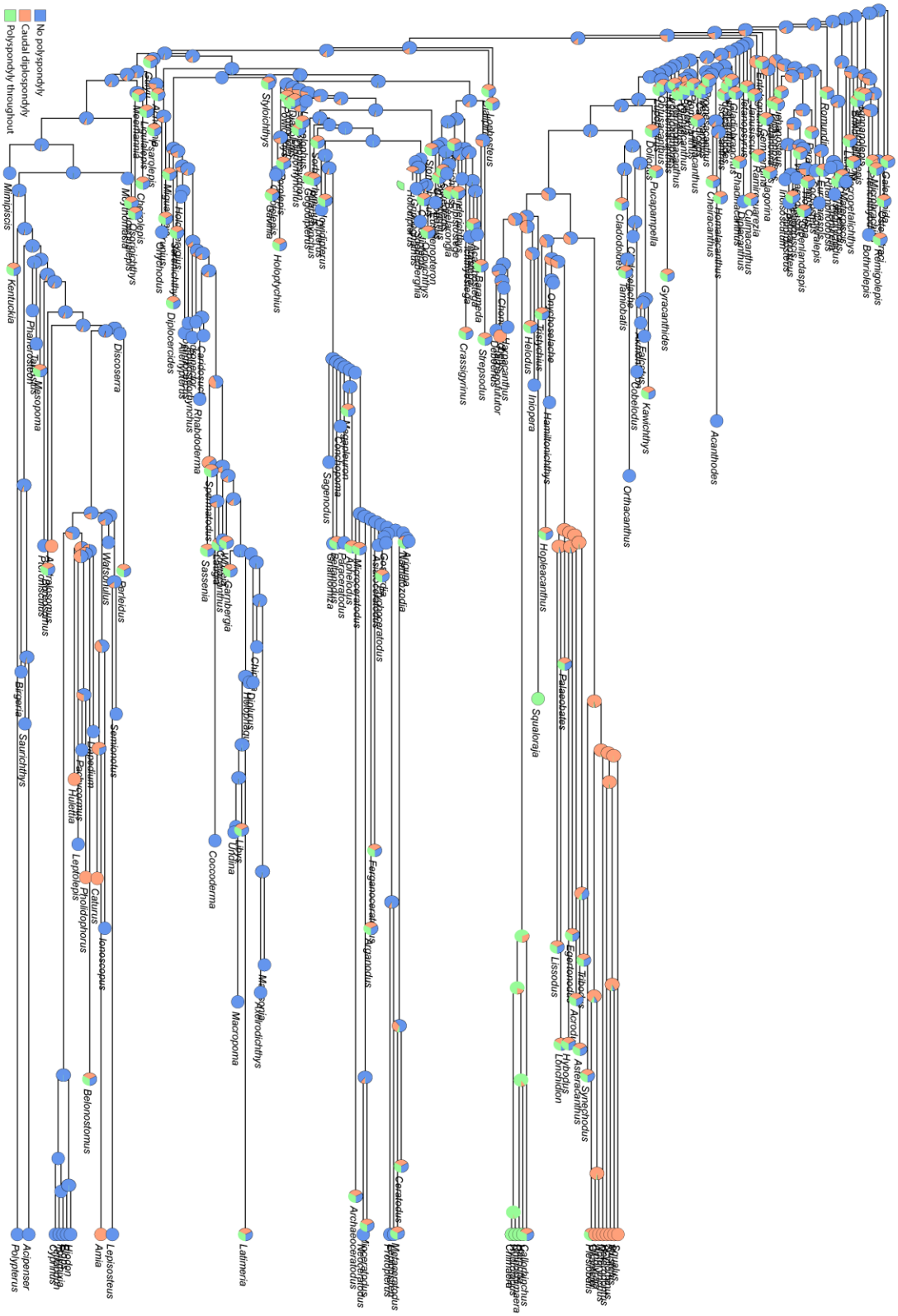

Figure A7.26. Threshold model ancestral state reconstruction for polyspondyly on tree 9.

References

Agassiz, L. 1836. Recherches Sur Les Poissons Fossiles, Livraison VI. Imprimerie de Petitpierre, Neuchâtel.

Ahlberg, P. E. 1991. A re-examination of sarcopterygian interrelationships, with special reference to the Porolepiformes. Zoological Journal of the Linnean Society 103:241–287.

Ahlberg, P. E., and N. H. Trewin. 1994. The postcranial skeleton of the Middle Devonian lungfish *Dipterus valenciennesi*. Transactions of the Royal Society of Edinburgh: Earth Sciences 85:159–175.

Ahlberg, P. E., Z. Johanson, and E. B. Daeschler. 2001. The late Devonian lungfish *Soederberghia* (Sarcopterygii, Dipnoi) from Australia and North America, and its biogeographical implications. Journal of Vertebrate Paleontology 21:1–12.

Ahlberg, P. E., J. A. Clack, and H. Blom. 2005. The axial skeleton of the Devonian tetrapod *Ichthyostega*. Nature 437:137–140.

Ahlberg, P. E., J. A. Clack, E. Luk&sbreve, evi&cbreve, and s. 1996. Rapid braincase evolution between Panderichthys and the earliest tetrapods. Nature 381:61–64.

Ahlberg, P. E., J. A. Clack, E. Lukševičs, H. Blom, and I. Zupiņš. 2008. *Ventastega curonica* and the origin of tetrapod morphology. Nature 453:1199–1204.

Alekseev, A. A., O. A. Lebedev, I. S. Barskov, M. I. Barskova, L. I. Kononova, and V. A. Chizhova. 1994. On the stratigraphic position of the Famennian and Tournaisian fossil vertebrate beds in Andreyevka, Tula Region, Central Russia. Proceedings of the Geologists' Association 105:41–52.

Anderson, M. E., J. A. Long, F. J. Evans, J. E. Almond, J. N. Theron, and P. A. Bender. 1999. Biogeographic affinities of Middle and Late Devonian fishes of South Africa. Records of the Western Australian Museum, Supplement 57:157–168.

Andrews, M., J. Long, P. Ahlberg, R. Barwick, and K. Campbell. 2005. The structure of the sarcopterygian *Onychodus jandemarrai* n. sp. from Gogo, Western Australia: with a functional interpretation of the skeleton. Transactions of the Royal Society of Edinburgh: Earth Sciences 96:197–307.

Andrews, S. M., and T. S. Westoll. 1970a. The postcranial skeleton of *Eusthenopteron foordi* Whiteaves*. Earth and Environmental Science Transactions of The Royal Society of Edinburgh 68:207–329.

Andrews, S. M., and T. S. Westoll. 1970b. The Postcranial Skeleton of Rhipidistian Fishes Excluding *Eusthenopteron**. Earth and Environmental Science Transactions of The Royal Society of Edinburgh 68:391–489.

Aoyama, H., and K. Asamoto. 2000. The developmental fate of the rostral/caudal half of a somite for vertebra and rib formation: experimental confirmation of the resegmentation theory using chick-quail chimeras. Mechanisms of Development 99:71–82.

Applegate, S. P. 1967. A survey of shark hard parts; pp. 37–67 in P. W. Gilbert, R. F. Mathewson, and D. P. Rall (eds.), Sharks, Skates and Rays. The Johns Hopkins Press, Baltimore, Maryland.

Arratia, G., and R. Cloutier. 1996. Reassessment of the morphology of *Cheirolepis vanadensis* (Actinopterygii); pp. 165–197 in H.-P. Schultze and R. Cloutier (eds.), Devonian Fishes and Plants of Miguasha, Quebec, Canada. Verlag Dr. Friedrich Pfeil, München, Germany.

Arratia, G., and R. Cloutier. 2004. A new cheriolepidid fish from the Middle-Upper Devonian of Red Hill, Nevada, USA; pp. 583–598 in G. Arratia, M. V. Wilson, and R. Cloutier (eds.), Recent Advances in the Origin and Early Radiation of Vertebrates. Verlag Dr. Friedrich Pfeil, München, Germany.

Arratia, G., and D. Hikuroa. 2010. Jurassic fishes from the Latady Group, Antarctic Peninsula, and the oldest teleosts from Antarctica. Journal of Vertebrate Paleontology 30:1331–1342.

Arratia, G., and H.-P. Schultze. 2013. Outstanding features of a new Late Jurassic pachycormiform fish from the Kimmeridgian of Brunn, Germany and comments on current understanding of pachycormiforms; pp. 87–120 in G. Arratia, H.-P. Schultze, and M. V. Wilson (eds.), Mesozoic Fishes 5: Global Diversity and Evolution. Verlag Dr. Friedrich Pfeil, München, Germany.

Arratia, G., H.-P. Schultze, and J. Casciotta. 2001. Vertebral column and associated elements in dipnoans and comparison with other fishes: development and homology. Journal of Morphology 250:101–172.

Aschliman, N., K. M. Claeson, and J. D. McEachran. 2012. Phylogeny of Batoidea; pp. 57–95 in J. C. Carrier, J. A. Musick, and M. R. Heithaus (eds.), Biology of Sharks and Their Relatives. CRC Press, Boca Raton, Florida.

Avaron, F., L. Hoffman, D. Guay, and M. a. Akimenko. 2006. Characterization of two new zebrafish members of the hedgehog family: Atypical expression of a zebrafish indian hedgehog gene in skeletal elements of both endochondral and dermal origins. Developmental Dynamics 235:478–489.

Backiel, T., B. Kokurewicz, and A. Ogorzałek. 1984. High incidence of skeletal anomalies in carp, Cyprinus carpio, reared in cages in flowing water. Aquaculture 43:369–380.

Bagnall, K. M., S. J. Higgins, and E. J. Sanders. 1988. The contribution made by a single somite to the vertebral column: experimental evidence in support of resegmentation using the chick-quail chimaera model. Development 103:69–85.

Balfour, F. 1878. A Monograph on the Development of the Elasmobranch Fishes. Macmillan and Co., London, 295 pp.

Balfour, F. 1885. A Treatise on Comparative Embryology. Macmillan and Co., London, 792 pp.

Balfour, F. M., and W. N. Parker. 1882. On the Structure and Development of Lepidosteus. Philosophical Transactions of the Royal Society of London 173:359–442.

Ballard, W. W., J. Mellinger, and H. Lechenault. 1993. A series of normal stages for development of *Scyliorhinus canicula*, the lesser spotted dogfish (Chondrichthyes:Scyliorhinidae). Journal of Experimental Zoology 267:318–336.

Balling, R., A. Neubüser, and B. Christ. 1996. Pax genes and sclerotome development. Seminars in Cell & Developmental Biology 7:129–136.

Bapst, D. W. 2012. paleotree: an R package for paleontological and phylogenetic analyses of evolution. Methods in Ecology and Evolution 3:803–807.

Barnes, R. M., and A. B. Firulli. 2009. A twist of insight - the role of Twist-family bHLH factors in development. The International Journal of Developmental Biology 53:909–924.

Bartram, A. W. H. 1975. The holostean fish genus *Ophiopsis* Agassiz. Zoological Journal of the Linnean Society 56:183–205.

Bartsch, P., and S. Gemballa. 1992. On the anatomy and development of the vertebral column and pterygiophores in *Polypterus senegalus* CUVIER, 1829 ("Pisces", Polypteriformes). Zoologische Jahrbücher. Abteilung Für Anatomie Und Ontogenie Der Tiere 122:497–529.

Barwick, R. E., and K. S. W. Campbell. 1996. A Late Devonian dipnoan, *Pillararhynchus*, from Gogo, Western Australia, and its relationships. Palaeontographica Abteilung A 1–42.

Basden, A. M., and G. C. Young. 2001. A primitive actinopterygian neurocranium from the Early Devonian of southeastern Australia. Journal of Vertebrate Paleontology 21:754–766.

Baum, B. R. 1992. Combining Trees as a Way of Combining Data Sets for Phylogenetic Inference, and the Desirability of Combining Gene Trees. Taxon 41:3–10.

Baum, K. A., and R. Lund. 1974. Vertebral centra in Haplolepis (Haplolepidae, Paleonisciformes) from the Allegheny Group, Pennsylvanian. Journal of Paleontology 48:199–200.

de Beer, G. R. 1924. Memoirs: Contributions to the study of the development of the head in *Heterodontus*. Journal of Cell Science s2-68:39–65.

Bensimon-Brito, A., J. Cardeira, M. L. Cancela, A. Huysseune, and P. E. Witten. 2012. Distinct patterns of notochord mineralization in zebrafish coincide with the localization of Osteocalcin isoform 1 during early vertebral centra formation. BMC Developmental Biology 12:28.

Berman, D. S. 1976. Cranial morphology of the Lower PermianlLungfish *Gnathorhiza* (Osteichthyes: Dipnoi). Journal of Paleontology 50:1020–1033.

Bernacsek, G. M. 1977. A lungfish cranium from the Middle Devonian of the Yukon Territory, Canada. Palaeontographica Abteilung A 175–200.

Bernacsek, G. M., and D. L. Dineley. 1977. New acanthodians from the Delorme Formation (Lower Devonian) of N. W. T. Canada. Palaeontographica Abteilung A 1–25.

Bininda-Emonds, O. R. P., and M. J. Sanderson. 2001. Assessment of the Accuracy of Matrix Representation with Parsimony Analysis Supertree Construction. Systematic Biology 50:565–579.

Bird, N. C., and P. M. Mabee. 2003. Developmental morphology of the axial skeleton of the zebrafish, *Danio rerio* (Ostariophysi: Cyprinidae). Developmental Dynamics 228:337–357.

Blom, H. 2005. Taxonomic revision of the Late Devonian tetrapod Ichthyostega from East Greenland. Palaeontology 48:111–134.

Blom, H., J. A. Clack, P. E. Ahlberg, and M. Friedman. 2007. Devonian vertebrates from East Greenland: a review of faunal composition and distribution. Geodiversitas 29:119–141.

Bogan, S., L. Taverne, and F. L. Agnolin. 2011. Description of a new aspidorhynchid fish, *Belonostomus lamarquensis* sp. nov. (Halecostomi, Aspidorhynchiformes), from the continental Upper Cretaceous of Patagonia, Argentina. Bulletin de l'Institut Royal Des Sciences Naturelles de Belqique, Sciences de La Terre 81:235–245.

Bordat, C. 1987. Etude ultrastructurale de l'os des vertèbres du Sélacien Scyliorhinus canicula L. Canadian Journal of Zoology 65:1435–1444.

Brazeau, M. D. 2009. The braincase and jaws of a Devonian "acanthodian" and modern gnathostome origins. Nature 457:305–308.

Brazeau, M. D., and M. Friedman. 2015. The origin and early phylogenetic history of jawed vertebrates. Nature 520:490–497.

Brito, P. M., G. Arratia, and H.-P. Schultze. 1999. The caudal skeleton of aspidorhynchids (Actinopterygii, Halecostomi): phylogenetic implications; pp. 249–264 in Mesozoic Fishes 2: Systematics and Fossil Record. Verlag Dr. Friedrich Pfeil, München, Germany.

Brown, R. W. 1946. Fossil egg capsules of chimaeroid fishes. Journal of Paleontology 261–266.

Bryant, L. 1987. *Belonostomus* (Teleostei: Aspidorhynchidae) from the Late Paleocene of North Dakota. PaleoBios 43:1–3.

Buchholtz, E. A. 2001. Vertebral osteology and swimming style in living and fossil whales (Order: Cetacea). Journal of Zoology 253:175–190.

Burke, A. C., C. E. Nelson, B. A. Morgan, and C. Tabin. 1995. Hox genes and the evolution of vertebrate axial morphology. Development 121:333–346.

Burrow, C. J., G. C. Young, and others. 2012. New information on "*Culmacanthus*" (Acanthodii: Diplacanthiformes) from the? Early-middle Devonian of southeastern Australia. Proceedings of the Linnean Society of New South Wales 134:21.

Burrow, C. J., R. G. Davidson, J. L. Den Blaauwen, and M. J. Newman. 2015. Revision of *Climatius reticulatus* Agassiz, 1844 (Acanthodii, Climatiidae), from the Lower Devonian of Scotland, based on new histological and morphological data. Journal of Vertebrate Paleontology 35:e913421.

Campbell, K. S. W., and R. E. Barwick. 1984. *Speonesydrion*, an Early Devonian dipnoan with primitive toothplates. PaleoIchthyologica 2:1–48.

Campbell, K. S. W., and R. E. Barwick. 1988. *Uranolophus*: a reappraisal of a primitive dipnoan. Memoirs of the Association of Australasian Palaeontologists 7:87–144.

Cappetta, H. 1975. Sélaciens et Holocéphale du Gargasien de la région de Gargas (Vaucluse). Géologie Méditerranéenne 2:115–134.

Cappetta, H. 1976. Sélaciens nouveaux du London Clay de l'Essex (Yprésien du bassin de Londres). Geobios 9:551–575.

Cappetta, H. 1987. Chondrichthyes II: Mesozoic and Cenozoic Elasmobranchii. Gustav Fischer Verlag, Stuttgart, 193 pp.

Carpenter, D. K., H. J. Falcon-Lang, M. J. Benton, and E. Henderson. 2014. Carboniferous (Tournaisian) fish assemblages from the Isle of Bute, Scotland: systematics and palaeoecology. Palaeontology 57:1215–1240.

de Carvalho, M. S. S. 1982. O Gênero de Mawsonia na ictiofáunula do cretáceo do estado da Bahia. Anais Da Academia Brasileira de Ciências 52:519–539.

de Carvalho, M. S. S., and J. G. Maisey. 2008. New occurrence of *Mawsonia* (Sarcopterygii: Actinistia) from the Early Cretaceous of the Sanfranciscana Basin, Minas Gerais, southeastern Brazil. Geological Society, London, Special Publications 295:109–144.

Casier, E. 1943. Contributions à l'étude des poissons fossiles de la Belgique. III. Quelques espèces nouvelles ou peu connues du Landénien marin. Bulletin Du Musée Royal d'Histoire Naturelle de Belgique 19:1–16.

Cavin, L. 2010. Diversity of Mesozoic semionotiform fishes and the origin of gars (Lepisosteidae). Naturwissenschaften 97:1035–1040.

Cavin, L., V. Suteethorn, E. Buffetaut, and H. Tong. 2007. A new Thai Mesozoic lungfish (Sarcopterygii, Dipnoi) with an insight into post-Palaeozoic dipnoan evolution. Zoological Journal of the Linnean Society 149:141–177.

Chang, M. 1984. Structure and phyogenetic significance of *Diabolepis speratus* gen. et sp. Nov., a new dipnoan-like form from the Lower Devonian of eastern Yunnan, China. Proceedings of the Linnean Society of New South Wales10 107:171–184.

Chapman, F. 1916. On the generic position of "Asterolepis ornata var. australis' McCoy, with description of a new variety." Proceedings of the Royal Society of Victoria 28:211–215.

Choo, B. 2011. Revision of the actinopterygian genus *Mimipiscis* (=*Mimia*) from the Upper Devonian Gogo Formation of Western Australia and the interrelationships of the early Actinopterygii. Earth and Environmental Science Transactions of the Royal Society of Edinburgh 102:77–104.

Choo, B. 2015. A new species of the Devonian actinopterygian *Moythomasia* from Bergisch Gladbach, Germany, and fresh observations on *M. durgaringa* from the Gogo Formation of Western Australia. Journal of Vertebrate Paleontology 35:e952817.

Christ, B., and J. Wilting. 1992. From somites to vertebral column. Annals of Anatomy - Anatomischer Anzeiger 174:23–32.

Christ, B., R. Huang, and J. Wilting. 2000. The development of the avian vertebral column. Anatomy and Embryology 202:179–194.

Christ, B., R. Huang, and M. Scaal. 2004. Formation and differentiation of the avian sclerotome. Anatomy and Embryology 208:333–350.

Clack, J. A. 1988. New material of early tetrapod *Acanthostega* from the Upper Devonian of East Greenland. Palaeontology 31:699–724.

Clack, J. A., E. L. Sharp, and J. A. Long. 2011. The fossil record of lungfishes; pp. 1–42 in J. M. Jørgensen and J. Joss (eds.), The Biology of Lungfishes. Science Publishers, Enfield, New Hampshire.

Claeson, K. M. 2011. The synarcual cartilage of batoids with emphasis on the synarcual of Rajidae. Journal of Morphology 272:1444–1463.

Cloutier, R. 1996. The primitive actinistian *Miguashaia bureaui* Schultze (Sarcopterygii); pp. 227–247 in Devonian Fishes and Plants of Miguasha, Quebec, Canada. Verlag Dr. Friedrich Pfeil, München, Germany.

Cloutier, R., and P. L. Forey. 1991. Diversity of extinct and living actinistian fishes (Sarcopterygii). Environmental Biology of Fishes 32:59–74.

Cloutier, R., and P. E. Ahlberg. 1995. Sarcopterygian interrelationships: how far are we from a consensus? Geobios 19:241–248.

Cloutier, R., and P. E. Ahlberg. 1996. Morphology, characters, and the interrelationships of basal sarcopterygians; pp. 445–479 in M. L. J. Stiassny, L. R. Parenti, and J. G. David (eds.), Interrelationships of Fishes. Academic Press, San Diego, California.

Cloutier, R., S. Loboziak, A.-M. Candilier, and A. Blieck. 1996. Biostratigraphy of the Upper Devonian Escuminac Formation, eastern Québec, Canada: a comparative study based on miospores and fishes. Review of Palaeobotany and Palynology 93:191–215.

Coates, M. I. 1996. The Devonian tetrapod *Acanthostega gunnari* Jarvik: postcranial anatomy, basal tetrapod interrelationships and patterns of skeletal evolution. Transactions of the Royal Society of Edinburgh: Earth Sciences 87:363–421.

Coates, M. I. 1999. Endocranial preservation of a Carboniferous actinopterygian from Lancashire, UK, and the interrelationships of primitive actinopterygians. Philosophical Transactions of the Royal Society of London B: Biological Sciences 354:435–462.

Coates, M. I., and S. E. K. Sequeira. 2001a. Early sharks and primitive gnathostome interrelationships; pp. 241–262 in P. E. Ahlberg (ed.), Major Events in Early Vertebrate Evolution. Taylor and Francis, New York.

Coates, M. I., and S. E. K. Sequeira. 2001b. A new stethacanthid chondrichthyan from the Lower Carboniferous of Bearsden, Scotland. Journal of Vertebrate Paleontology 21:438–459.

Coates, M. I., and R. W. Gess. 2007. A new reconstruction of *Onychoselache traquairi*, comments on early chondrichthyan pectoral girdles and hybodontiform phylogeny. Palaeontology 50:1421–1446.

Coburn, M. M., and P. G. Grubach. 1998. Ontogeny of the Weberian apparatus in the armored catfish *Corydoras paleatus* (Siluriformes: Callichthyidae). Copeia 1998:301.

Conway Morris, S., and J.-B. Caron. 2014. A primitive fish from the Cambrian of North America. Nature 512:419–422.

Cope, E. D. 1894. New and little-known Paleozoic and Mesozoic fishes. Journal of the Academy of Natural Sciences of Philadelphia 9:427–448.

Corning, H. 1891. Ueber die sogenannte Neugliederung der Wirbelsäule und über das Schicksal der Urwirbelhohle bei Reptilien. Morphologisches Jahrbuch 17:611–622.

Cote, S., R. Carroll, R. Cloutier, and L. Bar-Sagi. 2002. Vertebral development in the Devonian Sarcopterygian fish *Eusthenopteron foordi* and the polarity of vertebral evolution in non-amniote tetrapods. Journal of Vertebrate Paleontology 22:487–502.

Criswell, K. E. 2015. The comparative osteology and phylogenetic relationships of African and South American lungfishes (Sarcopterygii: Dipnoi). Zoological Journal of the Linnean Society 174:801–858.

Cunningham, C. W., K. E. Omland, and T. H. Oakley. 1998. Reconstructing ancestral character states: a critical reappraisal. Trends in Ecology & Evolution 13:361–366.

Dalgleish, A. E. 1985. A study of the development of thoracic vertebrae in the mouse assisted by autoradiography. Acta Anatomica 122:91–98.

Dalquest, W. W., M. J. Kocurko, and J. V. Grimes. 1989. Aspects of the postcranial skeleton of the Lower Permian lungfish, Gnathorhiza. Journal of Paleontology 63:919–930.

Daniel, J. F. 1922. The Elasmobranch Fishes. University of California Press, Berkeley, California, 334 pp.

Davis, S. P., J. A. Finarelli, and M. I. Coates. 2012. *Acanthodes* and shark-like conditions in the last common ancestor of modern gnathostomes. Nature 486:247–250.

Dean, B. 1906. Chimaeroid Fishes and Their Development. Carnegie Institution of Washington, Washington, D. C., 194 pp.

Dean, B. 1907. Notes on acanthodian sharks. American Journal of Anatomy 7:209–222.

Dean, M. N., and A. P. Summers. 2006. Mineralized cartilage in the skeleton of chondrichthyan fishes. Zoology 109:164–168.

Denison, R. H. 1968. Early Devonian lungfishes from Wyoming, Utah, and Idaho. Fieldiana Geology Memoirs 4:353–413.

Denison, R. H. 1969. New Pennsylvanian lungfishes from Illinois. Fieldiana Geology 12:193–211.

Denison, R. H. 1978. Placodermi. Gustav Fischer Verlag, Stuttgart, 128 pp.

Denison, R. H. 1983. Further Consideration of Placoderm Evolution. Journal of Vertebrate Paleontology 3:69–83.

Dennis-Bryan, K. 1987. A new species of eastrnanosteid arthrodire (Pisces:Placodermi) from Gogo, Western Australia. Zoological Journal of the Linnean Society 90:1–64.

Dennis-Bryan, K., and R. S. Miles. 1981. A pachyosteomorph arthrodire from Gogo, Western Australia. Zoological Journal of the Linnean Society 73:213–258.

Dick, J. R. F. 1978. On the Carboniferous shark *Tristychius arcuatus* Agassiz from Scotland. Earth and Environmental Science Transactions of The Royal Society of Edinburgh 70:63–108.

Dick, J. R. F., and J. G. Maisey. 1980. The Scottish Lower Carboniferous shark *Onychoselache traquairi*. Palaeontology 23:363–374.

Didier, D. 1995. Phylogenetic systematics of extant chimaeroid fishes (Holocephali, Chimaeroidei). American Museum Novitates 3119:1–86.

Duffin, C. J. 1993. The palaeospinacid shark *"Synechodus" jurensis* SCHWEIZER, 1964 from the Late Jurassic of Germany. Belgian Geological Survey, Elasmobranches et Stratigraphie 264:157–174.

Dupret, V. 2010. Revision of the genus *Kujdanowiaspis* Stensiö, 1942 (Placodermi, Arthrodira, "Actinolepida") from the Lower Devonian of Podolia (Ukraine). Geodiversitas 32:5–63.

Dupret, V., S. Sanchez, D. Goujet, P. Tafforeau, and P. E. Ahlberg. 2014. A primitive placoderm sheds light on the origin of the jawed vertebrate face. Nature 507:500–503.

Eames, B. F., N. Allen, J. Young, A. Kaplan, J. A. Helms, and R. A. Schneider. 2007. Skeletogenesis in the swell shark *Cephaloscyllium ventriosum*. Journal of Anatomy 210:542–554.

Eastman, C. R. 1907. Devonic Fishes of the New York Formations. New York State Education Department, Albany, 235 pp.

Eeden, F. J. van, M. Granato, U. Schach, M. Brand, M. Furutani-Seiki, P. Haffter, M. Hammerschmidt, C. P. Heisenberg, Y. J. Jiang, D. A. Kane, R. N. Kelsh, M. C. Mullins, J. Odenthal, R. M. Warga, M. L. Allende, E. S. Weinberg, and C. Nusslein-Volhard. 1996. Mutations affecting somite formation and patterning in the zebrafish, Danio rerio. Development 123:153–164.

Egerton, P. M. de G. 1845. Description of the mouth of a *Hybodus* found by Mr. Boscawen Ibbetson in the Isle of Wight. Quarterly Journal of the Geological Society 1:197–199.

Ekanayake, S., and B. K. Hall. 1987. The development of acellularity of the vertebral bone of the Japanese medaka, *Oryzias latipes* (Teleostei; Cyprinidontidae). Journal of Morphology 193:253–261.

Elliott, D. K. 1987. A new specimen of Chinlea sorenseni from the Chinle Formation, Dolores River, Colorado. Journal of the Arizona-Nevada Academy of Science 47–52.

Enault, S., D. N. Muñoz, W. T. A. F. Silva, V. Borday-Birraux, M. Bonade, S. Oulion, S. Ventéo, S. Marcellini, and M. Debiais-Thibaud. 2015. Molecular footprinting of skeletal tissues in the catshark *Scyliorhinus canicula* and the clawed frog *Xenopus tropicalis* identifies conserved and derived features of vertebrate calcification. Frontiers in Genetics 6.

Fan, C.-M., and M. Tessier-Lavigne. 1994. Patterning of mammalian somites by surface ectoderm and notochord: Evidence for sclerotome induction by a hedgehog homolog. Cell 79:1175–1186.

Farias, C., J. Canoura, and J. Gil. 2008. First record of Polymixia nobilis (Polymixiformes: Polymixiidae) close to the Strait of Gibraltar (south-western Spain). Marine Biodiversity Records 1.

Filleul, A., and D. B. Dutheil. 2004. A peculiar diplospondylous actinopterygian fish from the Cretaceous of Morocco. Journal of Vertebrate Paleontology 24:290–298.

Finarelli, J. A., and M. I. Coates. 2014. Chondrenchelys problematica (Traquair, 1888) redescribed: a Lower Carboniferous, eel-like holocephalan from Scotland. Earth and Environmental Science Transactions of the Royal Society of Edinburgh 105:35–59.

Fischer, A. H., K. A. Jacobson, J. Rose, and R. Zeller. 2008. Hematoxylin and eosin staining of tissue and cell sections. Cold Spring Harbor Protocols 2008:pdb.prot4986.

Fleming, A., R. J. Keynes, and D. Tannahill. 2001. The role of the notochord in vertebral column formation. Journal of Anatomy 199:177–180.

Fleming, A., R. Keynes, and D. Tannahill. 2004. A central role for the notochord in vertebral patterning. Development 131:873–880.

Fleming, A., M. G. Kishida, C. B. Kimmel, and R. J. Keynes. 2015. Building the backbone: the development and evolution of vertebral patterning. Development 142:1733–1744.

Forey, P. L., P. E. Ahlberg, E. Lukševičs, and I. Zupinš. 2000. A new coelacanth from the Middle Devonian of Latvia. Journal of Vertebrate Paleontology 20:243–252.

Foster, K. L., and T. E. Higham. 2010. How to build a pectoral fin: functional morphology and steady swimming kinematics of the spotted ratfish (*Hydrolagus colliei*). Canadian Journal of Zoology 88:774–780.

Friedman, M. 2007a. The interrelationships of Devonian lungfishes (Sarcopterygii: Dipnoi) as inferred from neurocranial evidence and new data from the genus *Soederberghia* Lehman, 1959. Zoological Journal of the Linnean Society 151:115–171.

Friedman, M. 2007b. *Styloichthys* as the oldest coelacanth: Implications for early osteichthyan interrelationships. Journal of Systematic Palaeontology 5:289–343.

Friedman, M. 2015. The early evolution of ray-finned fishes. Palaeontology 58:213–228.

Friedman, M., and M. I. Coates. 2006. A newly recognized fossil coelacanth highlights the early morphological diversification of the clade. Proceedings of the Royal Society B: Biological Sciences 273:245–250.

Gadow, H. 1896. On the evolution of the vertebral column of Amphibia and Amniota. Philosophical Transactions of the Royal Society of London. Series B, Biological Sciences 187:1–57.

Gadow, H. 1933. The Evolution of the Vertebral Column. Cambridge University Press, Cambridge, 356 pp.

Gadow, H., and E. C. Abbott. 1895. On the evolution of the vertebral column of fishes. Philosophical Transactions of the Royal Society of London. B 186:163–221.

Gagnier, P.-Y. 1996. Acanthodii; pp. 149–164 in Devonian Fishes and Plants of Miguasha, Quebec, Canada. Verlag Dr. Friedrich Pfeil, München, Germany.

Gagnier, P.-Y., and M. V. Wilson. 1996. Early Devonian acanthodians from northern Canada. Palaeontology 39:241–258.

Gardiner, B. G. 1983. Gnathostome vertebrae and the classification of the Amphibia. Zoological Journal of the Linnean Society 79:1–59.

Gardiner, B. G. 1984a. The relationships of the palaeoniscid fishes, a review based on new specimens of *Mimia* and *Moythomasia* from the Upper Devonian of Western Australia. Bulletin of the British Museum (Natural History) Geology Series 37:173–428.

Gardiner, B. G. 1984b. Sturgeons as living fossils; pp. 148–152 in N. Eldredge and S. M. Stanley (eds.), Living Fossils. Springer-Verlag, New York.

Gardiner, B. G., and R. S. Miles. 1994. Eubrachythoracid arthrodires from gogo, western australia. Zoological Journal of the Linnean Society 112:443–477.

Gardiner, B. G., B. Schaeffer, and J. A. Masserie. 2005. A review of the lower actinopterygian phylogeny. Zoological Journal of the Linnean Society 144:511–525.

Garvey, J. M., Z. Johanson, and A. Warren. 2005. Redescription of the pectoral fin and vertebral column of the rhizodontid fish *Barameda decipiens* from the lower carboniferous of Australia. Journal of Vertebrate Paleontology 25:8–18.

Gegenbaur, C. 1862. Untersuchungen Zur Vergleichenden Anatomie Der Wirbelsaule Bei Amphibien and Reptilien. Wilhelmn Engelmann, Leipzig, 71 pp.

Gegenbaur, C. 1872. Untershuchungen Zur Vergleichenden Anatomie Der Wirbelthiere: Das Kopfskelet Der Selachier, Ein Beitrage Zur Erkenntniss Der Genese Des Kopfskeletes Der Wirbelthiere. Wilhelm Engelmann, Leipzig, 316 pp.

Geoffroy-Saint-Hilaire, E. 1822. Considérations générales sur la vertèbre. 89–119.

Gess, R. W., and M. I. Coates. 2015. Fossil juvenile coelacanths from the Devonian of South Africa shed light on the order of character acquisition in actinistians. Zoological Journal of the Linnean Society 175:360–383.

Giles, S., M. Friedman, and M. D. Brazeau. 2015. Osteichthyan-like cranial conditions in an Early Devonian stem gnathostome. Nature 520:82–85.

Gillis, J. A., and B. K. Hall. 2016. A shared role for sonic hedgehog signalling in patterning chondrichthyan gill arch appendages and tetrapod limbs. Development 143:1313–1317.

Gillis, J. A., R. D. Dahn, and N. H. Shubin. 2009. Chondrogenesis and homology of the visceral skeleton in the little skate, *Leucoraja erinacea* (Chondrichthyes: Batoidea). Journal of Morphology 270:628–643.

Goodrich, E. 1930. Studies on the Structure and Development of Vertebrates. Dover Publications, London, 837 pp.

Goujet, D. 1975. *Dicksonosteus*, un nouvel arthrodire du Dévonien du Spitsberg remarques sur le squelette visceral des Dolichothoraci; pp. 218 in J.-P. Lehman (ed.), Problèmes actuels de Paléontologie—Evolution des Vertébrés. Colloques internationaux du Center National de la Recherche Scientifique, Paris.

Grande, L. 2010. An empirical synthetic pattern study of gars (Lepisosteiformes) and closely related species, based mostly on skeletal anatomy. The resurrection of Holostei. American Society of Ichthyologists and Herpetologists Special Publication 6:1–871.

Grande, L., and W. E. Bemis. 1998. A comprehensive phylogenetic study of amiid fishes (Amiidae) cased on comparative skeletal anatomy. An empirical search for interconnected patterns of natural history. Journal of Vertebrate Paleontology 18:1–696.

Grogan, E. D., and R. Lund. 2000. *Debeerius ellefseni* (Fam. Nov., Gen. Nov., Spec. Nov.), an autodiastylic Chondrichthyan from the Mississippian Bear Gulch Limestone of Montana

(USA), the relationships of the Chondrichthyes, and comments on gnathostome evolution. Journal of Morphology 243:219–245.

Gross, W. 1933. Die Wirbeltiere des rheinischen Devons. Abhandlungen Der Preußischen Geologischen Landesanstalt 154:1–83.

Gross, W. 1936. Beiträge zur Osteologie baltischer und rheinischer Devon-Crossopterygier. Paläontologische Zeitschrift 18:129–155.

Gross, W. 1956. Über Crossopterygier Und Dipnoer Aus Dem Baltischen Oberdevon Im Zusammenhang Einer Vergleichenden Untersuchung Des Porenkanalsystems Paläozoischer Agnathen Und Fische. Almqvist and Wiksell, Stockholm, Sweden, 140 pp.

Gross, W. 1963. *Gemuendina stuertzi* Traquair. Neuuntersuchung. Notizblatt Des Hessischen Landesamtes Für Bodenforschung Zu Wiesbaden 91:36–73.

Grotmol, S., H. Kryvi, K. Nordvik, and G. K. Totland. 2003. Notochord segmentation may lay down the pathway for the development of the vertebral bodies in the Atlantic salmon. Anatomy and Embryology 207:263–272.

Grotmol, S., K. Nordvik, H. Kryvi, and G. K. Totland. 2005. A segmental pattern of alkaline phosphatase activity within the notochord coincides with the initial formation of the vertebral bodies. Journal of Anatomy 206:427–436.

Haga, Y., V. J. Dominique, and S. J. Du. 2009. Analyzing notochord segmentation and intervertebral disc formation using the twhh:gfp transgenic zebrafish model. Transgenic Research 18:669–683.

Hall, B. K. 2005. Bones and Cartilage: Developmental and Evolutionary Skeletal Biology. Elsevier Academic Press, San Diego, California, 760 pp.

Hanke, G. F. 2008. *Promesacanthus eppleri* n. gen., n. sp., a mesacanthid (Acanthodii, Acanthodiformes) from the Lower Devonian of northern Canada. Geodiversitas 30:287–302.

Hanke, G. F., and M. V. Wilson. 2004. New teleostome fishes and acanthodian systematics; pp. 189–216 in Recent Advances in the Origin and Early Radiation of Vertebrates. Verlag Dr. Friedrich Pfeil, München, Germany.

Hanke, G. F., and M. V. H. Wilson. 2006. Anatomy of the early Devonian acanthodian *Brochoadmones milesi* based on nearly complete body fossils, with comments on the evolution and development of paired fins. Journal of Vertebrate Paleontology 26:526–537.

Hanke, G. F., and S. P. Davis. 2008. Redescription of the acanthodian *Gladiobranchus probaton* Bernacsek & Dineley, 1977, and comments on diplacanthid relationships. Geodiversitas 30:303–330.

Hanke, G. F., and S. P. Davis. 2012. A re-examination of *Lupopsyrus pygmaeus* Bernacsek & Dineley, 1977 (Pisces, Acanthodii). Geodiversitas 34:469–487.

Hanke, G. F., S. P. Davis, and M. V. Wilson. 2001. New species of the acanthodian genus *Tetanopsyrus* from northern Canada, and comments on related taxa. Journal of Vertebrate Paleontology 21:740–753.

Hasse, K. 1879. Das Natürliche System Der Elasmobranchier Auf Grundlage Des Baues Und Der Entwicklung Ihrer Wirbelsäule: Eine Morphologische Und Paläontologische Studie. Gustav Fischer, Jena, 284 pp.

Hauser, L. M., and D. M. Martill. 2013. Evidence for coelacanths in the Late Triassic (Rhaetian) of England. Proceedings of the Geologists' Association 124:982–987.

Hay, O. P. 1895. On the Structure and Development of the Vertebral Column of *Amia*. Field Columbian Museum Zoology Series 1:1–54.

Head, J. J., and P. D. Polly. 2015. Evolution of the snake body form reveals homoplasy in amniote Hox gene function. Nature 520:86–89.

Hemmings, S. K. 1978. The Old Red Sandstone Antiarchs of Scotland: *Pterichthyodes* and *Microbrachius*. Adlard & Son Ltd., Great Britain, 64 pp.

Hilton, E. J., L. Grande, and W. E. Bemis. 2011. Skeletal anatomy of the shortnose sturgeon, *Acipenser brevirostrum* Lesueur, 1818, and the systematics of sturgeons (Acipenseriformes, Acipenseridae). Fieldiana Life and Earth Sciences 3:1–168.

Holtzer, H. 1952. An experimental analysis of the development of the spinal column. Part II. The dispensability of the notochord. Journal of Experimental Zoology 121:573–591.

Homberger, D. G., and W. F. Walker Jr. 2004. Vertebrate Dissection. Thomson Brooks/Cole, China, 379 pp.

Huang, R., Q. Zhi, C. Schmidt, J. Wilting, B. Brand-Saberi, and B. Christ. 2000. Sclerotomal origin of the ribs. Development 127:527–532.

Hurley, I. A., R. L. Mueller, K. A. Dunn, E. J. Schmidt, M. Friedman, R. K. Ho, V. E. Prince, Z. Yang, M. G. Thomas, and M. I. Coates. 2007. A new time-scale for ray-finned fish evolution. Proceedings of the Royal Society B: Biological Sciences 274:489–498.

Inohaya, K., Y. Takano, and A. Kudo. 2007. The teleost intervertebral region acts as a growth center of the centrum: In vivo visualization of osteoblasts and their progenitors in transgenic fish. Developmental Dynamics 236:3031–3046.

Inoue, J. G., M. Miya, K. Lam, B.-H. Tay, J. A. Danks, J. Bell, T. I. Walker, and B. Venkatesh. 2010. Evolutionary origin and phylogeny of the modern holocephalans (Chondrichthyes: Chimaeriformes): a mitogenomic perspective. Molecular Biology and Evolution 27:2576–2586.

Jaekel, O. 1921. Die Stellung der Paläontologie zu einigen Problemen der Biologie und Phylogenie. Paläontologische Zeitschrift 3:213–239.

Janvier, P. 1996. Early Vertebrates. Clarendon Press, Oxford, 393 pp.

Janvier, P., and A. Ritchie. 1977. Le genre *Groenlandaspis* Heintz (Pisces, Placodermi, Arthrodira) dans le Devonien d'Asie. Colloques Researches Academie Des Sciences de Paris, Series D 284:1385–1388.

Janvier, P., and M. Arsenault. 2007. The anatomy of *Euphanerops longaevus* Woodward, 1900, an anaspid-like jawless vertebrate from the Upper Devonian of Miguasha, Quebec, Canada. Geodiversitas 29:143–216.

Janvier, P., M. Arsenault, and S. Desbiens. 2004. Calcified cartilage in the paired fins of the osteostracan *Escuminaspis laticeps* (Traquair 1880), from the Late Devonian of Miguasha (Québec, Canada), with a consideration of the early evolution of the pectoral fin endoskeleton in vertebrates. Journal of Vertebrate Paleontology 24:773–779.

Janvier, P., F. Lethiers, O. Monod, and Ö. Balkaş. 1984. Discovery of a vertebrate fauna at the Devonian-Carboniferous boundary in SE Turkey (Hakkari Province). Journal of Petroleum Geology 7:147–168.

Jarvik, E. 1980a. Basic Structure and Evolution of Vertebrates. Academic Press, London, 575 pp.

Jarvik, E. 1980b. Basic Structure and Evolution of Vertebrates. Academic Press, London, 337 pp.

Jessen, H. 1973. Weitere fischreste aus dem Oberen Plattenkalk der Bergisch-Gladbach–Paffrather Mulde (Oberdevon, Rheinisches Schiefergebirge). Palaeontographica Abteilung A Palozoologie-Stratigraphie 143:159–187.

Johanson, Z., S. Turner, and A. Warren. 2000. First East Gondwanan record of *Strepsodus* (Sarcopterygii, Rhizodontida) from the Lower Carboniferous Ducabrook Formation, central Queensland, Australia. Geodiversitas 22:161–169.

Johanson, Z., R. Carr, and A. Ritchie. 2010. Fusion, gene misexpression and homeotic transformations in vertebral development of the gnathostome stem group (Placodermi). The International Journal of Developmental Biology 54:71–80.

Johanson, Z., K. Trinajstic, R. Carr, and A. Ritchie. 2013. Evolution and development of the synarcual in early vertebrates. Zoomorphology 132:95–110.

Kaneko, T., K. Freeha, X. Wu, M. Mogi, S. Uji, H. Yokoi, and T. Suzuki. 2016. Role of notochord cells and sclerotome-derived cells in vertebral column development in fugu, *Takifugu rubripes*: histological and gene expression analyses. Cell and Tissue Research 366:37–49.

Kemp, A. 1991. Australian Mesozoic and Cainozoic lungfish; pp. in P. Vickers-Rich, J. M. Monaghan, R. F. Baird, and T. Rich (eds.), Vertebrate Palaeontology of Australasia. Pioneer Deisgn Studio, Melbourne.

Kemp, A. 1993. Problematic Triassic dipnoans from Australia; pp. in S. C. Lucas and M. Morales (eds.), The Nonmarine Triassic., . New Mexico Museum of Natural History and Science Bulletin vol. 3. New Mexico Museum of Natural History, Albuquerque, New Mexico.

Kemp, A. 1994. Australian Triassic lungfish skulls. Journal of Paleontology 68:647–654.

Kemp, A. 1996. Triassic lungfish from Gondwana; pp. 409–416 in Mesozoic Fishes: Systematics and Paleoecology. Verlag Dr. Friedrich Pfeil, München, Germany.

Kemp, A. 1997a. A revision of Australian Mesozoic and Cenozoic lungfish of the family Neoceratodontidae (Osteichthyes: Dipnoi), with a description of four new species. Journal of Paleontology 71:713–733.

Kemp, A. 1997b. Four species of *Metaceratodus* (Osteichthyes: Dipnoi, Family Ceratodontidae) from Australian Mesozoic and Cenozoic deposits. Journal of Vertebrate Paleontology 17:26–33.

Kemp, A. 1998. Skull structure in post-Paleozoic lungfish. Journal of Vertebrate Paleontology 18:43–63.

Kemp, N. E., and S. K. Westrin. 1979. Ultrastructure of calcified cartilage in the endoskeletal tesserae of sharks. Journal of Morphology 160:75–101.

Keynes, R. J., and C. D. Stern. 1988. Mechanisms of vertebrate segmentation. Development 103:413–429.

Kitchin, I. C. 1949. The effects of notochordectomy in *Ambystoma mexicanum*. Journal of Experimental Zoology 112:393–415.

Klaatsch, H. 1893a. Beitrage zur vergleichenden Anatomie der Wirbelsaule. II. Ueber die Bildung knorpeliger Wirbelknorper bei Fischen. Morphologisches Jahrbuch 20:143–186.

Klaatsch, H. 1893b. Beitrage zur vergleichenden Anatomie der Wirbelsaule. I. Ueber den Urzustand der Fischwirbelsaule. Morphologisches Jahrbuch 19:649–680.

Klymkowsky, M. W., and J. Hanken. 1991. Whole-mount staining of *Xenopus* and other vertebrates. Methods in Cell Biology 36:419–441.

Kokubu, C., K. Horie, K. Abe, R. Ikeda, S. Mizuno, Y. Uno, S. Ogiwara, M. Ohtsuka, A. Isotani, M. Okabe, K. Imai, and J. Takeda. 2009. A transposon-based chromosomal engineering method to survey a large cis-regulatory landscape in mice. Nature Genetics 41:946–952.

Koob, T. J., and J. H. Long. 2000. The vertebrate body axis: evolution and mechanical function. American Zoologist 40:1–18.

Krupina, N. I., R. R. Reisz, and D. Scott. 2001. The skull and tooth system of *Orlovichthys limnatis*, a Late Devonian dipnoan from Russia. Canadian Journal of Earth Sciences 38:1301–1311.

Ladich, F. 2001. Sound-generating and -detecting motor system in catfish: Design of swimbladder muscles in doradids and pimelodids. The Anatomical Record 263:297–306.

Laerm, J. 1976. The development, function, and design of amphicoelous vertebrae in teleost fishes. Zoological Journal of the Linnean Society 58:237–254.

Laerm, J. 1979a. The origin and homology of the chondrostean vertebral centrum. Canadian Journal of Zoology 57:475–485.

Laerm, J. 1979b. On the Origin of Rhipidistian Vertebrae. Journal of Paleontology 53:175–186.

Laerm, J. 1982. The origin and homology of the neopterygian vertebral centrum. 56:191–202.

Lambers, P. H. 1996. A redescription of the coelacanth *Macropoma willemoesii* VETTER from the lithographic limestone of Solnhofen (Upper Jurassic, Bavaria); pp. in G. Arratia and G. Viohl (eds.), Mesozoic Fishes - Systematics and Paleoecology. Verlag Dr. Friedrich Pfeil, München, Germany.

Lane, J. A., and J. G. Maisey. 2012. The visceral skeleton and jaw suspension in the durophagous hybodontid Shark *Tribodus limae* from the Lower Cretaceous of Brazil. Journal of Paleontology 86:886–905.

Lauder, G. V. 1980. On the relationship of the myotome to the axial skeleton in vertebrate evolution. Paleobiology 6:51–56.

Lebedev, O. A. 1995. Middle Famennian (Upper Devonian) chondrichthyans and sarcopterygians from Oryol region, Central Russia. Geobios 19:361–368.

Lefebvre, V., and P. Bhattaram. 2010. Chapter Eight - Vertebrate Skeletogenesis; pp. 291–317 in P. Koopman (ed.), Current Topics in Developmental Biology., . Organogenesis in Development vol. 90. Academic Press.

Lengner, C. J., M. Q. Hassan, R. W. Serra, C. Lepper, A. J. van Wijnen, J. L. Stein, J. B. Lian, and G. S. Stein. 2005. Nkx3.2-mediated Repression of Runx2 Promotes Chondrogenic Differentiation. Journal of Biological Chemistry 280:15872–15879.

Lewis, P. O. 2001. A Likelihood Approach to Estimating Phylogeny from Discrete Morphological Character Data. Systematic Biology 50:913–925.

Li, G.-Q., and M. V. Wilson. 1994. An Eocene species of Hiodon from Montana, its phylogenetic relationships, and the evolution of the postcranial skeleton in the Hiodontidae (Teleostei). Journal of Vertebrate Paleontology 14:153–167.

Liu, H. T. 1957. A new fossil cyprinid fish from Maoming, Kwangtung. Vertebrata PalAsiatica 1:151–153.

Liu, Y.-H. 1991. On a new petalichthyid, *Eurycaraspis incilis* gen. et sp. nov., from the middle Devonian of Zhanyi, Yunnan; pp. 139–177 in M.-M. Chang, Zhang, G.-R., and Y.-H. Liu (eds.), Early vertebrates and related problems of evolutionary biology. Science Press, Beijing.

Lombardo, C., Z.-Y. Sun, A. Tintori, D.-Y. Jiang, and W.-C. Hao. 2011. A new species of the genus *Perleidus* (Actinopterygii: Perleidiformes) from the Middle Triassic of Southern China. Bollettino Della Società Paleontologica Italiana 50:75–83.

Long, J. A. 1983. New bothriolepid fish from the Late Devonian of Victoria, Australia. Palaeontology 26:295–320.

Long, J. A. 1987. An unusual osteolepiform fish from the Late Devonian of Victoria, Australia. Palaeontology 30:839–852.

Long, J. A. 1988. New palaeoniscoid fishes from the Late Devonian and Early Carboniferous of Victoria. Memoirs of the Association of Australasian Palaeontologists 7:1–64.

Long, J. A. 1989. A new rhizodontiform fish from the Early Carboniferous of Victoria, Australia, with remarks on the phylogenetic position of the group. Journal of Vertebrate Paleontology 9:1–17.

Long, J. A. 1992. *Gogodipterus paddyensis* (Miles), gen. nov., a new chirodipterid lungfish from the Late Devonian Gogo Formation, Western Australia. The Beagle, Records of the Northern Territory Museum of Arts and Sciences 9:11–20.

Long, J. A. 1995. A new groenlandaspidid arthrodire (Pisces: Placodermi) from the Middle Devonian Aztec Siltstone, southern Victoria Land, Antarctica. Records of the Western Australian Museum 17:35–41.

Long, J. A. 1999. A new genus of fossil coelacanth (Osteichthyes: Coelacanthiformes) from the Middle Devonian of southeastern Australia. Records of the Western Australian Museum, Supplement 57:37–53.

Long, J. A., and A. M. Clement. 2009. The postcranial anatomy of two Middle Devonian lungfishes (Osteichthyes, Dipnoi) from Mt. Howitt, Victoria, Australia. .

Long, J. A., R. E. Barwick, and K. S. W. Campbell. 1997. Osteology and functional morphology of the osteolepiform fish *Gogonasus andrewsae* Long, 1985, from the Upper Devonian Gogo Formation, Western Australia. Records of the Western Australian Museum, Supplement 53:1–89.

Long, J. A., K. Trinajstic, G. C. Young, and T. Senden. 2008. Live birth in the Devonian period. Nature 453:650–652.

Long, J. A., G. C. Young, T. Holland, T. J. Senden, and E. M. G. Fitzgerald. 2006. An exceptional Devonian fish from Australia sheds light on tetrapod origins. Nature 444:199–202.

Long, J. A., E. Mark-Kurik, Z. Johanson, M. S. Y. Lee, G. C. Young, Z. Min, P. E. Ahlberg, M. Newman, R. Jones, J. den Blaauwen, B. Choo, and K. Trinajstic. 2015. Copulation in antiarch placoderms and the origin of gnathostome internal fertilization. Nature 517:196–199.

Lukševičs, E., O. A. Lebedev, and G. V. Zakharenko. 2010. Palaeozoogeographical connections of the Devonian vertebrate communities of the Baltica Province. Part I. Eifelian–Givetian. Palaeoworld 19:94–107.

Lund, R. 1982. *Harpagofututor volsellorhinus* new genus and species (Chondrichthyes, Chondrenchelyiformes) from the Namurian Bear Gulch Limestone, *Chondrenchelys problematica* Traquair (Visean), and their sexual dimorphism. Journal of Paleontology 56:938–958.

Lund, R. 1985. The morphology of Falcatus falcatus (St. John and Worthen), a Mississippian stethacanthid chondrichthyan from the Bear Gulch Limestone of Montana. Journal of Vertebrate Paleontology 5:1–19.

Lund, R. 2000. The new actinopterygian order Guildayichthyiformes from the Lower Carboniferous of Montana (USA). Geodiversitas 22.

Lund, R., and W. Lund. 1984. New genera and species of coelacanths from the Bear Gulch Limestone (Lower Carboniferous) of Montana (U.S.A.). Geobios 17:237–244.

Lund, R., E. D. Grogan, and M. Fath. 2014. On the relationships of the Petalodontiformes (Chondrichthyes). Paleontological Journal 48:1015–1029.

Macadie, C. I. 2007. A placoderm fish plate from the Lower Devonian of Reefton, New Zealand. Records of the Canterbury Museum 21:21–26.

Maisey, J. G. 1982. The Anatomy and Interrelationships of Mesozoic Hybodont Sharks. American Museum of Natural History, pp.

Maisey, J. G. 1983. Cranial Anatomy of *Hybodus basanus* Egerton from the Lower Cretaceous of England. American Museum Novitates 2578:1–64.

Maisey, J. G. 1989. *Hamiltonichthys mapesi* , g. & sp. nov. (Chondrichthyes; Elasmobranchii), from the Upper Pennsylvanian of Kansas. American Museum Novitates 2931:1–42.

Maisey, J. G. 2001. A primitive chondrichthyan braincase from the Middle Devonian of Bolivia; pp. 263–288 in P. E. Ahlberg (ed.), Major events in early vertebrate evolution. Taylor and Francis, New York.

Maisey, J. G. 2005. Braincase of the Upper Devonian shark *Cladodoides wildungensis* (Chondrichthyes, Elasmobranchii), with observations on the braincase in early chondrichthyans. Bulletin of the American Museum of Natural History 288:1–103.

Maisey, J. G. 2007. The braincase in Paleozoic symmoriiform and cladoselachian sharks. Bulletin of the American Museum of Natural History 307:1–122.

Maisey, J. G., and M. E. Anderson. 2001. A primitive chondrichthyan braincase from the Early Devonian of South Africa. Journal of Vertebrate Paleontology 21:702–713.

Maisey, J. G., G. J. P. Naylor, and D. J. Ward. 2004. Mesozoic elasmobranchs, neoselachian phylogeny and the rise of modern elasmobranch diversity; pp. 17–56 in G. Arratia and A. Tintori (eds.), Mesozoic Fishes 3: Systematics, Paleoenvironments and Biodiversity. Verlag Dr. Friedrich Pfeil, München, Germany.

Marinelli, W., and A. Strenger. 1954. Vergleichende Anatomie Und Morphologie Der Wirbeltiere. 1. *Lampetra Fluviatilis*. Franz Deuticke, Vienna, 80 pp.

Marshall, C. R. 1988. A large, well preserved specimen of the Middle Pennsylvanian lungfish *Conchopoma edesi* (Osteichthyes: Dipnoi) from Mazon Creek, Illinois, U.S.A. Journal of Vertebrate Paleontology 8:383–394.

Martin, M. 1981. Les Dipneustes et Actinistiens du Trias supérieur continental marocain. Stuttgarter Beiträge Zur Naturkunde Serie B (Geologie Und Paläontologie) 69:1–29.

Martin, M., and S. Wenz. 1984. Découverte d'un nouveau Coelacanthidé, *Garnbergia ommata* n. g., n. sp., dans le Muschelkalk supérieur du Baden-Württemberg. Stuttgarter Beiträge Zur Naturkunde, B (Geologie Und Paläontologie) 105:1–17.

Maxwell, E. E., N. B. Fröbisch, and A. C. Heppleston. 2008. Variability and conservation in late chondrichthyan development: Ontogeny of the winter skate (*Leucoraja ocellata*). The Anatomical Record: Advances in Integrative Anatomy and Evolutionary Biology 291:1079–1087.

Maxwell, E. E., H. Furrer, and M. R. Sánchez-Villagra. 2013. Exceptional fossil preservation demonstrates a new mode of axial skeleton elongation in early ray-finned fishes. Nature Communications 4:2570.

Maxwell, E. E., C. Romano, F. Wu, and H. Furrer. 2015. Two new species of *Saurichthys* (Actinopterygii: Saurichthyidae) from the Middle Triassic of Monte San Giorgio, Switzerland, with implications for character evolution in the genus: New *Saurichthys* species (Actinopterygii). Zoological Journal of the Linnean Society 173:887–912.

McCoy, V. E., E. E. Saupe, J. C. Lamsdell, L. G. Tarhan, S. McMahon, S. Lidgard, P. Mayer, C. D. Whalen, C. Soriano, L. Finney, S. Vogt, E. G. Clark, R. P. Anderson, H. Petermann, E. R. Locatelli, and D. E. G. Briggs. 2016. The "Tully monster" is a vertebrate. Nature advance online publication.

McCune, A. R. 1996. Biogeographic and Stratigraphic Evidence for Rapid Speciation in Semionotid Fishes. Paleobiology 22:34–48.

McMahon, J. A., S. Takada, L. B. Zimmerman, C.-M. Fan, R. M. Harland, and A. P. McMahon. 1998. Noggin-mediated antagonism of BMP signaling is required for growth and patterning of the neural tube and somite. Genes & Development 12:1438–1452.

Miles, R. S. 1967. Observations on the ptyctodont fish, *Rhamphodopsis* Watson. Zoological Journal of the Linnean Society 47:99–120.

Miles, R. S. 1970. Remarks on the vertebral column and caudal fin of acanthodian fishes. Lethaia 3:343–362.

Miles, R. S. 1971. The Holonematidae (placoderm fishes), a review based on new specimens of *Holonema* from the Upper Devonian of Western Australia. Source: Philosophical Transactions of the Royal Society of London. Series B, Biological Sciences 263:101–234.

Miles, R. S. 1973. Articulated acanthodian fishes from the Old Red Sandstone of England, with a review of the structure and evolution of the acanthodian shoulder-girdle. Bulletin of the British Museum (Natural History) Geology Series 24:113–213.

Miles, R. S. 1977. Dipnoan (lungfish) skulls and the relationships of the group: a study based on new species from the Devonian of Australia. Zoological Journal of the Linnean Society 61:1–328.

Miles, R. S., and T. S. Westoll. 1968. The placoderm fish *Coccosteus cuspidatus* Miller ex Agassiz from the Middle Old Red Sandstone of Scotland. Part 1. Descriptive morphology. Transactions of the Royal Society of Edinburgh 67:373–476.

Miles, R. S., and G. C. Young. 1977. Placoderm interrelationships reconsidered in the light of new ptyctodontids from Gogo, Western Australia. Linnean Society of London, Seminar Series 4:123–198.

Miller, H. 1841. The Old Red Sandstone. John Johnstone, Edinburgh, 275 pp.

Miller, R. F., R. Cloutier, and S. Turner. 2003. The oldest articulated chondrichthyan from the Early Devonian period. Nature 425:501–504.

Minikh, M. G. 1977. Triassic Dipnoan Fishes of the Eastern European Part of the USSR. Saratov University Press, Saratov, Russia, 96 pp.

Mise, T., M. Iijima, K. Inohaya, A. Kudo, and H. Wada. 2008. Function ofPax1 andPax9 in the sclerotome of medaka fish. Genesis 46:185–192.

Monsoro-Burq, A.-H. 2005. Sclerotome development and morphogenesis: when experimental embryology meets genetics. The International Journal of Developmental Biology 49:301–308.

Mori-Akiyama, Y., H. Akiyama, D. H. Rowitch, and B. de Crombrugghe. 2003. Sox9 is required for determination of the chondrogenic cell lineage in the cranial neural crest. Proceedings of the National Academy of Sciences 100:9360–9365.

Morin-Kensicki, E. M., and J. S. Eisen. 1997. Sclerotome development and peripheral nervous system segmentation in embryonic zebrafish. Development 124:159–167.

Morin-Kensicki, E. M., E. Melancon, and J. S. Eisen. 2002. Segmental relationship between somites and vertebral column in zebrafish. Development 129:3851–3860.

Moy-Thomas, J. A. 1935. The coelacanth fishes from Madagascar. .

Moy-Thomas, J. A. 1936. On the structure and affinities of the Carboniferous cochliodont *Helodus simplex*. Geological Magazine 73:488–503.

Moy-Thomas, J. A., and T. S. Westoll. 1935. On the Permian coelacanth, *Coelacanthus granulatus*, Ag. Geological Magazine 72:446–457.

Moy-Thomas, J. A., and R. S. Miles. 1971. Palaeozoic Fishes. Chapman and Hall, London, pp.

Munster, G. 1842. Beitrag zur Kenntnis einiger neuen seltenen Versteinerungen aus den lithographischen Schiefern in Baiern. Neues Jahrbuch Für Mineralogie, Geognosie. Geologie Und Petrefaktenkunde 1842:35–46.

Nakamura, T., J. Klomp, J. Pieretti, I. Schneider, A. R. Gehrke, and N. H. Shubin. 2015. Molecular mechanisms underlying the exceptional adaptations of batoid fins. Proceedings of the National Academy of Sciences 112:15940–15945.

Nakashima, K., X. Zhou, G. Kunkel, Z. Zhang, J. M. Deng, R. R. Behringer, and B. de Crombrugghe. 2002. The Novel Zinc Finger-Containing Transcription Factor Osterix Is Required for Osteoblast Differentiation and Bone Formation. Cell 108:17–29.

Near, T. J., R. I. Eytan, A. Dornburg, K. L. Kuhn, J. A. Moore, M. P. Davis, P. C. Wainwright, M. Friedman, and W. L. Smith. 2012. Resolution of ray-finned fish phylogeny and timing of diversification. Proceedings of the National Academy of Sciences 109:13698–13703.

Nelson, J. S. 2006. Fishes of the World, 4th ed. John Wiley, Hoboken, N.J, 601 pp.

Newberry, J. S. 1857. New fossil fishes from the Devonian rocks of Ohio. American Journal of Science 24:147–149.

Newman, M. J., E. Mark-Kurik, J. L. D. Blaauwen, and I. Zupiņš. 2015. Scottish Middle Devonian fishes in Estonia. Scottish Journal of Geology 51:141–147.

Nielsen, E. 1942. Studies on Triassic Fishes from East Greenland 1. *Glaucolepis* and *Boreosomus*. C. A. Reitzels Forlag, Copenhagen, 399 pp.

Nielsen, E. 1949. Studies on Triassic Fishes from East Greenland II: *Australosomus* and *Birgeria*. C. A. Reitzels Forlag, Copenhagen, 309 pp.

Nordvik, K., H. Kryvi, G. K. Totland, and S. Grotmol. 2005. The salmon vertebral body develops through mineralization of two preformed tissues that are encompassed by two layers of bone. Journal of Anatomy 206:103–114.

Ota, K. G., S. Fujimoto, Y. Oisi, and S. Kuratani. 2011. Identification of vertebra-like elements and their possible differentiation from sclerotomes in the hagfish. Nature Communications 2:373.

Otero, O., A. Likius, P. Vignaud, and M. Brunet. 2006. A new polypterid fish: *Polypterus faraou* sp. nov. (Cladistia, Polypteridae) from the Late Miocene, Toros-Menalla, Chad. Zoological Journal of the Linnean Society 146:227–237.

Oulion, S., V. Borday-Birraux, M. Debiais-Thibaud, S. Mazan, P. Laurenti, and D. Casane. 2011. Evolution of repeated structures along the body axis of jawed vertebrates, insights from the *Scyliorhinus canicula* Hox code. Evolution & Development 13:247–259.

Owen, R. 1843. Lectures on the Comparative Anatomy and Physiology of the Invertebrate Animals : Delivered at the Royal College of Surgeons, in 1843. Longman, Brown, Green, and Longmans, London, 392 pp.

Owen, R. 1848. On the Archetype and Homologies of the Vertebrate Skeleton. Richard and John E. Taylor, London, 203 pp.

Panchen, A. L. 1985. On the amphibian *Crassigyrinus scoticus* Watson from the Carboniferous of Scotland. Philosophical Transactions of the Royal Society of London. Series B, Biological Sciences 309:505–568.

Panchen, A. L. 1992. Classification, Evolution, and the Nature of Biology. Cambridge University Press, Cambridge, 405 pp.

Paton, R. L. 1976. A catalogue of fossil vertebrates in the Royal Scottish Museum, Part 5, Acanthodii. Royal Scottish Museums, Information Series, Geology 6:1–40.

Patterson, C. 1982. Morphological characters and homology; pp. 21–74 in K. A. Joysey and A. E. Friday (eds.), Problems of Phylogenetic Reconstruction. New York, Academic Press.

Patterson, C. 1988. Homology in classical and molecular biology. Molecular Biology and Evolution 5:603–625.

Peignoux-Deville, J., F. Lallier, and B. Vidal. 1982. Evidence for the presence of osseous tissue in dogfish vertebrae. Cell and Tissue Research 222:605–614.

Peters, H., B. Wilm, N. Sakai, K. Imai, R. Maas, and R. Balling. 1999. Pax1 and Pax9 synergistically regulate vertebral column development. Development 126:5399–5408.

Piekarski, N., and L. Olsson. 2014. Resegmentation in the mexican axolotl, *Ambystoma mexicanum*. Journal of Morphology 275:141–152.

Pierce, S. E., P. E. Ahlberg, J. R. Hutchinson, J. L. Molnar, S. Sanchez, P. Tafforeau, and J. A. Clack. 2013. Vertebral architecture in the earliest stem tetrapods. Nature 494:226–229.

Pisani, D., and M. Wilkinson. 2002. Matrix Representation with Parsimony, Taxonomic Congruence, and Total Evidence. Systematic Biology 51:151–155.

Porter, M. E., and J. H. Long. 2010. Vertebrae in compression: Mechanical behavior of arches and centra in the gray smooth-hound shark (*Mustelus californicus*). Journal of Morphology 271:366–375.

Porter, M. E., C. M. Roque, and J. H. Long. 2009. Turning maneuvers in sharks: Predicting body curvature from axial morphology. Journal of Morphology 270:954–965.

Powrie, J. 1864. On the Fossiliferous Rocks of Forfarshire and their Contents. Quarterly Journal of the Geological Society 20:413–429.

Pradel, A., P. Tafforeau, and P. Janvier. 2010. Study of the pectoral girdle and fins of the Late Carboniferous sibyrhynchid iniopterygians (Vertebrata, Chondrichthyes, Iniopterygia) from Kansas and Oklahoma (USA) by means of microtomography, with comments on iniopterygian relationships. Comptes Rendus Palevol 9:377–387.

Pradel, A., J. G. Maisey, P. Tafforeau, and P. Janvier. 2009. An enigmatic gnathostome vertebrate skull from the Middle Devonian of Bolivia. Acta Zoologica 90:123–133.

Pradel, A., P. Tafforeau, J. G. Maisey, and P. Janvier. 2011. A new Paleozoic Symmoriiformes (Chondrichthyes) from the Late Carboniferous of Kansas (USA) and cladistic analysis of Early chondrichthyans. PLoS ONE 6:e24938.

Pridmore, P. A., and R. E. Barwick. 1993. Post-cranial morphologies of the Late Devonian dipnoans *Griphognathus* and *Chirodipterus* and locomotor implications. Memoirs of the Association of Australasian Palaeontologists 15:161–182.

Pritchard, A. C., A. H. Turner, S. J. Nesbitt, R. B. Irmis, and N. D. Smith. 2015. Late Triassic tanystropheids (Reptilia, Archosauromorpha) from northern New Mexico (Petrified Forest Member, Chinle Formation) and the biogeography, functional morphology, and evolution of Tanystropheidae. Journal of Vertebrate Paleontology 35:e911186.

Ragan, M. A. 1992. Phylogenetic inference based on matrix representation of trees. Molecular Phylogenetics and Evolution 1:53–58.

Rayner, D. H. 1952. On the Cranial Structure of an Early Palæoniscid, *Kentuckia*, gen. nov. Earth and Environmental Science Transactions of The Royal Society of Edinburgh 62:53–83.

Rees, J., and C. J. Underwood. 2002. The status of the shark genus *Lissodus* Brough, 1935, and the position of nominal *Lissodus* species within the Hybodontoidea (Selachii). Journal of Vertebrate Paleontology 22:471–479.

Remak, R. 1855. Untersuchungen Über Die Entwickelung Der Wirbelthiere. Reimer, Berlin, pp.

Renn, J., and C. Winkler. 2009. Osterix-mCherry transgenic medaka for in vivo imaging of bone formation. Developmental Dynamics 238:241–248.

Revell, L. J. 2014. Ancestral Character Estimation Under the Threshold Model from Quantitative Genetics. Evolution 68:743–759.

Ridewood, W. 1921. On the calcification of the vertebral centra in sharks and rays. Philosophical Transactions of the Royal Society of London, Series B, Containing Papers of a Biological Character 210:311–407.

Ridewood, W. G. 1899. Some observations on the caudal diplospondyly of sharks. Journal of the Linnean Society of London, Zoology 27:46–59.

Ritchie, A. 1973. *Wuttagoonaspis* gen. nov., an unusual arthrodire from the Devonian of Western New South Wales, Australia. Palaeontographica Abteilung A 58–72.

Ritchie, A. 1981. First complete specimen of the dipnoan *Gosfordia truncata* Woodward from the Triassic of New South Wales. Records of the Australian Museum 33:606–615.

Ritchie, A. 2005. *Cowralepis*, a new genus of phyllolepid fish (Pisces, Placodermi) from the Late Middle Devonian of New South Wales, Australia. Proceedings of the Linnean Society of New South Wales 126:215–259.

Rodrigo, I., R. E. Hill, R. Balling, A. Münsterberg, and K. Imai. 2003. Pax1 and Pax9 activate Bapx1 to induce chondrogenic differentiation in the sclerotome. Development 130:473–482.

Romano, C., and W. Brinkmann. 2010. A new specimen of the hybodont shark *Palaeobates polaris* with three-dimensionally preserved Meckel's cartilage from the Smithian (Early Triassic) of Spitsbergen. Journal of Vertebrate Paleontology 30:1673–1683.

Ronquist, F. 2004. Bayesian inference of character evolution. Trends in Ecology & Evolution 19:475–481.

Roth, V. L. 1984. On homology. Biological Journal of the Linnean Society 22:13–29.

Ruta, M., J. E. Jeffery, and M. I. Coates. 2003. A supertree of early tetrapods. Proceedings of the Royal Society of London B: Biological Sciences 270:2507–2516.

Sallan, L. C. 2012. Tetrapod-like axial regionalization in an early ray-finned fish. Proceedings of the Royal Society B: Biological Sciences 279:3264–3271.

Sansom, R. S., S. E. Gabbott, and M. A. Purnell. 2013. Unusual anal fin in a Devonian jawless vertebrate reveals complex origins of paired appendages. Biology Letters 9:20130002.

Schaeffer, B. 1952. The Triassic coelacanth fish *Diplurus*, with observations on the evolution of the Coelacanthini. Bulletin of the American Museum of Natural History 99:25–78.

Schaeffer, B. 1967a. Osteichthyan vertebrae. Journal of the Linnean Society of London, Zoology 47:185–195.

Schaeffer, B. 1967b. Late Triassic fishes from the western United States. Bulletin of the American Museum of Natural History 135:285–342.

Schaeffer, B. 1981. The xenacanth shark neurocranium, with comments on elasmobranch monophyly. Bulletin of the American Museum of Natural History 169:1–66.

Schaeffer, B., and M. Mangus. 1976. An Early Triassic Fish Assemblage from British Columbia. American Museum of Natural History, pp.

Schaeffer, B., and C. Patterson. 1984. Jurassic fishes from the western United States, with comments on Jurassic fish distribution. American Museum novitates ; no. American Museum Novitates 2796:1–86.

Schaumberg, G. 1982. *Hopleacanthus richelsdorfensis* ngn sp., ein Euselachier aus dem permischen Kupferschiefer von Hessen (W-Deutschland). Paläontologische Zeitschrift 56:235–257.

Schultze, H.-P. 1969. *Griphognathus* Gross, ein langschnauziger Dipnoer aus dem Oberdevon von Bergisch-Gladbach (Rheinisches Schiefergebirge) und von Lettland. Geologica et Palaeontologica 3:21–61.

Schultze, H.-P. 1973. Crossopterygier mit heterozerker Schwanzflosse aus dem Oberdevon Kanadas, nebst einer Beschreibung von Onychodontida-Resten aus dem Mitteldevon Spaniens und aus dem Karbon der USA. Palaeontographica Abteilung A 188–208.

Schultze, H.-P. 1977. *Megapleuron zangerli* a new dipnoan from the Pennsylvanian, Illinois. Fieldiana Geology 33:375–396.

Schultze, H.-P. 1981. Das Schädeldach eines ceratodontiden Lungenfisches aus der Trias Süddeutschlands (Dipnoi, Pisces). Stuttgarter Beiträge Zur Naturkunde Serie B (Geologie Und Paläontologie) 70:1–31.

Schultze, H.-P. 1991. Lungfish from the El Molino (Late Cretaceous) and Santa Lucia (Early Paleocene) formations in southcentral Bolivia; pp. 441–448 in R. Suárez-Soruco (ed.), Fósiles y Facies de Bolivia, Vol. 1, Revista Técnica de Yacimientos Petrolíferos Fiscales Bolivianos. Santa Cruz, Bolivia.

Schultze, H.-P. 1992. A new long-headed dipnoan (Osteichthyes) from the Middle Devonian of Iowa, USA. Journal of Vertebrate Paleontology 12:42–58.

Schultze, H.-P. 2004. Mesozoic sarcopterygians; pp. 463–492 in G. Arratia and A. Tintori (eds.), Mesozoic Fishes 3: Systematics, Paleoenvironments and Biodiversity. Verlag Dr. Friedrich Pfeil, München, Germany.

Schultze, H.-P. 2010. The late Middle Devonian fauna of Red Hill I, Nevada, and its paleobiogeographic implications. Fossil Record 13:285–295.

Schultze, H.-P., and J. Zidek. 1982. Ein primitiver acanthodier (pisces) aus dem unterdevon lettlands. Paläontologische Zeitschrift 56:95–105.

Schultze, H.-P., and M. Arsenault. 1985. The panderichthyid fish *Elpistostege*: a close relative of tetrapods? Palaeontology 28:293–309.

Schultze, H.-P., and G. Arratia. 1988. Reevaluation of the caudal skeleton of some actinopterygian fishes: II. *Hiodon*, *Elops*, *and Albula*. Journal of Morphology 195:257–303.

Schultze, H.-P., and J. Chorn. 1997. The Permo-Carboniferous genus *Sagenodus* and the beginning of modern lungfish. Contributions to Zoology 67:9–70.

Schultze, H.-P., and S. L. Cumbaa. 2001. *Dialipina* and the characters of basal actinopterygians; pp. 315–332 in P. E. Ahlberg (ed.), Major Events in Early Vertebrate Evolution. Taylor and Francis, London.

Schultze, H.-P., and T. Märss. 2004. Revisiting *Lophosteus*, a primitive osteichthyan. Acta Universitatis Latviensis 679:57–78.

Sharma, S., D. Londono, W. L. Eckalbar, X. Gao, D. Zhang, K. Mauldin, I. Kou, A. Takahashi, M. Matsumoto, N. Kamiya, K. K. Murphy, R. Cornelia, L. Karol, K. Rathjen, D. Sucato, J. Birch, C. Johnston, B. S. Richards, T. Milbrandt, V. Talwakar, H. Iwinski, R. Muchow, J. C. Tassone, X.-C. Liu, R. Shindell, W. Schrader, C. Eberson, A. Lapinsky, R. Loder, J. Davey, N. Hosogane, Y. Ogura, Y. Takahashi, A. Miyake, K. Watanabe, K. Chiba, Y. Toyama, K. Kono, N. Kawakami, T. Tsuji, K. Uno, T. Suzuki, M. Ito, H. Sudo, S. Minami, T. Kotani, H. Yanagida, H. Taneichi, I. Yonezawa, K. Kaneko, J. A. Herring, D. Burns, N. Ahituv, S. Ikegawa, D. Gordon, and C. A. Wise. 2015. A PAX1 enhancer locus is associated with susceptibility to idiopathic scoliosis in females. Nature Communications 6:6452.

Shu, D.-G., S. C. Morris, J. Han, Z.-F. Zhang, K. Yasui, P. Janvier, L. Chen, X.-L. Zhang, J.-N. Liu, Y. Li, and H.-Q. Liu. 2003. Head and backbone of the Early Cambrian vertebrate *Haikouichthys*. Nature 421:526–529.

Sigogneau-Russell, D., and G. Hahn. 1994. Late Triassic microvertebrates from central Europe; pp. 197–213 in N. Fraser and H.-D. Sues (eds.), In the Shadow of the Dinosaurs. Early Mesozoic Tetrapods. Cambridge University Press, Cambridge.

Smith, J. L. B. 1953. The second cœlacanth. Nature 171:99–101.

Smithson, T. R., S. P. Wood, J. E. A. Marshall, and J. A. Clack. 2012. Earliest Carboniferous tetrapod and arthropod faunas from Scotland populate Romer's Gap. Proceedings of the National Academy of Sciences 109:4532–4537.

Stahl, B. J. 1999. Chondrichthyes III: Holocephali. Verlag Dr. Friedrich Pfeil, München, Germany, 164 pp.

Stensiö, E. 1919. Einige Bemerkungen über die systematische Stellung von *Saurichthys mougeotoi* Agassiz. Senckenbergiania 1:177–181.

Stensiö, E. 1932. Triassic fishes from East Greenland collected by the Danish expeditions 1929-1931. Meddelelser Om Grønland 83:1–305.

Stensiö, E. 1969. Elasmobranchiomorphi. Placodermata. Arthrodires.; pp. 71–692 in J. Piveteau (ed.), Traité de paléontologie. vol. 4.2. Masson, Paris.

Stensiö, E. A. 1921. Triassic Fishes from Spitzbergen. Adolf Holzhausen, Vienna, 307 pp.

Stern, C. D. 1990. Two distinct mechanisms for segmentation? Seminars in Developmental Biology 1:109–116.

Stern, C. D., and R. J. Keynes. 1987. Interactions between somite cells: the formation and maintenance of segment boundaries in the chick embryo. Development 99:261–272.

Stewart, K. 2003. Fossil fish remains from the Pliocene Kanapoi site, Kenya; pp. 21–38 in J. M. Harris and M. G. Leakey (eds.), Contributions in Science: Geology and Vertebrate Paleontology of the Early Pliocene Site of Kanapoi, Northern Kenya. Allen Press, Inc., Lawrence, Kansas.

Strudel, G. 1955. Etude des conséquences d'excisions de somites sur l'organogenèse vertébral de l'embryon de poulet. Archives D'anatomie Microscopique et de Morphologie Expérimentale 44:209–235.

Tabaste, N. 1963. Étude de restes de poissons du Crétacé saharien. Mémoire IFAN, Mélanges Ichthyologiques 68:437–485.

Taverne, L. 1997. "*Osorioichthys marginis*." Paléonisciforme" du Famennien de Belgique, et la phylogénie des Actinoptérygiens dévoniens (Pisces). Bulletin de l'Institut Royal Des Sciences Naturelles de Belqique, Sciences de La Terre 67:57–78.

Teillet, M.-A., C. Kalcheim, and N. M. Le Douarin. 1987. Formation of the dorsal root ganglia in the avian embryo: Segmental origin and migratory behavior of neural crest progenitor cells. Developmental Biology 120:329–347.

Thies, D. 1983. Jurazeitliche Neoselachier aus Deutschland und S-England. Courier Forschungsinstitut Senckenberg 58:1–116.

Thomson, K. S. 1965. The endocranium and associated structures in the Middle Devonian rhipidistian fish *Osteolepis*. Proceedings of the Linnean Society of London 176:181–195.

Traquair, R. H. 1886. On *Harpacanthus*, a new genus of Carboniferous Selachian Spines. Annals and Magazine of Natural History 18:493–496.

Traquair, R. H. 1888. Notes on the Nomenclature of the Fishes of the Old Red Sandstone of Great Britain. Geological Magazine (Decade III) 5:507–517.

Traquair, R. H. 1893. Notes on the Devonian Fishes of Campbelltown and Scaumenac Bay in Canada. Geological Magazine 10:145–149.

Trinajstic, K. 2001. Acanthodian microremains from the Frasnian Gneudna Formation, Western Australia. Records of the Western Australian Museum 20:187–198.

Trinajstic, K., and J. A. Long. 2009. A new genus and species of Ptyctodont (Placodermi) from the Late Devonian Gneudna Formation, Western Australia, and an analysis of Ptyctodont phylogeny. Geological Magazine 146:743.

Turner, S., C. J. Burrow, and A. Warren. 2005. *Gyracanthides hawkinsi* sp. nov. (Acanthodii, Gyracanthidae) from the Lower Carboniferous of Queensland, Australia, with a review of gyracanthid taxa. Palaeontology 48:963–1006.

Underwood, C. J., and D. J. Ward. 2008. Sharks of the order Carcharhiniformes from the British Coniacian, Santonian, and Campanian (Upper Cretaceous). Palaeontology 51:509–536.

Upeniece, I. 1995. A new species of *Strunius* (Sarcopterygii; Onychodontida) from Latvia; Lode quarry (Upper Devonian). Geobios 28:281–284.

Valiukevičius, J. 1992. First articulated Poracanthodes from the Lower Devonian of Severnaya Zemlya; pp. 193–214 in E. Mark-Kurik (ed.), Fossil fishes as living animals. Academy of Sciences of Estonia, Tallinn.

Van Buren, C. S., and D. C. Evans. 2016. Evolution and function of anterior cervical vertebral fusion in tetrapods: Evolution and function of the tetrapod syncervical. Biological Reviews n/a-n/a.

Van Valen, L. M. 1982. Homology and causes. Journal of Morphology 173:305–312.

Vorobyeva, E. 1967. Triasovbii ceratod iz juznoi fergany I nekotorye zamecanija o sisteme I filogenii ceratodontid. Palaeontologichevski Zhurnal 1967:102–11.

Vorobyeva, E., and H.-P. Schultze. 1991. Description and systematics of panderichthyid fishes with comments on their relationships to tetrapods; pp. in H.-P. Schultze and L. Trueb (eds.), Origins of the Higher Groups of Tetrapods: Controversy and Consensus. Comstock Publishing Associates, Ithaca, New York.

Wagner, G. P. 1989. The biological homology concept. Annual Review of Ecology and Systematics 51–69.

Wagner, G. P. 1999. A research programme for testing the biological homology concept; pp. 125–140 in Homology. John Wiley & Sons, New York.

Wake, D. B., and R. Lawson. 1973. Developmental and adult morphology of the vertebral column in the plethodontid salamander *Eurycea bislineata*, with comments on vertebral evolution in the Amphibia. Journal of Morphology 139:251–299.

Wallin, J., J. Wilting, H. Koseki, R. Fritsch, B. Christ, and R. Balling. 1994. The role of *Pax-1* in axial skeleton development. Development 120:1109–1121.

Wang, J.-Q., and G.-R. Zhang. 1999. New material of *Microbrachius* from Lower Devonian of Qujing, Yunnan, China. Vertebrata PalAsiatica 7:200–211.

Wang, S., H. Kryvi, S. Grotmol, A. Wargelius, C. Krossøy, M. Epple, F. Neues, T. Furmanek, and G. K. Totland. 2013. Mineralization of the vertebral bodies in Atlantic salmon (*Salmo salar* L.) is initiated segmentally in the form of hydroxyapatite crystal accretions in the notochord sheath. Journal of Anatomy 223:159–170.

Wang, W., Q.-M. Qu, and M. Zhu. 2010. A brief review of the Middle Palaeozoic vertebrates from Southeast Asia. Palaeoworld 19:27–36.

Ward, D. J. 1973. The English Palaeogene chimaeroid fishes. Proceedings of the Geologists' Association 84:315–330.

Ward, L., S. E. Evans, and C. D. Stern. 2016. A resegmentation-shift model for vertebral patterning. Journal of Anatomy n/a-n/a.

Watanabe, Y., D. Duprez, A.-H. Monsoro-Burq, C. Vincent, and N. M. Le Douarin. 1998. Two domains in vertebral development: antagonistic regulation by SHH and BMP4 proteins. Development 125:2631–2639.

Watson, D. M. S. 1934. The interpretation of arthrodires. Proceedings of the Zoological Society of London 104:437–464.

Watson, D. M. S. 1937. The acanthodian fishes. Philosophical Transactions of the Royal Society of London. Series B, Biological Sciences 228:49–146.

Watson, D. M. S. 1938. On *Rhamphodopsis*, a Ptyctodont from the Middle Old Red Sandstone of Scotland. Earth and Environmental Science Transactions of The Royal Society of Edinburgh 59:397–410.

Werdelin, L. 1986. A new chimaeroid fish from the Cretaceous of Lebanon. Geobios 19:393–397.

Werner, C. 1994. Die kontinentale Wirbeltierfauna aus der unteren Oberkreide des Sudan (Wadi Milk Formation). Berliner Geowissenschaftliche Abhandlungen E (B. Krebs-Festschrift) 13:221–249.

White, E. I., and H. A. Toombs. 1972. The buchanosteid arthrodires of Australia. Bulletin of the British Museum (Natural History) Geology Series 22:317–419.

van Wijhe, J. W. 1922. Frühe Entwicklungsstadien des Kopf- und Rumpfskeletts von *Acanthias vulgaris*. Bijdragen Tot de Dierkunde 1922:271–298.

Williams, E. E. 1959. Gadow's arcualia and the development of tetrapod vertebrae. The Quarterly Review of Biology 34:1–32.

Williams, J. L. 1942. The development of cervical vertebrae in the chick under normal and experimental conditions. American Journal of Anatomy 71:153–179.

Williams, M. E. 1998. A new specimen of *Tamiobatis vetustus* (Chondrichthyes, Ctenacanthoidea) from the Late Devonian Cleveland Shale of Ohio. Journal of Vertebrate Paleontology 18:251–260.

Woodward, A. S. 1890. On the discovery of a Jurassic fish-fauna in the Hawkesbury Beds of New South Wales. Annals and Magazine of Natural History 6:423–423.

Woodward, A. S. 1891. The Hybodont and cestraciont sharks of the Cretaceous Period. Proceedings of the Yorkshire Geological and Polytechnic Society 12:62–68.

Woodward, A. S. 1895. Catalogue of the Fossil Fishes in the British Museum:(Natural History.). Printed by order of the Trustees, pp.

Woodward, A. S. 1908. On some fossil fishes discovered by Prof. Ennes de Souza in the Cretaceous formation at Ilheos (State of Bahia), Brazil. Quarterly Journal of the Geological Society 64:358–362.

Woodward, A. S. 1917. The Fossil Fishes of the English Wealden and Purbeck Formations. The Palaeontological Society, London, 1-148 pp.

Woodward, A. S. 1941. The Head Shield of a new Macropetalichthyid Fish (*Notopetalichthys hillsi*, gen. et sp. nov.) from the Middle Devonian of Australia. Annals and Magazine of Natural History 8:91–96.

Wyffels, J., B. L. King, J. Vincent, C. Chen, C. H. Wu, and S. W. Polson. 2014. SkateBase, an elasmobranch genome project and collection of molecular resources for chondrichthyan fishes. F1000Research 3.

Xu, G.-H., L.-J. Zhao, K.-Q. Gao, and F.-X. Wu. 2012. A new stem-neopterygian fish from the Middle Triassic of China shows the earliest over-water gliding strategy of the vertebrates. Proceedings of the Royal Society B: Biological Sciences 280:20122261–20122261.

Yamagushi, H. 2004. Elasmobranch remains from the Taho Limestone (Lower-Middle Triassic) of Ehime Prefacture, Southwest Japan; pp. in Mesozoic Fishes 3 – Systematics, Paleoenvironments and Biodiversity. Verlag Dr. Friedrich Pfeil, München, Germany.

Yeo, G. H., F. S. H. Cheah, C. Winkler, E. W. Jabs, B. Venkatesh, and S. S. Chong. 2009. Phylogenetic and evolutionary relationships and developmental expression patterns of the zebrafish twist gene family. Development Genes and Evolution 219:289–300.

Young, G. C. 1974. Stratigraphic occurrence of some placoderm fishes in the Middle and Late Devonian. Newsletters on Stratigraphy 3:243–261.

Young, G. C. 1979. New information on the structure and relationships of *Buchanosteus* (Placodermi: Euarthrodira) from the Early Devonian of New South Wales. Zoological Journal of the Linnean Society 66:309–352.

Young, G. C. 1989. The Aztec fish fauna (Devonian) of Southern Victoria Land: Evolutionary and biogeographic significance; pp. 43–62 in J. A. Crame (ed.), Origins and Evolution of the Antarctic Biota. Geological Society of London, London.

Yu, X. 1998. A new porolepiform-like fish, *Psarolepis romeri*, gen. et sp. nov. (Sarcopterygii, Osteichthyes) from the Lower Devonian of Yunnan, China. Journal of Vertebrate Paleontology 18:261–274.

Zangerl, R. 1981. Chondrichthyes I: Paleozoic Elasmobranchii. Gustav Fischer Verlag, Stuttgart, 115 pp.

Zangerl, R., and G. R. Case. 1973. Iniopterygia, a new order of chondrichthyan fishes from the Pennsylvanian of North America. Fieldiana Geology Memoirs 6:1–67.

Zangerl, R., and G. R. Case. 1976. *Cobelodus aculeatus* (Cope) an anacanthous shark from Pennsylvanian black shales of North America. Palaeontographica Abteilung A Paläozoologie-Stratigraphie 154:107–157.

Zeng, L., H. Kempf, L. C. Murtaugh, M. E. Sato, and A. B. Lassar. 2002. Shh establishes an Nkx3.2/Sox9 autoregulatory loop that is maintained by BMP signals to induce somitic chondrogenesis. Genes & Development 16:1990–2005.

Zhao, Q., H. Eberspaecher, V. Lefebvre, and B. de Crombrugghe. 1997. Parallel expression of Sox9 and Col2a1 in cells undergoing chondrogenesis. Developmental Dynamics 209:377–386.

Zhu, M., and J. Fan. 1995. *Youngolepis* from the Xishancun Formation (Early Lochkovian) of Qujing, China. Geobios 19:293–299.

Zhu, M., and X. Yu. 2002. A primitive fish close to the common ancestor of tetrapods and lungfish. Nature 418:767–770.

Zhu, M., and P. E. Ahlberg. 2004. The origin of the internal nostril of tetrapods. Nature 432:94–97.

Zhu, M., X. Yu, and P. Janvier. 1999. A primitive fossil fish sheds light on the origin of bony fishes. Nature 397:607–610.

Zhu, M., X. Yu, and P. E. Ahlberg. 2001. A primitive sarcopterygian fish with an eyestalk. Nature 410:81–84.

Zhu, M., X. Yu, B. Choo, J. Wang, and L. Jia. 2012. An antiarch placoderm shows that pelvic girdles arose at the root of jawed vertebrates. Biology Letters 8:453–456.

Zhu, M., W. Zhao, L. Jia, J. Lu, T. Qiao, and Q. Qu. 2009. The oldest articulated osteichthyan reveals mosaic gnathostome characters. Nature 458:469–474.

Zhu, M., X. Yu, P. E. Ahlberg, B. Choo, J. Lu, T. Qiao, Q. Qu, W. Zhao, L. Jia, H. Blom, and Y. Zhu. 2013. A Silurian placoderm with osteichthyan-like marginal jaw bones. Nature 502:188–193.

Zidek, J. 1993. Juvenile *Orthacanthus platypternus* (Cope 1883) (Elasmobranchii: Xenacanthiformes) from the Upper Carboniferous near Hamilton, Kansas, USA; pp. 53–65 in U. Heitdke (ed.), New Research on Permo-Carboniferous faunas. Pollichia-Buch. vol. 29. Pollichia-Buch, Bad Dürkheim.

Zupiņš, I. 2008. A New Tristichopterid (Pisces, Sarcopterygii) from the Devonian of Latvia. Proceedings of the Latvian Academy of Sciences. Section B. Natural, Exact, and Applied Sciences. 62.